Gene Transfer Vector Development to Treat Lung Disease

Thesis submitted for the degree of Doctor of Philosophy

Rebekka Harding-Smith

Gene Medicine Research Group, Nuffield Department of Clinical Laboratory Sciences and

Lincoln College, University of Oxford

Supervisors: Dr. Deborah R. Gill and Dr. Steve C. Hyde

Trinity Term, 2014

Preface

Abstract

Gene transfer vector development to treat lung disease

Rebekka Harding-Smith
Nuffield Department of Clinical Laboratory Sciences and Lincoln College, University of Oxford
Thesis submitted for the degree of Doctor of Philosophy, Trinity Term 2014

Cystic Fibrosis (CF) is a degenerative disorder that is often associated with chronic lung disease. CF is caused by mutations in the gene encoding the Cystic Fibrosis Transmembrane Conductance Regulator (CFTR) chloride channel, which lead to defective chloride and sodium ion movement across epithelia. Subsequent dehydration of the airway surface liquid (ASL) on airway epithelia, is associated with poor mucociliary clearance and chronic lung infection. The monogenic nature of CF, along with the accessibility of the lung, makes the disease amenable to gene replacement therapy. Gene therapy clinical trials have focused on replacing the mutated CFTR with a functional copy, which has led to improved chloride transport, but has shown no significant effects on sodium transport. An alternative strategy for CF gene therapy therefore, could be to reduce the expression of the epithelial sodium channel (ENaC) in the lung, using RNA interference (RNAi), combined with CFTR delivery. Developing a dual-function gene transfer vector could potentially restore chloride and sodium levels in the ASL and help alleviate CF lung disease. The aim of this thesis was to develop a recombinant lentivirus delivery system capable of simultaneously delivering CFTR expression and knocking down ENaC expression in the airways. A modular HIV vector genome plasmid was developed to allow simple insertion of various promoter elements, transgenes and knockdown sequences, for subsequent virus production. Insertion of the CFTR transgene and a short-hairpin RNA (shRNA) sequence targeting the ENaC alpha subunit (ENaCα) resulted in significant knockdown of human ENaCα and simultaneous expression of CFTR in A549 (human lung carcinoma) cell culture. Replacement of the ENaCα shRNA with an shRNA targeting the transcription factor BACH1 resulted in target gene knockdown and concomitant HMOX1 up-regulation, confirming specific knockdown effects, and demonstrating that the dual-function rLV vector could mediate target gene knockdown irrespective of the target. Attempts were made to knock down BACH1 in primary cultures of human bronchial epithelial cells grown at the air-liquid interface (ALI), but improved transduction efficiencies from the apical surface will be required to generate successful knockdown in this experimental model. These studies provide proof-of-principle for the utility of this versatile dual-function prototype virus. The dual function vector not only has the potential for treatment of CF lung disease, but could be readily altered to target other lung diseases where combinations of prolonged target gene knockdown and gene expression/up-regulation could collectively provide an appropriate therapy. In conclusion, the focus on the rational design of gene transfer vectors for specific therapeutic effects will aid the development and translation of gene therapy approaches to human studies.

Acknowledgements

First and foremost I would like to thank my supervisors, Dr. Deborah Gill and Dr. Stephen Hyde, for their continued support throughout my DPhil. Luckily my tears of frustration when things inevitably did not go my way never fazed them and they continued to drive and encourage me until the bitter end. Thank you so much for all the guidance, late nights, BBQs, cakes and honesty. This means that I can finally forgive Steve for writing off my car. The debt is paid.

All of the members of the Gene Medicine group have contributed to the success of my DPhil, not only by helping me to learn the techniques required, and to bounce ideas off of, but also as friends and cake-providers. All of these people have contributed to the retention of my sanity over the past four years: Ian Pringle, Karen Bamford, Graciela Nunez-Alonso, Anna Lawton, Mary Connolly, Laura Moyce, Rebecca Coles, Jack Tiong Kit, Jean-Francois Gelinas, Natasha Davie, Cathy Oliveira and Charlotte Rush, with particular mention to Stephanie Sumner-Jones and Lee Davies who have put up with a lot of complaining and questions from me. Particular thanks also go to Anna Lawton for teaching me cloning techniques and singing to me on a daily basis, Lee Davies for showing me how to perform lentivirus productions, how to use the FACS machine, and for producing, concentrating and purifying copious volumes of rLV for my perusal, Stephanie Sumner-Jones for teaching me all there is to know about TaqMan analyses and cell culture, and Mary Connolly for her guidance in immunoblotting techniques. I would also like to thank my college advisors Pietro Roversi, Dunja Aksentijevic and Ioannis Vakonakis for their support at various points throughout my studies. Thanks also to Carmella Elan-Gaston, Louise Durning and the other academic support staff in Lincoln college who have helped with all of my paperwork and given me loads of great advice; Tim Knowles for helping me at various points with my financial situation so that I never had to live off beans on toast; Kati Ali for always being understanding if I arrived late to hall for dinner and letting me sneak in; and Simon Faulkner for lending me a gown on more occasions than I can count!

A large part of my life during my DPhil has revolved around the extra-curricular activities that have helped to keep me sane in the intense post-graduate environment in Oxford. As such, I would like to thank all of the members of the Oxford University Ice Hockey Club Women's team since 2010 for their friendship and dedication to this fantastic sport, what better way to get out the frustrations of the day than skating around the ice at full speed hitting pucks. Thanks also to the members of the Beaver's softball team, especially Isabel and Jem Lough who made me feel so welcome from the offset, and always arrange the best bunkhouse

retreats for the Beaver family. Also, thanks to the Lincoln College Boat Club who have always encouraged me to come and hop in a boat, even when other commitments rendered me unreliable. Thanks as well to Colin Pearson, Ben White and Tim Hands at Magdalen College School in Oxford who have been more understanding that I could possibly have imagined, making it possible for me to finish writing my thesis whilst also starting a full-time job as a teacher at the school. I feel that I should also apologise to my pupils for not being able give myself as fully as I would have liked for this first month of my new position.

I would like to acknowledge my friends, who I have sadly neglected this past year, but who have made living and studying in Oxford one of the most enjoyable times of my life, with a particular mention to Tim Green, Callum Doherty, Danielle Costa, Harry Fisher, Torben Schiffner, Izzy Paterson-Taylor, Pollyanna FitzGerald, Mitch Breisner, Paul Birmingham, Joanna Palermo, Jess McMurray, Emma Dyson for always being there to carry on the conversation when we haven't spoken for months, and Laura Walton for introducing me to ladies powerlifting! Further thanks are definitely necessary for Sabrina Sheikh and Ian Pringle who provided accommodation for me when my funding ran out and I had experiments to finish off in Oxford.

Last and definitely not least I would like to thank my family for being so supportive and just generally amazing throughout this entire process: my Mum and Dad especially for giving up their room back home in Wales so I would have more space to write up, even though I ended up taking over the living room instead, and for supporting me tremendously for the past four years; my brothers, David and Jonny and our extended family for providing me with laughs and entertainment whenever I found the time to come home to visit, and Pen and Ollie Marriage for providing me with a home-away-from-home here in the South. Most importantly I'd like to thank my non-related family, Ioana Gagea and Kirstin Bilham for their continued friendship, love and support throughout the bad times and the good times; Liz Williams for never complaining about my awful electronic communication skills and making it easy to pick up where we left off whenever I got the chance to go back to Wales; Ioana for keeping me happy with regular pictures of cute, fluffy animals and checking in on me to make sure that I'm doing OK; and Kirstin for providing distractions, energy drinks, and nutritional support for the past few weeks and generally making sure that I've still got my head screwed on.

Declaration

This thesis has been composed by myself and has not been used in any previous application for a degree. The results herein were obtained by myself, except where acknowledged in the text. All sources of published or unpublished information have been specifically acknowledged by means of a reference or personal communication notation, respectively

Table of contents

Table of figures

Table of tables

Abbreviations

ABC	ATP-binding cassette
AECs	Airway epithelial cells
ASIC	Acid-sensing ion channel 1
ASL	Airway surface liquid
ATP	Adenosine triphosphate
ATPase	Adenosine triphosphatase
Bash	Anti-Bach1 shRNA
Ca^{2+}	Calcium ions
cAMP	cyclic adenosine monophosphate
CF	Cystic Fibrosis
CFTR	Cystic Fibrosis Transmembrane Conductance Regulator
Cl^-	Chloride ion
CMV	Cytomegalovirus
CMV-	CMV promoter/enhancer element without introns
COPD	Chronic obstructive pulmonary disease
DNA	De-oxy Ribonucleic Acid
ds	double-stranded
ECL	Extracellular loop
EF1-α	Human elongation factor-1 α promoter
EGFP	Enhanced green fluorescent protein
EGFPLux	EGFP-Luciferase fusion protein
EIAV	Equine infectious anemia virus
ENaC	Epithelial sodium channel
ER	Endoplasmic reticulum
FIV	Feline immunodeficiency virus
GAPDH	Glyceraldehyde 3-phosphate dehydrogenase

GL	EGFPLux
HCO_3^-	Bicarbonate ion
HIV	Human immunodeficiency virus
Hsp70	Heat shock protein 70kDa
Hsp90	Heat shock protein 90kDa
IC	integrase-competent
ID	Integrase-deficient
IL-8	Interleukin-8
IRT	Immunoreactive trypsin
LPC	lysophosphatidylcholine
LTR	Long terminal repeat
LV	Lentivirus
miR30	Micro RNA 30. An endogenous microRNA.
miRNA	Micro RNA
ML	Mucus layer
mRNA	Messenger RNA
MSD	Membrane spanning domain
mWPRE	Mouse Woodchuck Hepatitis Virus post-regulatory element
N	Channel number
Na^+	Sodium ion
NaCl	Sodium chloride
Nash	Anti-ENaCα shRNA
NBD	Nucleotide binding domain
NE	Neutrophil elastase
OAS1	2'-,5'-oligoadenylate synthetase 1
PCL	Periciliary liquid
PEG	Polyethylene glycol
PGK	phospho-glycerate kinase

PHA-1	Pseudohypoaldosteronism-1
PIP_2	Phosphatidylinositol 4,5-bisphosphate
PIP_3	Phosphatidylinositol 3,4,5-triphosphate
PKA	Protein kinase A
PKR	Protein kinase R
P_O	Open probability
R	Regulatory
RNA	Ribonucleic Acid
RNAi	RNA interference
RV	Retrovirus
shRNA	Short hairpin RNA
shRNAmir	shRNA embedded in the miR30 context
siRNA	Small interfering RNA
SIV	Simian immunodeficiency virus
SPLUNC1	Short palate lung and nasal epithelial clone 1
TLR9	Toll-like receptor 9
TM	Transmembrane
UbC	Human polyubiquitin-C promoter
UKCFGTC	UK Cystic Fibrosis Gene Therapy Consortium
VSVG	Vesicular stomatitis virus glycoprotein

Chapter 1: Introduction

1.1 CFTR in Cystic Fibrosis lung disease

Cystic fibrosis (CF) is caused by mutations in the Cystic Fibrosis Transmembrane Conductance Regulator (*CFTR*) gene, which encodes the epithelial chloride channel, CFTR (Riordan et al., 1989). CF affects the mucosal surfaces of the body, including those in the pancreas, reproductive tract and the lungs leading to poor quality of life and varying rates of morbidity and mortality dependent on the specific mutation(s) causing the disease in an individual.

CF is the most common monogenic recessive disorder amongst Caucasians with an incidence of approximately 1 in 2500 live births in the UK (Dodge et al., 1997; Farrell, 2008). Early indicators of the disease can occur as early as birth with some CF newborns exhibiting meconium ileus (MI), which is an obstruction of the intestines caused by thickened first stools (meconium) (Boue et al., 1986; Kerem et al., 1989). Infants often also exhibit poor growth despite adequate calorific intake (failure to thrive) (Giglio et al., 1997). Confirmation of CF disease was initially detected with the sweat chloride test (Gibson and Cooke, 1959), however this test did not detect all forms of CF, therefore, in 1979 a blood spot test was developed for CF screening in newborns, based on raised serum immunoreactive trypsin (IRT, Crossley et al., 1979), which was first used in the 1980s in some NHS hospitals (Crossley et al., 1981). Following the identification of the CFTR gene, a further test was offered to determine whether the child had the F508del mutation. By 2007 all parents were offered the choice to screen their newborns for up to 31 different CF mutations, after which suspected CF newborns were referred for clinical assessment (NHS, 2014). A similar practice is in place in the USA, Australia, New Zealand and France, and has led to a decrease in infant mortality and improved quality of life for CF sufferers by offering early intervention.

1.1.1 Structure, function and activation of CFTR

The CFTR gene was discovered in 1989 and mapped to chromosome 7 (Rommens et al., 1989), leading to extensive research into the CFTR gene and mutations therein. The CFTR gene is 189 kb long with 26 exons and 27 introns producing a 1480 amino acid long polypeptide, consisting of two membrane-spanning domains (MSD-1 and MSD-2), two nucleotide-binding domains (NBD1 and 2) and a regulatory (R) domain with the carboxy (C)- and amino (N)- termini both located intracellularly (Riordan et al., 1989) (Figure 1.1).

CFTR is a member of the ATP-binding cassette (ABC) family of ion transporters and acts as the main chloride (Cl^-) and bicarbonate (HCO_3^-) transporter in epithelial cells. Nascent CFTR (127kDa) is processed primarily in the endoplasmic reticulum (ER) where core glycosylation occurs (131kDa), followed by trafficking to the golgi apparatus where the protein is fully glycosylated resulting in a mature 160kDa protein and transport to the apical plasma membrane (Cebotaru et al., 2008). The mechanism of activation of the channel is dependent upon intracellular cyclic adenosine monophosphate (cAMP) and ATP activation at the R and NBD domains respectively. The cAMP-activated protein kinase A (PKA) activates the CFTR channel by phosphorylation of the R domain (Anderson et al., 1991), an action that stimulates ATPase activity, increasing ATP binding and hydrolysis at the NBDs (Sheppard and Welsh, 1999). ATP hydrolysis at the NBDs is responsible for CFTR channel gating such that an increase in intracellular ATP concentration increases CFTR open probability (P_O) by decreasing the duration of the channel closed state (Winter et al., 1994). Inactivation of the channel is mediated through phosphatase activity at the R domain (Sheppard and Welsh, 1999). The activation of CFTR and gating activity is also highly dependent on intracellular sodium chloride (NaCl) concentration, with a decrease in intracellular NaCl resulting in a lower stable, concentration dependent open probability (P_O), due to an increase in mean closing time (Wu et al., 2001).

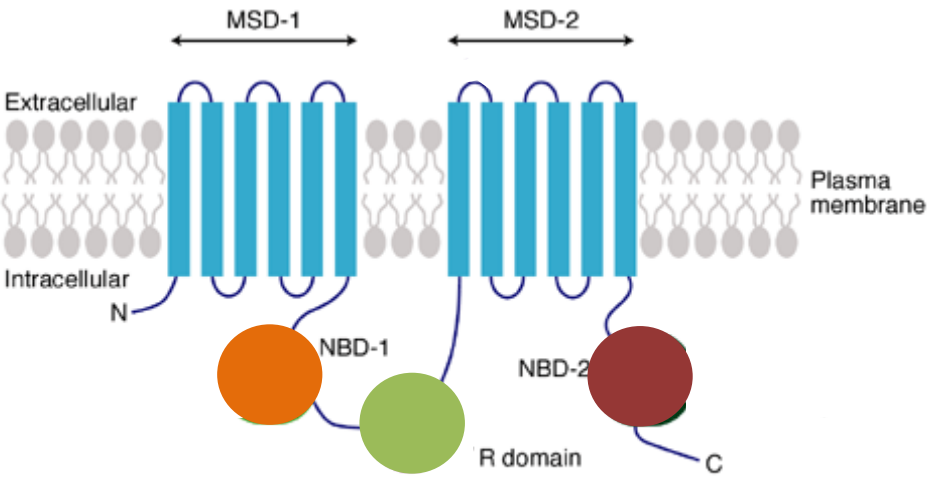

Figure 1.1. Structure of the Cystic Fibrosis Transmembrane Conductance Regulator (CFTR)

The CFTR protein forms a channel in the apical membrane of epithelial cells. The channel consists of two membrane-spanning domains (MSD-1 and MSD-2 indicated in blue) that each contain six intramembrane α helices and form the pore of the channel. These domains are connected via an intracellular loop containing a nucleotide-binding domain (NBD-1; orange) and a regulatory domain (R; green). The carboxy (C)- and amino (N)- termini are also located intracellularly along with a second nucleotide-binding domain (NBD-2; brown) in the C-terminal tail. Phosphorylation of the R domain results in ATPase activity that initiates activation of the channel by increasing ATP binding and hydrolysis at the NBD-1 and NBD-2 domains. Phosphatase activity at the R domain inactivates the channel. Figure amended from Davidson and Dorin (2001).

1.1.2 Mutations in CFTR

Mutations in CFTR can affect the structure, function and activation of the channel; 1977 mutations of CFTR have been identified to date (CF Mutations Database, 2014) and these have been characterised into six classes with increasing levels of functional state (Boyle and De Boeck, 2013): no production of nascent protein due to nonsense mediated decay (Class I; G542X mutation), trafficking defects (Class II; F508del), defective channel gating (Class III; G551D mutation), defective channel conductance (Class IV; R117H mutation), reduced synthesis of nascent protein (Class V; 3849+10kbC→T) and decreased protein stability at the plasma membrane (Class VI; 4326delTC).

Over 90% of patients with CF are at least heterozygous for the F508del mutation which is a class II mutation resulting in abnormal translocation of CFTR to the plasma membrane; normally the Hsp70 protein mediates CFTR processing and is dissociated from CFTR during transport to the golgi (Yang et al., 1993), however F508del-CFTR remains associated with Hsp70 in the ER (Brooks, 1999) blocking its transport to the golgi (Cheng et al., 1990; Gregory et al., 1991) and decreasing surface expression. A small number of CFTR channels succeed in reaching the plasma membrane, however these have a decreased P_O although conductance, anion selectivity ($Br^- > Cl^- > I^-$) and opening kinetics are similar to wild-type. The decreased P_O is due to an increased closing time (Dalemans et al., 1991) suggesting faulty gating; the F508del mutation occurs in NBD-1 close to one of the sites at which NBD-1 and NBD-2 bind to one another via ATP to alter channel conformation and open the channel pore (Huang et al., 2009; Zhou et al., 2006; Lewis et al., 2004). Another common mutation, G551D, is also located within NBD-1 and results in a decreased P_O due to lack of further activation by ATP (Bompadre et al., 2007). Defects in CFTR affect Cl^- transport in organs with large epithelial surfaces such as the lungs, pancreas, liver and reproductive organs.

However, the main cause of morbidity and mortality in CF sufferers is the lung pathophysiology.

1.1.3 Pathophysiology of CF lung disease

Dysfunction of CFTR in CF sufferers causes changes in the composition of luminal fluids, including those in the airways, due to decreased CFTR activity at the apical surface of epithelia (Figure 1.2). The airway surface liquid (ASL) consists of the periciliary liquid (PCL) layer and the mucus layer (ML). The PCL in normal cells is maintained at 6-7μm in height, which is approximately the height of outstretched cilia, allowing full cilia movement that creates the motion for effective mucus clearance (Matsui et al., 1998a). The abnormal fluid composition in the airways produces an environment more susceptible to infection; CF lung disease is characterised by low PCL height, mucus hyperviscosity, reduced mucociliary clearance and increased infections, particularly by *Pseudomonas aeruginosa* and *Burkholderia cepacia* that do not often cause pathogenesis in people without the disease (Lyczak et al., 2002). The chronic infection present in CF lungs leads to increased leukocyte infiltration, further contributing to mucus viscosity via phagocytosis of bacteria and release of extracellular DNA from both the bacteria and leukocytes, which is not sufficiently cleared or degraded: 10.3% of the dry weight of CF sputum (mucus coughed up from the lower airways) is DNA (Chernick and Barbero, 1959). Antibiotic treatments have been successful in decreasing DNA concentration in the sputum and relatively enhancing pulmonary function (Smith et al., 1988). There are three main hypotheses regarding the molecular cause of abnormal mucosal surfaces in CF sufferers: a) the high salt hypothesis; b) the low volume hypothesis; and c) the bicarbonate hypothesis.

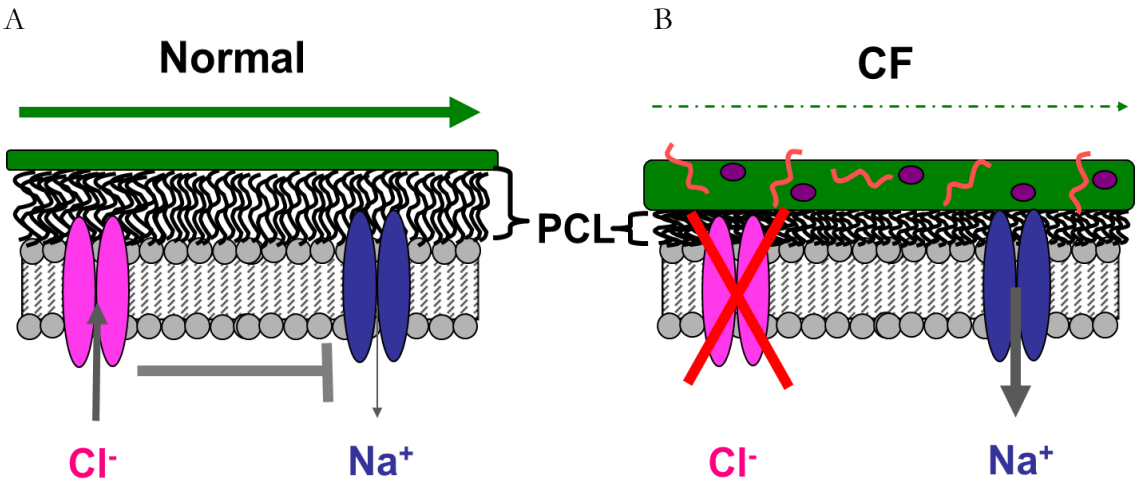

Figure 1.2. CF *versus* non-CF airway epithelia.

In non-CF airway epithelia (A) the PCL is maintained at a height of 6-7μm, the approximate height of fully extended mature cilia, allowing normal cilia beating and mucociliary clearance. In CF airway epithelia (B) the PCL height is decreased, flattening the cilia and reducing cilia beating and mucociliary clearance, leading to a build-up of mucus. ASL dehydration in CF also results in increased mucus viscosity further reducing mucus clearance and providing an environment beneficial for opportunistic pathogen infection and bacterial plaque formation. Neutrophil infiltration followed by respiratory burst releases extracellular DNA that contributes to mucus viscosity.

The high salt hypothesis was first described in 1996, based on experiments in primary cultures of airway epithelial cells grown on permeable filters with the apical surface exposed to the air. Direct application of *Pseudomonas aeruginosa* or *Staphylococcus aureus* colonies to normal cells resulted in fewer or no recovered bacteria after 24 hours, however the same treatment in CF cells grown under the same conditions resulted in a greater number of bacteria being recovered. As these cells were grown in culture the cause of the increased bacterial killing in the normal cells was not due to the contribution of immune or inflammatory cells. Removing the apical fluid from normal cultures resulted in removal of the anti-bacterial properties in the epithelia however the diluted apical fluid removed from normal and CF cells using distilled water successfully killed *P. aeruginosa* cultures. Conversely, apical fluid rinsed from normal and CF cells using a high salt solution (150mM NaCl) failed to kill the bacteria in both cases, suggesting that the cause of the failure to kill bacteria in CF cells was caused by the high salt concentration on CF airway epithelia, rather than any other components present in the apical fluid. Further analysis of the composition of normal and CF ASL suggested that the NaCl concentration in CF cells was greater than in normal cells and was associated with the ability to kill bacteria (Smith et al., 1996). Whilst many groups confirmed this hypertonicity of CF apical fluid (Joris et al., 1993; McShane et al., 2003; Zabner et al., 1998), others argued that there was no difference in NaCl concentration between CF and normal airway cultures and that both conditions tended towards isotonicity (Knowles et al., 1997; Matsui et al., 1998a).

In contrast, the low volume hypothesis argues that the apical fluid in CF cells remains isotonic and that the cause of high mucus viscosity and increased bacterial infection in the airways is a decrease in ASL volume, mainly due to a decrease in PCL height: In CF, lack of the main Cl^- channel, CFTR, leads to hyperabsorption of Na^+ from the ASL, accompanied by water, leading to a decrease in ASL height below the height of the outstretched cilia, causing cilia to collapse thus decreasing mucociliary transport rates (Matsui et al., 1998a; Figure 1.2).

Increased Na^+ absorption in CF epithelia was observed as early as 1986 (Knowles et al., 1986), and the low volume hypothesis has been further investigated in primary human cell culture, where addition of ATP to cultures results in fluid secretion onto the apical surface of normal, but not CF, cultures (Jiang et al., 1993). Matsui and colleagues tested the credibility of the high salt and low volume hypotheses in a study in primary human bronchial epithelial cells grown at the air-liquid interface (ALI; planar), and a hollow fibre culture model (cylindrical). Assays measuring ASL fluid height, mucus transport and Cl^- concentration revealed that most fluid absorption was Na^+ dependent, and that this was the main cause of the decrease in PCL height to less than the height of outstretched cilia (<7μm) in CF cells, which led to decreased cilia motility and mucus transport, all of which occurred under isotonicity (Matsui et al., 1998a; Matsui et al., 1998b). The scientific debate continues, largely based on discussion of the differences in the assays used to collect and measure ASL. The role of the epithelial sodium channel, ENaC, in this process is discussed further in section 1.2.2.

Most recently, the bicarbonate (HCO_3^-) hypothesis has focused on the cause of mucus hyperviscosity in CF. Mucin glycoproteins contribute to the mucus gel in the lumen of hollow organs and are compacted and stored as intracellular granules. Mucins are polyanionic therefore their compaction requires high local concentrations of calcium ions (Ca^{2+}) and hydrogen ions (H^+) that shield their negative charges, allowing compaction by almost 1000x (Perez-Vilar et al., 2005; Verdugo et al., 1987; Espinosa et al., 2002). Under normal conditions mucin granules are secreted and expand within 1-2s of release (Espinosa et al., 2002) via unshielding of the repulsive negative charges through removal of Ca^{2+} and H^+. The role of HCO_3^- in this process is in the sequestration of these cations away from the granule. HCO_3^- is normally secreted onto the apical surface of epithelial cells along with Cl^- via CFTR (Poulsen et al., 1994). However, in CF the decrease in secreted HCO_3^- impairs Ca^{2+} removal, resulting in excessive Ca^{2+} and H^+ in mucus secretions, and limited mucus expansion resulting in mucus hyperviscosity, as evidenced by the increased Ca^{2+} concentration in CF secretions, the inability

of pancreatic granules to disaggregate without HCO_3^- (Freedman and Scheele, 1994) and the decreased rate of mucus expansion in cells with low pH and increased Ca^{2+} concentration (Espinosa et al., 2002). Decreased HCO_3^- transport is also a major indicator of whether a CF patient will suffer pancreatic insufficiency, more so than differences in Cl^- transport (Wine, 2001). More recent data obtained from tracheal explants of wild-type and CF pigs complement the HCO_3^- hypothesis. The CFTR (-/-) pig model was developed by targeted disruption of both *CFTR* genes resulting in lack of CFTR protein expression (Rogers et al., 2008). The resulting offspring developed symptoms typical of Cystic Fibrosis disease observed in humans such as meconium ileus, mucus accumulation, and airway inflammation and infection (Stoltz et al., 2010). A positive correlation between PCL height and mucociliary transport rates was observed in wild-type pigs, whereas in CF pigs greater PCL heights were associated with decreased transport rates, a phenomena that was also observed with inhibition of HCO_3^- transport in wild-type cultures. The authors observed that decreased HCO_3^- concentration could explain why mucociliary transport rates in CF cells were reduced even where there was adequate PCL hydration (Birket et al., 2014). Mucus plugging was also more prevalent in CF airways than non-CF; this is where mucus is partly secreted from submucosal glands but remains tethered to the mucus gland (Hoegger et al., 2014), due to dehydration and inflammation of the cells surrounding the gland.

The recent identification and characterisation of the pH-dependent protein, SPLUNC1, could marry the low volume and bicarbonate hypotheses. Under normal conditions SPLUNC1 inhibits the sodium channel ENaC, however, at the low pH observed in CF ASL (a by-product of decreased HCO_3^- concentration), SPLUNC1 is no longer inhibitory. This is a putative cause of Na^+ hyperabsorption through ENaC (main premise of the low volume hypothesis) that drives dehydration of the PCL (Bingle et al., 2007; Garcia-Caballero et al., 2009; Garland et al., 2013; Tarran and Redinbo, 2014).

1.2 The role of the epithelial sodium channel (ENaC) in CF lung disease

According to the low volume hypothesis (Section 1.1.3) a major cause of CF lung disease is the hyperabsorption of Na^+ from the apical surface of airway epithelial cells, which acts as a driving force for water absorption from the ASL and leads to the airway surface dehydration observed in CF lung disease. The apical Na^+ transporter responsible for Na^+ absorption from the ASL is the epithelial sodium channel, ENaC.

1.2.1 Structure, function and activation of ENaC

ENaC is a multimeric protein formed of three subunits: ENaCα, ENaCβ, and ENaCγ, that are coded for by the genes *SCNN1A* (31kb), located on the short arm of chromosome 12 (Meisler et al., 1994; Drwinga et al., 1993; Dubois and Naylor, 1993) , and *SCNN1B* (103kb) and *SCNN1G* (34kb) located on the short arm of chromosome 16. These subunits are similar in length (α: 669, β: 640, γ: 649 amino acids) and size (α: 76kDa, β: 73kDa, γ: 74kDa) yet share only 30-40% sequence similarity (Canessa et al., 1994b). There is also an ENaCδ subunit, which is expressed predominantly in the brain and has not been observed to form channels in the lung. Northern blot analyses of *ENaC* RNA indicated that large amounts were expressed in the kidney, lung, and colon, with lower amounts in the liver, thyroid and pancreas. Even lower levels were detected in the placenta and brain, and none in heart or skeletal muscle (McDonald et al., 1994; Voilley et al., 1994).

Although the crystal structure of the ENaC channel has not yet been successfully determined, a protein belonging to the ENaC/degenerin family, ASIC1, has had its crystal structure analysed (Jasti et al., 2007). These data confirmed the proposed structure of ENaC from sequence analyses where two α-helices form the membrane-spanning domains (MSD-1 and MSD-2), linked by a large extracellular loop (ECL; >500 residues) and containing short

intracellular hydrophobic C- and N-termini (~10kDa each) (Canessa et al., 1994a). The extracelluar domains form a structure likened to a clenched hand holding a ball (Figure 1.3) with 'palm', 'knuckle', 'thumb' and 'finger' domains surrounding a β-helix 'ball' domain, and the 'wrist' domain controlling channel gating.

ENaC is highly selective for Na^+ (Voilley et al., 1994) and plays an important role in the reabsorption of fluid in the organs in which it is expressed, by using Na^+ as a driving force for the paracellular movement of water across the epithelium (Gaillard et al., 2010). ENaC is inhibited by amiloride, which directly blocks the channel and has been used extensively as an ENaC-specific inhibitor for determining the contribution of ENaC to cell current (McDonald et al., 1994).

ENaCα is the most highly expressed subunit in the lungs, followed by ENaCβ then ENaCγ (Caci et al., 2009). The stoichiometry of subunits in ENaC channels in airway epithelia has been a subject of much controversy: early evidence suggested that the channel formed was a nonamer with a stoichiometry of $\alpha_3\beta_3\gamma_3$ (Snyder et al., 1998), followed by multiple studies suggesting a heterotetrameric formation with a stoichiometry of $\alpha_2\beta_1\gamma_1$ (Wang et al., 2013; Kosari et al., 1998; Firsov et al., 1998), however most recent evidence suggests a heterotrimeric conformation with a stoichiometry of $\alpha_1\beta_1\gamma_1$, with the possibility of trimers-of-trimers formations that could explain the previous observation of nonamers (Kashlan and Kleyman, 2011; Stewart et al., 2011).

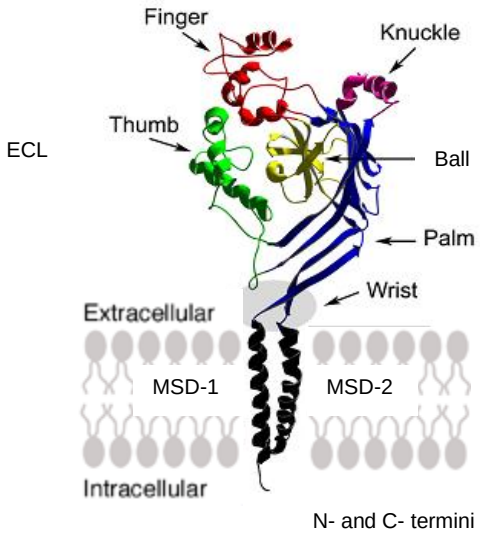

Figure 1.3. The proposed structure of the epithelial sodium channel (ENaC)

Individual ENaC subunits have minimal intracellular domains, two membrane-spanning domains (MSD-1 and MSD-2) and a large extracellular loop (ECL; Duneclift et al., 1997) with a structure described as a hand clenching a ball. The majority of cleavage sites reside in the 'finger' domain, which is important for activation of the channel, and the 'wrist' domain is involved in channel gating (Jasti et al., 2007). Figure amended from Kleyman et al. (2009).

Cell surface expression of ENaC channels relies on *N*-glycosylation of the ECL in ENaCα and ENaCγ (Canessa et al., 1994a) with the delivery of ENaC out of the ER to the apical membrane also requiring all three subunits assembling into a multimeric complex, such that ENaC trafficking out of the ER is limited by the number of subunits available (Yueksekdag et al., 2010; Carattino et al., 2008a), although some groups have shown that ENaCα (Kashlan and Kleyman, 2011), ENaCβ and ENaCγ are also capable of forming homotrimers (Stewart et al., 2011). The activity of ENaC can be mediated extracellularly by cleavage with serine proteases: proteolytic cleavage by furin at two consensus sites in the finger domains of ENaCα and ENaCγ induces an intermediate P_O (Hughey et al., 2004) followed by further cleavage in the finger domain of ENaCγ by prostasin, to result in a high P_O and the fully activated channel (Hughey et al., 2007; Bruns et al., 2007). These cleavage events release inhibitory peptides (Carattino et al., 2008b) that are normally located in the finger domains of ENaCα and ENaCγ, and cause the channel's slow gating kinetics (Voilley et al., 1994). This sets the ENaC channel apart from other members of the ENaC/degenerin superfamily, which are mostly prone to rapid inactivation (Mano and Driscoll, 1999). Control of ENaC activation also occurs via intracellular mediators, such as the anionic lipids PIP_2 and PIP_3 (Ma et al., 2002) and PKA (Stutts et al., 1997).

It is clear that ENaCα and ENaCγ play important roles in channel activation, however what is the role of ENaCβ? This subunit does not contain any consensus cleavage sites (Hughey et al., 2003) but contains more *N*-glycosylation sites in its ECL than any other subunit (13, compared to 6 in ENaCα and 5 in ENaCγ (Canessa et al., 1994a). One role of ENaCβ appears to be inhibition of channel activation, as a premature stop inserted into the C-terminus of ENaCβ results in a 3-fold increase in the amiloride-sensitive Na^+ current when expressed with wild-type ENaCα and ENaCγ in *Xenopus laevis*. This is caused by an increase in ENaC channel activity and in the number of active channels, without any alteration in biophysical or

pharmacological properties (Schild et al., 1995). Truncation of the C-terminus in either ENaCβ or ENaCγ (but not ENaCα) also significantly increased the half-life of the channel from 3.6 hrs to >30 hrs and it is suggested that the C-termini of these two subunits are involved in clathrin-mediated endocytosis and turnover of the ENaC channel (Shimkets et al., 1997). Finally, ENaCβ has been implicated as the limiting factor in ENaC activation since only over-expression of ENaCβ, and not ENaCα or ENaCγ, increased epithelial Na^+ absorption in mice (Mall et al., 2004).

1.2.2 The interaction of CFTR and ENaC in CF lung disease

The maintenance of ASL hydration is thought to be highly dependent on ENaC channel number and P_O. Na^+ is transported into airway epithelial cells (AECs) via ENaC channels expressed on the apical surface of these cells, and is exported from the basolateral surface of AECs via Na^+/K^+-ATPase channels. Cl^- and water follow Na^+ via intracellular and paracellular pathways respectively (Hobbs et al., 2013b). In normal AECs ENaC is thought to be inhibited by CFTR such that the lack of functional CFTR in CF leads to hyperabsorption of Na+ from the apical surface of AECs, via ENaC, leading to dehydration of the ASL and poor mucociliary transport. The consequent build-up of hyperviscous mucus is a major cause of the chronic lung disease associated with CF (Gentzsch et al., 2010; Mall et al., 2004) (Section 1.1.3). The exact mechanism of this interaction is unclear, but CFTR and ENaC regulation could occur through either direct or indirect interaction, or include aspects of both. Mutations in ENaC were observed in patients with CF-like lung disease, but with no CFTR mutations; one of the most common mutations encountered is p.W493R-SCNN1A (ENaCα), a mutation in the thumb domain of ENaCα which results in an increase in the amiloride-sensitive current in the nasal epithelia of patients. Expression of p.W493R-SCNN1A along with wild-type ENaCβ and ENaCγ also led to a 4-fold increase in ENaC activity in *X. laevis* oocytes (Azad et al., 2009; Rauh et al., 2013). Another ENaCα mutation, p.V114I-SCNN1A,

was discovered in a patient with no disease-causing CFTR mutations; this patient presented with elevated Na^+ and Cl^- in sweat tests, subnormal lung function and reduced fertility. This patient was originally diagnosed with CF, but did not suffer from pancreatic insufficiency or chronic inflammation (Mekus et al., 1998). Gain-of-function mutations in ENaC are usually associated with Liddle's disease and occur predominantly in ENaCβ or ENaCγ (Shimkets et al., 1994) where an increase in the ENaC channel number and P_O are observed (Firsov et al., 1996; Snyder et al., 1995). Studies in immortalised (Stutts et al., 1995b) and primary (Boucher et al., 1988) CF cell cultures confirmed Na^+ hyperabsorption in these conditions, and nasal potential difference measurements in CF patients also show an increased amiloride-sensitive current (Boucher et al., 1986).

These studies suggest that ENaC hyperactivation could be a major contributor to CF lung disease. Furthermore, loss-of-function mutations in ENaCα, ENaCβ and ENaCγ cause a condition called pseudohypoalderosteronism-1 (PHA-1) (Chang et al., 1996; Chang and Fujita, 1996) which is characterised by increased ASL volume (Kerem et al., 1999) but no chronic lung disease or progressive decline in lung function (Schaedel et al., 1999) highlighting the role of ENaC channels in ASL hydration.

Direct interaction of CFTR and ENaC has been proposed to play a role in ENaC regulation under normal conditions. Co-expression studies in *X. laevis* oocytes suggest that CFTR protects ENaC from proteolytic cleavage (Gentzsch et al., 2010) and ENaC increases CFTR-mediated Cl^- conductance (Ji et al., 2000; Yan et al., 2004). CFTR and ENaC were also shown to physically interact with one another by co-immunoprecipitation (Gentzsch et al., 2010) and fluorescence resonance energy transfer (FRET) (Berdiev et al., 2007) analyses, although the high density of ENaC channels in motile cilia, where no CFTR channels appear to be expressed (Enuka et al., 2012) suggests that direct inhibition of ENaC by CFTR is not the only mechanism by which CFTR regulates ENaC. As such, indirect regulation of ENaC has also been suggested: increasing the intracellular Cl^- concentration inhibits ENaC and requires

the C-terminus of ENaCβ, further implying that this subunit is important in ENaC channel activation in the airways (Bachhuber et al., 2005; Konig et al., 2001). This effect of Cl^- concentration on ENaC could explain why the presence of apical non-CFTR Cl^- channels in CFTR mutant mice attenuate lung disease in this model (Grubb and Boucher, 1999), and why the ENaCβ-overexpressing mouse exhibits CF-like lung disease whereas the ENaCα- and ENaCγ- overexpressing mice do not (Mall et al., 2004). The CFTR activator cAMP has also been implicated in ENaC activation: when expressed alone cAMP activates ENaC, whereas when CFTR and ENaC are co-expressed cAMP inhibits ENaC activation (Stutts et al., 1995a). Whether the inhibition of ENaC by CFTR is caused by direct or indirect effects there is plenty of evidence that such an interaction exists. The extent of ENaC inhibition is thought to be such that a 2-fold decrease in CFTR results in a 2-fold increase in ENaC activation (Azad et al., 2009) and the absence of degenerative lung disease in people with Liddle's disease (ENaC gain-of-function) further suggests that the presence of CFTR is important for inhibiting ENaC (Hopf et al., 1999; Mall et al., 2010).

SPLUNC1, recently identified as major factor in ENaC regulation, is a pH dependent inhibitor of ENaC (Garland et al., 2013) and is abundant in the ASL, making up 10% of the total soluble proteins therein (Campos et al., 2004). Under normal conditions the ASL is near-neutral pH and SPLUNC1 acts extracellularly on ENaC to prevent proteolysis of the inhibitory domain (Garcia-Caballero et al., 2009) thereby inhibiting ENaC activation. However, in CF airways CFTR-dependent secretion of HCO_3^- is drastically reduced (bicarbonate hypothesis; Section 1.1.3) resulting in a lower HCO_3^- concentration in the ASL and reduction in ASL pH (Coakley et al., 2003), which inactivates SPLUNC1 releasing its inhibitory effect on ENaC (Garland et al., 2013). ENaC is therefore hyperactivated contributing to ASL volume depletion (low volume hypothesis; section 1.1.3).

It has been hypothesised that inhibition or knockdown of ENaC subunits could aid restoration of ASL height and help alleviate CF symptoms in the lung (Li and Folkesson,

2006). The inhalation of amiloride (a potent ENaC inhibitor) has been shown to reduce sputum viscosity and elasticity, increase mucociliary transport rates, and improve cough clearance in patients with CF, with no indication of systemic, respiratory or subjective toxicity (Knowles et al., 1990).

1.3 Treatments for CF lung disease

The prognosis for CF sufferers continues to improve. In 1970 the median life expectancy for someone born with CF was 8 years, but with recent advances in treatments the CF registry predicted a median survival of 36.6 years in the UK in 2013, although the median age at death in the UK was 29±2 years for the same year (CF Trust, 2014). Of the 146 deaths reported from CF in 2013 the age at death ranged from 0 years to 74 years reflecting that different CF-causing mutations have different effects on mortality.

The large epithelial surface area of the human lung makes the treatment of CF lung disease challenging. Current disease management is effective for treating CF in non-lung tissues and include pancreatic-enzyme replacement therapy, dietary counselling, and nutritional education (Ramsey et al., 1992), however the management of CF lung disease has proven more challenging. Current lung disease management for CF sufferers consists of mainly inhaled or oral antibiotics, and anti-inflammatories to reduce the bacterial load and chronic inflammation associated with CF respectively (Knowles et al., 1995b) although anti-inflammatory use is limited due to the potential for nephrotoxicity (Kovesi et al., 1998), and co-administration of antibiotics and anti-inflammatories is not advised due to the lack of toxicity data of this combination of treatments (Touw et al., 1995). Patients are regularly required to undergo longer courses of intravenous antibiotics in hospital following pulmonary exacerbations (Flume et al., 2009). Perhaps the most effective current lung disease management therapy for CF is airway clearance therapy, combined with antibiotics (Bosworth and Nielson, 1997).

Airway clearance therapies include daily physiotherapy to massage the chest and back aiding in airway mucus clearance, and the use of mucolytics that break down mucins thereby decreasing mucus viscosity and improving mucociliary clearance. Physical exercise is also highly effective in increasing mucociliary clearance and many CF patients regularly take part in sports and exercise as part of their disease management strategy.

1.3.1 DNase

One medication used to manage CF lung disease is recombinant human DNase (rhDNase; marketed under Pulmozyme or Dornase-α), Endogenous DNase I is normally present in saliva, urine, pancreatic secretions and blood and is involved in degradation of extracellular DNA released from bacteria and host cells following an immune response. In CF lungs excessive extracellular DNA, due to respiratory burst of neutrophils, is a major contributor to mucus hyperviscosity (Section 1.1.3) and therefore degradation of the DNA component can help make lung mucus easier to clear during physiotherapy. In 1994 rhDNase was licenced for use in the UK and now >50% of CF patients receive the drug in a nebulised format (CF Trust, 2014) one to two times daily with no severe adverse effects (Jones and Wallis, 2010). Use of rhDNase has been linked to a significantly reduced risk of death in CF patients (George et al., 2011) along with improved airway clearance and lung function, and fewer exacerbations (Fuchs et al., 1994; Shah et al., 1995).

1.3.2 Ivacaftor

The global biotechnology company Vertex received European approval of the drug ivacaftor in July 2012. Ivacaftor (developed as VX-770 and manufactured as Kalydeco) is a CFTR potentiator and causes increased CFTR channel activity by increasing the P_O of channels already present at the apical membrane (Van Goor et al., 2009). As such, this drug is most effective in the treatment of patients with class III mutations (Section 1.1.2), such as G551D,

that account for ~6% of patients with CF in the UK (CF Trust, 2014). The current treatment regime involves oral administration once every 12 hours alongside pre-established treatments. This dose led to improvements in the forced expiratory volume in one second (FEV_1), a standard clinical end-point observation for CF clinical trials, and in decreased sweat chloride levels (Accurso et al., 2010). More recently, ivacaftor has also been shown to increase mucociliary clearance, and decrease colonisation of the lungs by *P. aeruginosa* in patients with at least one G551D allele (Rowe et al., 2014). A second small molecule, lumacaftor (VX-809), is currently under investigation as a corrector of the F508del genotype. In cell culture lumacaftor enhances the processing of F508del-CFTR and its delivery to the cell membrane (Van Goor et al., 2009) through stabilisation of the MSD-1 (Loo et al., 2013) leading to improved processing of the mutant CFTR in the ER and enhanced Cl^- secretion to ~14% of that of non-CF cells (Van Goor et al., 2011). In the clinic lumacaftor delivery alone led to a decrease in sweat Cl^- levels but no significant enhancement in lung function, nasal potential difference or patient-related outcomes (Clancy et al., 2012). Recent clinical data involving co-delivery of lumacaftor and ivacaftor has produced more promising results, showing a further decrease in sweat Cl^- levels and a significant increase in FEV_1 compared to placebo (Boyle et al., 2014). Further work is ongoing into combining lumacaftor with other possible CFTR correctors has produced promising results but these combination therapies have yet to be assessed in the clinic (Phuan et al., 2014). Although some of these small molecule CFTR correctors have shown clinical amelioration of CF symptoms, they are taken in combination with already established CF treatments and further work is required to improve the effect of these molecules on CF pathophysiology. Each of these molecules acts to enhance a particular aspect of CFTR trafficking, processing or activation and therefore each treatment would only be effective for certain classes of mutations. Gene therapy, whereby a functional copy of the CFTR gene is delivered to cells, has the potential to correct all CF phenotypes, regardless of the underlying mutation causing the disease.

1.4 Gene therapy for CF lung disease

CF lung disease is a prime candidate disease for gene replacement therapy as CF is monogenic recessive and the lungs are relatively accessible. Most current treatments are geared towards managing the symptoms of lung disease rather than correcting the underlying defect (Section 1.3). Treatments targeting specific mutations, such as those in development by Vertex (Section 1.3.2) have been successful in ameliorating lung dysfunction; however, gene replacement therapy has the potential to treat CF regardless of the specific mutation. .

CF is sometimes described as a disease of the small airways; lung pathology in CF initially presents in the ciliated epithelial cells of the bronchioles (Engelhardt et al., 1994) and in the submucosal glands (Hoegger et al., 2014), therefore targeting these locations is important for the success of CF gene therapy. It is suggested that only 6-10% of cells are required to express CFTR to restore normal Cl^- transport in CF lungs (Johnson et al., 1992), suggesting that gene therapy targeted at the AECs could be achieved with a relatively low level of cell correction. There are two classes of gene therapy which have been investigated in CF patients clinically: non-viral and viral, which are discussed in the following sections. Importantly, the turnover of ciliated airway epithelial cells is thought to be ~17 months in the lungs (Rawlins and Hogan, 2008), and therefore all non-integrating vectors will require repeated administration to treat the chronic effects of CF lung disease.

1.4.1 Non-viral gene therapy

This class of gene therapy is based on synthetic gene transfer agents, without viral protein components. Plasmid DNA (pDNA) can be delivered 'naked' in either PBS, saline or water, with no additional components and has been successful in partially correcting the Cl^- transport defect in nasal epithelia of CF patients (Zabner et al., 1997) and airway epithelial cells in a murine model (Davies et al., 2007). Sequence optimisation has been shown to increase the level and duration of gene expression (Gill et al., 2009; Yew et al., 1997). For

example the use of human endogenous promoter sequences such as human polyubiquitin-C (UbC) or elongation factor-1α (EF-1α) resulted in increased duration of expression, compared with viral promoters, detectable up to 6 months post-delivery (Gill et al., 2001). However naked pDNA is not very efficient and is rapidly degraded by intra- and extra-cellular DNases often inducing an immune response mediated via toll-like receptor 9 (TLR9).

Complexes of pDNA and cationic lipids or polymers are less susceptible to degradation and may offer a more efficient cellular uptake. (Nishikawa and Hashida, 2002). The first non-viral gene therapy clinical trial for CF was performed using DC-Chol/DOPE lipoplexes (cationic lipid-nucleic acid complexes; Felgner et al., 1997) in 1995: delivery of CFTR to the nose with this vector resulted in partial correction of the Cl^- transport defect in CF patients but only for up to 7 days post-delivery (Caplen et al 1995). Repeat administration was well-tolerated and resulted in similar levels of expression to a single dose, but it was postulated that improved efficiency would be required for treating lung disease (Hyde et al., 2000). Lipoplexes containing GL67:DOPE have shown some promise in the lungs, including partial correction of the potential difference (Alton et al., 1999; Ruiz et al., 2001) in the lower airways following aerosol administration. However, lipoplex delivery was associated with mild flu-like symptom for approximately 2 days post-delivery (Ruiz et al., 2001) that were in part attributed to the presence of unmethylated CpG dinucleotides in the DNA sequence via stimulation of the TLR9-mediated immune response (Scheule, 2000). This effect was mainly observed with the lipoplexes and not the GL67A liposomes alone (Chadwick et al., 1997), but was also increased in lipoplexes compared to naked DNA formulations (Freimark et al., 1998). The presence of even a single unmethylated CpG in the pDNA sequence might be sufficient to initiate this immune response, thus removal of all CpGs from the pDNA can result in sustained inflammation-free transgene expression in excess of 56 days following aerosolisation to the mouse lung (Hyde et al., 2008; Bazzani et al., 2011). These data led to the use of CpG-free pDNA in the largest gene therapy trial for CF to date run by the UK Cystic Fibrosis Gene

Therapy Consortium (UKCFGTC; Evaluation of safety and gene expression with a single dose of pGM169 or GL67A administered to the nose and lungs of the individuals with CF. EudraCT reference: 2007-004050-85). Initial Phase I and IIa studies indicated that delivery of pDNA/GL67A lipoplexes expressing CFTR to CF patients by nebulisation can result in partial correction of Cl^- transport defects and is well-tolerated (Davies et al 2011; Alton et al 1999). A Phase IIb multi-dose, double-blind, placebo-controlled study recruiting around 120 subjects was initiated in 2013, where subjects are being administered 12 doses of pDNA/GL67A complexes at 28±5 day intervals (Alton et al., 2014; Alton et al., 2013b). Initial results confirm that repeat administration at these intervals and doses is safe with results due in 2015 (Deborah Gill, personal communication).

Another non-viral therapy showing promise in the clinic is DNA nanoparticles developed by Copernicus: in these studies single plasmid DNA molecules were coated with 30-mer lysine polymers covalently bonded to polyethylene glycol (PEG). These nanoparticles are 18-25mm in diameter allowing their passive diffusion through the nuclear pores (Liu et al., 2003). In a phase I clinical trial DNA nanoparticles were delivered to the nasal epithelium of CF patients resulting in partial correction of the chloride defect in some cases at 3 days post-delivery (Konstan et al., 2004).

Polyethylenimine (PEI; Kopeikin et al., 2014) is another cationic polymer that can bind to pDNA to form a "polyplex" that can enter the cytoplasm via the endocytic pathway. Once inside the cell, PEI mediates endosomal escape by acting as a 'proton sponge' during acidification of the endolysosome, protecting the pDNA from lysosomal degradation (Demeneix et al., 1998). Transgene expression upon delivery of polyplexes was similar to with lipoplexes (Wiseman et al., 2003), although instillation of polyplexes into mouse lungs caused toxicity and was not amenable to repeat administration (Rudolph et al., 2000). Aerosol delivery on the other hand was well tolerated and resulted in high transgene expression for up to 28 days post-delivery (Gautam et al., 2001). Repeat administration via aerosol was also well-

tolerated, however transgene expression decreased with increasing doses (Davies et al., 2012). As little is known about the half-life of PEI toxicity, an accumulation of PEI in the cells could be of concern, therefore until more is known the use of PEI in the clinic is likely to be minimal. Non-viral vectors show great promise in the clinic for the treatment of CF lung disease and research continues into the development of new non-viral vectors, including the refinement of plasmid vector design (reviewed in Pringle et al., 2009).

1.4.2 Viral gene therapy

Recombinant adenoviral vectors were one of the first viral vectors to be evaluated clinically in CF patients. Adenovirus is a non-integrating double stranded DNA virus that mostly infects the upper respiratory tract in humans. Recombinant Adenovirus vectors (rAd) expressing CFTR delivered to human nose and lungs expressed mRNA (Knowles et al., 1995a) and protein (Crystal et al., 1994) with partial correction of Cl^- transport (Hay et al., 1995; Zabner et al., 1993) but evidence of inflammation (Crystal et al., 1994; Knowles et al., 1995a), efficiency was low, and the gene transfer was transient due to lack of integration with these vectors (Harvey et al., 1999; Zuckerman et al., 1999). Attempts at re-administration of rAd vectors produced partial correction of the Cl^- transport defect after the initial dose but showed a decreased effect with subsequent doses possibly due to the initiation of an immune response to the vector, also triggering humoral immunity (Zabner et al., 1996). Relatively high levels of vector-derived mRNA (Harvey et al., 1999) along with a low (<1%) proportion of cells determined positive for CFTR (Zuckerman et al., 1999) suggested that high expression was achieved from only a few transduced cells. Since these early trials, there has been very little interest in further testing Adenoviral vectors for CF, until the development of 'gutless' or helper-dependent Ad vectors (HDAd), which are devoid of all coding viral regions, and require co-transfection with a helper virus that contains the packaging and capsid information, during production. These vectors have been shown to be less immunogenic than the first-

generation rAd vectors (O'Neal et al., 2000) permitting longer term transgene expression (Palmer et al., 2005; reviewed in Alba et al., 2005). Delivery to the liver of nonhuman primates resulted in up to 7 years transgene expression from a single dose, with a decline to 10% of peak expression by this time but still 2-110 fold higher than baseline levels with no long-term adverse effects (Brunetti-Pierri et al., 2013). However, achieving high levels of transgene expression for a longer duration would require vector re-administration, which has been problematic due to the production of neutralising antibodies against the capsid (Dai et al., 1995). This issue could be circumvented by switching the serotype of the HDAd in subsequent administrations (Mastrangeli et al., 1996), however there are limited HDAd capsid proteins that could be used, therefore for the treatment of a chronic disorder, such as CF, where repeated administration would be necessary for the lifetime of a patient, these vectors require further development.

Adeno-associated virus (AAV) is a single-stranded DNA virus that integrates into a specific site on chromosome 19, but does not cause any known disease in humans and only elicits a mild inflammatory response. Recombinant AAV vectors (rAAV) are currently non-integrating and showed greater promise than rAd in CF patients in Phase I and II clinical trials. A single dose of AAV2 delivered to the nose (Wagner et al., 1998; Wagner et al., 1999) and lungs (Aitken et al., 2001; Flotte et al., 2003) resulted in vector-derived DNA detection up to 10 weeks post-delivery with no adverse effects, and transient correction of the chloride transport defect in the nose for up to 2 weeks post-delivery; however vector-derived mRNA could not be detected. Due to the apparent low clinical transduction efficiency of the AAV2 vectors in the lungs, preclinical studies using alternative AAV serotypes, AAV5 and AAV6, have been carried out; these serotypes exhibited increased delivery efficiency to airway epithelial cells (Zabner et al., 2000; Halbert et al., 2001). In particular, AAV6 in combination with a cell-specific promoter resulted in up to 90% transduction efficiency in murine airways (Halbert et al., 2007), but these vectors have not yet been evaluated in the clinic.

A viral vector with high affinity for airways is recombinant murine parainfluenza virus type 1 (or Sendai virus; SeV) (Jain et al., 2001; Griesenbach et al., 2005), a single-stranded RNA virus vector that exhibits 10 – 100 times greater levels of gene transfer in mice and ferrets compared with other viral vectors, transducing terminally differentiated cells in the airway (Yonemitsu et al., 2000). Correction of the Cl^- transport defect in nasal epithelium of CF transgenic mice has also been confirmed but the effects were transient, lasting only a few days and associated with inflammation (Ferrari et al., 2007). More recently rSeV-mediated reporter gene expression was assessed in the ovine lungs (which are the most morphologically similar to human lungs) where high levels of reporter gene expression could be observed after one dose but repeat administration was inefficient, leading to the conclusion that rSeV as a vector to treat chronic disorders, such as CF, that would involve repeat administration, is not currently viable (Griesenbach et al., 2011).

1.4.3 Development of Lentiviral vectors for lung gene transfer

Lentivirus is an integrating, double-stranded RNA virus. Recombinant Lentivirus (rLV) can transduce non-dividing cells and has been developed for CF lung replacement therapy (Mitomo et al., 2010; Stocker et al., 2009). The UKCFGTC and others have also been developing Lentiviral (LV) vectors for CF lung gene replacement therapy, with the aim of long-term expression (Limberis et al., 2002; Mitomo et al., 2010; Stocker et al., 2009). The commonly used third-generation HIV vector system of Trono and Naldini (Dull et al., 1998) was developed in an effort to improve the safety of rLV vectors by introducing a deletion in the 3′ long terminal repeat (LTR): during reverse transcription this deletion is transmitted to the 5′ LTR therefore ablating the ability of the virus to self-replicate within cells. Although there have been no clinical trials of Lentivirus in the lung, subretinal administration is currently under assessment in the clinic in the USA and France (Trial ID: US-1061, US-1085, US-1102, FR-0060), and an EIAV-based vector, ProSavin has shown promise with the first-

in-man *in vivo* delivery of an rLV vector to the striatum of patients with Parkinson'd Disease (Palfi et al., 2014) showing an improvement in motor function up to 12 months post-dosing with no clinically significant adverse effects.

The Human Immunodeficiency Virus (HIV) is a lentivirus that has a natural selectivity for cells of the immune system due to the envelope protein expressed as part of the HIV virion, but to increase the tropism for other target cells, HIV can be pseudotyped with envelope proteins from other viruses. The vesicular stomatitis virus glycoprotein (VSVG) is a commonly-used pseudotype for rLV and permits transduction of lung cells as this coat protein shows very broad cell tropism (Yee et al., 1994a; Yee et al., 1994b; Burns et al., 1994). However, the receptors for VSVG reside only on the basolateral surface of airway epithelial cells (Thomas and Roth, 1994), therefore pre-treatment with lysophosphatidylcholine (LPC) is necessary to allow access to these receptors, by disrupting the tight junctions between epithelial cells. Transgene expression from such vectors can persist for >12 months and >26 days in the mouse nose and human airway cells respectively (Limberis et al., 2002; Stocker et al., 2009), however, this approach might compromise the already delicate CF airway epithelia (Cmielewski et al., 2010). As such, there have been efforts to improve rLV efficiency to the lung focused on developing new pseudotypes to improve the efficiency of lung cell transduction and to avoid the use of tight junction openers or ciliastatic agents, such as lysophosphatidylcholine (LPC).

The UKCFGTC has developed LV vectors pseudotyped with the Sendai Virus (SeV) (Jain et al., 2001) Fusion (F) and hemagglutinin-neuraminidase (HN) envelope proteins, which are highly selective for ciliated airway epithelial cells, without the need for pre-treatment. Expression with this pseudotype was able to persist for the lifetime of mice when delivered to the nose (Mitomo et al., 2010) or lungs (Griesenbach et al., 2012). Importantly, the rLV-FHN vectors mediated increased reporter gene expression upon repeat administration of up to

three doses with no evidence of chronic toxicity. A possible treatment for CF is the delivery of a normal *CFTR* gene to the affected airway epithelial cells.

However, while correction of the CF chloride defect by this approach has been demonstrated in CF mice and CF patients, correction of the Na+ defect has proven more difficult (Alton, 1999, Grubb, 1994).

1.5 RNA interference as a potential therapy for CF lung disease

1.5.1 RNA interference mechanism

RNA interference (Consortium, 2012)(RNAi) refers to forms of gene knockdown initiated by small double-stranded RNA molecules, such as micro RNAs (miRNAs), short hairpin RNAs (shRNAs) and short interfering RNAs (siRNAs) (Meister, 2004). The endogenous RNAi mechanism in mammals consists of miRNAs that are long sections of non-coding RNA with often multiple hairpin structures along their length. Many miRNAs have been identified in humans that are proposed to regulate gene expression via degradation or sequestration of target mRNA (Carthew and Sontheimer, 2009). MiRNAs are usually expressed from RNA polymerase II (Pol II) promoters. The primary transcribed miRNA sequence is known as pri-miRNA and contains a stem-loop structure(s). The stem contains an anti-sense knockdown sequence that is complementary to the target mRNA and directs its knockdown. The pri-miRNA is recognised by the nuclear RNaseIII complex, Drosha, which processes these long pri-miRNAs, often containing multiple knockdown sequences, into pre-miRNAs that contain only the stem and loop portion of the structure (Lee et al., 2003). Pre-miRNA is then rapidly exported from the nucleus via Exportin-5 (Yi et al., 2003; Lund et al., 2004) where the structure is recognised by the dsRNA-specific endonuclease, Dicer, which cleaves the pre-miRNA approximately 20-22 nucleotides from the bottom of the stem (Lund et al., 2004) and

results in a short interfering RNA (siRNA) with a 2bp 3' overhang on both the sense and anti-sense strands. The anti-sense strand is recognised by the RNA-induced silencing complex (RISC) which contains four different subunits that direct and carry out target mRNA degradation. Once bound to the RISC complex the sense strand of the siRNA is released from the duplex by the helicase domain and the loaded RISC is then primed ready to target mRNA for degradation. Homology searching domains in RISC recognise mRNA sequences complementary to the loaded anti-sense strand (Nykanen et al., 2001) and one of two things may occur: the target mRNA is cleaved at a single site in the centre of the siRNA-mRNA duplex by the endonuclease and exonuclease subunits (Elbashir et al., 2001) and the mRNA is subsequently degraded, or the loaded RISC remains bound to the target mRNA preventing its translation via sequestration (Shankar et al., 2005). Whether the target mRNA is degraded or sequestered appears to be dependent on the extent of complementarity between the anti-sense siRNA and the target mRNA: full complementarity results in degradation of the target, whereas even a single mismatch could result in sequestration (Shankar et al., 2005).

The processed siRNA duplex can be chemically synthesised, and is often done so as a 23 nucleotide siRNA including the 3' two nucleotide overhangs, and can be used directly to confer target mRNA knockdown (Dykxhoorn and Lieberman, 2005). These sequences are recognised by the RISC complex, bypassing the Dicer step of the RNAi mechanism and also abolishing the need for delivery to the nucleus (Dykxhoorn et al., 2003). However, simple siRNA sequences such as these are less efficient than siRNAs naturally produced by Dicer (Shankar et al., 2005), do not readily permeate the cell membrane due to their large size and polar surface area, and are rapidly degraded by both intracellular and extracellular nucleases. Chemical modifications, such as cholesterol conjugation of these siRNAs (Lorenz et al., 2004), or delivery using cationic lipids and polymers can enhance the stability and permeability of the sequences (Reviewed in Lee and Sinko, 2006). The use of siRNAs in this context serves only as a method for transient knock down of target gene expression. For RNAi to be used in

the context of disease management and as a therapy therefore would involve repeated administration. Alternatively the siRNA sequences can be expressed from a plasmid allowing the production of a greater number of siRNA molecules due to continued expression from the plasmid that is not subject to cytoplasmic RNA degradation. Combining this technology with integration-competent viral delivery could allow prolonged expression of the knockdown sequence.

There are two main types of sequence that are used to produce plasmid-encoded RNAi sequences (Figure 1.4): short hairpin RNA sequences (shRNAs) or pre-miRNA-like sequences (shRNAmir). The latter consists of the desired siRNA duplex embedded in an endogenous miRNA sequence, replacing the endogenous miRNA (Figure 1.4B). These shRNAmirs are designed to form a stem-loop structure reminiscent of endogenous miRNA to ensure processing via the endogenous RNAi pathway (Figure 1.4C). Multiple shRNA sequences can be inserted into the miRNA context to allow targeting of multiple mRNA sequences, either within the same mRNA target, or in alternative mRNAs as required (Shao et al., 2011; Mueller et al., 2012). The shRNA option involves inserting the stem-loop structure of the required knockdown sequence downstream of an RNA polymerase III (Pol III) promoter bypassing the nuclear Drosha cleavage step in the RNAi pathway. Both methods have been used to knock down target gene expression both *in vitro* and *in vivo* (Reviewed in Ramachandran and Ignacimuthu, 2013).

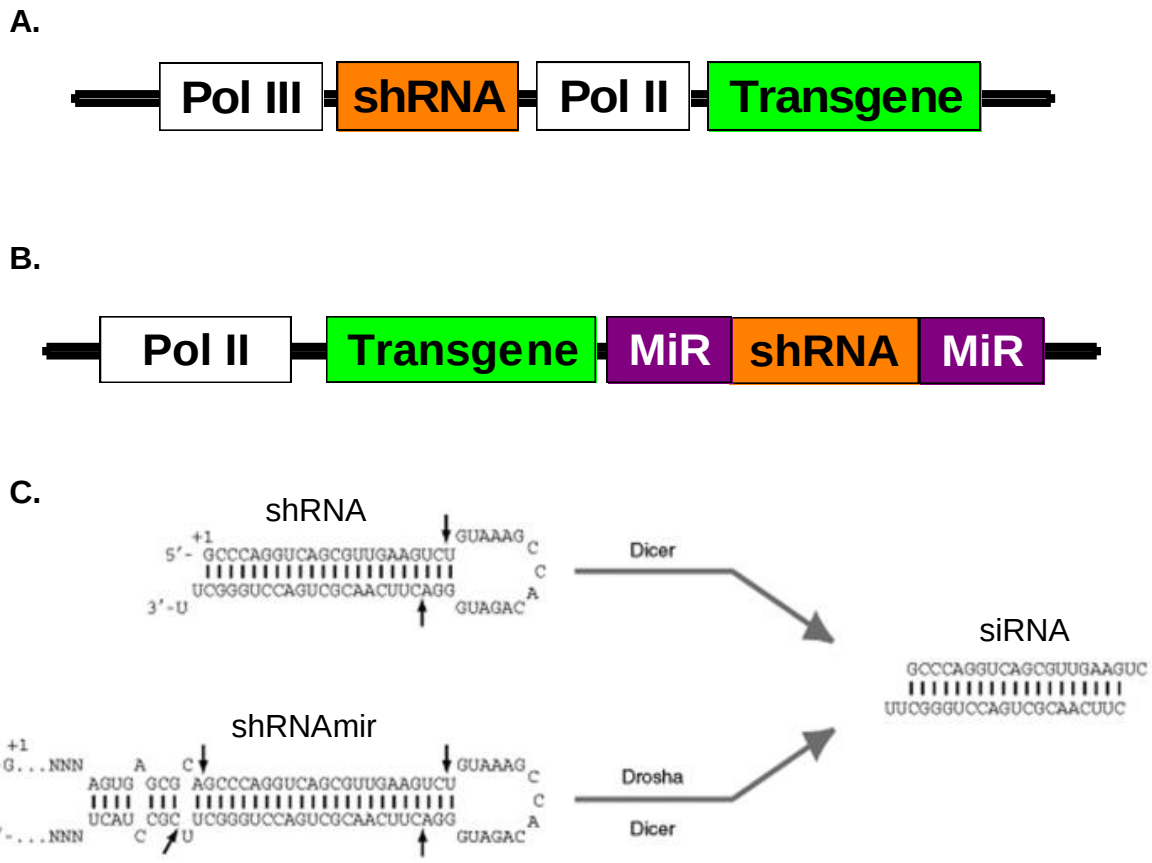

Figure 1.4. Diagram to show the structure of the shRNA and shRNAmir expression cassettes

Short hairpin RNA (shRNA) sequences are placed downstream of a Pol III promoter to allow expression of this small RNA (A). This can be followed by a transgene expressed from a Pol II promoter. shRNAmir sequences are composed of an shRNA flanked by miRNA (miR) contextual sequences, and can be placed downstream of a transgene to produce a bi-cistronic, dual-function construct (B). shRNAs and shRNAmirs are both processed similarly by the RNAi machinery (C): the miRNA context flanking the shRNA in shRNAmirs is cleaved by Drosha in the nucleus to produce a construct similar to the shRNA. These hairpins are then processed by Dicer in the cytoplasm into short double-stranded RNAs similar to short interfering RNAs (siRNAs). One of the strands (referred to as the guide strand) is recruited to the RNA-Induced Silencing Complex (RISC) to target mRNA degradation. Figure C is amended from Boudreau et al. (2009).

1.5.2 Knockdown of ENaC as a treatment for CF lung disease

A possible treatment for CF is the delivery of a normal *CFTR* gene to the affected airway epithelium. However, while correction of the CF chloride defect by this approach has been demonstrated in CF mice and CF patients, correction of the sodium defect has proven more difficult (Alton et al., 1999; Grubb et al., 1994). The use of RNA interference to knock down some, or all, of the ENaC subunits could aid restoration of ASL height and help alleviate CF symptoms in the lung (Tarran et al., 2006). Repeat dosing of wild-type mice with naked anti-ENaCγ siRNA, via nasal perfusion, resulted in significant knockdown of *ENaCγ* mRNA in nasal epithelium (34% knockdown) and lung tissue (62%), which corresponded to ~40% reduction in protein expression in these tissues, and did not induce an inflammatory response (Yueksekdag et al., 2010). Human bronchial epithelial cells grown at the air-liquid interface (ALI cultures) differentiate into pseudostratified layers representing the cell layers observed in airway epithelia *in vivo*. Transfection of ALI cultures with anti-ENaC siRNAs targeting either the α, β, or γ subunit, using Lipofectamine 2000® (L2k) as the gene transfer agent, resulted in 50-65% knockdown of the targeted subunit and a reduction in fluid absorption from the apical surface of the ALI culture (Caci et al., 2009). Delivery to CF mutant ALI cells, of siRNAs targeting both *ENaCα* and *ENaCβ* resulted in a significant increase in ASL height, similar to that observed with a combination of the CFTR potentiators ivacaftor and lumacaftor, suggesting that knockdown of ENaC could have a similar effect on ASL height to expression of CFTR (Gianotti et al., 2013). In this study siRNA targeting *ENaCα* or *ENaCβ* alone did not affect ASL height but did cause a significant reduction in the amiloride-sensitive sodium current. In another study an siRNA targeting *ENaCα* was delivered to primary nasal epithelial cells resulting in significant knockdown of ENaCα that caused a decrease in the amiloride sensitive sodium current, without stimulation of a TLR response to the dsRNA (Clark et al., 2013). In the same study the ENaCα siRNA was delivered to mice intranasally

using a lipid nanoparticle vehicle, resulting in significant knockdown of *ENaCa* in the mouse lung, and no evidence of *OAS1* induction (up-regulated during interferon response causing global degradation of mRNA). The only study so far to evaluate knockdown of ENaC with an rLV vector used a sequence targeting ENaCα: plasmid-encoded anti-ENaCα shRNA was delivered, using an rLV vector, to human bronchial ALI cells resulting in significant knockdown and a decrease in the amiloride-sensitive Na^+ current. Delivery of the same vector to CF mutant ALI cells resulted in a significant decrease in the rate of fluid absorption from the apical surface (Aarbiou et al., 2012).

1.6 Aims

The aim of this study was to construct and evaluate a novel dual-function recombinant lentivirus (rLV) vector, with a modular design to allow insertion of various promoters, transgenes and RNA interference elements. Insertion of sequences to simultaneously mediate ENaCα knockdown and CFTR transgene expression could allow the use of this vector for treatment of CF lung disease.

Chapter 2: Materials and methods

2.1 Chemicals, reagents, solvents and solutions

Chemicals, reagents and solvents were typically of research grade, analytical grade or tissue culture grade. Potable water from the municipal water supply was further purified by reverse-osmosis (Merk Millipore, Watford, UK) to prepare reagent grade (≥10M ohm) or analytical grade (≥18M ohm) quality; or supplied as water for injection (Baxter, Newbury, UK). Solutions of chemicals and reagents were prepared using analytical grade water or water for injection except for electrophoresis solutions which were prepared with reagent grade water. Solution pH was determined using a glass-electrode pH meter (Mettler Toledo, Leicester, UK) and adjusted using concentrated acidic or basic solutions as appropriate for the ionic composition of the solution. Solutions were sterilised by autoclaving or by 0.2μm filtration (Nalgene; Thermo Fisher Scientific, Loughborough, UK). Solutions were typically stored in re-useable glass bottles or single-use polypropylene or polystyrene containers. Reactions were typically performed in single-use polypropylene or polystyrene containers. Reaction temperature control was achieved by the use of temperature controlled heating blocks or water bath. Solutions containing predominantly DNA were typically stored at ≤-20°C. Solutions containing predominantly RNA and viruses were typically stored at ≤-80°C. Other solutions were typically stored at room temperature.

2.2 Construction of novel plasmid DNA molecules

Plasmid DNA molecules were cleaved using New England Biolabs (NEB; Hitchin, UK) restriction enzymes according to the manufacturer's instructions. DNA fragments were typically separated using 0.7% submarine agarose gel electrophoresis, using TAE running buffer incorporating ethidium bromide (Ogden and Adams, 1987). On some occasions where

the DNA fragment size of interest was <1kb, 2% agarose gels were preferred. DNA fragments were purified by excision from agarose gels using the QIAEX II gel extraction kit (Qiagen, Manchester, UK). Ligation of DNA fragments was achieved using T4 DNA Ligase (NEB) according to the manufacturer's instructions. Ligated DNA fragments were transformed into One Shot STBL3 Chemically Competent *E. coli* cells (Life Technologies), Transformed *E. coli* were cultured on LB agar plates containing Ampicillin or Kanamycin (Sigma) as appropriate. Individual *E. coli* colonies were isolated and cultured for DNA extraction in LB liquid media containing the appropriate antibiotic. Plasmid DNA was isolated from small scale (~5ml cultures) using the Wizard Plus SV MiniPrep kit (Promega, Southampton, UK) according to the manufacturer's instructions. Correctly assembled DNA molecules were identified following restriction enzyme digestion and submarine agarose gel electrophoresis. Plasmid DNA was isolated from large scale (200-400ml cultures) using HiSpeed Prep (Qiagen) or Endofree Prep (Qiagen) kits according to the manufacturer's instructions. All plasmids for use in cell culture transfection studies were purified using the Endofree Prep method. DNA sequencing was performed by a commercial DNA sequencing service (Source Biosciences, Oxford, UK) using either custom-designed (synthesised by Sigma) or the widely used M13F and M13R primers. DNA sequence analysis and custom DNA sequencing primer design was performed using MacVector software (MacVector, Cambridge, UK) to confirm successful cloning and ensure the absence of mutations that could be introduced by PCR amplification of fragments.

pGM number	Plasmid short name	Construct description	source	VSV-G vGM	FHN vGM
N/A	N/A	RRLSIN.cPPT.PGK-GFP.WPRE	AddGene	N/A	
pGM279	N/A	RRLSIN.cPPT.PGK-GFP.mWPRE	Anna Lawton	N/A	
pGM290	pHIV.EGFPLux2.NotMod	RRLSIN.cPPT.CMV-EGFPLux2.mWPRE	Ian Pringle	vGM004	vGM035
N/A	pAlmostMod1	RRLSIN.cPPT.EGFP.mWPRE	R. Harding-Smith	N/A	
pGM340	pMod	RRLSIN.cPPT.EGFPLux.mWPRE	R.Harding-Smith	N/A	
pGM341	pHIV.EGFPLux2	RRLSIN.cPPT.CMV-EGFPLux.mWPRE	R.Harding-Smith	vGM029	
pGM342	pEGFPLux2-shmir-6	RRLSIN.cPPT.CMV-EGFPLux.shmir6.mWPRE	R.Harding-Smith	vGM030	
pGM346	pEGFPLux2-shmir-2	RRLSIN.cPPT.CMV-EGFPLux.shmir2.mWPRE	R.Harding-Smith	vGM049	
pGM347	pEGFPLux2-shmir-3	RRLSIN.cPPT.CMV-EGFPLux.shmir3.mWPRE	R.Harding-Smith	vGM050	
pGM348	pEGFPLux2-shmir-4	RRLSIN.cPPT.CMV-EGFPLux.shmir4.mWPRE	R.Harding-Smith	vGM051	
pGM349	pEGFPLux2-shmir-5	RRLSIN.cPPT.CMV-EGFPLux.shmir5.mWPRE	R.Harding-Smith	vGM052	
pGM390	psoCFTR2	RRLSIN.cPPT.CMV-CFTR.mWPRE	R.Harding-Smith	vGM081	
pGM391	pBash3-EGFPLux2	RRLSIN.hU6-Bash3.cPPT.CMV-CFTR.mWPRE	R.Harding-Smith	vGM082	vGM123
pGM392	pNash8-EGFPLux2	RRLSIN.hU6-Nash8.cPPT.CMV-CFTR.mWPRE	R.Harding-Smith	vGM083	
pGM393	pScramble-EGFPLux2	RRLSIN.hU6-non-target-shRNA.cPPT.CMV-CFTR.mWPRE	R.Harding-Smith	vGM084	
pGM394	pBash3-soCFTR2	RRLSIN.hU6-Bash3.cPPT.CMV-CFTR.mWPRE	R.Harding-Smith	vGM085	
pGM395	pNash8-soCFTR2	RRLSIN.hU6-Nash8.cPPT.CMV-CFTR.mWPRE	R.Harding-Smith	vGM086	vGM096
pGM396	pScramble-soCFTR2	RRLSIN.hU6- scrambleshRNA.cPPT.CMV-CFTR.mWPRE	R.Harding-Smith	vGM087	
pGM416	pNash4.EGFPLux	RRLSIN.hU6-Nash4.cPPT.CMV-EGFPLux.mWPRE	R.Harding-Smith	vGM128	
pGM417	pNash4.CFTR	RRLSIN.hU6-Nash4.cPPT.CMV-CFTR.mWPRE	R.Harding-Smith	vGM129	
pGM418	pNash5.EGFPLux	RRLSIN.hU6-Nash5.cPPT.CMV-EGFPLux.mWPRE	R.Harding-Smith	vGM130	
pGM419	pNash5.CFTR	RRLSIN.hU6-Nash5.cPPT.CMV-CFTR.mWPRE	R.Harding-Smith	vGM131	
	pGIPZ-1	GIPZ.CMV-tGFP-Puro-shmir-1	Open Biosystems	vGM060	
	pGIPZ-2	GIPZ.CMV-tGFP-Puro-shmir-2	Open Biosystems	vGM061	
	pGIPZ-3	GIPZ.CMV-tGFP-Puro-shmir-3	Open Biosystems	vGM062	
	pGIPZ-4	GIPZ.CMV-tGFP-Puro-shmir-4	Open Biosystems	vGM064	
	pGIPZ-5	GIPZ.CMV-tGFP-Puro-shmir-5	Open Biosystems	vGM063	

pGIPZ-6	GIPZ.CMV-tGFP-Puro-shmir-6	Open Biosystems	vGM063
pLKO.Bash1	LKO.hU6-Bash1.cPPT.PGK-Puro	Sigma-Aldrich	vGM132
pLKO.Bash2	LKO.hU6-Bash2.cPPT.PGK-Puro	Sigma-Aldrich	vGM133
pLKO.Bash3	LKO.hU6-Bash3.cPPT.PGK-Puro	Sigma-Aldrich	vGM066
pLKO.Bash4	LKO.hU6-Bash4.cPPT.PGK-Puro	Sigma-Aldrich	vGM034
pLKO.Bash5	LKO.hU6-Bash5.cPPT.PGK-Puro	Sigma-Aldrich	vGM035
pLKO-Nash6	LKO.hU6-Nash6.cPPT.PGK-Puro	Sigma-Aldrich	vGM060
pLKO-Nash7	LKO.hU6-Nash7.cPPT.PGK-Puro	Sigma-Aldrich	vGM061
pLKO-Nash8	LKO.hU6-Nash8.cPPT.PGK-Puro	Sigma-Aldrich	vGM062
pLKO-Nash9	LKO.hU6-Nash9.cPPT.PGK-Puro	Sigma-Aldrich	vGM064
pLKO-Nash10	LKO.hU6-Nash10.cPPT.PGK-Puro	Sigma-Aldrich	vGM063
pLKO-Scramble	LKO.hU6-Scramble.cPPT.PGK-Puro	Sigma-Aldrich	vGM070
pLKO-Nash1	LKO.hU6-Nash1.cPPT.PGK-Puro	Open Biosystems	vGM112
pLKO-Nash2	LKO.hU6-Nash2.cPPT.PGK-Puro	Open Biosystems	vGM113
pLKO-Nash3	LKO.hU6-Nash3.cPPT.PGK-Puro	Open Biosystems	vGM114
pLKO-Nash4	LKO.hU6-Nash4.cPPT.PGK-Puro	Open Biosystems	vGM115
pLKO-Nash5	LKO.hU6-Nash5.cPPT.PGK-Puro	Open Biosystems	vGM116

Table 2.1. Plasmid DNA and rLV vector names, suppliers and compositions

vGM: virus gene medicine number; pGM plasmid gene medicine number; hU6: human U6 promoter; Nash: anti-ENaCα shRNA; Bash: anti-BACH1 shRNA; PGK: human phosphoglycerate kinase promoter; CMV: CMV promoter/enhancer; RRLSIN: self-inactivating (mutation in 3'LTR; cPPT: central polypurine tract; Puro: Puromycin resistance; shmir: anti-ENaCα shRNA embedded in the miR30 sequence; mWPRE: mutated Woodchuck Hepatitis Virus regulatory element; GFP: green fluorescent protein; EGFPLux: GFP-luciferase fusion reporter; CFTR: Cystic Fibrosis transmembrane conductance regulator; GIPZ: commercial backbone; tGFP: turbo GFP; VSV-G: Vesicular Stomatitis Virus G protein.

2.2.1 Polymerase Chain Reaction amplification of DNA sequences

Polymerase chain reaction (PCR) DNA primers were designed using MacVector software and synthesised by Sigma. shRNAmir sequences were amplified from the GIPZ plasmid backbone (Sigma; (Silva et al., 2005) using primers GM11-499 and GM11-500 (Table 2.2) to introduce a 5' NotI site and a 3' ApaI site flanking the shRNAmir sequence.

shRNA sequences, including the hU6 promoter sequence, shRNA sequence and cPPT, were amplified from the LKO plasmid backbone (Sigma; (Moffat et al., 2006) using primers GM12-648 and GM12-659 (Table 2.2) to introduce a 5' HpaI site and 3' ClaI/EcoRV sites flanking the shRNA cassette, The PCR conditions were as described in Table 2.3.

Primer name	Forward (F) or reverse (R)	Sequence (5' - 3')	Purpose
GM09-362	F	GGGTCGACAATCAACCTCTGGATTACAAAAT	mutant WPRE
GM09-363	R	GGGGTACCCAGGCGGGGAGGCGGCCCAAAG	
GM10-396	F	CCCTCGAGTCAATATTGGCCATTAGCCATATTATTC	CMVprom/enh
GM10-397	R	CCGGATCCCTGCCCAGTGCCTCACGACCAAC	
GM10-409	F	GGGGATCCACCGGTCGCCACCATGGTGAGCAAG	EGFPLuc fragment
GM10-410	R	GGGTCGACGCGGCCGCTTTACACGGCGATCTTTCCGCCCTT	
GM11-482	F	GGCTCGAGATTTGAGTCCGGCCGGACTTG	EGFPLux2
GM11-483	R	GTCTAGAGCTAGCCACCATGGTGAGCAAGGGCGAG	
GM11-499	F	GGGCGGCCGCTGTTTGAATGAGGCTTCAG	shRNAmir from pGIPZ
GM11-500	R	GGGGGCCCAAAGTGATTTAATTTATACC	
GM12-648	F	GGGTTAACGCCGCCCCCTTCACCGAGGG	shRNA from pLKO.1
GM12-649	R	GGGATATCATCGATTCGAGCCGCGGCCAAAGTGG	

Table 2.2. Primers used to amplify shRNAmir/shRNA sequences

Stage	Temperature (°C)	Time (s)	Cycles
Denaturation	98	30	30
Annealing	47.8	30	30
Extension	72	60	30
Final extension	72	420	1

Table 2.3. PCR conditions for amplification of shRNAmir sequences

shRNA name	Plasmid backbone	Clone ID (The RNAi Consortium)	Gene	Target species	Size (nt)	Mature Sequence (sense): 5'-3': same as mRNA sequence	Mature sequence (antisense): 5' - 3': seed sequence is 2-6 nt from 5' end
shmir-1	pGIPZ	V3LHS_390481	SCNN1A	Human	19	CCCGUCAGCCUCAACAUCA	UGAUGUUGAGGCUGACGGG
shmir-2	pGIPZ	V2LHS_93911	SCNN1A	Human	19	GCUCUUUGACCUGUACAAA	UUUGUACAGGUCAAAGAGC
shmir-3	pGIPZ	V2LHS_93913	SCNN1A	Human	19	CGAUGUAUGGAAACUGCUA	UAGCAGUUUCCAUACAUCG
shmir-4	pGIPZ	V3LHS_390479	SCNN1A	Human	19	UGCUAUACUUUCAAUGACA	UGUCAUUGAAAGUAUAGCA
shmir-5	pGIPZ	V2LHS_93915	SCNN1A	Human	19	GCUGUGCCUACAUCUUCUA	UAGAAGAUGUAGGCACAGC
shmir-6	pGIPZ	V3LHS_413051	SCNN1A	Human	19	AGGAAGUUGCUCCAAGAAC	GUUCUUGGAGCAACUUCCU
Nash1	pLKO.1	TRCN0000069085	SCNN1A	Mouse	21	GCACCCUUAAUCCUUACAGAU	AUCUGUAAGGAUUAAGGGUGC
Nash2	pLKO.1	TRCN0000069084	SCNN1A	Mouse	21	CCCUGCAAUCAGGCGAAUUAU	AUAAUUCGCCUGAUUGCAGGG
Nash3	pLKO.1	TRCN0000069086	SCNN1A	Mouse	21	CGAGAUGCUAUCCUUGCAGAA	UUCUGCAAGGAUAGCAUCUCG
Nash4	pLKO.1	TRCN0000069087	SCNN1A	Mouse	21	CGGAGUUGCUAAACUCAACAU	AUGUUGAGUUUAGCAACUCCG
Nash5	pLKO.1	TRCN0000069083	SCNN1A	Mouse	21	GCUGUAUUAGAUGCUCACAUU	AAUGUGAGCAUCUAAUACAGC
si-ENaCα	GSK ENaCα shRNA	GSK2225745	SCNN1A	Both	19	UGUGCAACCAGAACAAAUC	GAUUUGUUCUGGUUGCACA
Nash6	pLKO.1	TRCN0000044561	SCNN1A	Human	21	CCCGGAAAUUAAAGAGGAGCU	AGCUCCUCUUUAAUUUCCGGG
Nash7	pLKO.1	TRCN0000044558	SCNN1A	Human	21	CCAGAACAAAUCGGACUGCUU	AAGCAGUCCGAUUUGUUCUGG
Nash8	pLKO.1	TRCN0000044559	SCNN1A	Human	21	CGAUGUAUGGAAACUGCUAUA	UAUAGCAGUUUCCAUACAUCG
Nash9	pLKO.1	TRCN0000044562	SCNN1A	Human	21	CGCAGAGCAGAAUGACUUCAU	AUGAAGUCAUUCUGCUCUGCG
Nash10	pLKO.1	TRCN0000044560	SCNN1A	Human	21	GAACAAUUACACCGUCAACAA	UUGUUGACGGUGUAAUUGUUC

Bash1	pLKO.1	TRCN0000013594	BACH1	Human	21	CCUAUGAAUCUUCUGUGCAUA	UAUGCACAGAAGAUUCAUAGG
Bash2	pLKO.1	TRCN0000013596	BACH1	Human	21	CCAGCAAGAAUGCCCAAGAAA	UUUCUUGGGCAUUCUUGCUGG
Bash3	pLKO.1	TRCN0000013597	BACH1	Human	21	GCCCAUAUGCUUGUGUCAUUA	UAAUGACACAAGCAUAUGGGC
Bash4	pLKO.1	TRCN0000013595	BACH1	Human	21	GCUGGAUUGUAUCCAUGAUAU	AUAUCAUGGAUACAAUCCAGC
Bash5	pLKO.1	TRCN0000013593	BACH1	Human	21	CCCUAGAAUCUGGAGAGCUUA	UAAGCUCUCCAGAUUCUAGGG
Bash78	pLKO.1	TRCN0000084278	BACH1	Mouse	21	GCUCCUUCAAAGUCCAGCAUU	AAUGCUGGACUUUGAAGGAGC
Bash79	pLKO.1	TRCN0000084279	BACH1	Mouse	21	GCGUACACAAUAUCGAGGAAU	AUUCCUCGAUAUUGUGUACGC
Bash80	pLKO.1	TRCN0000084280	BACH1	Mouse	21	GCUCGACUGUAUCCAUGACAU	AUGUCAUGGAUACAGUCGAGC
Bash81	pLKO.1	TRCN0000084281	BACH1	Mouse	21	CCUGAAGAGGUAACGGUUAAA	UUUAACCGUUACCUCUUCAGG
Bash82	pLKO.1	TRCN0000084282	BACH1	Mouse	21	GCCCGUAUGCUUGUGUGAUUA	UAAUCACACAAGCAUACGGGC

Table 2.4. Knockdown sequences, target mRNA and clone number

2.3 Maintenance of A549 and M-1 cells

A549 human lung carcinoma cells (ATCC cat. no. CCL-185) were maintained in Ham's F-12K culture media (Life Technologies, Paisley, UK) supplemented with 10% heat-inactivated fetal calf serum (FCS; Sigma, UK). M-1 mouse kidney cells (ATCC product no. CRL-2038) were maintained in DMEM/F-12 (1:1) plus L-Glutamine (Life Technologies,) supplemented with 0.005mM dexamethasone (Sigma, Gillingham, UK) and 5% FCS, according to the manufacturer's instructions. A549 and M-1 cells were cultured in static single-use, gas-permeable, tissue culture flasks (Nalgene) within a 37°C incubator with a humidified 5% CO_2 atmosphere. All cell culture manipulations were performed using aseptic technique within a sterile air laminar flow cabinet.

2.4 Transient transfection of M-1 and A549 cells

To facilitate transient transfection, M-1 and A549 cells were seeded at a density of 1 x 10^5 cells/well in 24-well plates in a volume of 500µl cell culture media. Twenty four hours later, cell culture media was removed and the cells were transiently transfected, typically with three experimental replicates, with either 0.8µM siRNA and 1µl Lipofectamine2000® (Life Technologies) or 0.8µg plasmid DNA and 2.4µl Lipofectamine2000® (1:3 DNA:Lipo ratio) in 100µl Serum-free Opti-MEM media (Life Technologies). Cells were incubated overnight at 37°C/5% CO_2. Sham treatments received Opti-MEM alone. After 24 hours, media was replaced with 500µl cell culture media. Cells were typically harvested 48 hours post-transduction.

2.5 Lentiviral vector production

Lentiviral vectors were generated using four (for VSV-G pseudotype) or five (for F/HN pseudotype) plasmid transient transfection of HEK293T cells. HEK293T cells were grown in suspension, under constant agitation, in serum-free Freestyle media (Life Technologies). Depending on production scale, cells were cultured in single-use 6-well tissue culture dishes (Nalgene), 20-200ml Erlenmeyer flasks (Nalgene) or WAVE Bioreactors (GE Life Sciences, Little Chalfont, UK). Cells were grown in dishes and flasks within a 37°C incubator with a humidified 8% CO_2 atmosphere. Cells grown in WAVE bioreactors were incubated at 37°C and maintained at pH 7.2 by a varying CO_2 atmosphere within the bioreactor headspace. Typically cells were grown to 1-3 x 10^6 cells /ml and transfected with cocktail of plasmid DNA molecules at 1.5μg total DNA per 1x 10^6 cells using Polyethylenimine at an N:P ratio of 15:1. For VSV-G pseudotype production, the four plasmids were used at the following ratios indicate in Table 2.5 (Dull et al., 1998). For F/HN pseudotype production, the five plasmids were used at the ratios indicated in Table 2.6 (Mitomo et al., 2010).

At 24 hours post-transfection, media was replaced with fresh FreeStyle media containing 5 mM sodium butyrate (Sigma). Viral supernatant was harvested 48 (culture dishes/Erlenmeyer flasks) or 72 (WAVE Bioreactors) hours post-transfection and filtered through a 0.45μm polytetrafluoroethylene (PTFE) filter (Nalgene) before aliquoting and storage at -80°C. All WAVE bioreactor lentiviral vector productions were performed by Dr Lee Davies, University of Oxford.

Plasmid 1	Vector genome	as indicated	10
Plasmid 2a	Gag and Pol	pGM281	5
Plasmid 2b	Rev	pRSV-Rev	2.5
Plasmid 3	VSVG (envelope)	pMD2-G	3.5

Table 2.5. Plasmids used and ratio thereof for multi-plasmid transfection into HEK293T suspension cells to produce VSVG-pseudotyped rLV vectors.

Plasmid 1	Vector genome	as indicated	10
Plasmid 2a	Gag and Pol	pGM281	5
Plasmid 2b	Rev	pRSV-Rev	2.5
Plasmid 3a	Sendai F protein	pGM301	3.5
Plasmid 3a	Sendai HN protein	pGM303	3.5

Table 2.6. Plasmids used and ratio thereof for multi-plasmid transfection into HEK293T suspension cells to produce FHN-pseudotyped rLV vectors.

2.6 Lentiviral vector purification/concentration

Lentiviral vectors produced in WAVE bioreactors were purified/concentrated using an unpublished in-house process involving anion-exchange membrane chromatography and tangential-flow ultrafiltration/diafiltration. Viral vectors were concentrated x500-1000 fold by this approach and formulated in FreeStyle media before aliquoting and storage at-80°C. All such studies were performed by Dr Lee Davies, University of Oxford.

2.7 Determination of Lentiviral titre

2.7.1 Viral particle titre (VP/ml)

Physical lentiviral particle titre (VP/ml) was determined by quantitative reverse transcriptase PCR (qRT-PCR), assuming each intact lentiviral particle contains 2 copies of viral RNA. Viral RNA was extracted from virus supernatants using the QiaAMP viral RNA mini kit (Qiagen) according to the manufacturer's instructions. Complete DNA removal from viral RNA preparations was ensured by incubation with an excess of DNase (Ambion DNA-free kit; Life Technologies), during viral RNA extraction. Viral RNA copy number was determined using TaqMan real-time qRT-PCR instrumentation and reagents (Life Technologies). For lentiviral vectors containing Woodchuck Hepatitis Virus post-regulatory element (WPRE) sequences, viral RNA copy number was determined using the WPRE primer and TaqMan probe set (Table 2.4) and a standard curve of WPRE RNA molecules prepared by *in vitro* transcription (a kind gift of Dr Stephanie Sumner-Jones). For lentiviral vectors lacking WPRE sequences, viral RNA copy number was determined using the HIVbb primer and TaqMan probe set (Table 2.7) and a standard curve of DNA molecules containing the HIV Psi sequence.

2.7.2 Functional titre (FTU/ml)

Functional lentiviral particle titre (FTU/ml) was determined for certain viral vectors using an assay that was dependent upon expression of an EGFP containing transgene. For such vectors, viral titre was determined following transduction of HEK293F suspension cells (Life Technologies), grown as described for HEK293T cells above, with viral suspensions diluted (x2 or x5 fold dilution series) in FreeStyle media in the presence of 8μg/ml polybrene. Cells were harvested 72 hours post-transduction, stained with LIVE/DEAD® stain (Life Technologies), fixed in 20% paraformaldehyde, before storage in FACS buffer (10% (w/v) bovine serum albumin (BSA; Sigma, UK) and 10mM Ethylene diamine tetraacetic acid (EDTA; Sigma, UK) in PBS) at 4°C prior to FACS analysis using a FACSCaliber flow cytometer (BD Biosciences, Oxford, UK). Cells were counted by FACS with gating of cells negative for LIVE/DEAD stain and subsequent gating for cells positive for EGFP fluorescence. Numbers of EGFP positive and negative cells were determined using CellQuest Pro software (BD Biosciences). Functional transducing units per ml of virus supernatant (FTU/ml) were calculated as the mean of those viral dilutions that produced between 0.1% and 20% of EGFP positive cells.

2.7.3 Functional titre (TTU/ml)

As an alternative to the FTU/ml functional titre method presented in Section 2.7.2, the functional titre of certain viral vector preparations was determined by an assay that was dependent upon the genomic integration of WPRE DNA sequences. For this approach, functional viral titre (TTU/ml) was determined following transduction of HEK293F suspension cells with viral suspensions diluted (x2 or x5 fold dilution series) in FreeStyle media in the presence of 8μg/ml polybrene. Cells were harvested 72 hours post-transduction and genomic DNA prepared using the QIAamp DNA mini kit (Qiagen). WPRE copy number was determined using TaqMan real-time qPCR instrumentation and reagents (Life

Technologies), the WPRE primer and TaqMan probe set (Table 2.4); and, a standard curve of WPRE containing plasmid DNA molecules. Functional transducing units per ml of virus supernatant (TTU/ml) were determined from the slope of a linear regression curve generated from the dilution series using Prism software (GraphPad La Jolla, CA, USA).

2.8 Transduction of A549 and M-1 cells

To facilitate viral vector transduction, M-1 and A549 cells were seeded at a density of either 1 x 10^5 cells/well in 24-well plates in a volume of 500µl cell culture media, or 2 x 10^5 cells/well in 12-well plates in a volume of 1ml cell culture media. Twenty four hours later, cell culture media was removed and the cells were transiently transduced in the presence of 8µg/ml polybrene, to enhance viral transduction (Davis et al., 2002), with the viral dose stated in the text. Cells were subsequently incubated at 37°C/5% CO_2. After 24 hours, media was replaced with the appropriate volume of cell culture media except where explicitly stated. Cells were harvested 72 hours post-transduction unless otherwise stated.

2.9 Gene expression analyses

2.9.1 Quantification of mRNA levels by relative expression qRT-PCR

Total cellular RNA was extracted from cells grown *in vitro* using the RNeasy® kit (Qiagen), according to the manufacturer's instructions. Complete DNA removal from total RNA preparations was ensured by incubation with an excess of DNase (Life Technologies), during RNA extraction. Total RNA yield was determined using the Quant-IT Ribogreen® assay kit (Life Technologies) according to the manufacturer's instructions. Messenger RNA (mRNA) copy number was determined using two-step TaqMan real-time qRT-PCR instrumentation and reagents (Life Technologies). Primers and TaqMan probes for target mRNA quantification are detailed in Table 2.7. Where target mRNA levels were to be determined

using the relative expression approach, the comparative $\Delta\Delta C_T$ method (Schmittgen and Livak, 2008) was adopted. Three independent replicates were carried out for each RNA sample for both the target mRNA (typically ENaCα, HMOX or Bach1) and a normalising mRNA (typically GAPDH). Cycle thresholds (Ct) values were determined for both target and normalising mRNA and the difference between these values was used to calculate an RNA sample ΔCt value ($\Delta Ct = Ct_{normalising\ mRNA} - Ct_{,target\ mRNA\alpha}$). One RNA sample, typically an experimental sample that was mock or sham treated control or alternatively a sample treated with an irrelevant or scrambled RNAi molecule was defined as the comparator. The difference in ΔCt values between the comparator and all remaining RNA samples was determined to calculate ΔΔCt values ($\Delta\Delta Ct = \Delta Ct_{comparator} - \Delta Ct_{,RNA\ Sample}$). Mean ΔΔCt values for each RNA sample were calculated from the three replicates and transformed into relative expression values using the formulae relative expression = $2^{-\Delta\Delta Ct}$ (Schmittgen and Livak, 2008). Using this approach, the relative expression of the target mRNA for the comparator RNA sample was deemed to be 1, and the relative expression of the target mRNA in each of the other RNA samples in a given experiment were expressed relative to this value. Copy DNA (cDNA) synthesis reactions (10µl final volume) included 10ng of total RNA and were primed with 400 nM reverse primer (Table 2.7). qPCR reactions (10µl final volume) included 300 nM forward and reverse primer and 100 nM TaqMan probe (Table 2.7). All RNA samples were analysed with and without reverse transcriptase in the cDNA synthesis step to control for the possible contribution of contaminating DNA to the calculated relative expression value. Where possible, samples containing the target mRNA and samples containing no RNA input were analysed in parallel as positive and negative controls. Ct values were determined using SDS software (Life Technologies).

Target	RPS/DPS	Primer (F/R) or probe (P)	Primer/probe sequence (5'-3')	Detector-quencher
hENaCα mRNA	hENaCα-B	F	ACATCCCAGGAATGGGTCTTC	
		R	ACTTTGGCCACTCCATTTCTCT	
		P	TGCTATCGCGACAGAACAATTACACCGTC	FAM-TAMRA
h/mGAPDH mRNA	GSK-GAP-D	F	CAAGGTCATCCATGACAACTTTG	
		R	GGGCCATCCACAGTCTTCTG	
		P	ACCACAGTCCATGCCATCACTGCCA	VIC-TAMRA
hBACH1 mRNA	hBach1-A	F	TGTGCGATGTCACCATCTTTG	
		R	CTTGAGTGGAAGTAACTGCTGC	
		P	ACAGCGGTTCCGCGCTCACC	FAM-TAMRA
hHMOX1 mRNA	hHmox1-A	F	AGGGAAGCCCCCACTCAAC	
		R	ACTGTCGCCACCAGAAAGCT	
		P	CCGCTCCCAGGCTCCGCTTC	FAM-TAMRA
mENaCα mRNA	mENaCα-A	F	GACCTCCATCAGTATGAGAAAGGAA	
		R	GACATCGCTGCCATTCTCAGT	
		P	CCTGGACAGCCTCGGAGGCAACTA	FAM-TAMRA
mBACH1 mRNA	mBach1-A	F	GCCAAAGGCTTCTGGAGTGA	
		R	GTGGGCGACAACTGCATTT	
		P	ATTTGCAGCACGGACTCGCCTTG	VIC-TAMRA
mHMOX1 mRNA	mHmox1-A	F	CCTCACTGGCAGGAAATCATC	
		R	CCTCGTGGAGACGCTTTACATA	
		P	CTTGCACGCCAGCCACACAGC	VIC-TAMRA
WPRE v/mRNA & DNA	WPRE-B	F	TGGCGTGGTGTGCACTGT	
		R	CCCGGAAAGGAGCTGACA	
		P	TTGCTGACGCAACCCCCACTGG	FAM-TAMRA
HIVbb-B v/mRNA	HIVbb-B	F	GGAAGCTTTAGACAAGATAGAGGAAGA	
		R	CTTCTCCAATTGTCCCTCATATCTC	
		P	CAAAACAAAAGTAAGACCACCGCACAGCA	VIC-TAMRA

Table 2.7. Primers and probes used in TaqMan RT-PCR and qRT-PCR analyses

2.9.2 Quantification of mRNA levels by absolute qRT-PCR

As an alternative to quantification of mRNA levels by the ΔΔCt relative expression method described in Section 2.9.1, certain mRNA quantification studies utilised an absolute qRT-PCR approach. This approach was only possible where known concentrations of RNA molecules containing the target mRNA were available to act as a standard curve. This approach was utilised to quantify levels of viral vector-derived mRNA that contained WPRE sequences. Total RNA purification and determination of yield was as described in Section 2.9.1. Quantification of WPRE containing mRNA was as described in Section 2.7.1. mRNA levels were expressed as WPRE copy number per ng of total RNA (c/ng).

2.9.3 Quantification of transgene expression by fluorescence-activated cell sorting (FACS)

Functional transgene expression from vectors directing the expression of EGFP containing transgenes was determined by FACS analysis essentially as described in Section 2.7.2. Transduction efficiency was determined as the percentage of live cells expressing EGFP above the level of background fluorescence from untransduced (sham treatment) cells.

2.9.4 Detection of protein expression by immunoblotting

Immunoblotting was used to detect ENaCα protein using an anti-ENaCα monoclonal IgG1 antibody (kind gift of GSK) generated using a peptide corresponding to amino acids 49 – 64 of hENaCα (Ac-LIEFHRSYRELFEFFC-amide).

Transduced wells from duplicate treatments were pooled before lysis with RIPA containing protease inhibitor. Subsequent shearing using a 21G needle was used to further break up the cells and DNA retaining the intact proteins. Insoluble material was removed by centrifugation and the total protein remaining in the supernatant quantified using the Bio-rad D_C protein

assay. 15μg of total protein from each extract was diluted 1:1 with Laemmli sample buffer, incubated at 37°C for 5 minutes and loaded into a 7% Tris-HCL gel for SDS-PAGE separation. Proteins were then transferred to either a polyvinylidene fluoride (PVDF) membrane. Membranes were washed using either TBST and non-specific binding sites blocked using buffer containing 5% skimmed milk powder. Blots were then incubated with primary anti-hCFTR mouse monoclonal IgG_1 antibody (1:500 Anti-CFTR, clone M3A7, Millipore, UK) or anti-ENaCα monoclonal IgG_1 antibody (1:500; kind gift of GSK, see above) in buffer with 5% skimmed milk powder. Primary antibody was detected by incubation with a 1:10,000 dilution of either secondary goat anti-mouse, or goat anti-rabbit HRP-conjugated antibodies as with 5% skimmed milk. Protein bands were detected by addition of ECL Western blot reagent followed by exposure of the blot to photographic paper.

For detection of Hsp90 the goat polyclonal HSP90α/β(N-17) primary antibody was used (sc-1055, Santa-Cruz Biotechnology) at a dilution of 1:1000, followed by incubation with a rabbit anti-goat HRP-conjugated antibody at a dilution of 1:2000.

Densitometry was carried out by scanning the immunoblot images and saving with a .tiff format. These images were imported into the ImageJ software and the density of each band detected following subtraction of background levels. The density of each band was determined relative to the chosen control band (indicated in the text for each immunoblot) and normalised to HSP90 expression.

2.10 CFTR Iodide efflux assay

The activity of CFTR protein produced following *in vitro* transfection with pNash8-soCFTR2 and pScramble-soCFTR2 plasmids was determined using an iodide efflux assay (Griesenbach et al., 2008). In brief, HEK293T cells were transfected with pNash8-soCFTR2, pScramble-soCFTR2, pCIKCFTR (positive control expressing functional CFTR; (Rose et al., 2002)) or

pCIK NLS β-Gal (negative control expressing β-Gal; (Gill et al., 2001)) using Lipofectamine2000®. At 24 hours post-transfection, transfection reagents were removed and replaced with cell culture media. At 48 hours post-transfection cells were initially bathed in efflux buffer and Iodide^{125}, subsequently the bathing solution was replaced at 1 minute intervals for 3 minutes with efflux buffer lacking Iodide^{125}. Subsequently, the bathing solution was replaced at 1 minute intervals for 7 minutes with efflux buffer containing forskolin and IBMX to stimulate CFTR activity. Iodide permeability is selectively enhanced by CFTR and thus an increase in I^{125} permeability is indicative of CFTR activity. Two separate experiments of six wells of a six-well dish were performed for each condition. All such studies were performed by Mario Chan, Imperial College, London.

2.11 Primary human air-liquid interface (ALI) cultures

2.11.1 Maintenance of ALI cultures

Fully differentiated human bronchial epithelial cells grown at the air-liquid interface on 6.5mm diameter Transwell supports (ALIs) were obtained from Epithelix Sàrl (Genève, Switzerland). The ALIs were maintained according to the manufacturer's instructions. Briefly, ALIs were supplied with MucilAir cell culture media (Epithelix Sàrl) bathing both apical and basolateral surfaces. Upon receipt, ALI Transwells were placed at 37°C within standard 24-well plates with 500µl MucilAir cell culture media bathing the basolateral surface and a humidified 5% CO_2 atmosphere exposed to the apical surface. Within a few days, rapidly beating cilia movement was discernible on the apical surface. Basolateral media was replaced every 3-4 days. The apical surface was periodically rinsed with 100µl MucilAir cell culture media to remove visible accumulations of mucus.

2.11.2 Normal dosing of ALI cultures

To facilitate transduction of ALI cultures with lentiviral vectors, the apical surface was briefly rinsed with 200µl PBS. Subsequently, 100µl of viral vector suspension in FreeStyle media was added directly to the apical surface. Where indicated, the viral vector suspension contained 10mM ethylene glycol tetraacetic acid (EGTA), pH 8.0. After 4 hours at 37°C in a humidified 5% CO_2 atmosphere, the virus suspension was removed and the apical surface re-exposed to the humidified 5% CO_2 atmosphere.

2.11.3 Interval dosing of ALI cultures

ALI cells were transduced with 10µl of virus at hourly intervals as indicated in Figure 6.10 with a 200µl PBS pre-wash between doses. The dose for each 10µl aliquot was determined in order to minimise over-crowding of the virus particles on the ALI filter insert and was estimated as follows: The diameter of a HIV particle is approximately 150nm, therefore the maximum number of viral particles that could fit snuggly onto the ALI surface (6.5mm diameter/33.183mm^2 area) would be 1.87 x 10^9 VP, which is equivalent to 5.3 x 10^6 TTU per ALI. As these calculations only provide an estimate, approximately half the number of viral particles was used (9 x 10^8 VP/2.5 x 10^6 TTU) per 10µl aliquot to ensure that overcrowding was not occurring. Therefore the 5 x 10^7 TTU dose was divided into twenty 2.5 x 10^6 TTU aliquots.

2.11.4 Bioluminescence imaging (BLI) of ALI cultures

100µl of D-Luciferin was added to the apical surface of cells for 20 minutes before detection of bioluminescence (BLI) using the IVIS *in vivo* imaging system (Perkin-Elmer). A region of interest (ROI) was determined for each ALI encompassing the entire well, and was kept the same size for all BLI measurements. The average radiance (p/s/cm^2/sr) was determined by

normalising values to the sham-treated controls. After BLI, the luciferin was removed and cells were washed three times to remove any residual luciferin.

2.12 Statistics

Statistical analysis was performed using Analysis of Variance (ANOVA), followed by Tukey's Post-Hoc test unless otherwise stated. For statistical analysis of FACS data (% GFP positive cells, Cell viability) and other percentage-based data, data were transformed using the arcsin function prior to ANOVA. For correlation statistics, Pearson's Correlation Co-efficient was calculated.

All statistical analyses were performed using Graphpad Prism 6, version 6.03.

Chapter 3: Design and construction of a modular recombinant Lentiviral (rLV) vector for dual-function therapy

3.1 Introduction

Dual-function vectors have the potential to deliver simultaneous transgene expression and target gene knockdown. Vectors with capacity for RNA knockdown that can also express cell selection marker genes are available (e.g. pGIPZ and pLKO.1 lentiviral vector systems; Section 2.2), but none have been reported that enable simple replacement and testing of different promoters, therapeutic transgenes and RNA interference (RNAi) elements. Such a vector would be a useful tool for analysing different combinations of gene expression elements and would be a versatile platform upon which to test dual-function therapies for multiple diseases. Creation of a modular dual-function vector in a recombinant lentiviral (rLV) system provides versatility, and potential tissue specificity through pseudotyping with alternative viral coat proteins (Section 1.4.3).

In this chapter, the design and construction of an rLV genome plasmid with a modular structure is described. The aim was to support the straightforward insertion of a variety of gene expression modules, including promoter, transgene and RNAi elements, with only minimal intermediate sub-cloning steps. This modular genome plasmid was then used to produce third generation rLV vectors which were then shown to be capable of transducing both human and mouse cell lines.

3.2 Results

3.2.1 Design and construction of a modular recombinant lentivirus (rLV) genome plasmid (pMod)

The modular rLV genome plasmid design was based on the Addgene plasmid pRRLSIN.cPPT.PGK-GFP.WPRE vector genome plasmid (Dull et al., 1998; Zufferey et al., 1999) shown in Figure 3.1 (Table 2.1). This plasmid is compatible with third generation rLV production (Section 2.5) and the resultant virus has produced robust levels of reporter gene expression both in cell culture and *in vivo* (Zufferey et al., 1998).

A modular rLV plasmid (named pMod or pGM340; Table 2.1, Figure 3.2C), was designed based on pRRLSIN.cPPT.PGK-GFP.WPRE (Figure 3.2A) to allow simple insertion of transgenes, transgene promoter/enhancers, and shRNA/shRNAmir elements into the genome plasmid (Table 3.1; Figure 3.2B). Other modifications included in the design were: (i) replacement of the Woodchuck Hepatitis Virus post-regulatory element (WPRE) with a mutant WPRE (mWPRE) to decrease the probability of trans-activation (Section 3.2.1.1; Schambach et al., 2006) (ii) mutation of the NotI site in the partial gag region to leave a unique NotI site for transgene module insertion (Section 3.2.1.2); (iii) replacement of the GFP transgene with an enhanced GFP-Luciferase fusion transgene (EGFPLux2; Section 3.2.1.3) to allow detection of the reporter gene using both fluorescence and luminescence; and (iv) replacement of the PGK promoter with a cytomegalovirus enhancer element (CMVenh) that is flanked by restrictions sites that will allow replacement of this module with promoters in our library (Section 3.2.1.2; Table 3.1; Figure 3.2C).

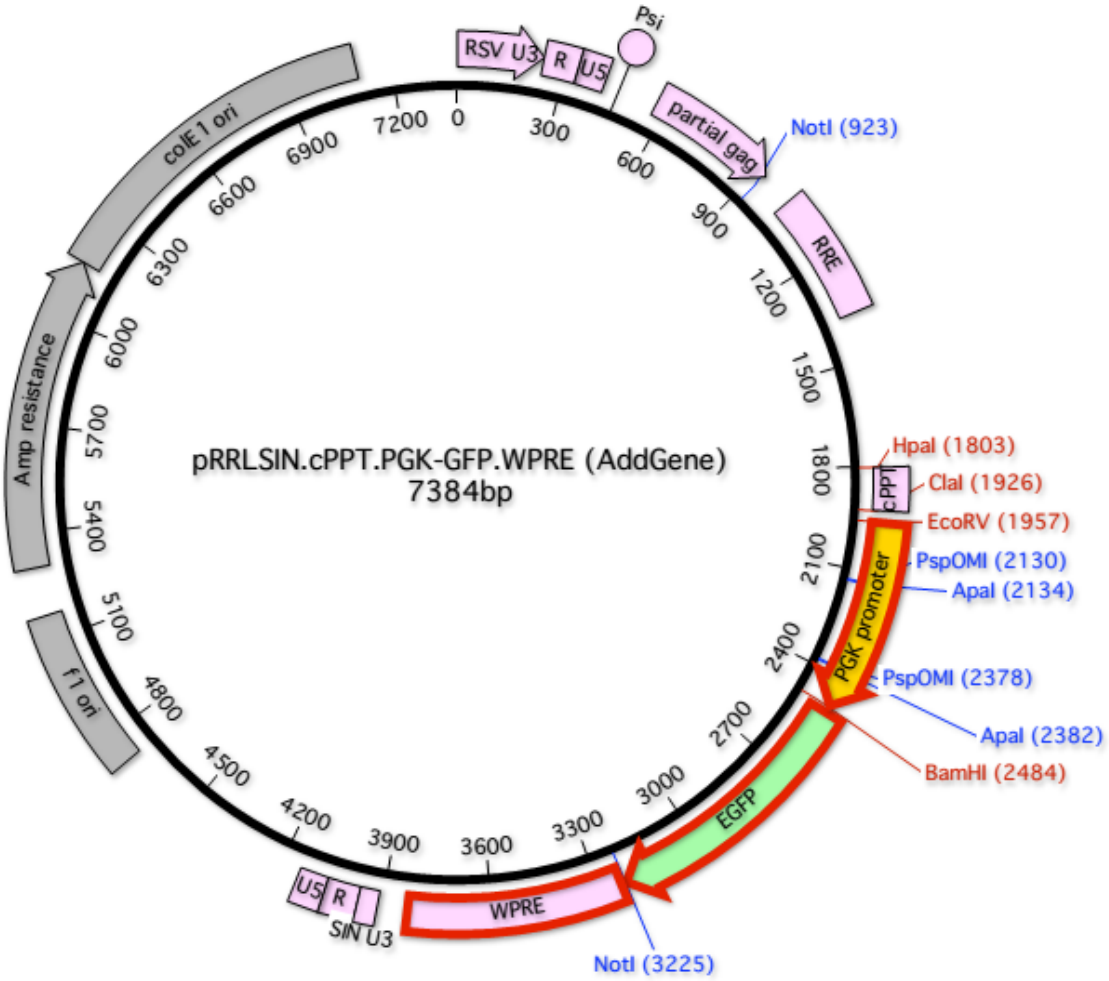

Figure 3.1 Map of plasmid pRRLSIN.cPPT.PGK-GFP.WPRE and design of the modular rLV

The pRRLSIN.cPPT.PGK-GFP.WPRE vector genome plasmid (Dull et al., 1998) is suitable for use in third generation rLV production. This plasmid contains features to allow amplification of the plasmid in bacterial cell culture (grey), and a HIV-based viral genome containing a 3' self-inactivating long-terminal repeat (SIN U3) to prevent propagation of virus within the host, a central polypurine tract (cPPT) to enhance nuclear import and integration, and the Woodchuck Hepatitis Virus post-regulatory element (WPRE) to enhance nuclear export of transgene mRNA (Zufferey et al., 1999). Also included are the green fluorescent protein (GFP) reporter transgene (light green) and human phosphoglycerate kinase (PGK) promoter (orange). Restriction sites are shown with their location in parentheses (Blue font indicates two cut sites, red font indicates one cut site).

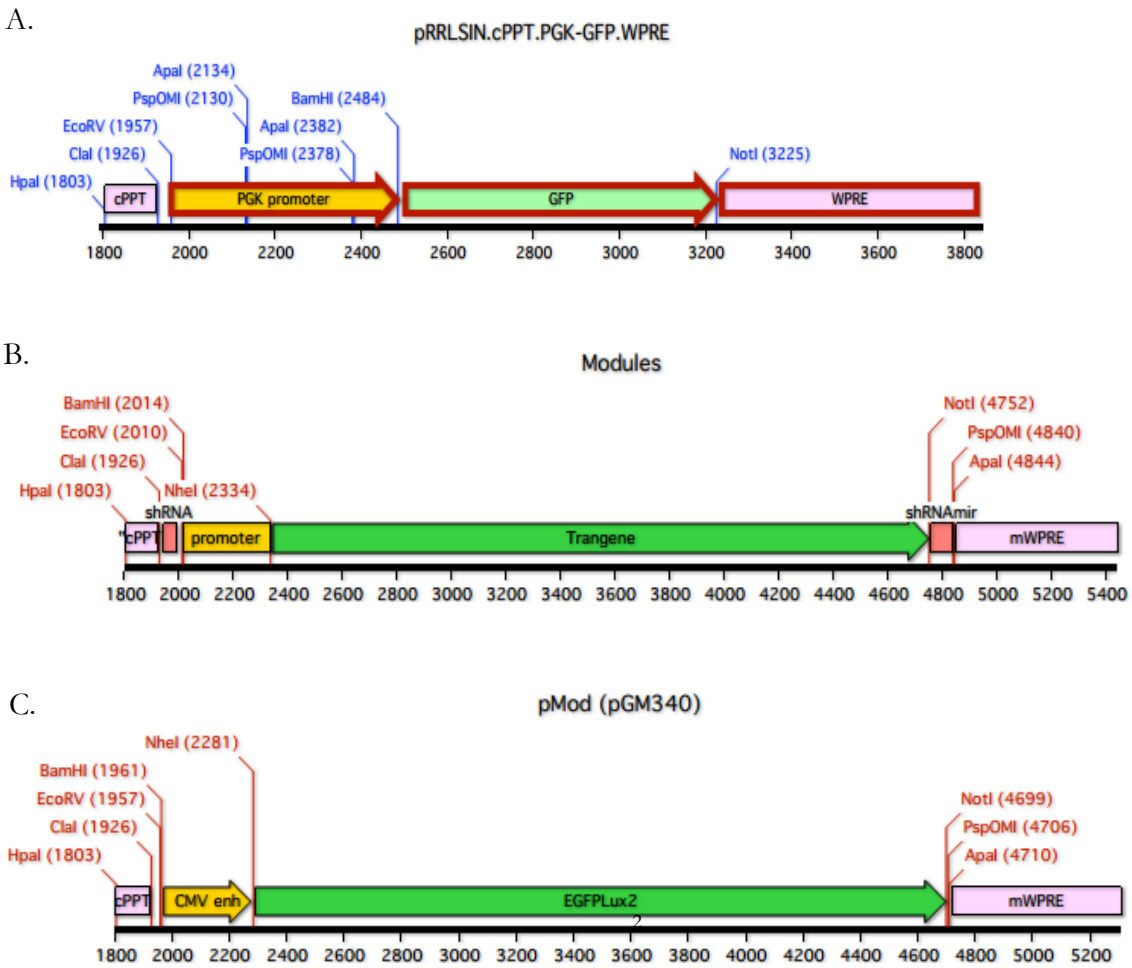

Figure 3.2. Map of amendments made to pRRLSIN.cPPT.PGK-GFP.WPRE to produce the modular rLV genome plasmid, pMod (pGM340)

The red highlighted sections in pRRLSIN.cPPT.PGK-GFP.WPRE (A) were altered in order to construct a modular rLV genome plasmid (B). In summary, the WPRE region was replaced by mutant WPRE (mWPRE; Section 3.2.1.1), the partial gag region was replaced with a modified partial gag containing a mutated NotI site (Section 3.2.1.2). Finally the EGFP transgene was replaced by an EGFP-Luciferase fusion (EGFPLux22; dark green), introducing a unique ApaI site downstream of the transgene to create pMod (C; Section 3.2.1.3). A CMV enhancer sequence (orange) was also inserted that contains restriction sites to allow insertion of other promoters available in our group (BamHI, EcoRI, NheI). Restriction sites used for insertion of modules into the modular rLV are shown above the sequences, with the cut site in parentheses.

Module	Upstream restriction site	Downstream restriction site
Promoter/enhancer	BamHI	NheI
Transgene	NheI	NotI
shRNA	HpaI/ClaI	EcoRV
shRNAmir	NotI	ApaI/PspOMI

Table 3.1 Modular design of plasmid pMod

A modular recombinant Lentivirus (rLV) genome plasmid was designed, based on pRRLSIN.cPPT.PGK-GFP.WPRE, to allow insertion of the modules above using the restriction sites indicated, which were selected based on access to a library of modular transgenes available on NheI-NotI DNA fragments, and promoter/enhancer elements available on BamHI-NheI fragments (Gill et al., 2001; Hyde et al., 2008).

3.2.1.1 Incorporation of a mutated WPRE and generation of the transgene module for the modular genome plasmid

It has been reported that the incorporation of WPRE into rLV vectors can significantly increase transgene expression *in vitro* and *in vivo* (Zufferey et al., 1999; Deglon et al., 2000) through enhanced nuclear export of transgene RNA. However, concerns have been raised about the possible oncogenicity of this 'wild-type' WPRE due to the expression of part of the hepadnavirus X protein, which in a limited number of studies has been associated with increased tumour formation (Kingsman et al., 2005). A mutated WPRE (mWPRE) sequence was obtained that has been shown to abrogate the X protein whilst retaining the enhancements in nuclear export and transgene expression (Zanta-Boussif et al., 2009). The mWPRE sequence was previously amplified by PCR (Section 2.2.1) from a source plasmid (Mitomo et al., 2010) and inserted into pRRLSIN.cPPT.PGK.GFP.WPRE (Table 2.1) replacing the 'wild-type' WPRE and creating pRRLSIN.cPPT.PGK-GFP.mWPRE (pGM279; Table 2.1; unpublished work, Anna Lawton). This pGM279 contains two NotI sites: one downstream of the transgene that is suitable for insertion of transgene and shRNAmir modules (Table 3.1), and one within the partial gag sequence (Figure 3.3B). To retain a unique NotI site in the modular vector, a partial gag was designed containing a mutated NotI site (Anna Lawton; plasmid not shown). This gag fragment was relatively small (<400bp) which can sometimes make DNA fragment manipulation more difficult. To increase the size of the fragment to be inserted into pGM279, the pol-cPPT region from pGM279 was digested using MfeI and EcoRV and inserted into pHIVgagNoNot to create pHIVgagNoNot.cPPT (Table 2.1, plasmid not shown). Enhanced GFP (EGFP) from pEGFP-N1 (Promega) was inserted into this plasmid on a NheI-NotI fragment, to act as a gap-filler for the transgene module, generating pHIVgagNoNot.EGFP (Table 2.1; Figure 3.3A).

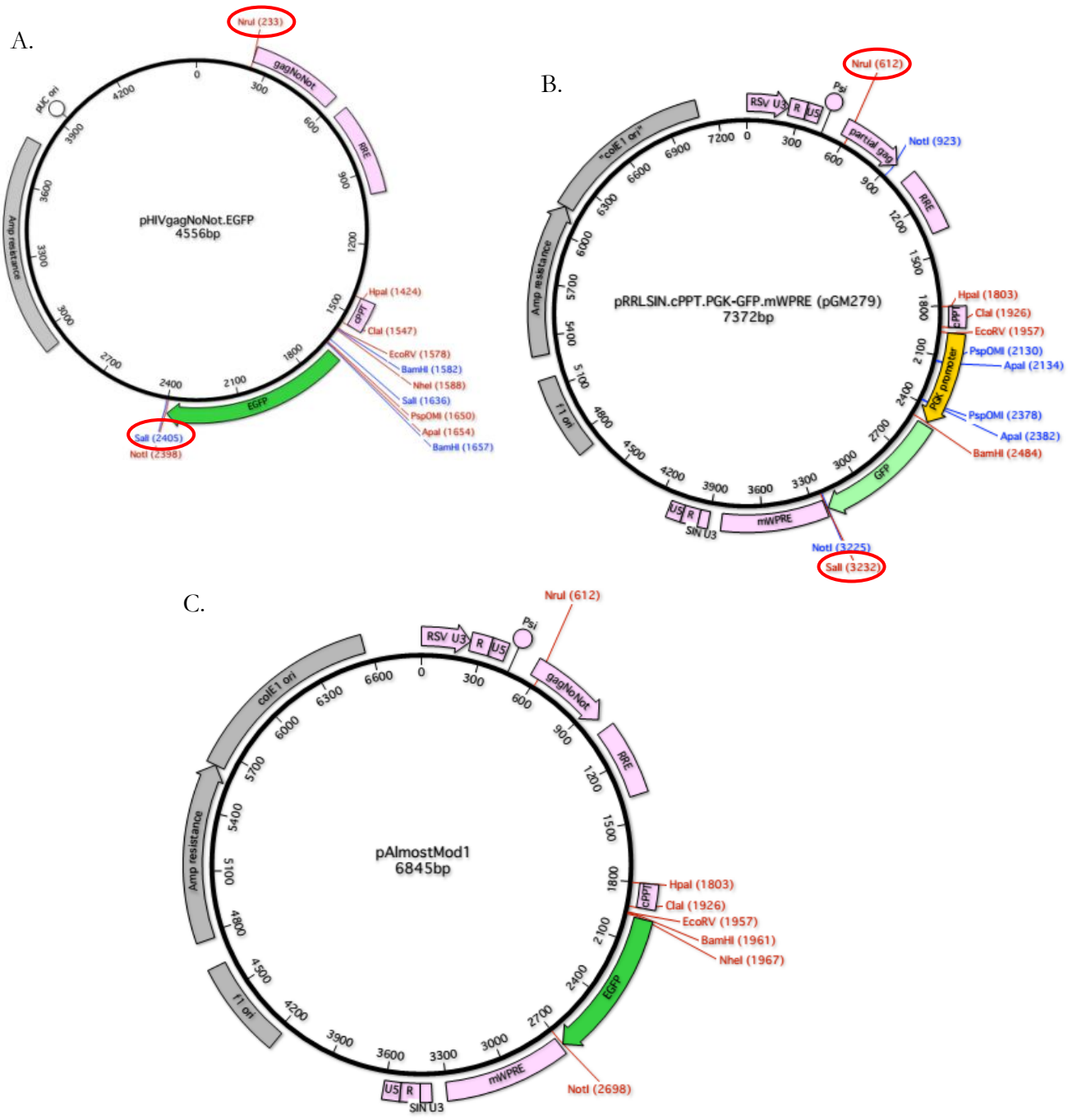

Figure 3.3. Generation of pAlmostMod1.

The pHIVgagNoNot.EGFP plasmid was digested with NruI and SalI (A) and inserted into the Nru-SalI sites in pGM279 (B) to generate pAlmostMod1. Restriction sites are indicated in red (single cut site) and blue (two cut sites) font. Red ellipses indicate the cut sites used in this step of the design.

The entire gag-pol-cPPT-transgene was then digested on an NruI-SalI fragment and inserted into pGM279 to generate pAlmostMod1 (Table 2.1; Figure 3.3C).

3.2.1.2 Insertion of the EGFP-Luciferase fusion transgene (EGFPLux2) as a dual reporter with a unique 3' ApaI restriction site.

EGFP fluorescence can be used to determine transduction efficiency using fluorescence microscopy, and luciferase expression can be detected via bioluminescence allowing the monitoring of transgene expression over time without the need to harvest cells. Therefore a protein fusion of EFGP and Luciferase was selected as the transgene with which to replace the EGFP transgene in pAlmostMod1. The EGFP-Luciferase fusion sequence was available commercially (pEGFPLuc, Promega) but did not contain a suitable 3' NotI site for insertion into the modular plasmid. Primers were therefore designed to introduce a 3' NotI site into the EGFPLuc transgene generating the transgene module (Table 3.1; performed by Anna Lawton). An internal BglII site was also mutated to improve compatibility with other plasmids in the group where a BglII site upstream of the promoter sequence was required (performed by Anna Lawton). The final sequence was named EGFPLux2 and contained the EGFP-Luciferase fusion transgene, flanked by NheI and NotI, and lacking an internal BglII site. The EGFPLux2 transgene contained the restriction sites required for insertion of sequences into the transgene module site (NheI and NotI; Table 3.1) and the 3' ApaI site required for shRNAmir module insertion (Table 3.1). In order to create the promoter module it was necessary to insert a BamHI site upstream of the promoter sequence. A commercial GeneArt plasmid (p15CpG.CMVenhancer) had been designed (Anna Lawton) to contain a CMV enhancer sequence with upstream BglII and BamHI sites, and an ApaI site downstream of the NheI site (Figure 3.4A). Digestion of the EGFPLux2 transgene from an available plasmid, pGM307 (Anna Lawton; Table 2; Figure 3.4B) using NheI and NotI allowed insertion of the transgene into p15CpG.CMVenhancer generating pCMVenh.EGFPLux2 (Figure 3.4C) which

contained the correctly positioned restriction sites for the promoter, transgene and shRNAmir modules. Subsequent digestion of pCMVenh.EGFPLux2 with BamHI and SalI (Figure 3.4C) and insertion into pAlmostMod1 (Figure 3.4D) generated the modular rLV genome plasmid pMod (pGM340; Figure 3.4E). This final pMod allows the insertion of different transgenes, promoter/enhancer sequences upstream of the transgene, shRNA sequences upstream of the transgene promoter, and shRNAmir sequences between the transgene and mWPRE, all using a few common restriction enzymes and minimal cloning steps (Table 3.1).

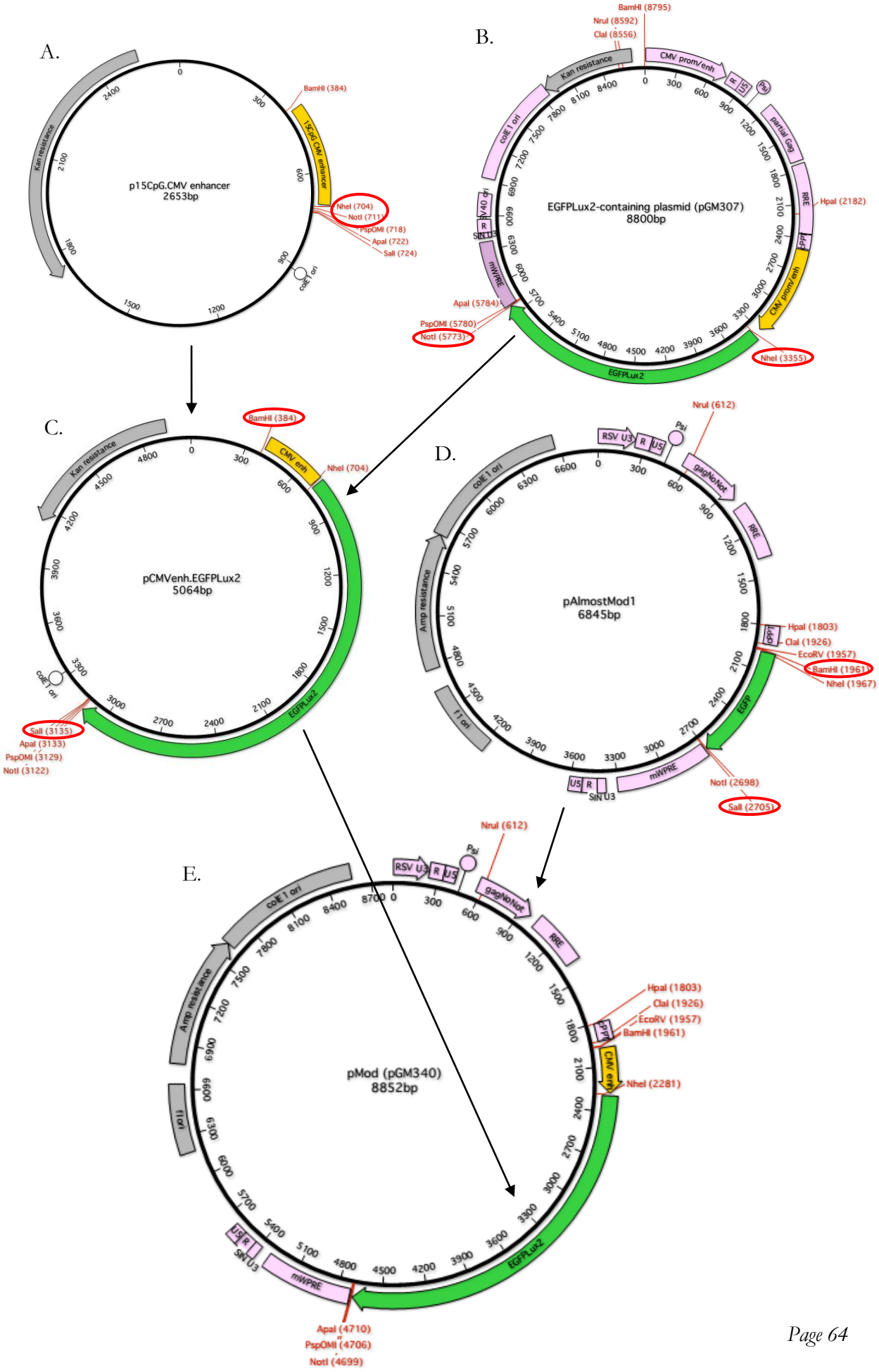
A.
p15CpG.CMV enhancer
2653bp
Kan resistance
15CpG CMV enhancer
BamHI (384)
NheI (704)
NotI (711)
PspOMI (718)
ApaI (722)
SalI (724)
colE1 ori
B.
EGFPLux2-containing plasmid (pGM307)
8800bp
BamHI (8795)
NruI (8592)
ClaI (8556)
Kan resistance
CMV prom/enh
partial Gag
RRE
HpaI (2182)
CMV prom/enh
NheI (3355)
EGFPLux2
mWPRE
ApaI (5784)
PspOMI (5780)
NotI (5773)
colE1 ori
C.
pCMVenh.EGFPLux2
5064bp
Kan resistance
BamHI (384)
CMV enh
NheI (704)
EGFPLux2
colE1 ori
SalI (3135)
ApaI (3133)
PspOMI (3129)
NotI (3122)
D.
pAlmostMod1
6845bp
NruI (612)
RSV U3
R
U5
Psi
gagNoNot
RRE
HpaI (1803)
ClaI (1926)
EcoRV (1957)
BamHI (1961)
NheI (1967)
EGFP
mWPRE
SIN U3
NotI (2698)
SalI (2705)
Amp resistance
colE1 ori
f1 ori
E.
pMod (pGM340)
8852bp
NruI (612)
RSV U3
R
U5
Psi
gagNoNot
RRE
HpaI (1803)
ClaI (1926)
EcoRV (1957)
BamHI (1961)
CMV enh
NheI (2281)
EGFPLux2
mWPRE
SIN U3
ApaI (4710)
PspOMI (4706)
NotI (4699)
Amp resistance
colE1 ori
f1 ori

Figure 3.4. Insertion of the 15CpG CMV enhancer and EGFPLux2 into pAlmostMod1 to introduce the restriction sites required for the promoter and shRNAmir modules

An ApaI site was introduced downstream of the commercially available EGFPLuc (pEGFPLuc, Promega) and an internal BglII site mutated (performed by Anna Lawton). To complete the promoter module a BamHI site was required upstream of the promoter; this layout was available in p15CpG.CMVenhancer (A) designed previously in the group (Anna Lawton). The EGFPLux2 transgene was inserted into p15CpG.CMVenhancer by digesting the transgene from an earlier group plasmid, pGM307 (B) using the NheI and NotI sites generating pCMVenh.EGFPLux2 (C). The promoter and transgene were then digested out using BamHI and SalI and the fragment inserted into pAlmostMod1 (D) to generate pMod (pGM340; E), which is the final modular genome plasmid containing all the restriction sites necessary for insertion of the modules designed in section 3.2.1 (Table 3.1). Restriction sites used in this design are indicated with red ellipses.

3.2.2 Production of modular recombinant Lentivirus (rLV) vectors and functional testing in human and mouse cell culture

3.2.2.1 Insertion of a CMV promoter/enhancer sequence for gene expression from pMod

To determine whether the modular rLV genome plasmid, pMod (pGM340; Table 2.1) could produce functional virus, the cytomegalovirus enhancer (CMVenh) in pMod was replaced with the human CMV immediate/early promoter/enhancer sequence (CMVenh/prom) capable of high and persistent reporter and CFTR transgene expression in cell culture and *in vivo*. The CMVenh/prom fragment was isolated from pCIKLux (Gill et al., 2001; Table 2.1) using primers designed to introduce a 5' BglII site and 3' NheI site (Anna Lawton). This amplified fragment was available in the pGM307 plasmid used previously (Figure 3.5A) and was not included in the original modular design as the 5' restriction site was BglII rather than BamHI, and the HIV backbone in the modular plasmid contains multiple BglII sites. However, due to the compatibility of BglII and BamHI sticky ends it was possible to digest the pGM307 with BglII and NheI to extract the CMV enhancer/promoter and insert this into the BamH1/NheI sites of pMod (Figure 3.5B), replacing the weaker 15CpG.CMVenhancer sequence and generating pHIV.EGFPLux2 (pGM341; Table 2.1; Figure 3.5C). This reporter construct was tested in cell culture alongside pHIV.EGFPLux2.NotMod (pGM290), which is an equivalent plasmid that does not contain the modifications made to generate the modular plasmid (Figure 3.5D). This comparison would allow confirmation that the modifications made to create the modular vector did not affect virus production and gene expression.

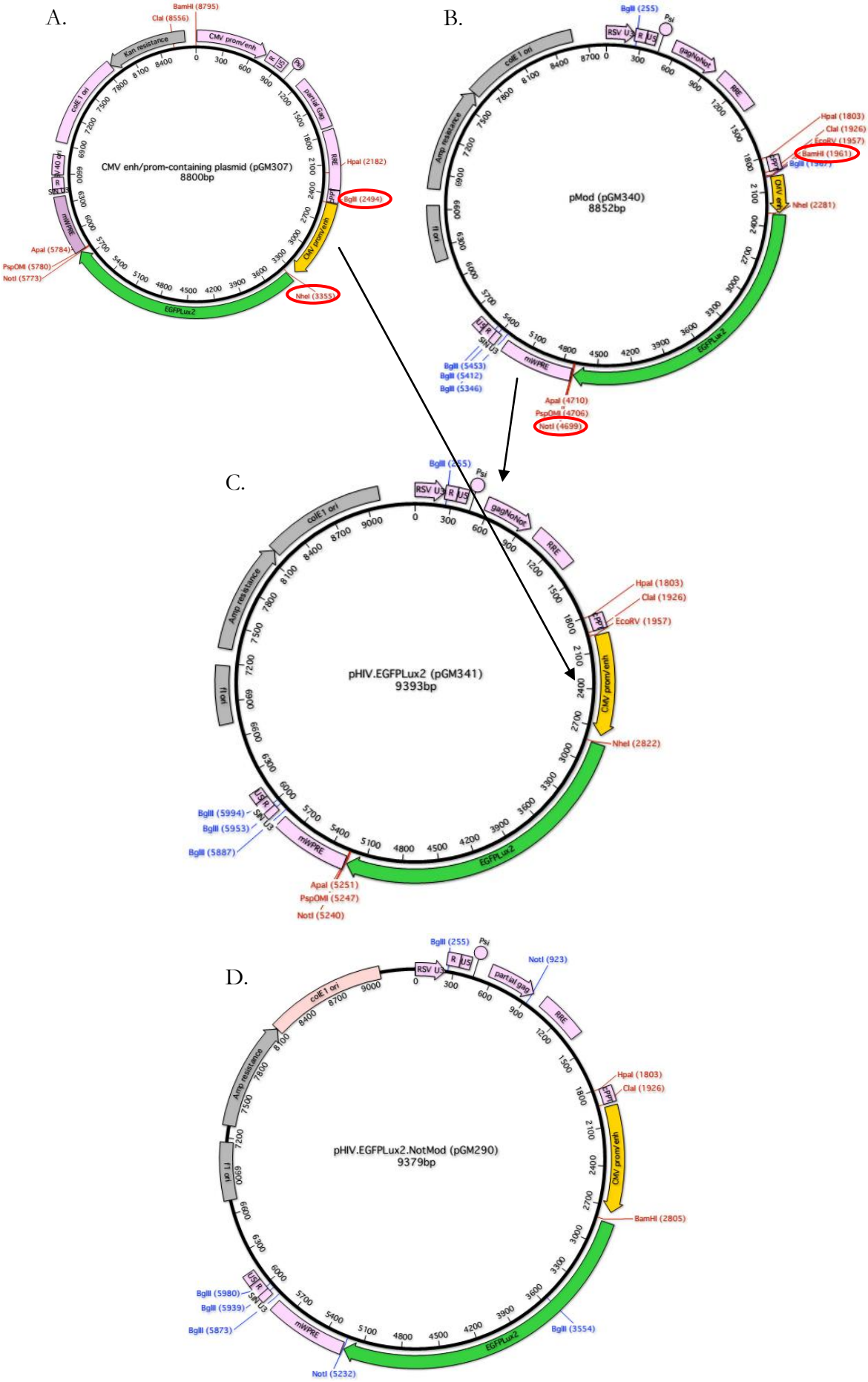
A.
CMV enh/prom-containing plasmid (pGM307)
8800bp
BamHI (8795)
ClaI (8556)
HpaI (2182)
BglII (2494)
NheI (3355)
ApaI (5784)
PspOMI (5780)
NotI (5773)
B.
pMod (pGM340)
8852bp
BglII (255)
HpaI (1803)
ClaI (1926)
EcoRV (1957)
BamHI (1961)
NheI (2281)
BglII (5453)
BglII (5412)
BglII (5346)
ApaI (4710)
PspOMI (4706)
NotI (4699)
C.
pHIV.EGFPLux2 (pGM341)
9393bp
BglII (255)
HpaI (1803)
ClaI (1926)
EcoRV (1957)
NheI (2822)
BglII (5994)
BglII (5953)
BglII (5887)
ApaI (5251)
PspOMI (5247)
NotI (5240)
D.
pHIV.EGFPLux2.NotMod (pGM290)
9379bp
BglII (255)
NotI (923)
HpaI (1803)
ClaI (1926)
BamHI (2805)
BglII (5980)
BglII (5939)
BglII (5873)
BglII (3554)
NotI (5232)

Figure 3.5 Insertion of the CMV immediate/early promoter/enhancer (CMVprom/enh) into pMod (pGM340) to generate pHIV.EGFPLux2 (pGM341).

A CMV immediate/early promoter/enhancer (CMV prom/enh) fragment was digested from pGM307 with BglII and NheI (A) and the fragment inserted into the BamHI and NheI digest of pMod (pGM340; B) to generate pHIV.EGFPLux2 (pGM341; C). The non-modular equivalent plasmid pHIV.EGFPLux2.NotMod (pGM290; D) is shown for comparison. Restriction sites are indicated in red (one cut site) or blue (multiple cut sites) font.

3.2.2.2 Production and titration of rLV using pHIV.EGFPLux2

The previous sections in this chapter describe the multiple manipulations required to construct the modular pHIV.EGFPLux2 (pGM341) vector genome plasmid suitable for production of third generation rLV. To confirm that these manipulations had not impaired virus production and expression, third generation rLV was produced in HEK293T suspension cells (Section 2.5) using the pHIV.EGFPLux2 (pGM341; Figure 3.5C) or the non-modular vector genome plasmid, pHIV.EGFPLux2.NotMod (pGM290; Table 2.1; Figure 3.5D), to generate vEGFPLux2 (vGM029) and vEGFPLux2.NotMod (vGM004; Table 2.1) respectively. All rLV vectors were produced pseudotyped with the vesicular stomatitis virus glycoprotein (VSVG) unless otherwise stated. To produce VSVG-pseudotyped rLV vectors from the genome plasmids, a multi-plasmid transfection was performed in HEK293T suspension cells using three other plasmids: pGM281 containing the HIV gag and pol sequences, pRSV-Rev, and pMD2-G containing the VSVG coat protein sequence (Table 2.5). GFP fluorescence was detected in producer cells by fluorescence microscopy indicating that the plasmid transfection was successful (Figure 3.6). After 48 hours virus supernatant was collected and virus titre determined by two different techniques: flow cytometry of GFP fluorescence (Section 2.7.2) and a viral particle TaqMan qRT-PCR assay (Section 2.7.1), to determine functional titration units (FTU) and viral particle number (VP) respectively, calculated per ml of harvested virus. Titration indicated that both vEGFPLux2 (vGM029) and vEGFPLux2.NotMod (vGM004) expressed the EGFPLux2 transgene, producing functional titres of 2 x 10^7 FTU/ml and 9.9 x 10^6 FTU/ml respectively. These titres were comparable to those observed routinely during VSVG-pseudotyped rLV vector production (1x10^7 FTU/ml on average; Lee Davies, Personal Communication).

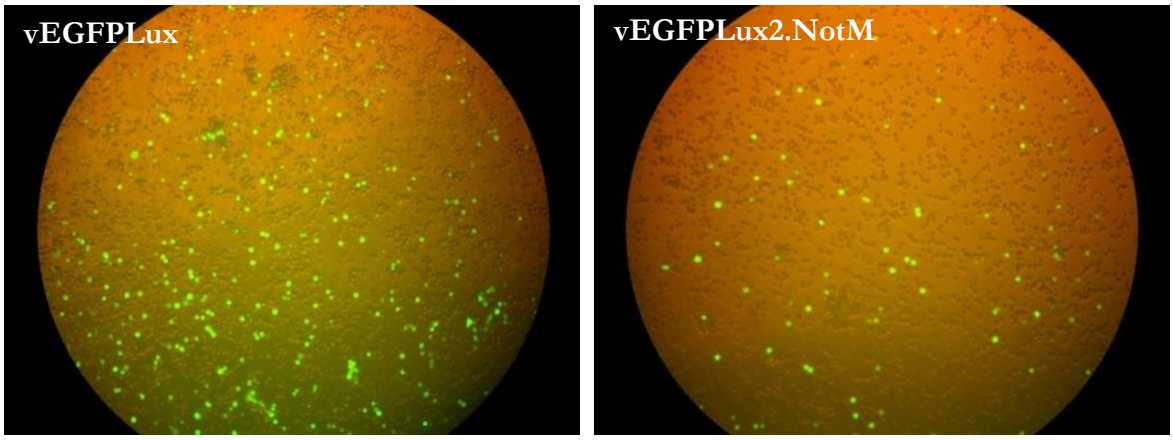

Figure 3.6. Representative micrographs of producer cells following multi-plasmid transfection to produce rLV vectors.

To produce third generation rLV vectors, the viral genome plasmids pHIV.EGFPLux2 (pGM341) and pEGFPLux2.NotMod (pGM290) were co-transfected into HEK293T suspension cells (producer cells) along with gag/pol, rev and VSVG coat protein plasmids to produce vEGFPLux2 (vGM029) and vEGFPLux2.NotMod (vGM004) respectively (full protocol details in section 2.5). Successful transfection was verified by the presence of EGFP fluorescence at 24 hours post-transduction as determined with fluorescence microscopy. (10x magnification)

The viral particle number (VP/ml), which is usually greater than functional titre due to the presence of defective viral particles in the supernatant, was 6 x 108 VP/ml and 5 x 108 VP/ml for vEGFPLux2 and vEGFPLux2.NotMod respectively (data not shown).

3.2.2.3 Transduction of human and mouse cells with modular rLV

The modular rLV developed as described in this chapter was used to transduce human and murine cell lines grown in culture. One of the aims of this thesis was to determine whether a dual-function anti-ENaC and CFTR delivery rLV vector could simultaneously knock down ENaC and express CFTR therefore two cell lines were chosen for developing a transduction protocol: the human A549 epithelial cell line, which is derived from a human lung carcinoma, does not express CFTR (Renier et al., 1995) and expresses ENaC at levels suitable for measuring ENaC knockdown (Clark et al., 2013), and the murine epithelial M-1 cell line, which is derived from the mouse kidney (Stoos et al., 1991) and has been shown to express detectable levels of ENaC suitable for knockdown studies (Painter, 2007). The endogenous levels of CFTR from the M-1 cell line is unimportant at this stage as detection of transgene CFTR expression would be using human CFTR-specific assays. To determine a suitable dose of virus for initial studies, A549 and M-1 cells were seeded overnight in a 6-well plate (Section 2.8) and then transduced with doses of vEGFPLux2 ranging from 4 x 10^6 to 1 x 10^7 FTU/well; media-only control wells (sham-treatments) were also included. Cells were harvested at 72 hours post-transduction and FACS analysis (Section 2.9.3) used to determine transduction efficiency and cell viability. The total RNA yield from each treatment sample was also quantified as an additional indication of cell viability (Section 2.9.1). Transduced cells were observed in both cell lines at all virus doses delivered (Figure 3.7A). At least 85% of A549 cells were transduced even at the lowest dose, with cell viability remaining >80% at all doses (Figure 3.7B; dark grey bars). No significant increase in transduction was observed between the two highest doses and the only significant difference in cell viability was between

the highest dose and the sham-treated cells ($p<0.05$, sham vs. 4 x 10^6 FTU/well). Although cell viability remained high, transduction of A549 cells resulted in a significant (approximately 2-fold) decrease in total RNA yield compared with media-only controls ($p<0.05$, sham vs. all doses; Figure 3.7C). While a trend for reduced RNA yield with increased viral dose was apparent, the magnitude of change was modest over the range of virus doses evaluated. Transduction with lower doses of virus would be required to determine whether there is a threshold of viral dose below which global RNA depletion is not observed.

Transduction of M-1 cells with vEGFPLux2 was similar overall, except that only a maximum of 65% GFP positive cells were observed (Figure 3.7A). In this study, there was no significant difference in transduction efficiency between the two highest doses applied. In contrast to A549 cells, M-1 cell viability decreased significantly following transduction with vEGFPLux2 ($p<0.05$, sham vs. all doses; Figure 3.7B) such that only 35% of cells were viable at the very highest dose. Total RNA yield reflected this change with at least a 2-fold decrease in yield between the media-only and vEGFPLux2 transduced cells ($p<0.05$, sham vs. all doses), and a further 2.5-fold decrease from the 6 x 10^6 FTU/well dosed cells to the highest dose ($p<0.05$, 6 x 10^6 FTU/well vs. 1 x 10^7 FTU/well; Figure 3.7C).

Overall, in both A549 and M-1 cells, given the narrow range of virus doses evaluated, the variation in transduction efficiency and cell viability appear appropriate.

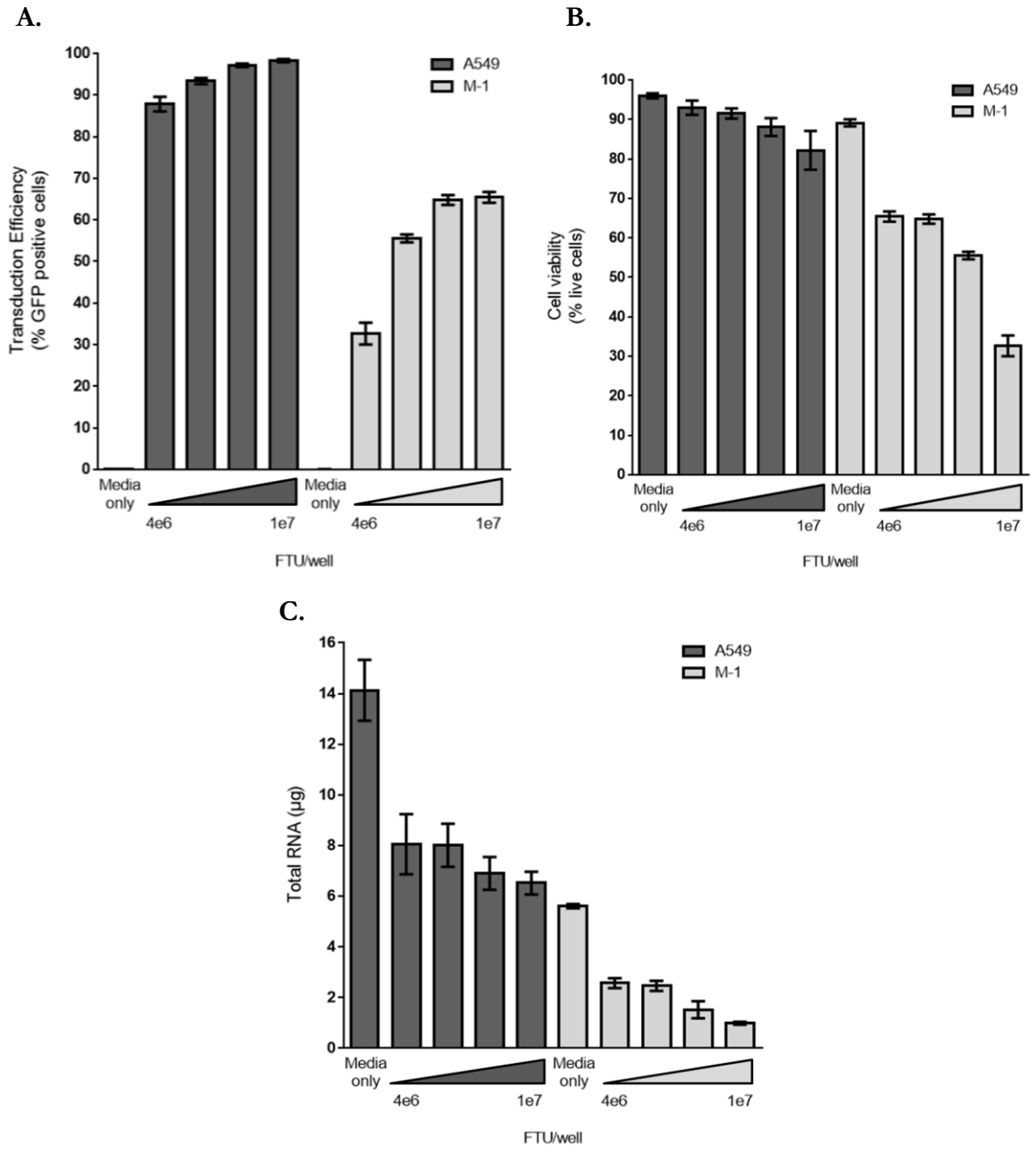

Figure 3.7. Analysis of A549 and M-1 cells transduced with increasing doses of vEGFPLux2

Human A459 cells (dark grey) and mouse M-1 cells (light grey) were seeded at 2 x 10^5 cells/well and transduced with four doses of virus (4 x 10^6, 6 x 10^6, 8 x $10^{6,}$ and 1 x 10^7 FTU/well). After 72 hours cells were harvested for FACS analysis to determine transduction efficiency as the percentage of GFP positive cells (A) and % cell viability (B). Total RNA yield was also measured (C). n=3 wells per dose; Media only: indicates addition of serum-free media to the cells, in lieu of virus.

3.3 Discussion

In this chapter a modular dual-function lentiviral vector genome plasmid (pMod; pGM340) was designed and constructed to allow insertion of different promoter, transgene and RNAi elements (Table 3.1), with minimal sub-cloning steps (Section 3.2.1). In published studies vectors have been designed to facilitate expression of multiple transgenes (Palfi et al., 2014), or multiple RNAi constructs (Mueller et al., 2012; Henry et al., 2006) for use as an investigative tool. Following insertion of the CMV immediate/early promoter/enhancer (CMVProm/enh) into pMod, the resulting EGFPLux2-expressing plasmid, pHIV.EGFPLux2 (pGM341; Figure 3.5D) was used to produce third generation rLV (vEGFPLux2) at titres comparable to those achieved previously using vectors with similar promoters (Lee Davies; Personal Communication). The titres for rLV preparations are often difficult to compare with published studies as there is neither a standardised protocol nor specific cell line used to determine viral titre; however the viral yields achieved here in this chapter are similar to reports of other non-purified, non-concentrated virus preparations performed at this scale (Lee Davies; Personal Communication). These data confirmed that the re-designed modular configuration was suitable for subsequent virus studies.

In order to develop a protocol to screen rLV vectors for knockdown of human mRNA, the A549 human epithelial cell line was used, as it has proved useful in non-viral lung gene transfer in the laboratory and ENaC expression studies (Clark et al., 2013). The vEGFPLux2 vector was shown to efficiently transduce this cell line, with a dose of 6 x 10^6 FTU/well leading to >90% of A549 cells being positive for GFP fluorescence, with no significant decrease in cell viability compared to media-only control cells (Figure 3.7A and B). However, despite cell viability being unaffected by rLV transduction, the total RNA yield was decreased by almost 50% (Figure 3.7C).

The mouse M-1 epithelial cell line, derived from kidney, expresses high levels of ENaC (Haerteis et al., 2012) and should be suitable for screening ENaC-targeting RNAi constructs. Following transduction with vEGFPLux2, approximately 60% of M-1 cells were positive for GFP fluorescence at a dose of 6 x 10^6 FTU/well, with approximately 60% cell viability. The observed 40% cell death coincided with a 2-fold decrease in total RNA yield compared with media-only cells. The reason for the observed decrease in RNA yield following transduction of both cell lines is unknown, but could be due to toxicity of the VSVG coat protein (Burns et al., 1993). However, transduction of A549 and M-1 cells with any of the doses tested here produced sufficient RNA with which to perform qRT-PCR analyses in subsequent knockdown studies.

In conclusion, these studies have identified cell culture transduction conditions suitable for detection of mRNA knockdown following delivery of a potent RNAi sequence. In the next chapter screening protocols were developed for selecting sequences that knock down ENaC in cell culture.

Chapter 4: Development of a protocol for screening RNA interference (RNAi) sequences in A549 cells.

4.1 Introduction

To choose an efficient RNA interference (RNAi) sequence for use in the dual-function vectors designed in chapter 3 it was necessary to develop a robust protocol for screening RNAi sequence function. The epithelial sodium channel, ENaC, was chosen as the primary target for RNAi-induced knockdown with the dual-function vector, as overexpression of ENaC is implicated in Cystic Fibrosis (CF) and CF-like lung disease (Section 1.2.2). The simultaneous knockdown of ENaC and expression of the CFTR transgene from a dual-function vector has the potential to treat the molecular deficiencies that cause CF and CF-like lung disease (Section 1.5.3). The ENaC channel is predicted to exist mainly as a heterotrimer consisting of one each of the α, β, and γ subunits (Stewart et al., 2011); the β subunit is thought to be the limiting factor in ENaC channel activation as overexpression of ENaCβ, and not ENaCα nor ENaCγ, results in Na^+ hyperabsorption (Mall et al., 2004). However, ENaCα is the most abundant subunit and is thought to form the Na^+-conducting pore of the ENaC channel (Canessa et al., 1994b; Alvarez de la Rosa et al., 2000). The ENaCα subunit has also been shown to form homotrimeric channels (Jain et al., 2001) and ENaCα hyperactivity has been observed in atypical CF (Rauh et al., 2010; Azad et al., 2009). These data suggest that knockdown of ENaCα could abrogate ENaC hyperactivity in CF therefore ENaCα was chosen as the target mRNA transcript for developing the dual-function vector.

The lung carcinoma cell line A549 was chosen as the cell culture model for developing the dual-function vector as this cell line does not express CFTR (Renier et al., 1995) but does express hENaCα. In this chapter, a qRT-PCR assay for detecting *hENaCa* knockdown was evaluated and a protocol was developed for the robust screening of RNAi sequence function.

4.2 Results

4.2.1 Detection of hENaCα knockdown with qRT-PCR

4.2.1.1 Comparative ΔΔCt RT-PCR detection of hENaCα mRNA

The earliest detectable knockdown with RNAi is manifest at the mRNA level; an RNAi sequence that is completely complementary to the target mRNA will initiate its degradation and therefore decrease target mRNA expression leading to a decrease in protein expression whilst even a single nucleotide mismatch could result in sequestration of mRNA and decrease protein expression but not mRNA expression (Su et al., 2009). A qRT-PCR assay (RPS-hENaCα-B; Table 2.7) was designed to amplify *hENaCa* mRNA (Section 2.9.1) and was previously tested to determine the sensitivity and dynamic linear range of the assay on total RNA (Ambion; Dixon, R. 2010, UKCFGTC unpublished data). No *hENaCa* mRNA standard curve was available for determining absolute mRNA copy number therefore the comparative ΔΔCt method was used (Section 2.9.1). In brief, the ΔΔCt method involves normalising the target gene mRNA levels to those of a housekeeping gene by calculating the ΔCt from the RT-PCR amplification plot (target Ct – housekeeping Ct). A control sample that should not exhibit any knockdown is used as the comparator to determine ΔΔCt (test ΔCt – comparator ΔCt). The ΔΔCt is then transformed into relative expression of the target mRNA compared to the comparator mRNA by using the formula $2^{-\Delta\Delta Ct}$ which assigns the comparator a relative expression of one. A relative expression of lower than one indicates knockdown of the target mRNA and a relative expression of greater than one indicates an increase in target mRNA. As this protocol involves quantification of two mRNAs it is desirable to "multiplex" the PCR reaction, that is, to perform qRT-PCR of the target and housekeeping mRNA in the same reaction. Alternatively, the reaction can be performed in "singleplex" (utilising separate reactions for the target and housekeeping qRT-PCR). The housekeeping gene chosen for

these ΔΔCt analyses was glyceraldehyde-3-phosphate dehydrogenase (GAPDH), which has previously been proven as a relatively stable housekeeping gene expressed in A549s (Stephanie Sumner-Jones, personal communication). Earlier studies (Dixon, R. 2010, UKCFGTC unpublished data) indicated that a total RNA input of 50ng into the qRT-PCR assay was appropriate for detecting endogenous *hENaCa* mRNA levels and knockdown in total RNA.

4.2.1.2 Detecting hENaCα knockdown in A549 cells using short-interfering RNA (siRNA) molecules.

To determine whether significant hENaCα knockdown could be detected with this qRT-PCR assay, A549 cells were transfected with a short interfering RNA (siRNA), si-ENaCα, that has been shown previously to knock down *hENaCa* mRNA levels in primary human lung and nasal epithelia, and the mouse lung (Clark , 2013; used with permission from GSK, UK). Lipofectamine2000 (L2K; Life Technologies) has been widely used in transient transfection of siRNA and shRNA in primary human cell culture, mice, and A549 cells (Almaca et al., 2013 2013; Clark et al., 2013). Therefore in this study L2K was used as the transfection reagent to deliver si-ENaCα to A549 cells (33nM per well based on the manufacturer's protocol). Media was replaced 24 hours post-transfection and total RNA was extracted from the cells 48 hours post-transfection. Total RNA was quantified and 50 ng used for comparative ΔΔCt qRT-PCR of hENaCα. ENaCα mRNA levels were normalised to GAPDH and expressed as the relative expression of hENaCα compared to treatment with a widely-used, non-target siRNA control, si-UC. A sham treatment was also included, where only media was added to the wells, and all hENaCα and GAPDH amplification plots were within the dynamic range of the assay (data not shown). Significant knockdown of hENaCα by 56% compared to si-UC levels was observed (Figure 4.1). This result confirmed that the RPS-hENaCα-B assay could detect endogenous hENaCα and GAPDH in A549 cells, and could detect at least 50% knockdown of hENaCα following RNAi treatment.

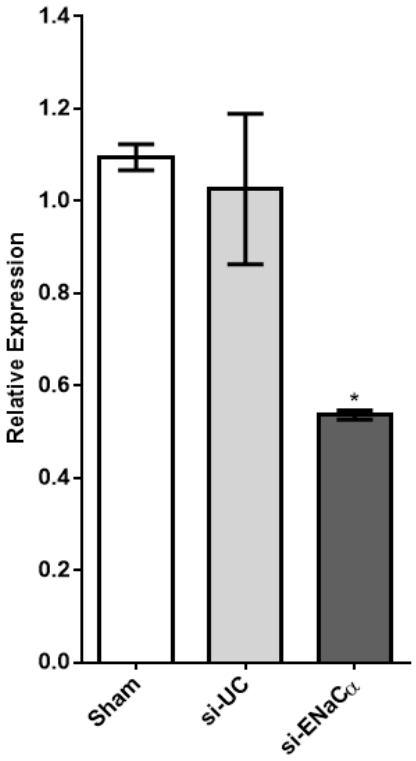

Figure 4.1. Relative expression of *hENaCα* mRNA in A549 cells transfected with si-ENaCα.

Cells were treated with 33nM of an anti-ENaCα siRNA (si-ENaCα), or a universal control non-target siRNA (si-UC), using Lipofectamine2000 (L2K; Section 2.4). Twenty four hours post-treatment, media was exchanged for fresh cell culture media and cells were harvested after a further 24 hours. Total RNA was extracted and the RPS-hENaCα-B and RPS-GSKGAP-D primer sets were used to determine the relative expression of ENaCα mRNA, using the comparative ΔΔCt method with si-UC as the comparator. Bars represent the mean ± SEM of n=3 wells. *$p<0.05$ versus si-UC, ANOVA and Tukey's multiple comparison post-hoc test.

4.2.2 Transient transfection for screening knockdown sequences

4.2.2.1 Structure and sequence of the knockdown constructs

Six RNAi sequences targeting human ENaCα (hENaCα) were obtained from OpenBiosystems (now part of Dharmacon). These sequences originated from the Hannon-Elledge library which is a collection of >85,000 human shRNAs and >75,000 mouse shRNAs. All of these shRNAs were developed by Rosetta Inpharmatics (Kirkland, USA) using proprietary algorithms based on siRNA experiments. These shRNAs are 22 nucleotides long and embedded in a miR-30 context to create shRNAmirs and were provided here in the pGIPZ backbone (Figure 4.2A) as short-hairpin RNAs (shRNAs) embedded within the human miR-30 sequence (shRNAmir; Section 1.5.2) (Zeng et al., 2002). When inserted downstream of RNA polymerase III (pol III) promoter (usually upstream of small non-coding RNAs) shRNAmirs have been shown to (a) be up to 12 times more efficient than the same shRNAs without the flanking miR sequences (Silva et al., 2005), (b) exhibit fewer off-target effects (Boudreau et al., 2009) and (c) have reduced RNAi-mediated cytotoxicity (McBride et al., 2008). The shRNAmir can also be expressed from an RNA polymerase II (pol II) promoter (usually upstream of protein-encoding genes) either alone, or in the same expression cassette as other shRNAmirs and/or transgenes (Figure 1.4). The GIPZ expression cassette consists of a CMV promoter driving transcription of the turbo GFP (tGFP) transgene, the Puromycin resistance transgene (PuroR) and the shRNAmir (Figure 4.2A). An internal ribosome entry site (IRES) drives translation of PuroR and the miR30 sequences flanking the shRNAmir leading to cleavage of this sequence via the endogenous miRNA pathway and further processing to release the embedded shRNA. This shRNA is then further cleaved by Dicer to produce a short interfering RNA duplex (siRNA) that is recognised by the RISC complex to direct target mRNA degradation.

A.

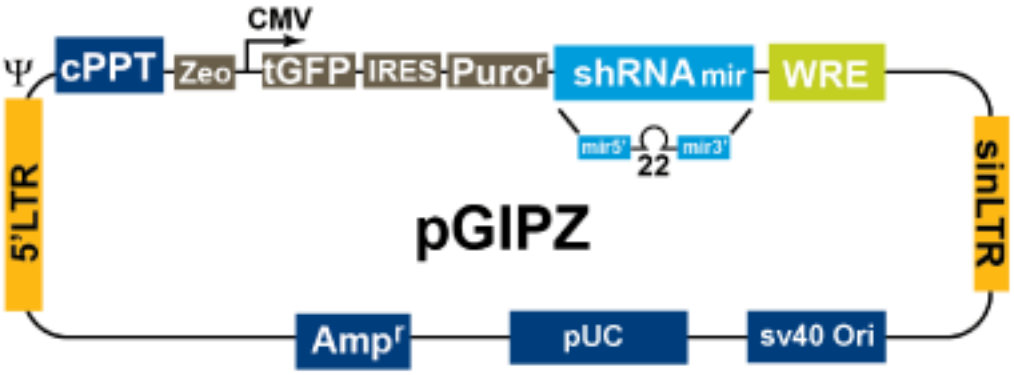

B.

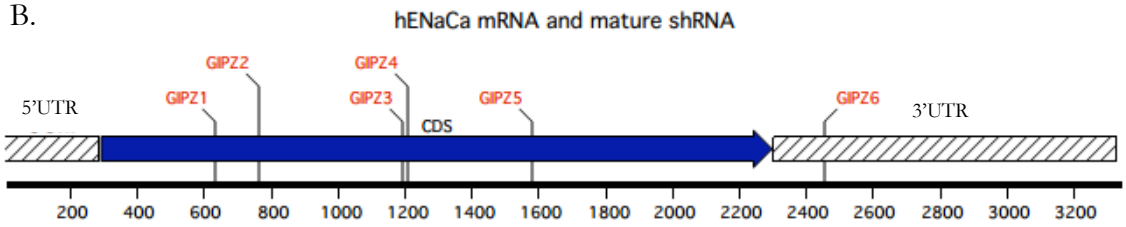

Figure 4.2. Schematic of the pGIPZ rLV plasmid and location of shRNAmir target sites along the *hENaCα* mRNA

The GIPZ plasmid (pGIPZ; A) contains the recombinant HIV sequences that allow generation of rLV viral particles in a second-generation rLV system. Other important features include the puromycin resistance gene (PuroR), turbo GFP transgene (tGFP), an internal ribosome entry site (IRES), the WPRE sequence and a shRNAmir sequence (red). Six shRNAmirs were obtained in the pGIPZ backbone (GIPZ-1 to GIPZ-6) that were designed to target the human epithelial sodium channel (hENaCα) transcript (NM_001038.5) at the locations indicated (B). The GIPZ schematic was provided by the manufacturer.

Six pGIPZ plasmids (pGIPZ-1 to pGIPZ-6; Table 2.4) were obtained containing shRNAmir sequences targeting the coding sequence (CDS) or 5'untranslated region (5'UTR) of *ENaCa* mRNA.

4.2.2.2 Screening shRNAmir sequences by transient transfection of A549 cells with pGIPZ.

The pGIPZ plasmids containing the selected shRNAmir sequences were designed for use in making recombinant HIV viral vectors in a second-generation rLV system and were incompatible with the third-generation rLV system. In order to screen the shRNAmir sequences quickly, cost-effectively and without the need for sub-cloning into the third-generation system at this early stage, the purified pGIPZ DNA was used to transfect A549 cells using L2K, rather than producing rLV viral particles. Cells were transfected with each of the six pGIPZs (pGIPZ-1 to pGIPZ-6; 0.8μg per well) and were screened alongside sham treated wells (no transfection mix) and a negative control plasmid (pLKO-Scramble) that contains a non-target shRNA sequence.

Successful transfection was demonstrated by fluorescent microscopy of tGFP positive cells, which could be detected in all pGIPZ-transfected wells (Figure 4.3). Media was replaced after 24 hours and cells were harvested 48 hours post-transfection for RNA extraction. The relative expression of hENaCα in pGIPZ transfected cells was determined by qRT-PCR. None of the pGIPZ plasmids decreased hENaCα expression levels compared with the pLKO-Scramble (Figure 4.4A). However, all plasmid-transfections decreased *hENaCa* mRNA levels by >50% compared with sham-treated controls, suggesting that plasmid transfection caused a non-specific decrease in hENaCα expression. In parallel, total RNA yields for each treatment decreased by >40% in cells transfected with plasmids, compared with the sham-treated controls (Figure 4.4B).

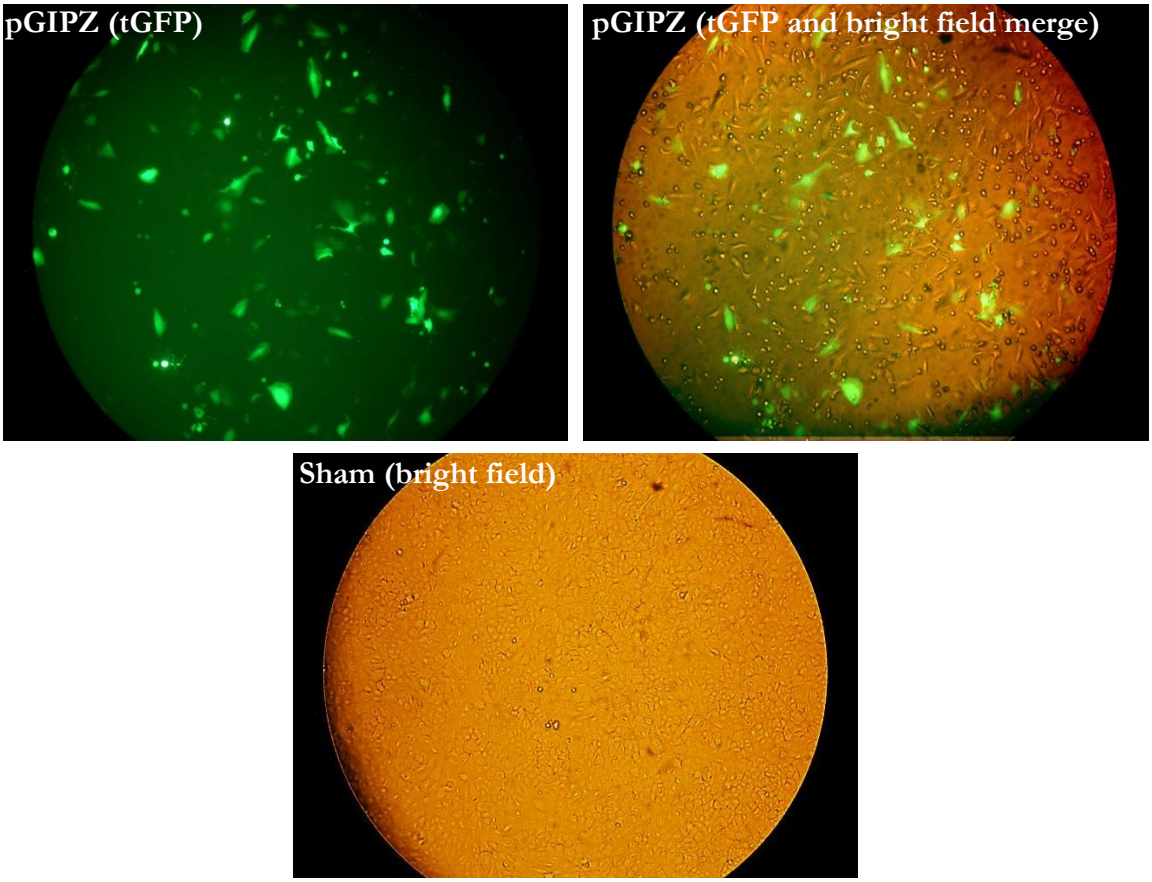

Figure 4.3. Representative micrographs of tGFP-expressing A549 cells following pGIPZ transfection using L2K.

A549 cells were seeded at 2 x 10^5 cells/ml 24 hours prior transfection with 0.8µg pDNA per well using L2K. Media was replaced after 24 hours and cells were visualised a further 24 hours later (immediately prior to harvest) using a fluorescence microscope. All images are the same field of view as seen down the microscope at 16x magnification. Sham-treated cells appeared densely packed and fully confluent with very few rounded detached cells whereas pGIPZ/L2K transfected cells appeared less confluent with many rounded detached cells suggesting cytotoxicity mediated by the pGIPZ/L2K transfection mixture.

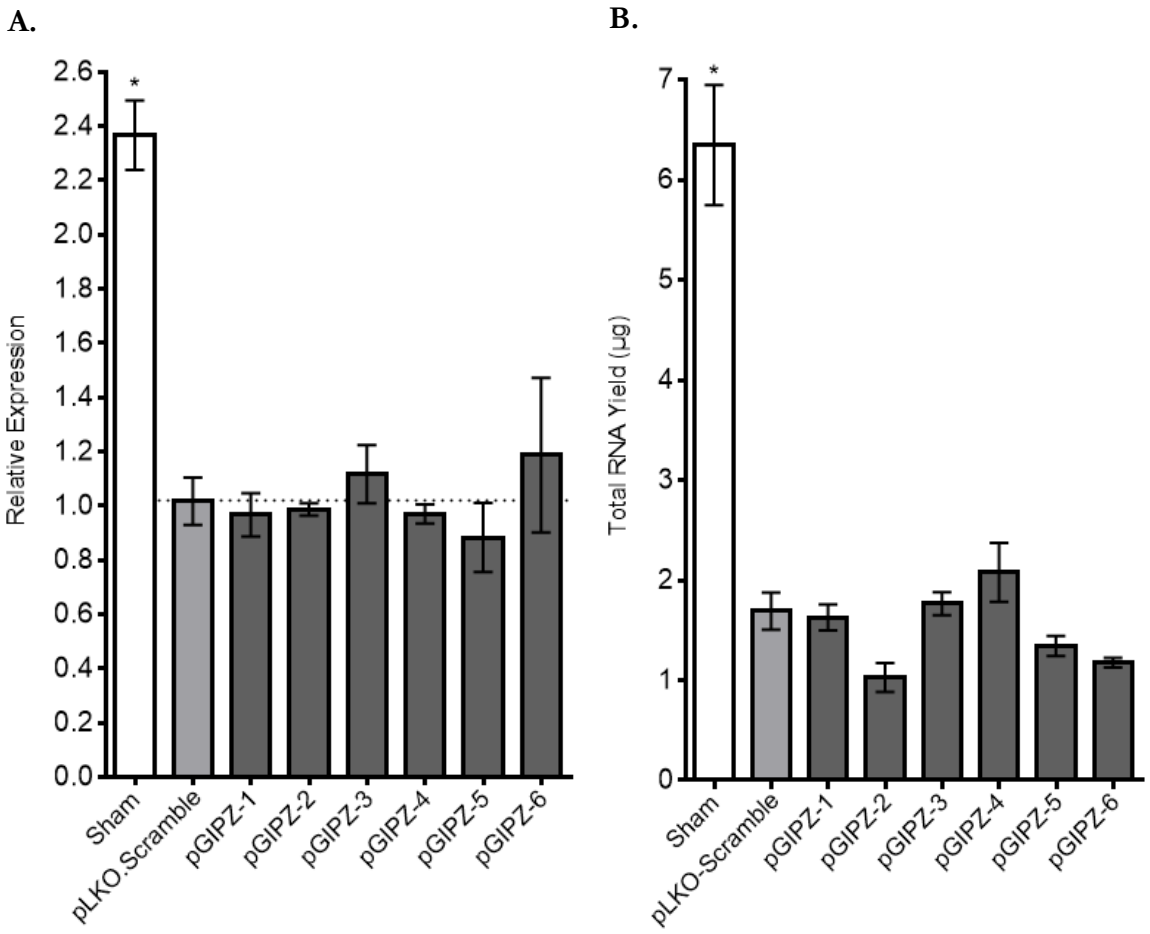

Figure 4.4 Relative expression of hENaCα and total RNA yield in A549 cells transfected with pGIPZ DNA using L2K.

A549 cells were seeded at 2 x 10^5 cells/ml 24 hours prior to transfected as in Figure 4.3 with one of six pGIPZ plasmids (pGIPZ-1 to pGIPZ-6) and harvested 48 hours post-transfection and RNA extracted. Total RNA was quantified (B) and the relative expression of hENaCα compared with the cells transfected with non-target shRNA (pLKO.Scramble; dotted line, B). Bars represent the means ± SEM of at least 3 wells. *$p<0.05$ versus. pLKO.Scramble, one-way ANOVA with Tukey's multiple comparison post-hoc test.

This significant decrease in both total RNA yield, and specific *hENaCa* mRNA levels, suggests that pGIPZ/L2K transfection caused toxicity in the cells. This difference in cellular health could also be observed in the micrographs of transfected and sham-treated cells (Figure 4.3). The A549 cells were rinsed with PBS prior to harvesting therefore many of the rounded, detached cells observed would be washed away at this stage, which could explain the decrease in total RNA yield observed. However, the number of cells remaining and total RNA yield should not cause a decrease in the relative expression of hENaCα in itself, as the hENaCα Ct of each sample is normalised to the GAPDH housekeeping gene Ct. In addition, the same quantity of total RNA is used in each qRT-PCR reaction, therefore, as a housekeeping gene, the GAPDH Ct should remain consistent for each sample, and this was observed in this study (data not shown). Subsequent repeats of this experiment highlighted inconsistencies in the relative expression in the pGIPZ-treated wells, and also in the controls. To determine whether these inconsistencies were due to overload of the RNAi cellular machinery, by transfecting cells with a large quantity of shRNAmir-producing plasmid DNA, the percentage of cells expressing tGFP, and therefore the expression cassette that produced the shRNAmir, was estimated using counts from the photomicrographs. These counts suggested that ~14% of the cells in a well were expressing tGFP irrespective of which shRNAmir sequence was evaluated (data not shown). Furthermore, flow cytometry studies from independent transfections indicated that only 5% of cells expressing tGFP remained following the PBS rinse and harvest (data not shown). Together, these low transfection efficiencies suggest that overload of the RNAi machinery was unlikely to be the cause of the RNA perturbations observed. Whatever the cause of the discrepancies observed here it was decided to pursue a different delivery approach to determine whether transfection using a plasmid designed for incorporation into rLV vectors was causing the inconsistencies observed here. As it was previously established that virus particles created with the modular dual-function design (Section 3.2.1) could

transduce both human and mouse cells lines by >60% (Figure 3.7), rLV-based vectors were used for further protocol development.

4.2.3 Viral transduction for screening shRNAmir sequences in A549 cells.

In this section, the development of a protocol to screen shRNAmir sequences for target mRNA knockdown is described. To facilitate LV production, the shRNAmir sequences were moved from the GIPZ backbone to the pEGFPLux2 backbone created in chapter 3.

4.2.3.1 Creating dual-function shRNAmir reporter rLV genome plasmids.

The rLV dual-function genome plasmid pEGFPLux2 (pGM341; Table 2.1) contains NotI and ApaI restriction enzyme sites between the EGFPLux2 transgene and the mWPRE specifically for insertion of shRNAmir sequences. However, the shRNAmir sequences in pGIPZ are not flanked by these restriction sites, therefore primers were designed to amplify the shRNAmir from the pGIPZ backbone whilst incorporating a 5' NotI site and a 3' ApaI site (Primers GM11-499 and GM11-500 respectively; Table 2.2). As PCR amplification of fragments containing hairpins may be problematic due to hairpins re-forming during amplification, addition of the hairpin destabilisers DMSO and betaine (Melchior and Von Hippel, 1973; Rees et al., 1993) to the PCR reactions was evaluated.

As an exemplar, the pGIPZ-6 shRNAmir sequence (shmir-6) targeting the 3'UTR of the *hENaCa* mRNA was chosen for further testing due to results obtained in replicate experiments that suggested that this sequence may be suitable for use. This sequence was amplified using the above primers with or without DMSO (5%) and betaine (1M) (Figure 4.5).

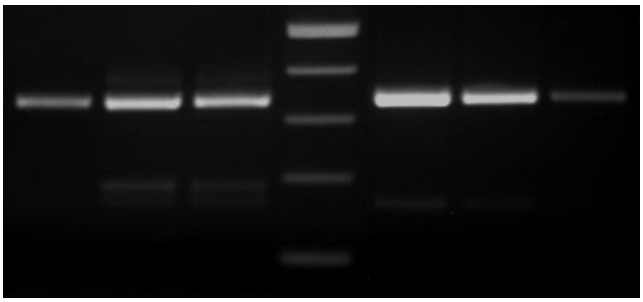

100mM $MgSO_4$ (µl)	0	2	4	L	0	2	4
DMSO (5%) /Betaine (1M)	-	-	-	L	+	+	+

Figure 4.5. Photograph of the 2% agarose gel showing amplification of the shmir-6 shRNAmir from pGIPZ-6 with or without the addition of DMSO and betaine.

The 339bp shRNAmir fragment from pGIPZ-6 (shmir-6) was amplified using the GM11-499 and GM11-500 primers (Table 2.2). The PCR reactions were prepared with or without DMSO (5%)/betaine (1M) and with three different volumes of 100mM $MgSO_4$. L indicates the kb ladder with bands from top to bottom indicating 500, 400, 300, 200 and 100 base pairs.

While the presence of DMSO/betaine appeared to enhance the yield of the 339bp PCR product when no additional $MgSO_4$ was added to the reaction, product yield was satisfactory when 2µl of 100mM $MgSO_4$ was added without DMSO/betaine; for simplicity, all future shRNAmir amplifications were performed with 2µl of 100mM $MgSO_4$ and no DMSO/betaine. Subsequent to amplification, the 339bp shmir-6 fragment was inserted into pCR-BluntII-TOPO to create pTOPO-shmir-6. The shmir-6 sequence was verified by sequencing.

The pTOPO-shmir-6 (Figure 4.6A) and pEGFPLux2 (Figure 4.6B) plasmids were both digested with NotI and ApaI, and the resultant 332bp shRNAmir fragment from pTOPO-shmir-6 inserted into the 9382bp pEGFPLux2 backbone to create pEGFPLux2-shmir-6 (pGM342; Figure 4.6C), which was then amplified and purified for use in rLV particle production. Restriction digest analyses confirmed the correct insertion of shmir-6.

4.2.3.2 Determining an appropriate dose for viral transduction in A549 cells.

The pEGFPLux2 and pEGFPLux2-shmir-6 viral genome plasmids were used to produce the VSV-G pseudotyped rLV viral particles vEGFPLux2 (vGM029) and vEGFPLux2-shmir-6 (vGM030) respectively, using the third generation rLV system (Section 2.5). The functional titres of vEGFPLux2 and vEGFPLux2-shmir-6 were 2.04 x 10^7 and 1.96 x 10^7 FTU/ml respectively which were within the expected range (Section 2.7.2). A549 cells were transduced with vEGFPLux2 or vEGFPLux2-shmir-6 at two different concentrations: 2 x 10^6 FTU/well (low dose) or 2 x 10^7 FTU/well (high dose), and cells were harvested 72 hours post-transduction for flow cytometry (Section 2.9.3) and RNA extraction. The low and high doses resulted in transduction of ~5% and ~80% of cells respectively with either virus, as judged by EGFP expression using fluorescence microscopy (Figure 4.7A).

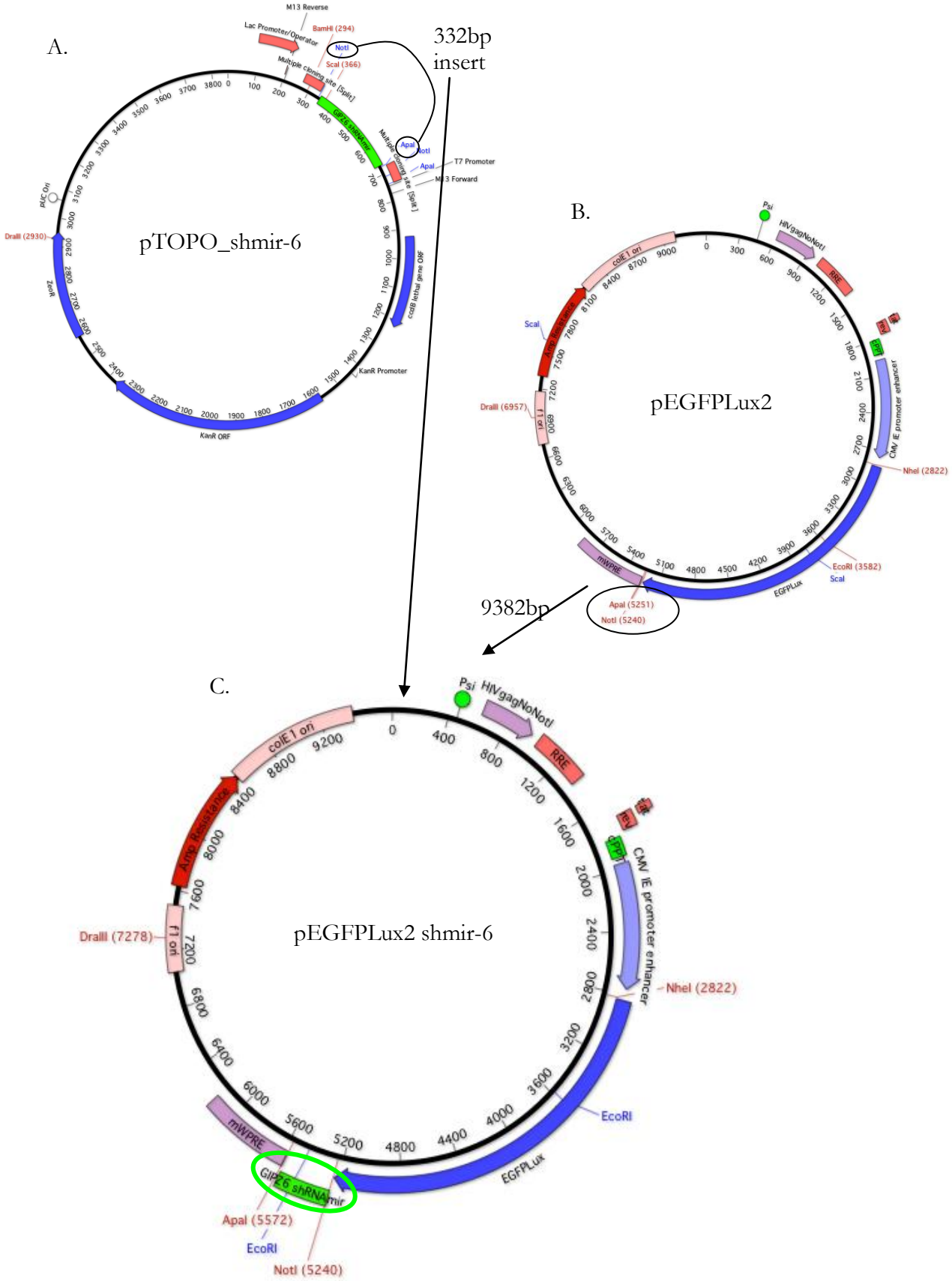

Figure 4.6. Schematic of the restriction digests required to make pEGFPLux2-shmir-6

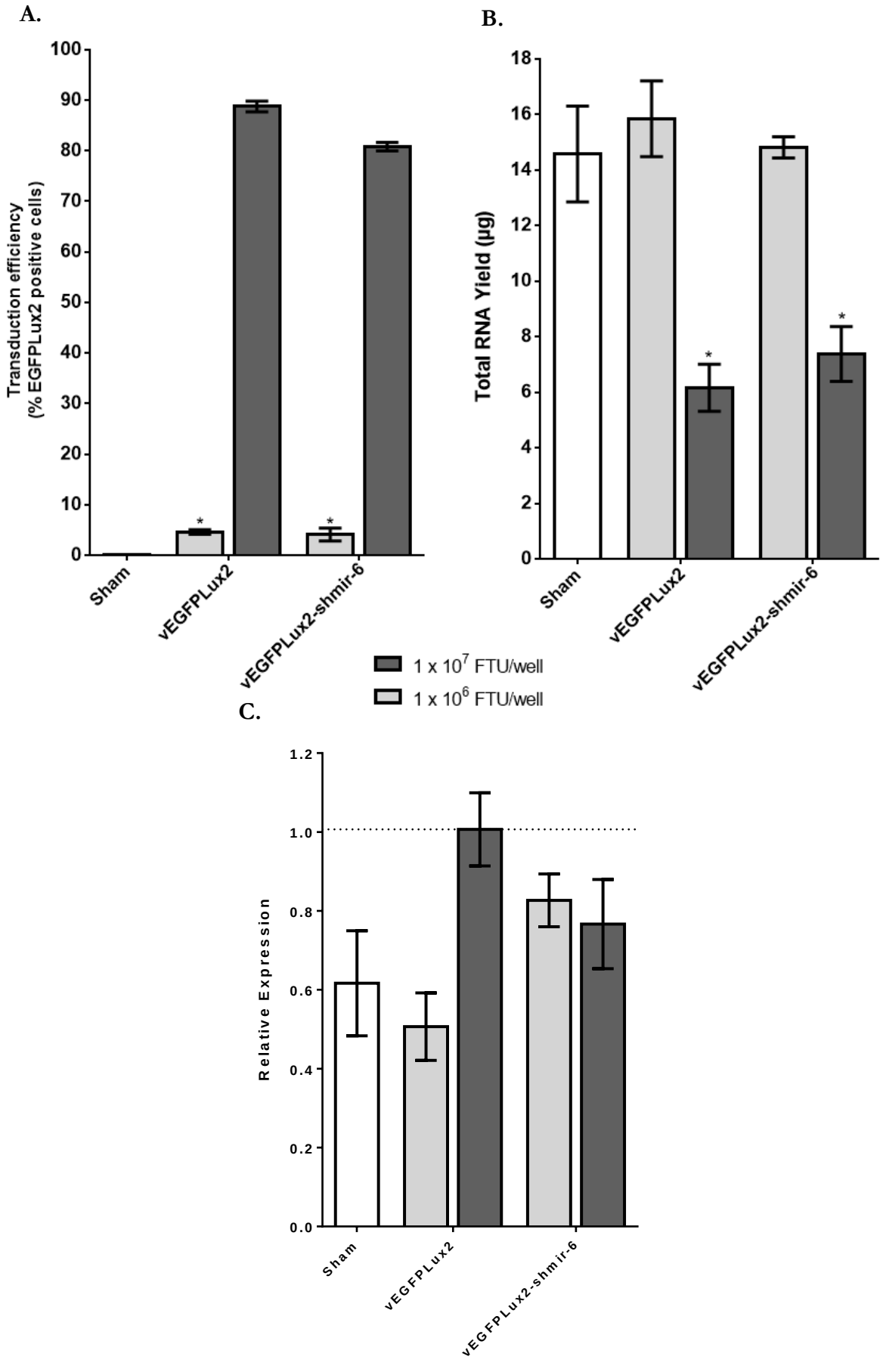
A.
Transduction efficiency (% EGFPLux2 positive cells)
100
90
80
70
60
50
40
30
20
10
0
*
*
Sham
vEGFPLux2
vEGFPLux2-shmir-6
B.
Total RNA Yield (µg)
18
16
14
12
10
8
6
4
2
0
*
*
Sham
vEGFPLux2
vEGFPLux2-shmir-6
1 x 10^7 FTU/well
1 x 10^6 FTU/well
C.
Relative Expression
1.2
1.0
0.8
0.6
0.4
0.2
0.0
Sham
vEGFPLux2
vEGFPLux2-shmir-6

Figure 4.7. Flow cytometry and RNA analyses of A549 cells transduced with vEGFPLux2 or vEGFPLux2-shmir-6 at two different doses

A549 cells were seeded at 2 x 10^5 cells/ml 24 hours prior to transduction with either 1 x 10^7 FTU (high dose; dark grey) or 1 x 10^6 FTU (low dose; light grey) of either vEGFPLux2 or vEGFPLux2-shmir-6. Sham treatments received media but no virus (white bars). Cells were harvested 72 hours post-transduction and the transduction efficiency determined as the percentage of EGFPLux2 positive cells (A). Total RNA was also extracted and RNA yield determined (B). The relative expression of hENaCα was calculated compared to the vEGFPLux2 (high dose) control (C). Bars represent the mean ± SEM for n=3 wells. * $p<0.05$ ANOVA versus vEGFPLux2 (high dose) with Tukey's multiple comparison post-hoc test.

There were no differences in total RNA yield between the sham and low dose treatments, However, the high dose treatment resulted in a significant decrease in total RNA yield to less than 50% of sham-treated cells (Figure 4.7B). The relative expression of hENaCα was determined for each treatment relative to the high dose of vEGFPLux2, as the non-shRNAmir-containing equivalent of vEGFPLux2-shmir-6. No significant decrease in hENaCα expression was observed between vEGFPLux2 and vEGFPLux2-shmir-6 at either dose (Low dose: $p=0.227$; High dose: $p=0.480$; Figure 4.7C).

Due to the significant decrease in total RNA yield at the high dose and the low transduction efficiency of virus at the low dose, the experiment was repeated with an extended range of viral doses: 1×10^7, 8×10^6, 6×10^6 and 4×10^6 FTU/well. A dose response was observed with both viruses, with higher doses achieving significantly greater transduction efficiencies than lower doses (Figure 4.8A). Total RNA yield was largely unaffected by viral dose, although most of the virus-treated wells had significantly lower total RNA than the sham treatment (Figure 4.8B). No significant reduction in hENaCα expression was observed between the vEGFPLux2 and vEGFPLux2-shmir-6 treated cells at any dose (Figure 4.8C).

A.

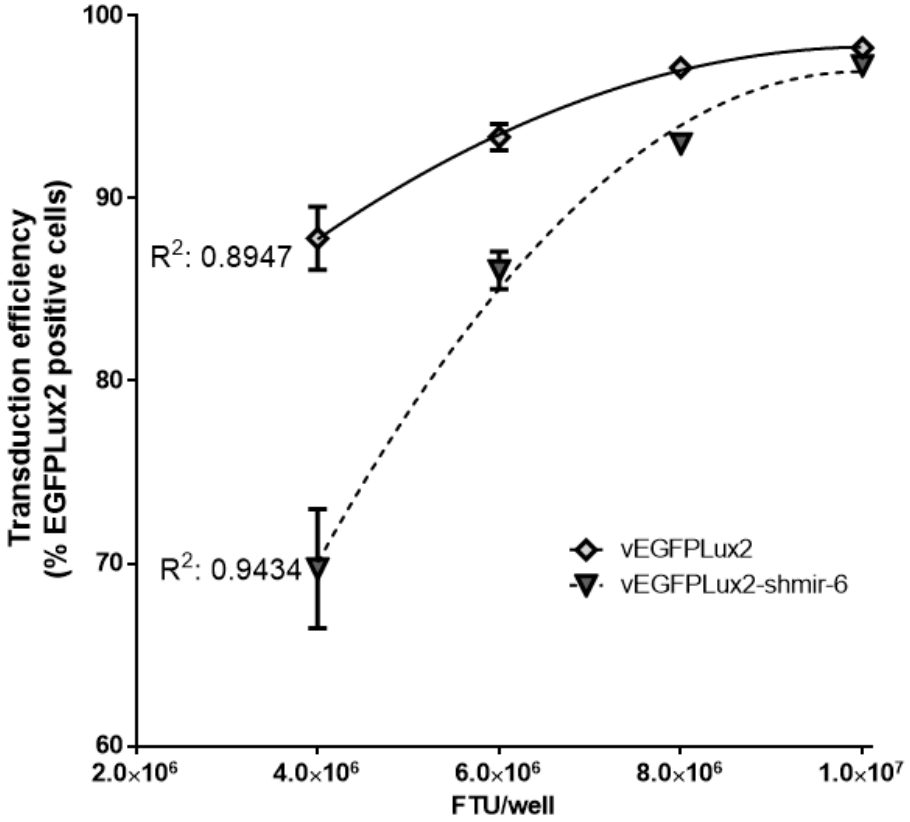
100
90
80
70
60
Transduction efficiency
(% EGFPLux2 positive cells)
R2: 0.8947
R2: 0.9434
vEGFPLux2
vEGFPLux2-shmir-6
2.0×10^6
4.0×10^6
6.0×10^6
8.0×10^6
1.0×10^7
FTU/well

B.

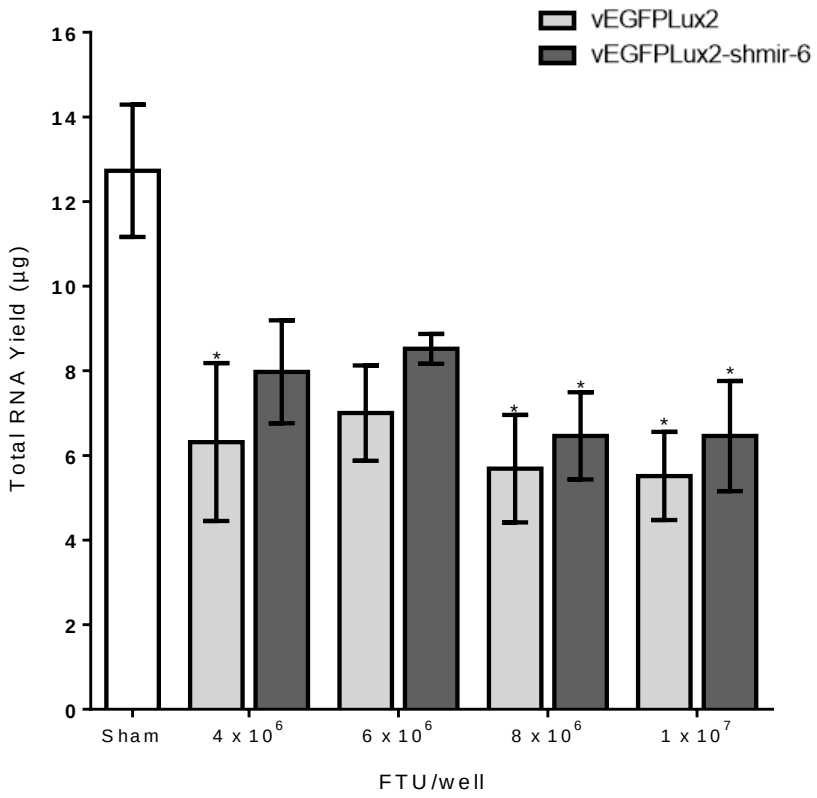
vEGFPLux2
vEGFPLux2-shmir-6
16
14
12
10
8
6
4
2
0
Total RNA Yield (µg)
Sham
4 x 10^6
6 x 10^6
8 x 10^6
1 x 10^7
FTU/well

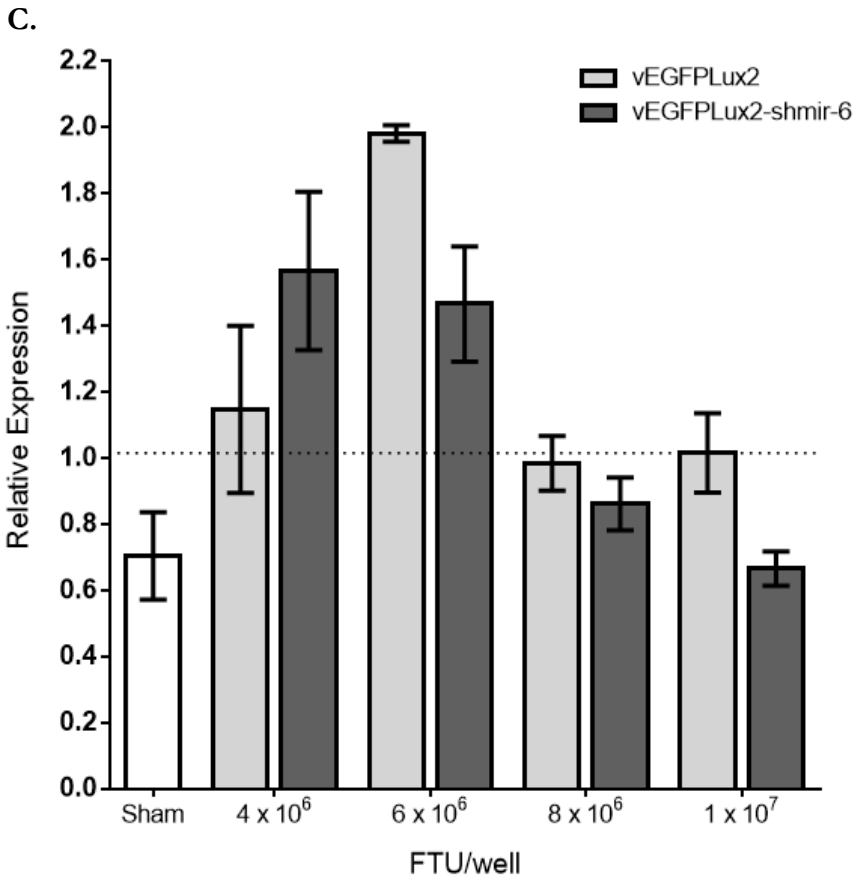

Figure 4.8. Flow cytometry and RNA analyses of A549 cells transduced with vEGFPLux2 or vEGFPLux2-shmir-6 at four different doses.

A549 cells were seeded at 2 x 10^5 cells/ml 24 hours prior to transduction with four different doses of vEGFPLux2 or vEGFPLux2-shmir-6. Flow cytometry was used to determine the percentage of EGFPLux2 positive cells, which was plotted against dose to reveal non-linear apparently saturating regression (A; R^2 as indicated). Total RNA yield was determined (B) and relative expression of hENaCα was compared to the vEGFPLux2 1 x 10^7 FTU dose. Bars represent the mean ± SEM for n=3 wells. * $p<0.05$ ANOVA versus sham with Tukey's multiple comparison post-hoc test.

4.2.3.3 Altering the viral incubation duration of vEGFPLux2 on A549 cells.

The dose response studies in section 4.2.3.2 led to the use of 6 x 10^6 FTU per well as the dose for future studies in A549 cells as this resulted in transduction of >80% of cells (Figure 4.8A) with no significant decrease in total RNA yield compared to the sham treatment (Figure 4.8B). However, no decrease in relative expression of hENaCα could be observed at this dose with vEGFPLux2-shmir-6 compared to vEGFPLux2 (Figure 4.8C). As the duration of virus incubation on the cells before harvest might contribute to the decrease in RNA yield observed (Figure 4.7B and Figure 4.8B), a subsequent study examined the impact of a post-transduction media change at 2, 4, 8 or 24 hours. Cells were harvested for flow cytometry and RNA analyses 72 hours post-transduction. Transduction efficiency increased with virus incubation duration (Figure 4.9A) showing a linear increase between 2 and 24 hours (broken line) of incubation with a plateau at 72 hours of incubation (solid line), suggesting that at some time between 24 and 72 hours of virus incubation the maximum transduction efficiency had been reached. Total RNA yield was not significantly lower with any incubation period compared with the sham treatment, (Figure 4.9B), however a significant decrease in cell viability, as determined by flow cytometry, was observed after 72 hours of incubation compared with the other incubation periods and the sham treatment (Figure 4.9C). The confluence and appearance of the cells was greatly improved with the 24 hour incubation compared with the 72 hour incubation, with fewer detached cells (Figure 4.9D). The 24 hour viral incubation duration was chosen for future studies; the transduction efficiency was >60% (Figure 4.9A), there is no significant decrease in total RNA yield (Figure 4.9B) or cell viability (Figure 4.9C) compared with the sham treatment, and the cells appear healthy at harvest (Figure 4.9D).

A.

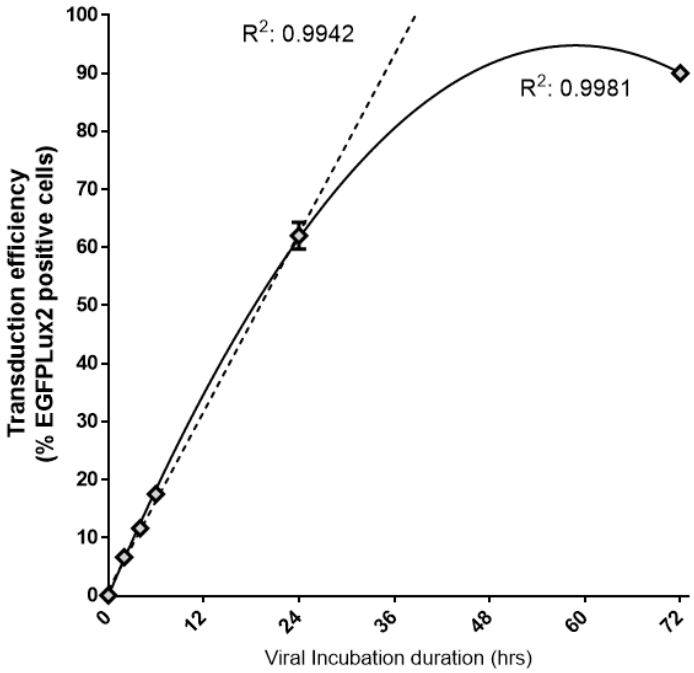
R2: 0.9942
R2: 0.9981
Transduction efficiency (% EGFPLux2 positive cells)
Viral Incubation duration (hrs)

B.

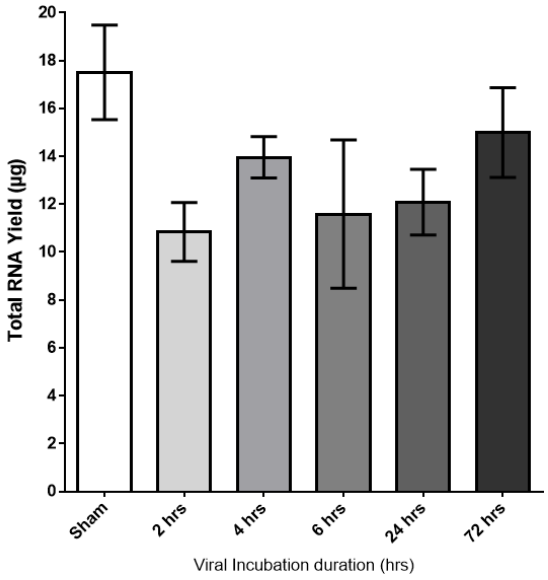
Total RNA Yield (µg)
Sham
2 hrs
4 hrs
6 hrs
24 hrs
72 hrs
Viral Incubation duration (hrs)

C.

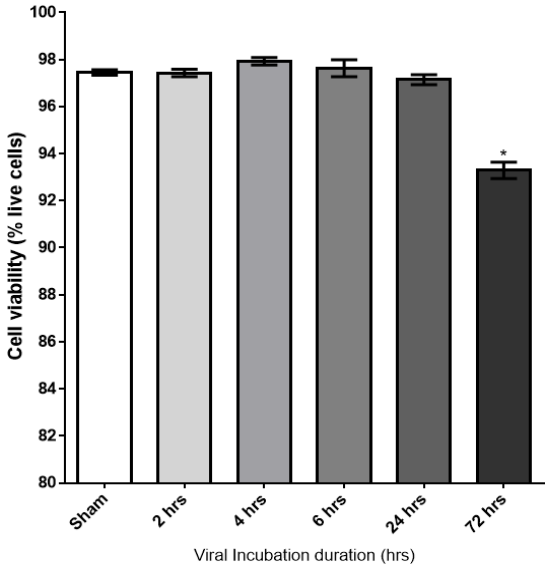
Cell viability (% live cells)
Sham
2 hrs
4 hrs
6 hrs
24 hrs
72 hrs
Viral Incubation duration (hrs)

D.

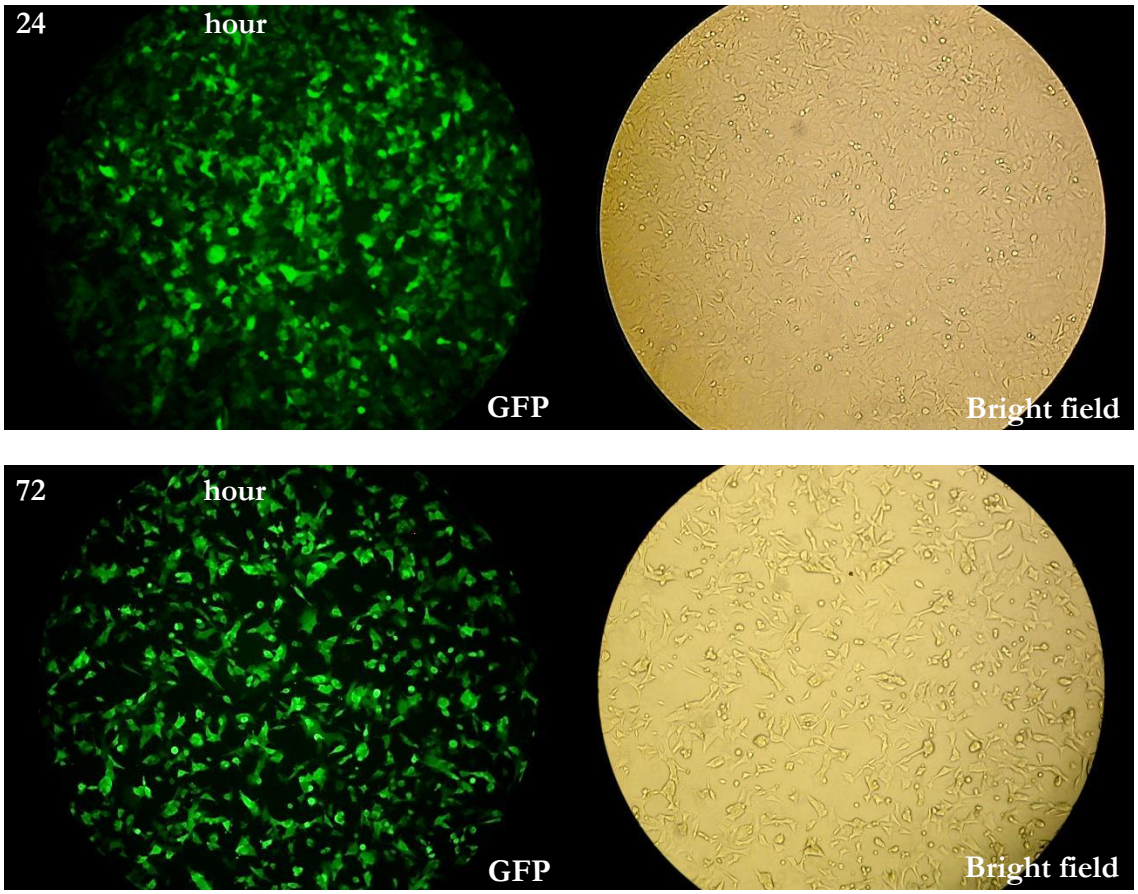

Figure 4.9. Flow cytometry and total RNA yield of A549 cells transduced with vEGFPLux2 for different viral incubation durations.

A549 cells were seeded at 2.5 x 10^5 cells/ml 24 hours prior to transduction with 6 x 10^6 FTU/well of vEGFPLux2 as in Figure 4.7 with varying virus incubation times. Non-linear (solid line) and linear (broken line) regression curves were fitted to the plot of virus incubation duration versus transduction efficiency (A). Total RNA yield was determined for each incubation duration (B) and cell viability was determined by flow cytometry (C). Representative photographs are shown of cells 72 hours post-transduction (D) following either 24 hours or 72 hours of viral incubation.

Bars and symbols represent the mean ± SEM for n=3 wells. * $p<0.05$ ANOVA versus sham treatment with Tukey's multiple comparison post-hoc test.

4.2.3.4 Screening shRNAmir sequences in A549 cells

The lack of detectable hENaCα knockdown when transducing A549 cells with vEGFPLux2-shmir-6 could be due to poor efficacy of the shmir-6 sequence. To determine whether any of the shRNAmir sequences significantly knocked down hENaCα, compared with the vEGFPLux2 control, the shRNAmir sequences from pGIPZ-1 to pGIPZ-5 (shmir-1 to shmir-5) were amplified by PCR as described in section 4.2.3.1 and inserted into pCR-BluntII-TOPO. Sequencing demonstrated that all five shRNAmir sequences were successfully modified with 5' NotI and 3' ApaI restriction enzyme sites to facilitate insertion into pEGFPLux2. Multiple attempts to insert the shmir-1 sequence into pEGFPLux2 were unsuccessful as determined by incorrect restriction digest profiles, whereas all other insertions were successful. The remaining shRNAmir-containing plasmids were used to produce vEGFPLux2-shmir-2 to vEGFPLux2-shmir-5 VSV-G pseudotyped rLV viral particles with titres of between 1.7 x 10^7 and 4.2 x 10^7 FTU/ml (data not shown). To determine whether any of the vEGFPLux2-shmir rLVs knocked down hENaCα, A549 cells were transduced with 6 x 10^6 FTU/well of vEGFPLux2-shmir-2 to vEGFPLux2-shmir-6. Media was replaced at 24 hours post-transduction and cells harvested 72 hours post-transduction for flow cytometry and RNA extraction. The viruses containing the shmir-2 and shmir-6 sequences had transduction efficiencies of >50% in A549 cells, whereas the other viruses had transduction efficiencies >70% (Figure 4.10A). Cell viability was not compromised by viral transduction (data not shown), which was reflected in the total RNA yield (Figure 4.10B). There was a tendency towards a decrease in hENaCα relative expression with all shRNAmir viruses except vEGFPLux2-shmir-6, although there were no significant differences compared with vEGFPLux2 alone (Figure 4.10C). Power calculations revealed that due to the large standard deviation (up to 0.23) of some of the results, a sample size of up to six wells per treatment would be required to detect a significant knockdown 40% or higher with vEGFPLux2-shmir-3 and vEGFPLux2-shmir-4.

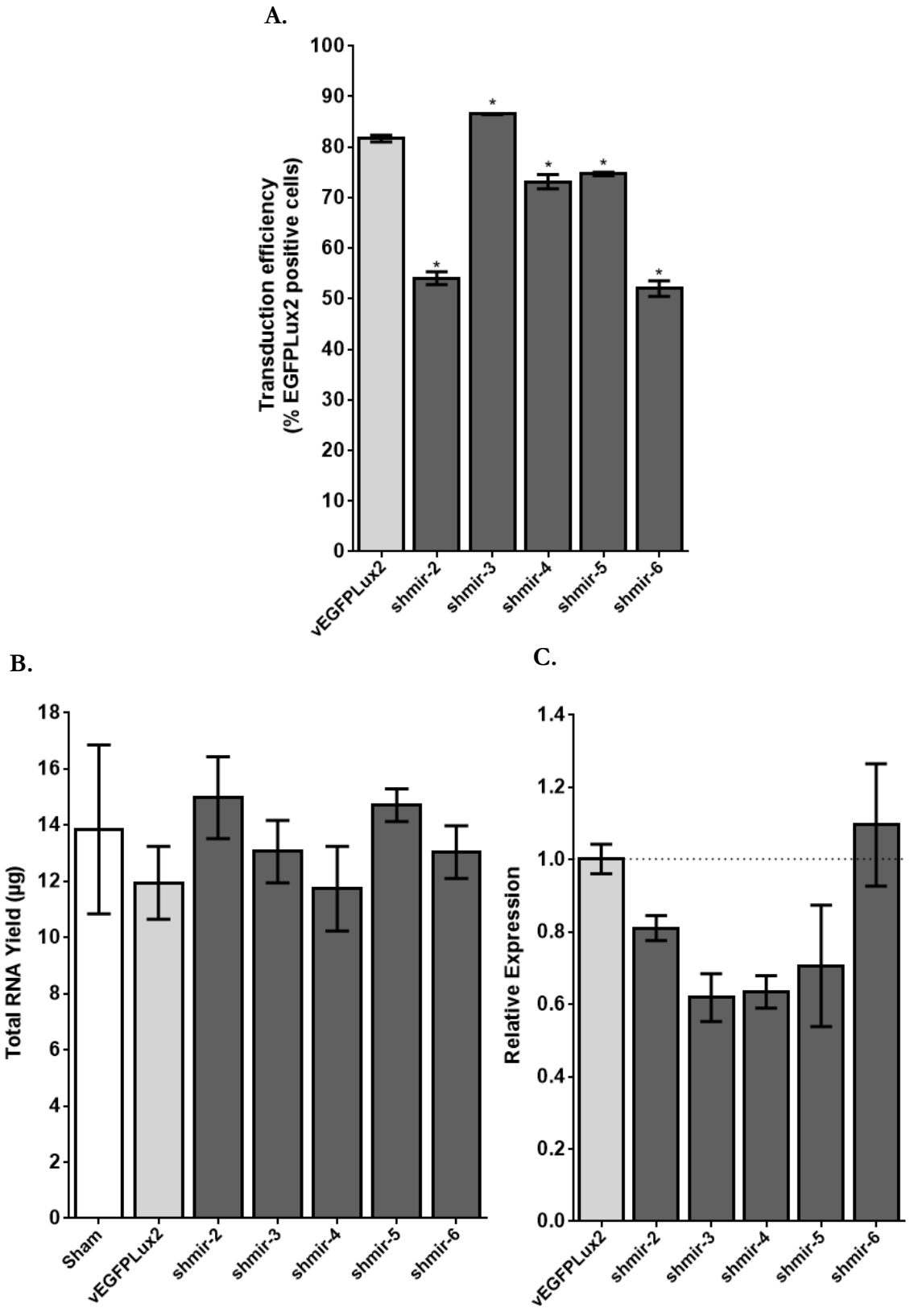
A.
Transduction efficiency (% EGFPLux2 positive cells)
100
90
80
70
60
50
40
30
20
10
0
*
vEGFPLux2
shmir-2
shmir-3
shmir-4
shmir-5
shmir-6
B.
Total RNA Yield (µg)
18
16
14
12
10
8
6
4
2
0
Sham
vEGFPLux2
shmir-2
shmir-3
shmir-4
shmir-5
shmir-6
C.
Relative Expression
1.4
1.2
1.0
0.8
0.6
0.4
0.2
0.0
vEGFPLux2
shmir-2
shmir-3
shmir-4
shmir-5
shmir-6

Figure 4.10. Flow cytometry and total RNA yield of A549 cells transduced with vEGFPLux2-shmir viruses.

A549 cells were seeded at 2 x 10^5 cells/ml 24 hours prior to transduction with 6 x 10^6 FTU/well of vEGFPLux2-shmir-2 to vEGFPLux2-shmir-6 (shmir-2 to shmir-6) with a media change at 24 hours post-transduction. Cells were harvested for flow cytometry and RNA extraction 72 hours post-transduction. The transduction efficiency (A), total RNA yield (B) and hENaCα relative expression (C) were determined as previously. Bars represent the mean ± SEM for n=3 wells. * $p<0.05$ ANOVA versus vEGFPLux2 (A and C) or sham treatment (B) with Tukey's multiple comparison post-hoc test.

Therefore, it is possible that vEGFPLux2-shmir3 and 4 were successful in knocking down hENaCα but the experiment lacked the power to detect this difference as being significant.

4.2.3.5 Improving the power of knockdown studies.

Virus vEGFPLux2-shmir-3 was selected to determine whether a significant difference in relative expression of hENaCα could be achieved by increasing the sample size from three to six, (>80% transduction efficiency and 38% knockdown; Figure 4.10). Cells were transduced, as previously, with vEGFPLux2 or vEGFPLux2-shmir-3 with a sample size of six. Both viruses had transduction efficiencies of >80% (data not shown) and there was no evidence of a decrease in total RNA yield in the vEFPLux2-shmir-3 treated wells (Figure 4.11A). However, there was no evidence of knockdown in vEGFPLux2-shmir-3 transduced wells compared with vEGFPLux2 alone (Figure 4.11B). One final attempt at knockdown using vEGFPLux2-shmir-3 was carried out, on this occasion with a sample size of 12, to determine whether the trend for knockdown observed in Figure 4.10C could be reproduced. A further 12 wells were transduced and allowed to express for a further 48 hours (120 hours post-transduction harvest, rather than 72 hours) to determine whether this longer time allowed for expression could increase knockdown effects. Cells were harvested 72 hours or 120 hours post-transduction for flow cytometry and RNA analyses. There was a significant decrease in the percentage of vEGFPLux2-shmir-3-transduced cells between 72 and 120 hours (Figure 4.12A) that was not observed with vEGFPLux2. This decrease could be due to the death of some of the vEGFPLux2-shmir3 transduced cells, however, there was no significant decrease in cell viability nor total RNA yield between time points suggesting that this is not the cause of the apparent lower transduction efficiency between time points (data not shown).

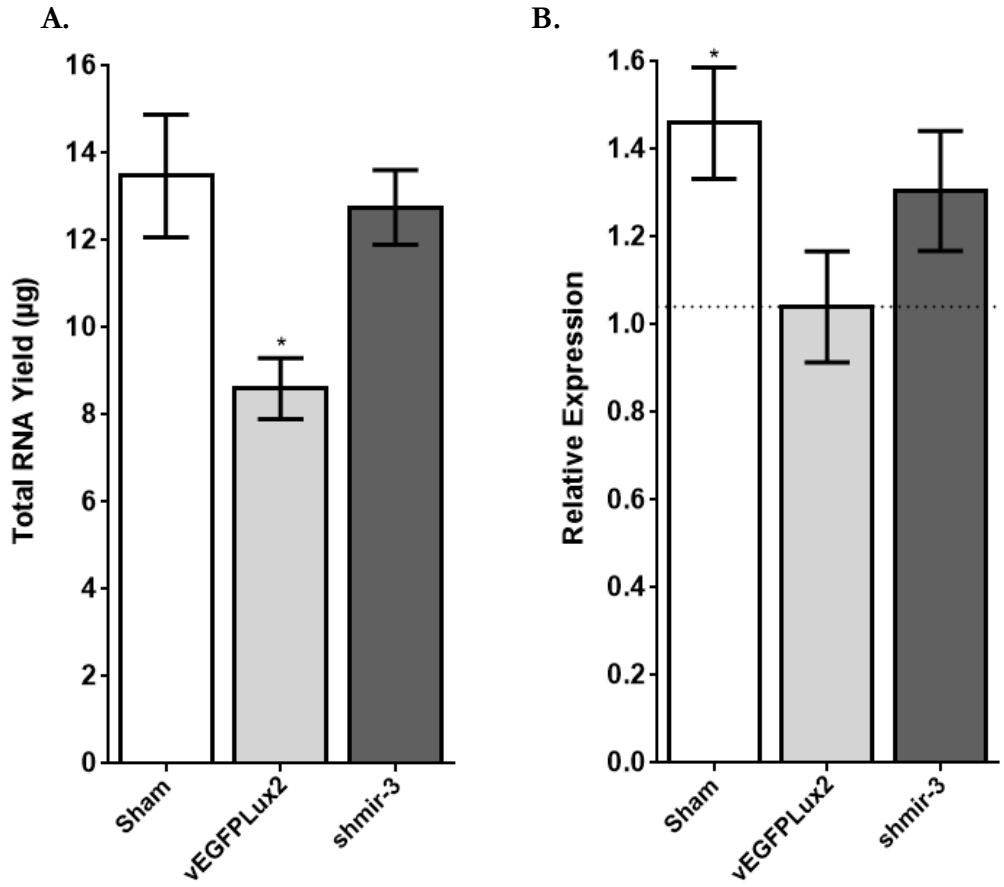

Figure 4.11. Yield and relative expression of RNA from A549 cells transduced with vEGFPLux2-shmir-3.

A549 cells were seeded at 2 x 10^5 cells/ml for 24 hours prior to transduction, as previously, with vEGFPLux2-shmir-3. Total RNA yield (A) and hENaCα relative expression (B) were determined as previously. Sham treatment was without virus (white). Bars represent the mean ± SEM for n=6 wells. * $p<0.05$ ANOVA versus sham treatment (A) or vEGFPLux2 (B) with Tukey's multiple comparison post-hoc test.

A.

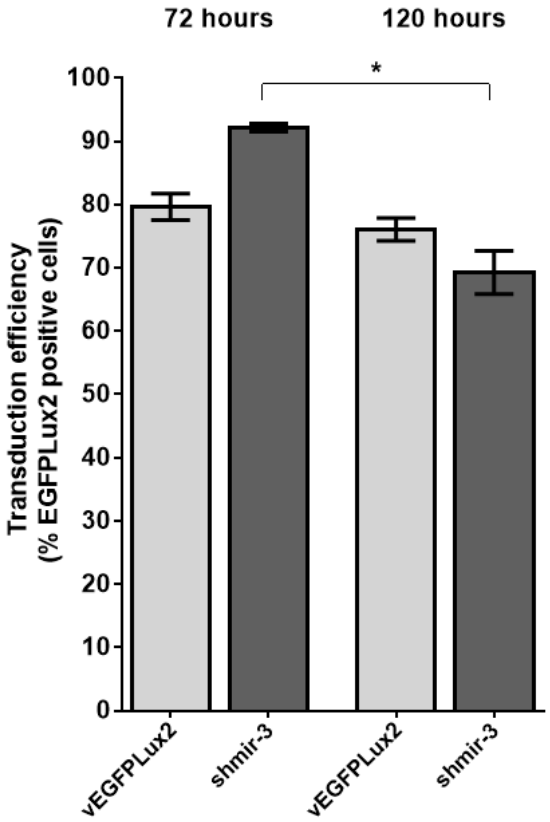
72 hours
120 hours
*
Transduction efficiency
(% EGFPLux2 positive cells)
100
90
80
70
60
50
40
30
20
10
0
vEGFPLux2
shmir-3
vEGFPLux2
shmir-3

B.

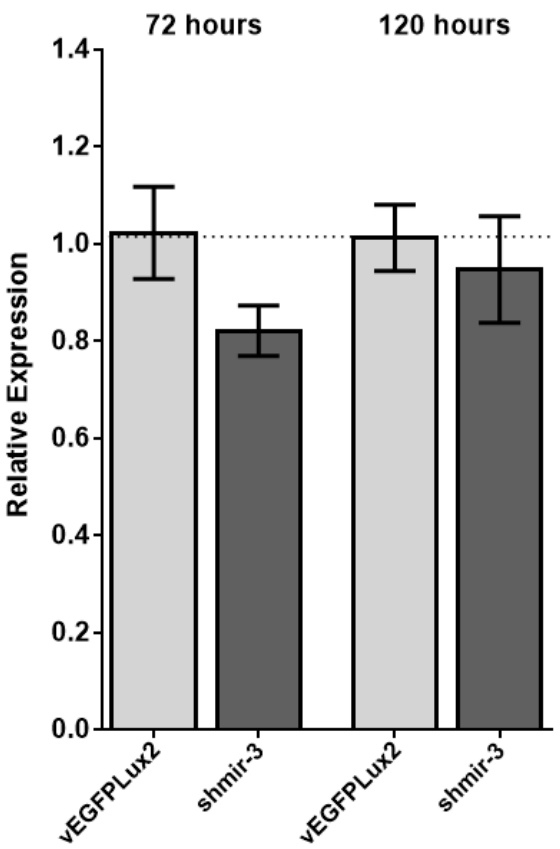
72 hours
120 hours
Relative Expression
1.4
1.2
1.0
0.8
0.6
0.4
0.2
0.0
vEGFPLux2
shmir-3
vEGFPLux2
shmir-3

C.

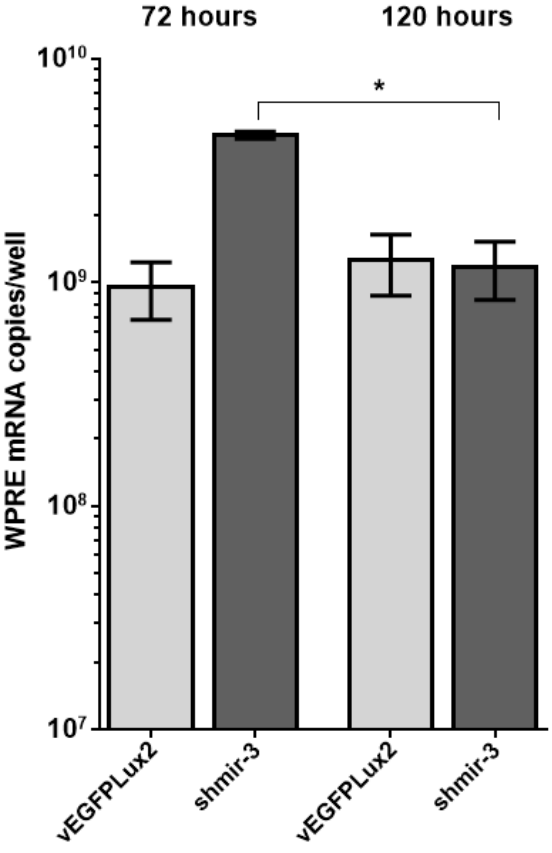
72 hours
120 hours
*
WPRE mRNA copies/well
10^{10}
10^{9}
10^{8}
10^{7}
vEGFPLux2
shmir-3
vEGFPLux2
shmir-3

Figure 4.12. Flow cytometry and RNA analyses of A549 cells transduced with vEGFPLux2-shmir-3 and harvested at 72 or 120 hours.

Cells were transduced as previously with vEGFPLux2 (light grey) or vEGFPLux2-shmir-3 (shmir-3; dark grey) and RNA was extracted at either 72 hours, or 120 hours post-transduction. Transduction efficiency (A) and hENaCα relative expression (B) were determined as previously. Transgene expression was also determined, by WPRE copy number analysis using an qRT-PCR assay (C). Bars represent the mean ± SEM for n=3 (A) and 6 or 12 (B and C) wells for vEGFPLux2 or vEGFPlux2-shmir-3 treated cells respectively.

* $p<0.05$ ANOVA with Tukey's multiple comparison post-hoc test.

There was no significant decrease in the relative expression of hENaCα in vEGFPLux2-shmir-3 transduced wells at either harvest time point (Figure 4.12B). The lack of knockdown observed with vEGFPLux2-shmir-3 could be due to the shRNAmir being processed incorrectly or not being expressed at all in the vector (Section 4.3). Although flow cytometry indicated that the EGFPLux2 transgene is expressed in >80% of cells in wells transduced with vEGFPLux2-mish3, it is possible that the downstream portion of the vector, encoding the shRNAmir, was not transcribed along with the transgene cassette (Figure 4.2). To determine whether this is the case, a qRT-PCR assay was used to quantify the copies of mWPRE mRNA present in the total RNA extracted from wells. An mWPRE RNA standard curve (gift of Stephanie Sumner-Jones) was run in parallel to interpolate the mWPRE copy number (Section 2.9.2; Sumner-Jones, personal communication). The shRNAmir sequence in vEGFPLux2-shmir-3 is situated between the EGFPLux2 sequence and the mWPRE sequence (Figure 4.6) therefore if the shRNAmir sequence is not expressed then mWPRE will not be expressed either. All transductions produced >9 x 10^8 mWPRE copies/well (c/well; Figure 4.12C) and there was a significant correlation between MFI and mWPRE copies/well ($p=0.009$, Pearson's correlation coefficient, $R^2 = 0.983$). These data confirm that the vEGFPLux2-shmir-3 transduced wells did produce mWPRE mRNA, which suggests that the entire expression cassette, including the shRNAmir, was expressed.

However, expression of the shRNAmir in the mRNA does not reveal whether the shRNAmir is subsequently processed correctly by the RNAi pathway (Section 4.3). It is also possible that shmir-3 does not effectively target hENaCα for knockdown. Overall, the use of shRNAmir in the vEGFPLux construct as a screening tool would require much further work to interpret (Section 4.3), therefore a more direct screening protocol was developed that would require fewer preparation steps.

4.2.4 Viral transduction for screening shRNA sequences in A549 cells.

To screen sequences more efficiently and in a viral context, it was anticipated that the original plasmid (pGIPZ) could be used directly to produce rLV viral particles. However, the pGIPZ backbone is not compatible with the third generation rLV production used routinely in the UKCFGTC and, combined with the concerns that the shRNAmir sequences may not be processed correctly in the dual-function system, this led to the use of shRNA sequences without the miR30 flanking sequence (Section 1.5.2). The shRNA sequences were chosen from an shRNA library designed by the RNAi Consortium (TRC) using an algorithm designed to rank potential 21mer anti-sense sequences based on their thermodynamic stability and potential off-target effects (Moffat et al., 2006). For a given target mRNA transcript five shRNAs were obtained in the pLKO backbone (pLKO-6 to pLKO-10): one targeting the 3'UTR of the target transcript, and four targeting the coding sequence (CDS): all spanning the entire transcript (Moffat et al., 2006). All of the sequences were shown previously to knock down hENaCα by 64 to 95% in the MCF-7 breast cancer cell line (Sigma-Aldrich) but there are no published reports of their use in A549 cells. These sequences were obtained in the pLKO.1 backbone (Figure 4.13A) that has the shRNA expressed from a polIII promoter (hU6), upstream of the puromycin selection gene (PuroR) expressed from a separate polII promoter (hPGK). The pLKO.1 plasmid is compatible with the third generation rLV production used within the UKCFGTC but does not contain a fluorescent reporter gene for functional titration via flow cytometry, nor the mWPRE sequence for particle titration. In this section a novel viral particle assay was developed to quantify preparations of HIV-based rLV vectors irrespective of their transgene or WPRE status.

A.

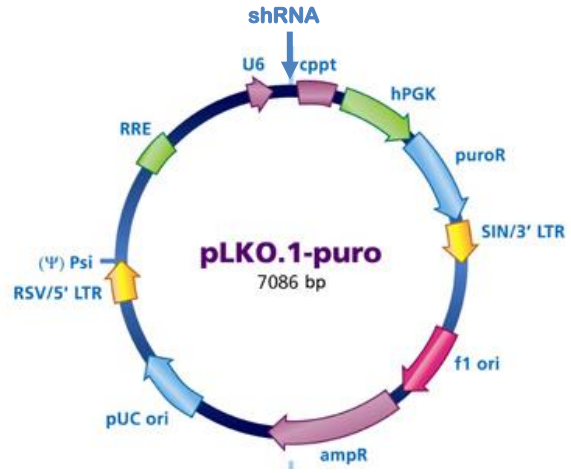

B.

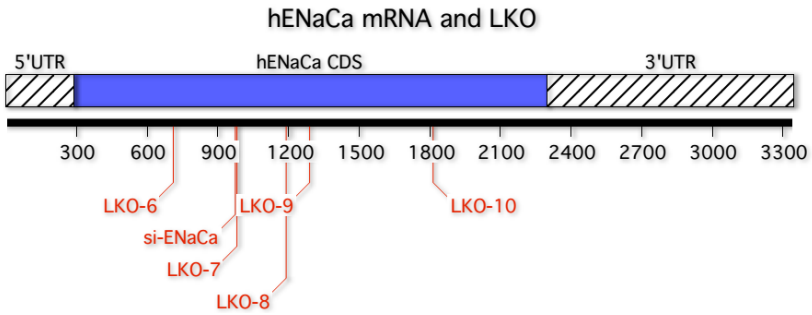

Figure 4.13. Map of the pLKO.1 backbone and the target sites of the anti-hENaCα sequences along the hENaCα transcript.

pLKO.1 viral genome plasmids (A) were used to produce rLV vectors for screening of shRNA sequences. This construct contains the puromycin resistance gene (PuroR) expressed from the human phosphoglycerate kinase (hPGK) polII promoter, downstream of the shRNA sequence expressed from a separate human U6 (hU6) polIII promoter. The target sequences of five anti-hENaCα shRNAs (LKO-6 to LKO-10) along the hENaCα transcript are indicated (B). Four target the coding sequence (CDS) whilst the fifth targets the 3' untranslated region (3'UTR). Figure A amended from the manufacturer's protocol (Sigma-Aldrich)

4.2.4.1 Design of a HIV backbone titration assay to determine the viral particle titre of LKO viral vectors.

Ideally, the new qRT-PCR assay would be based on amplifying a sequence shared between all HIV-based rLV genomes produced by the UKCFGTC to facilitate its usefulness. The plasmid design software MacVector (MacVector Inc., Waterbeach, Cambridge, UK) was used to determine whether there was a consensus sequence between the HIV-based plasmids and also the pLKO.1 backbone. Three plasmids were used to obtain the consensus sequence: pEGFPLux2.NotMod (pGM029; HIV not modular), pEGFPLux2 (pGM341; HIV modular), and pLKO.Scramble (HIV commercial; non-target shRNA; Table 2.1). All three plasmids shared some sequence identity, including in the region spanning the RSV/U3 hybrid to the cPPT that is incorporated into the rLV particle viral genome. This region is shared between all of the third generation HIV-based rLVs in the UKCFGTC. The consensus sequence was entered into Primer Design 3.0, and possible RNA primer sets (RPS: forward/reverse primer and probe) were examined for suitable target sites. A real-time TaqMan qRT-PCR primer set (RPS-HIVbb) was chosen for synthesis based its location between the Psi and RRE sequences (Table 2.2).

A standard curve was prepared for the HIVbb assay by making a five-fold dilution series of pLKO.Scramble. The standard curve was prepared to range from five to 78,125 copies per PCR reaction and copy numbers for the standards were calculated by determining the mass of a single pLKO.Scramble plasmid, and using this to determine the copy number per pg of DNA. All DNA standards could be detected and the assay had a dynamic linear range of between five and 78,125 DNA copies per PCR reaction, producing a >4 logs range (Figure 4.14A). The efficiency of the primers was ~99% as determined by the deviation of the slope from 100% efficiency (-3.32), with an R^2 of greater than 0.995). The primers were evaluated

with a range of lentiviral genome plasmids containing the target sequence and each was amplified efficiently (data not shown).

To examine the working range of the assay, viral RNA was extracted from aliquots of virus supernatant of vLKO-Scramble, vEGFPLux2 (vGM030) and vEGFPLux2.NotMod (vGM029) viral RNA were extracted (Section 2.7.1) and diluted 10-, 100- and 1000-fold and quantified using the RPS-HIVbb assay. All dilutions resulted in similar VP/ml values (Figure 4.14B) and for convenience only 100-fold dilutions were used in all future studies.

The pLKO-6 to pLKO-10 viral genome plasmids were used to produce VSVG-pseudotyped rLV vectors, as previously and subsequently, the RNA copies per ml, and thus viral particle titre (VP/ml; section 2.7.1) for each of the viral supernatants was determined by qRT-PCR with the RPS-HIVbb assay. To examine the working range of the assay, viral RNA was extracted (Section 2.7.1) and diluted 10-, 100- and 1000-fold and quantified using the RPS-HIVbb assay. All dilutions resulted in similar VP/ml values (Figure), for convenience, just 100-fold dilutions were used in all future studies.

4.2.4.2 Viral transduction for screening vLKO shRNAs in A549 cells.

Five pLKO.1 plasmids that target the CDS (pLKO-6 to pLKO-9) and 3'UTR (pLKO.10) of the hENaCα transcript (Figure 4.13B) were used as the rLV genome plasmid in production of VSV-G-pseudotyped rLV (vLKO-6 to vLKO-10). Viral genomic RNA (vRNA) was extracted from the vLKOs and particle titre determined using the RPS-HIVbb assay. All viruses were produced with over 1 x 10^8 VP/ml (Table 4.1), which were comparable to the titres observed previously for vLKO.Scramble production (Figure 4.14B). Vectors vLKO-7 and vLKO-8, which previously knocked down *hENaCa* mRNA expression to 64% and 95%, in the MCF-7 breast cancer cell line, relative to the non-target control (Table 4.1), were chosen for developing a knockdown screening protocol in A549 cells to determine whether a similar discrepancy in hENaCα knockdown could be observed.

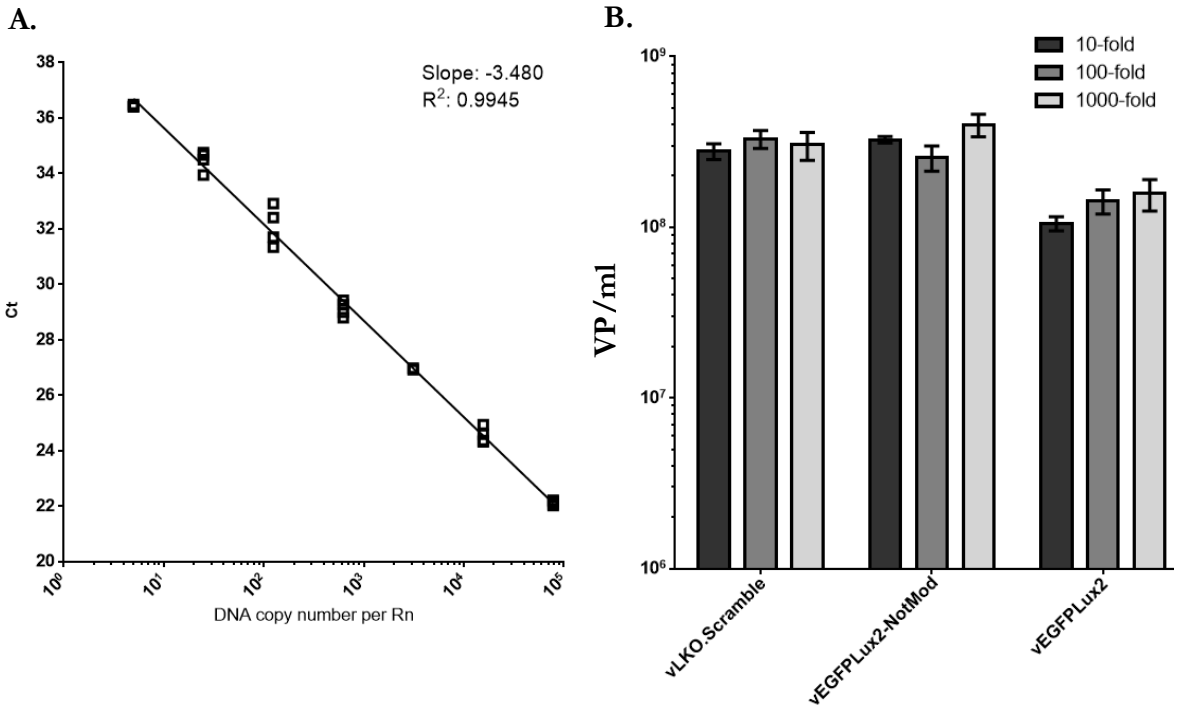

Figure 4.14. DNA copy number and viral particle titre using the RPS-HIVbb assay.

Plasmid DNA standards were prepared using pLKO.Scramble and used to test the efficiency and reproducibility of the RPS-HIVbb primer sets (A). Regression analysis was performed on the DNA copy number per reaction versus the cycle threshold (Ct). Representative plots are shown with the slope and R^2 regression indicated. Viral RNA from the rLV vectors produced in chapter 3 were used to determine the viral particle titre (VP/ml) using the RPS-HIVbb assays (B) using three dilutions of extracted viral RNA for input into the RT-PCR reaction. Bars represent the mean ± SEM of n=3 rLV preparations.

The vLKO.1 backbone contains the puromycin resistance gene (PuroR; Figure 4.13A), a selectable marker in mammalian cells, which can be used to enhance the percentage of transduced cells by addition of puromycin. In this section a screening protocol was developed for vLKO.1 shRNA sequences using vLKO-7 and vLKO-8 with puromycin selection.

The selected dose was based on the 6 x 10^6 FTU/well determined in chapter 3, which was approximately equivalent to 1.2 x 10^8 VP/well. Cells were transduced with 1.2 x 10^8 VP/well of vLKO.Scramble, vLKO-7 or vLKO-8. After 24 hours the media was replaced with fresh cell culture media containing 5μg/ml puromycin (Ahmed et al., 2010), and cells were harvested for RNA analyses 72 hours post-transduction. The vLKO-7 and vLKO-8 viruses knocked down hENaCα by 73% and 88% (Figure 4.15A). There were no significant decreases in total RNA yield between the sham-treated wells and wells transduced with virus (Figure 4.15B). The control virus, vLKO.Scramble, was assessed both with and without puromycin selection to determine whether puromycin altered the expression of hENaCα and to estimate the transduction efficiency of the LKO viruses. Puromycin did not significantly decrease *hENaCa* mRNA expression (Figure 4.15A) and cell counts suggested that a transduction efficiency of >90% was achieved (data not shown).

Virus name	vGM number	VP/ml	Knockdown in MCF-7 (%)
vLKO-6	vGM060	4.54×10^8	66
vLKO-7	vGM061	3.89×10^8	64
vLKO-8	vGM062	3.74×10^8	95
vLKO-9	vGM064	7.80×10^8	78
vLKO-10	vGM063	2.52×10^8	73

Table 4.1. Virus particle titres for anti-hENaCα vLKOs, determined using the RPS-HIVbb assay

The vLKO particles were titrated using the RPS-HIVbb viral particle assay developed in the previous sub-section. The percentage knockdown of hENaCα previously determined in MCF-7 cell lines by the supplier (Sigma-Aldrich, UK) is also shown. A list of all plasmids and viruses used in this thesis is provided in Table 2.1.

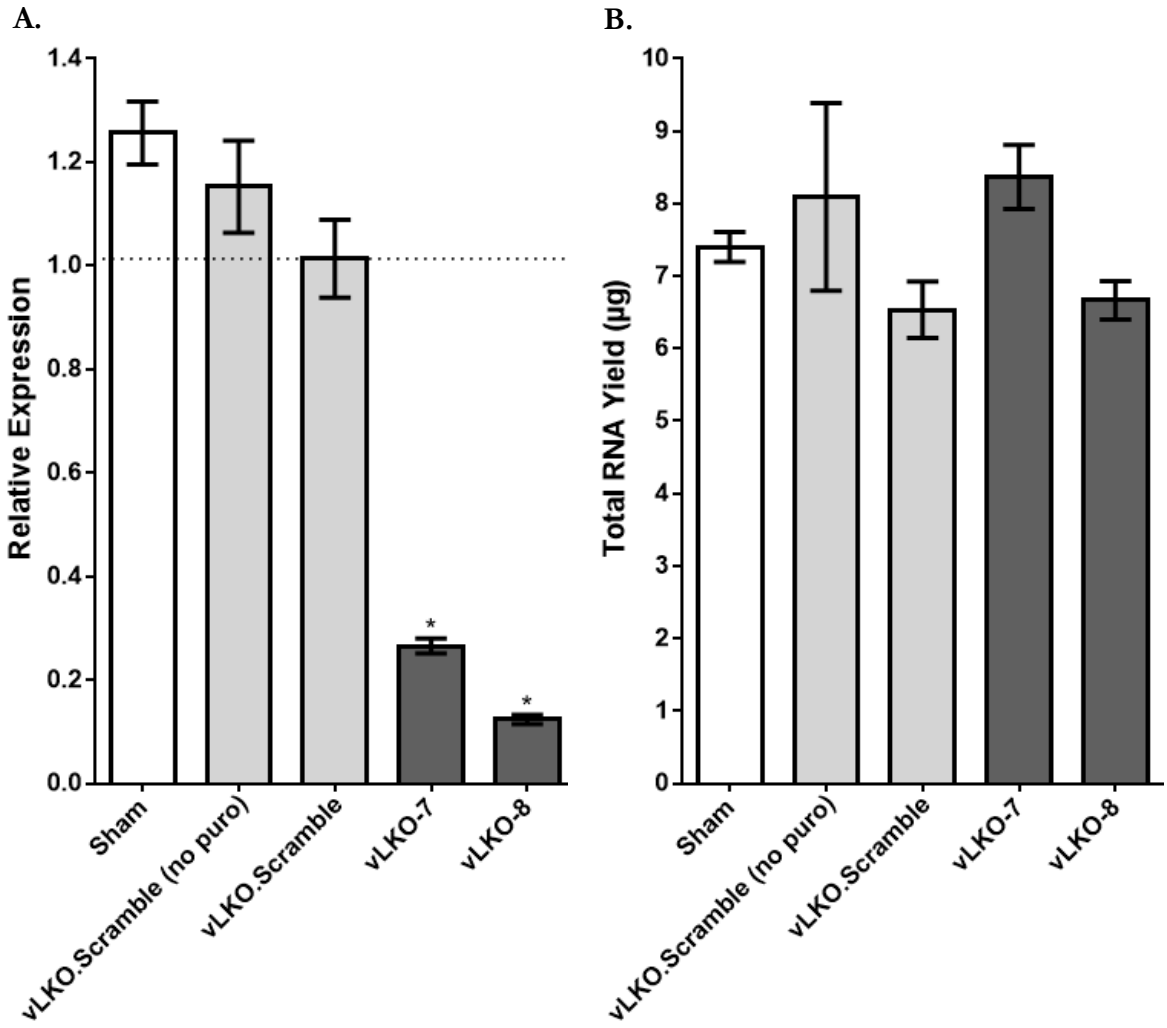

Figure 4.15. Total RNA yield and hENaCα relative expression of cells transduced with vLKO viruses and selected for with puromycin

Cells were transduced with 1.2 x 10^8 VP/well of vLKO.Scramble (light grey) or vLKO knockdown viruses (dark grey). Puromycin was added at the media change 24 hours post-transduction and cells were harvested 72 hours post-transduction for RNA analyses. The relative expression of hENaCα in vLKO-8 treated cells was determined compared with vLKO.Scramble treated cells (A) and total RNA yield was also measured (B). Sham treatments (white bars) and vLKO.Scramble (no puro) did not receive puromycin. Bars represent the mean ± SEM of n=6 wells. * $p<0.05$, ANOVA with Tukey's post-hoc versus vLKO.Scramble (A) or sham treatment (B).

4.3 Discussion

The aim of studies described in this Chapter was to develop a reliable protocol for screening potential knockdown sequences in A549 cells. Three protocols were evaluated: (a) transfection with plasmid DNA containing the RNAi expression cassette (Section 4.2.2); (b) transduction with rLV vectors containing an shRNAmir sequence expressed from the transgene cassette (Section 4.2.3), and finally, (c) transduction with rLV particles containing an shRNA sequence expressed from a separate promoter to the transgene (Section 4.2.4).

The knockdown target chosen for these studies was hENaCα due to implications of the overexpression of the ENaC channel in Cystic Fibrosis lung disease (Section 1.2.2). A qRT-PCR assay was evaluated to determine whether knockdown could be observed using an anti-ENaCα short interfering RNA (siRNA) that had been previously shown to significantly knock down ENaCα in both A549 cells and in mice (Clark et al., 2013). Human ENaCα was significantly knocked down by 66% compared to a scrambled siRNA molecule (siUC; Figure 4.1). This is similar to the >50% knockdown in ENaCα mRNA, and 63% knockdown in ENaCα protein observed in the published study (Clark et al., 2013).

Knockdown sequences were obtained either in the pGIPZ (Figure 4.2A) or pLKO.1 backbones (Figure 4.13A), both of which are suitable for producing rLV particles (Moffat et al., 2006). The pGIPZ viral genome plasmid contains an shRNA embedded in the human miR-30 sequence (shRNAmir; Figure 1.5) to allow processing of the knockdown sequence via the endogenous miRNA pathway (Boudreau et al., 2009) although this genome plasmid was only compatible with second generation rLV production and therefore could not be used to produce rLV vectors here.

The manufacturer suggests that pGIPZ plasmids can be used directly in transient transfection of cells, therefore a transfection protocol was developed to determine whether it was possible to screen the shRNAmir sequences in the pGIPZ backbone by transfecting A549 cells directly

with pGIPZ using Lipofectamine2000 (L2K).Although initial results, using sham-treated cells as the comparator, were encouraging suggesting that knockdown was achievable (data not shown), the use of pLKO.Scramble as a non-target shRNA control indicated that knockdown observed previously was not specific to ENaCα (Figure 4.4A). It has been reported that transfection of cells with pDNA can induce interferon production (Akusjarvi et al., 1987) and subsequent expression of interferon-stimulated genes (ISGs), particularly 2'-,5'-oligoadenylate synthetase 1 (OAS1), that leads to degradation of viral and cellular RNA (Samuel, 2001). This interferon response has also been observed when using L2K to transfect cells with rLV backbone plasmids expressing shRNA sequences (Bridge et al., 2003) so is not specific to the shRNAmir sequences. Interestingly, the same sequences transfected in the form of a chemically synthesised siRNA duplex rather than expressed from plasmid DNA did not induce the interferon response (Bridge et al., 2003). Although no analysis of interferon response was performed in the present study there was a significant decrease in total RNA yield, by >60% compared to the sham treatment control (Figure 4.4B). Furthermore, deterioration in cell morphology in transfected cells compared with the sham treatment could be observed (Figure 4.3) comprising of rounded, detached cells, similar to the effects observed upon transduction of cells with shRNA (Fish and Kruithof, 2004). Due to these issues complicating the interpretation of studies using pDNA transfection for knockdown studies, no further work was attempted using pDNA transfection.

Two different viral protocols were developed for viral screening: one using shRNAmir sequences (Section 4.2.3) and one using shRNA sequences (Section 4.2.4). The shRNAmir sequences were the preferred option due to an improved safety profile compared to shRNA. The toxicity concerns raised during the transfection protocol development are also relevant to transduction of RNAi sequences; transduction of rat neurons with shRNA-containing rLV particles induced the expression of ISGs including OAS1 and, at higher doses, protein kinase R (PKR) (Hutson et al., 2012), that leads to the global inhibition of mRNA synthesis (Samuel,

2001). In another study it was shown that rLV particles without the shRNA sequence did not significantly induce OAS1 over untransduced levels, but the particles containing the shRNA did (Fish and Kruithof, 2004). It is proposed that this increased induction of OAS1 is a result of the accumulation of unprocessed or aberrant RNA duplexes resulting from competition for RNAi machinery (Castanotto et al., 2007) and this is supported by the increased toxicity of shRNAs that are expressed more highly, independent of their knockdown efficacy (McBride et al., 2008). This toxicity may be abrogated by inserting the shRNA sequence into an shRNAmir context, without compromising the knockdown potential of the sequence (McBride et al., 2008), although elsewhere shRNAs have been proven more potent than the equivalent shRNAmir in knocking down target gene expression, and this has been attributed to greater levels of expression from a similar dose (Boudreau et al., 2008).

Since the shRNAmir-containing pGIPZ plasmids were incompatible with the preferred third generation rLV production, shRNAmir sequences from the pGIPZ were amplified using PCR and inserted into the third generation rLV compatible pHIV.EGFPLux2 (pGM341) plasmid, designed in chapter 3. The shRNAmir sequence was inserted between the EGFPLux2 transgene and the mWPRE sequence to create six hENaCα knockdown lentiviral vector genome plasmids: pEGFPLux2-shmir-1 to pEGFPLux2-shmir-6 (Figure 4.6). A dose of 6 x 10^6 FTU/well was established as the most suitable for screening as this dose of vEGFPLux2-shmir transduced over 80% of the cells in a well (Figure 4.8A) with minimal RNA loss (Figure 4.8B) and a tendency towards hENaCα knockdown (Figure 4.8C), although this was not statistically significant. The incubation time of the virus on the A549 cells was also reduced to 24 hours as this appeared to improve cell health compared with the 72 hour incubation (Figure 4.9D), and transduced over 60% of cells (Figure 4.9A). These parameters were used to screen the five vEGFPLux2-shmir VSV-G pseudotyped viruses that were successfully produced; unfortunately none gave significant hENaCα knockdown (Figure 4.10). The vEGFPLux2-shmir-3 virus had a tendency towards hENaCα knockdown and this virus was

re-tested using a greater number of samples to increase the statistical power; however no knockdown was observed (Figure 4.11B). One further attempt to detect knockdown was performed by harvesting cells at 120 hours rather than 72 hours post-transduction, to determine whether additional time allowed for increased shRNAmir expression resulting in detectable mRNA knockdown, however there were no significant differences in relative expression with either harvest time-point (Figure 4.12C). Whether the lack of predicted knockdown observed with these viral vectors was due to inefficient processing of the shRNAmir from the mRNA cassette, or due to the inability of the processed antisense sequence to knock down hENaCα was difficult to determine, therefore a protocol was developed to allow screening of RNAi sequences more directly.

Although toxicity has been observed with shRNA sequences in some cases (Boudreau et al., 2009), it is possible to minimise the stimulation of ISGs by careful selection of the dose and vector design to enable expression of sufficient shRNA for successful knockdown with minimal toxicity. The pLKO.1 backbone is compatible with third generation rLV particle production and contains the hU6 polIII promoter for expression of a 21-mer shRNA sequence (Figure 4.13A). Although sequences of this length have been associated with increased toxicity compared with 19-mer sequences (Fish and Kruithof, 2004; Grimm et al., 2006), delivered in rLV particles produced using the pLKO.1 backbone they have been shown not to induce the interferon pathway (Moffat et al., 2006). The backbone also contains the puromycin resistance gene (PuroR) expressed from the hPGK promoter for use as a selectable marker in mammalian cells. Five anti-hENaCα shRNA sequences were obtained in the pLKO.1 backbone (pLKO-6 to pLKO-10) and used to produce third generation rLV particles (vLKO-6 to vLKO-10; Table 4.1). The vLKO-7 and vLKO-8 viruses were chosen to use for development of the protocol as they had been shown previously to knock down hENaCα by 64% and 95% respectively in MCF-7 cells (Table 4.1), providing analysis of two shRNA sequences with potentially different efficacies in A549 cells. The protocol was tested

using the parameters established in section 4.2.3 (6 x 10^6 FTU/well; 24 hour viral incubation; 72 hour harvest) however, the LKO viruses do not contain a fluorescent reporter to readily measure functional viral titre therefore 1.2 x 10^8 VP/well was used which appeared to be equivalent to the 6 x 10^6 FTU/well (Section 4.2.4.2). Also, at the 24 hour media change puromycin was added for positive selection of transduced cells, which should result in the majority of cells at harvest expressing the shRNA. The vLKO-7 and vLKO-8 sequences significantly knocked down hENaCα by 73% and 88% respectively. Together, the estimated transduction efficiency of >90% without significant decrease in total RNA yield between sham and transduced cells (Figure 4.15B) and detection of knockdown similar to other studies (Moffat et al., 2006), suggest that delivery of 1.2 x 10^8 VP/well of vLKO with puromycin selection appear to be suitable conditions for screening shRNA sequences for knockdown.

Chapter 5: Simultaneous transgene expression and target gene knockdown, with recombinant Lentivirus (LV) in immortalised cell culture.

5.1 Introduction

In this chapter, the most effective anti-hENaCα shRNA sequence tested, Nash8, was inserted into the shRNA module of pEGFPLux2, and the EGFPLux2 reporter transgene replaced with soCFTR2, to create a dual-function plasmid for the production of rLV vectors capable of directing simultaneous hENaCα knockdown and CFTR transgene expression in A549 cells.

An alternative target for knockdown gene therapy in the lungs was also investigated: BACH1 is a transcription factor that is particularly involved in regulation of the cellular oxidative stress (OS) response and of the cell cycle (Warnatz et al., 2011). Pulmonary emphysema and chronic obstructive pulmonary disorder (COPD) can be caused by genetic disorders such as CF and alpha1-antitrypsin (AAT) deficiency and BACH1 upregulation has been reported in both (Goven et al., 2008; Tanimoto et al., 2009). Furthermore, the repression of BACH1 has been implicated in amelioration of symptoms associated with these diseases (Tanimoto et al., 2009; Hou et al., 2012). The involvement of BACH1 in the OS response is specifically through the repression of HMOX1, a molecule involved in the OS response in the lungs (Ryter and Choi, 2005; Ryter et al., 2007). Not only is BACH1 a target for gene knockdown for ameliorating the symptoms of chronic lung disease, but the concomitant upregulation of HMOX1 can act as a useful surrogate for specific BACH1 knockdown in cell culture: small decreases in BACH1 can cause large increases in HMOX1 expression (Raval et al., 2012; Wang et al., 2014). In section 5.2.7 BACH1 was assessed as a target for knockdown using the dual-function rLV vector system.

5.2 Results

5.2.1 Combining the Nash8 shRNA cassette and the soCFTR2 transgene to create a dual-function genome plasmid.

The shRNA sequence Nash8 knocked down *hENaCa* mRNA by 87% compared to the Scramble control shRNA (Figure 4.15), therefore Nash8 was chosen for insertion into the dual-function vector. The shRNA sequence was amplified from the LKO.1 backbone using PCR with primers designed to incorporate both the shRNA expression cassette and the adjacent cPPT sequence (Figure 5.1A and B). The PCR products were inserted into pCRII-Blunt-TOPO for amplification in TOP10 cells to produce pTOPO-Nash8 and pTOPO-Scramble, and subsequent sequencing of the shRNA expression cassette confirmed that the PCR was successful. The 546bp Nash8 and Scramble shRNA expression cassettes were removed from the pTOPO-shRNA plasmids using HpaI and EcoRV and inserted into the pHIV.EGFPLux2 (pGM341) backbone (Figure 5.1C), replacing the existing cPPT to create pNash8-EGFPLux2 (pGM392) and pScramble-EGFPLux2 (pGM393) respectively (Table 2.1; Figure 5.1D). To create a dual-function vector with therapeutic potential for CF lung disease, the EGFPLux2 transgene was replaced with a version of the CFTR cDNA known as soCFTR2 (Hyde et al., 2008).

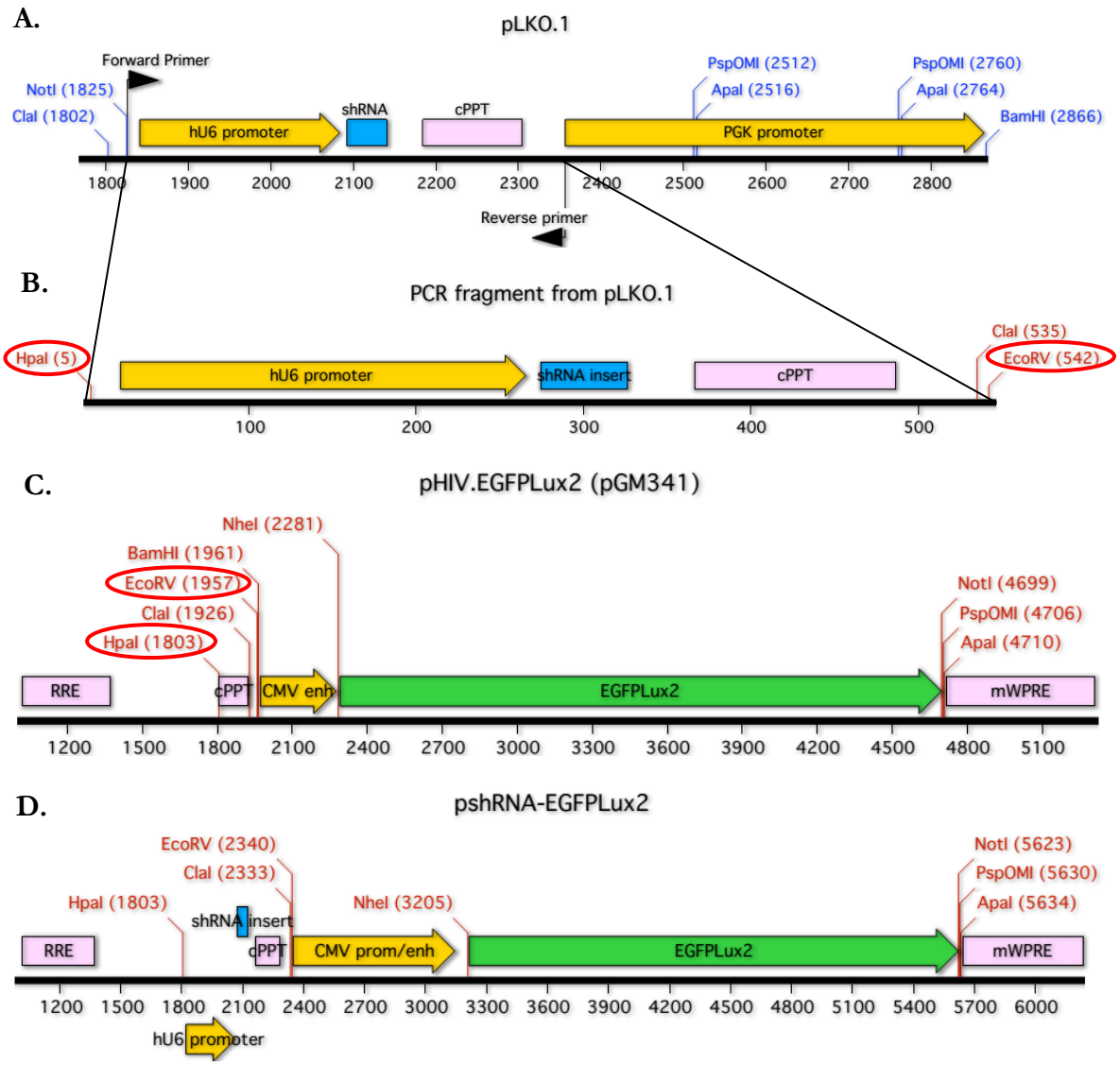

Figure 5.1. Amplification of the shRNA expression cassette in pLKO.1 and subsequent insertion into pHIV.EGFPLux2 to create the dual function genome plasmid

Primers were designed to introduce a 5' HpaI site and 3' ClaI/EcoRV sites into the pLKO.1 shRNA expression cassette (Primers GM12-648 and GM12-649 respectively; Table 2.2; A). These primers were used to amplify this region on the required fragments (B). Subsequent digestion with HpaI and EcoRV allowed insertion of the cPPT, hU6 promoter and shRNA into the HpaI/EcoRV site in pHIV.EGFPLux2 (pGM341; C), upstream of the transgene promoter, to generate the dual-function shRNA/EGFPLux2 virus genome plasmid (D). Restriction site are shown in red (single cut site) and blue (multiple cut sites) font.

The soCFTR2 cDNA has been codon-optimised to enhance translation and has been engineered to remove all CG dinucleotides from the sequences. The removal of CGs from promoters and transgenes has been shown to increase the duration of transgene expression following gene transfer in the lung (Hyde et al., 2008). Importantly, the soCFTR2 cDNA has been shown to encode a functional CFTR chloride channel in cell culture and to direct CFTR-specific chloride ion transport in the respiratory epithelial cells of CF patients (Jane Davies, Imperial College, London, personal communication). The 4453bp soCFTR2 fragment was digested from the soCFTR2-containing pGM169 (Table 2.2) using NheI and PspOMI and inserted into the NheI/PspOMI backbone of both pNash8-EGFPLux2 (pGM392) and pScramble-EGFPLux2 (pGM393) to produce pNash8-soCFTR2 (pGM395; Table 2.2) and pScramble-soCFTR2 (pGM396; Table 2.2) respectively. Both pNash8-soCFTR2 and pScramble-soCFTR2 shRNA expression cassettes were sequenced to confirm they were correct.

5.2.2 Functional assessment of pNash8-soCFTR2 using the iodide efflux assay.

In order to demonstrate that plasmids pNash8-soCFTR2 and pScramble-soCFTR2 were capable of expressing functional CFTR protein, they were used to transfect HEK293T cells in an iodide efflux assay performed by Mario Chan at Imperial College, London (Section 2.10). Plasmids pCIKCFTR (expressing CFTR) (McLachlan et al., 2011) and pCIK NLS β-Gal (expressing nuclear localising β-galactosidase) were used as positive and negative controls for functional CFTR expression respectively. Forty-eight hours post-transfection cells were incubated with Iodide^{125} (I^{125}) followed by forskolin addition to specifically stimulate CFTR activity. Radioactive iodide is used rather than chloride since the half-life of iodide is 59 days as opposed to the half-life of Cl^{36} which is ~300,000 years, and iodide is not transported by

many other non-CFTR Cl^- channels whereas Cl^- is. Thus the quantity of I^{125} present in the media surrounding the cells reflects the CFTR channel activity in the cell. Abundant CFTR activity was observed for both pNash8-soCFTR2 and pScramble-soCFTR2 in two separate experiments (n=6) (Figure 5.2 A and B) indicating that these dual-function plasmids express functional CFTR channels. Furthermore, presence of the anti-hENaCα shRNA Nash8 rather than the non-target control, Scramble, did not appear to negatively impact functional CFTR expression.

5.2.3 Target gene knockdown and transgene mRNA expression in A549 cells transduced with dual-function rLV vectors.

The dual-function viral genome plasmids created in section 5.2.1 were used to produce rLV vectors with the VSV-G pseudotype. The WPRE viral particle assay (Section 2.7.1) was used to quantify virus yield and indicated that virus preparations containing the EGFPLux2 transgene had 4-5x more viral particles (range: 1.48 x 10^9 to 1.88 x 10^9 VP/ml) than similar vector configurations containing the soCFTR2 cDNA (range: 3.55 x 10^8 to 4.70 x 10^8 to VP/ml) (Table 5.1). Inclusion of shRNA sequences appeared to have little or no effect on virus yield (Table 5.1). Virus configurations containing the EGFPLux2 transgene were also assessed using the functional titre assay based on EGFP expression in transduced cells, titres (Table 5.1; range: 1.97 x 10^7 to 2.48 x 10^7 FTU/ml) were similar to those of the shRNAmir-containing viruses produced in section 4.2.3.2. (2 x 10^7 FTU/ml)

To determine whether vNash8-EGFPLux2 or vNash8-soCFTR2 could knockdown *hENaCa* mRNA expression, A549 cells were transduced with 1775 VP/cell; a similar viral dose to the optimum (1550 VP/cell) for transduction, cell viability and RNA yield established in Section 3.3 (Figure 3.7). Parallel transductions with vScramble-EGFPLux2 and vScramble-soCFTR2 acted as experimental controls.

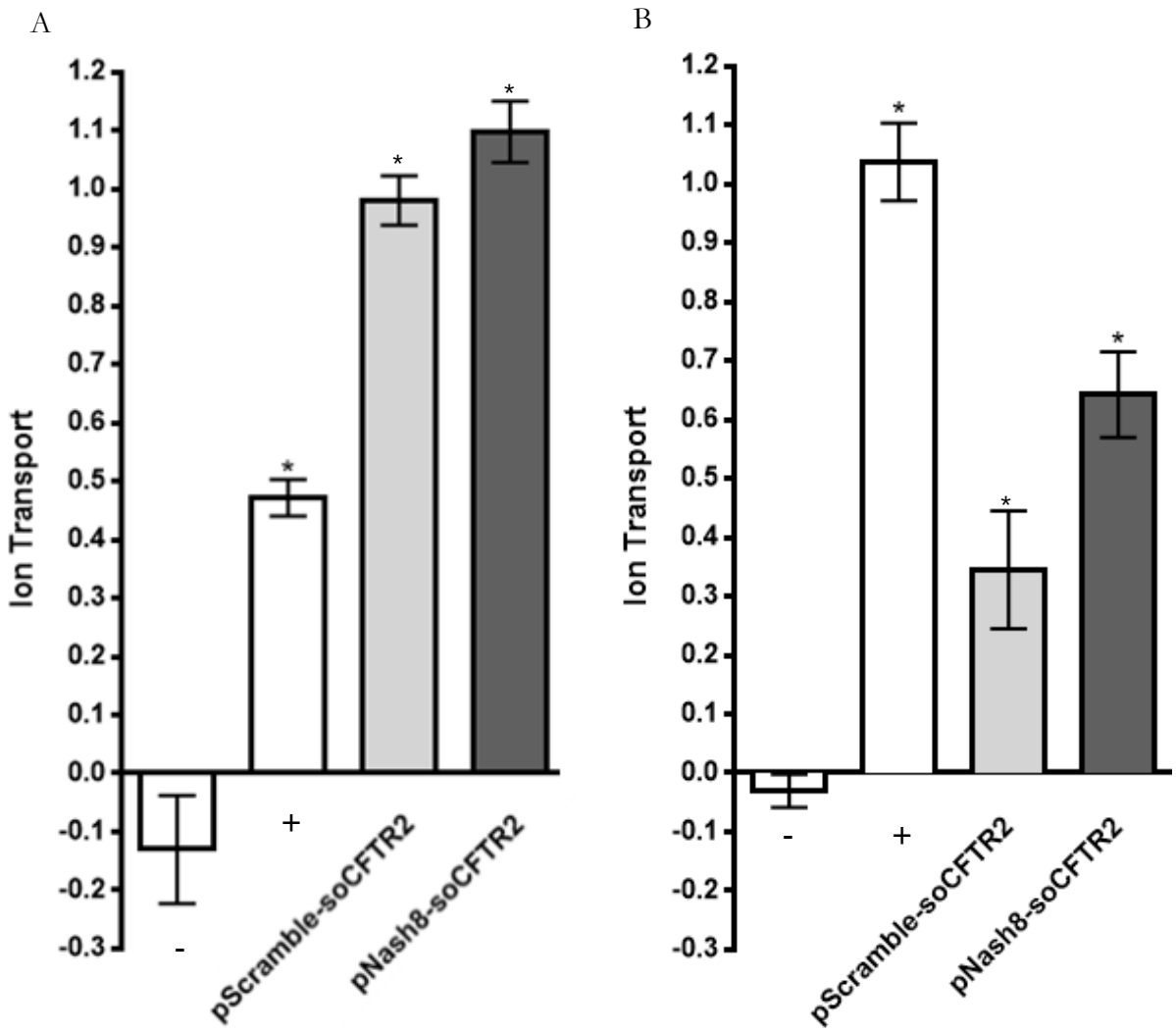

Figure 5.2. Functional CFTR channel detection in HEK293T cells

Adherent HEK293T cells were transfected with pScramble-soCFTR2 or pNash8-soCFTR2 and CFTR-specific ion transport detected using the iodide efflux assay (Section 2.10). Two independent experiments (A and B; n=6) were performed by Mario Chan (Imperial College, London) and I^{125} efflux detected. The plasmids pCIK CFTR (+) and pCIK NLS β-Gal (-) were used as the controls in this experiment. Bars represent the mean ± SEM. * $p<0.05$ versus pCIK NLS β-Gal (-), ANOVA with Tukey's post-hoc multiple comparison test.

Virus Name	vGM number	Functional titre FTU/ml	Particle titre WPRE VP/ml	EGFPLux2 to soCFTR2 fold difference
vEGFPLux2	vGM029	2.48×10^7	1.88×10^9	
vScramble-EGFPLux2	vGM084	2.04×10^7	1.48×10^9	
vNash8-EGFPLux2	vGM083	1.97×10^7	1.84×10^9	
vsoCFTR2	vGM081		4.70×10^8	4.00
vScramble-soCFTR2	vGM087		3.65×10^8	4.05
vNash8-soCFTR2	vGM086		3.55×10^8	5.18

Table 5.1. Titration details of dual-function rLV vectors pseudotyped with VSV-G

The dual-function viruses vEGFPLux2 (vGM029) and vsoCFTR2 (vGM081) were produced as VSV-G pseudotypes and given vGM numbers for cataloguing within the UKCFGTC. The functional titre, or number of Functional Transducing Units per ml of virus supernatant (FTU/ml) for vEGFPLux2 viruses was determined by flow cytometry, and the particle titre, or number of Virus Particles per ml (VP/ml) for all viruses was assayed using RT-PCR of WPRE. The fold difference between the vEGFPLux2 and the vsoCFTR2 preparations with the same shRNA sequences is indicated in the last column of the table. Functional titres are the average of three wells per virus, and WPRE particle titres are calculated from a single viral RNA extraction for each virus. For further details of the viruses see table 2.2.

Treatment with either of the Nash8 containing vectors resulted in significant hENaCα knockdown, by 71% and 85% respectively for vNash8-EGFPLux2 and vNash8-soCFTR2 compared with vScramble-EGFPLux2 ($p<0.05$; Figure 5.3A). Importantly, transgene expression (EGFPLux2 or soCFTR2) was confirmed for all dual vector configurations using the WPRE RT-PCR assay (Section 2.9.2) (Figure 5.3B). Interestingly, soCFTR2 expression was ~3x lower than EGFPLux2 expression, regardless of the shRNA present (Figure 5.3B) and unexpectedly, soCFTR2 transgene expression also appeared to significantly decrease hENaCα expression: a 31% decrease was observed between vScramble-EGFPLux2 and vScramble-soCFTR2, and a 48% decrease between vNash8-EGFPLux2 and vNash8-soCFTR2 (Figure 5.3A). These data indicate that the dual-function rLV vector can mediate both transgene expression and target mRNA knockdown.Optimising the CFTR Western blot assay for use in A549 cell culture

Although transgene RNA expression in cells transduced with dual-function rLV particles was detected by quantification of WPRE mRNA (Figure 5.3A) this does not prove that the complete transgene is expressed, or that it is successfully translated into protein. Expression of the EGFPLux2 protein was confirmed visually and by flow cytometry (data not shown). However, to determine whether the CFTR protein was successfully expressed Western blot analyses were performed. The detection of CFTR by Western blot has been difficult in the past due to poor antibodies available for this purpose, and various states of glycoprotein processing distorting CFTR band detection, often resulting in a large smear indicating the fully glycosylated CFTR protein, especially when the protein is expressed at high levels from a constitutive promoter.

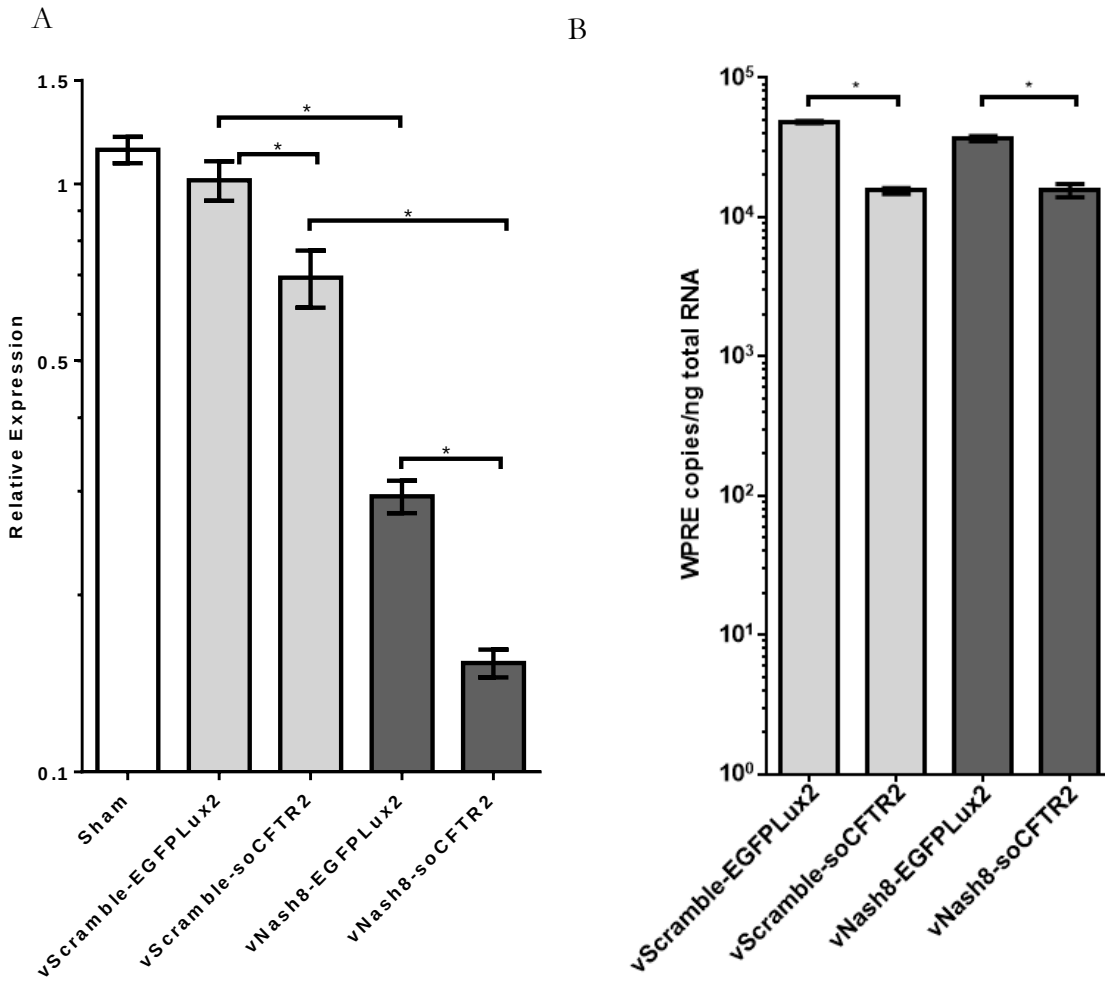

Figure 5.3. Relative hENaCα expression and transgene expression in A549 cells transduced with dual-function anti-ENaCα rLV vectors.

A549 cells were transduced with dual-function rLV targeting ENaCα (1775 VP/cell) and harvested at 72 hours post-transduction. The relative expression of *hENaCa* mRNA was determined using qRT-PCR with normalisation against GAPDH, and vScramble-EGFPLux2 as the comparator (A). Transgene expression was determined by calculating the WPRE mRNA copies per ng total RNA (B). The transduction efficiency of viruses expressing EGFP was ~60% according to flow cytometry (data not shown). Bars represent the mean ± SEM of n=6 cell culture wells. * $p<0.05$ ANOVA with Tukey's post-hoc multiple comparison test.

A549 cells, which do not express endogenous CFTR protein, and do not efflux iodide from CFTR-specific chloride channels (Uta Griesenbach, Imperial College, London, Personal Communication), were suitable for use as a negative control. Western blots performed with the established assay often resulted in a large amount of background and excess band detection when performed on protein extracted from HEK293T cells transduced with rLV particles expressing soCFTR2 (Mary Connolly, personal communication). Transfection of A549 and HEK293T cells here, with the non-viral pCIKCFTR vector using Lipofectamine 2000 also resulted in excess background, however, CFTR expression in HEK293T cells transfected with pCIKCFTR was evident (data not shown).

To choose the optimal conditions for the CFTR Western Blot, and to determine whether CFTR protein could be detected in A549 cells following transduction by rLV particles, A549 cells were transduced with either vEGFPLux2 or vsoCFTR2 at a dose of 1420 VP/cell and harvested 72 hours post-transduction. The transduction efficiency was approximately 55% according to manual cell counts of duplicate wells (data not shown). Bands corresponding to CFTR could be detected in total protein extracted from vsoCFTR2-transduced cells under all blotting conditions. The established blotting conditions (nitrocellulose with PBST buffer and no milk) were the only samples where background staining could be detected (Figure 5.4; left upper panel). Here, the CFTR was detected as an overexposed band spreading from around 130kDa to around 220kDa. Replacing the nitrocellulose membrane with polyvinylidene fluoride (PVDF) decreased the background and increased the resolution of the CFTR band (Figure 5.4; left lower-panel), as did the addition of 3% skimmed milk powder to the antibody incubation (Figure 5.4; centre and right panels). As observed in previous studies, three protein sizes could be detected for CFTR: the fully glycosylated protein (Band C), partially glycosylated protein (Band B) and the core glycosylated protein (Band A; Figure 5.4). Better resolution of these bands was obtained than when using PVDF as opposed to nitrocellulose (Figure 5.4).

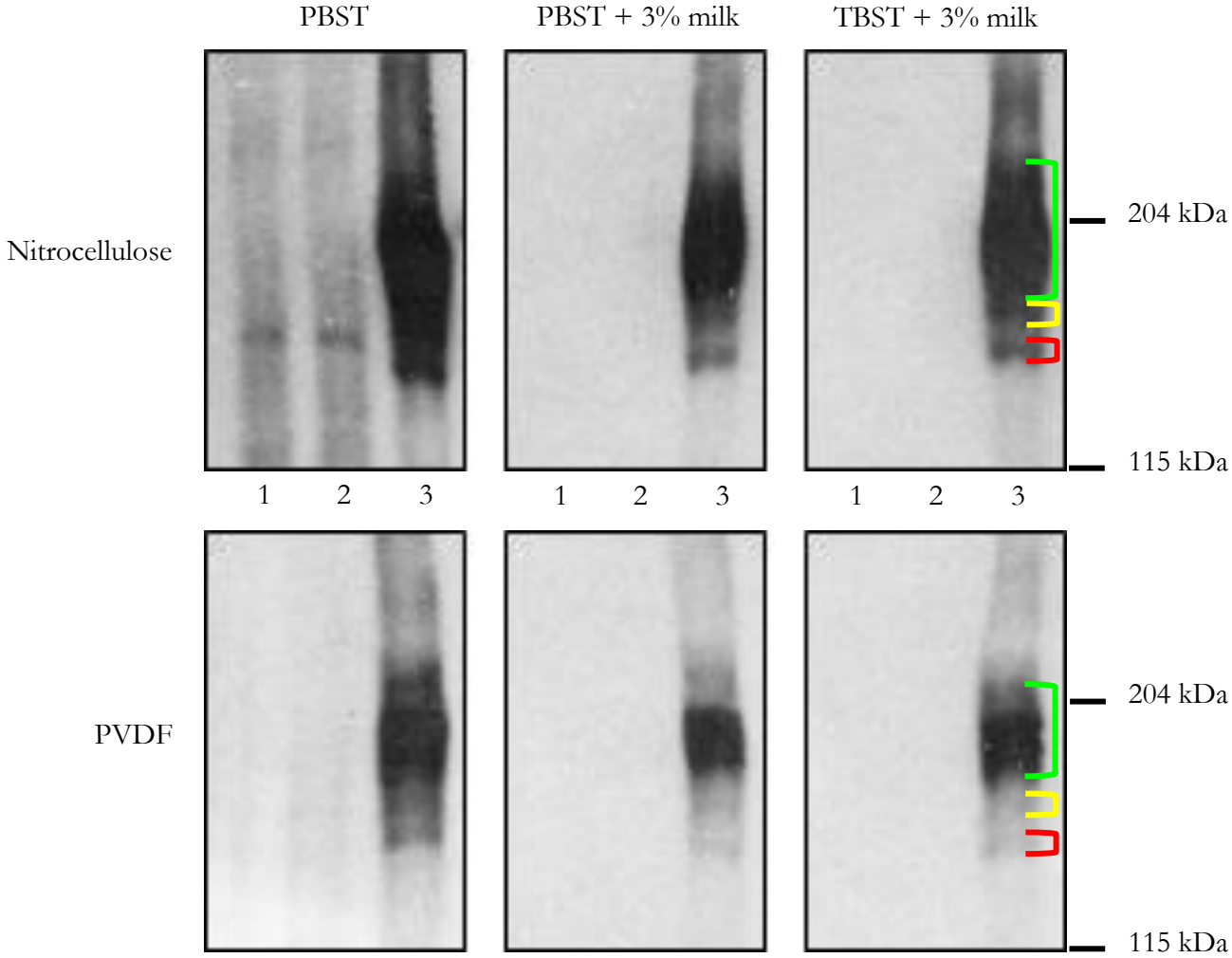

Figure 5.4. Images of CFTR Western blots of protein extracted from A549 cells transduced with vsoCFTR2.

A549 cells (Lane 1) were transduced with 1420 VP/cell of either vEGFPLux2 (Lane 2) or vsoCFTR2 (Lane 3). Total protein was extracted, and 15µg of protein in sample buffer separated by SDS-PAGE and blotted onto either a nitrocellulose (top panel) or polyvinylidene fluoride (PVDF; bottom panel) membrane. The antibody incubations on the membranes were performed in either PBST alone (left panel), PBST with 3% skimmed milk powder (middle panel) or TBST with 3% milk (right panel). Band A (red brackets; ~125kDa), band B (yellow brackets; ~130kDa) and band C (green brackets; ~160kDa) could be detected corresponding to core, partial and fully glycosylated CFTR respectively, where band C indicates the mature CFTR channel protein. Band sizes were estimated using the Precision Plus Kaleidoscope standards ladder (Bio-Rad). Photographs were taken of a 20s exposure to photographic film.

The data above suggest that the best conditions for detecting specific CFTR protein at a good resolution were blotting onto a PVDF membrane and using the TBST with 3% milk for antibody incubations (Section 2.9.4).

5.2.4 Optimising the ENaCα Western blot assay for use in A549 cell culture

The ENaCα protein is approximately 75kDa; however seven surface glycosylation sites result in a slower migration so that the protein appears to be approximately 100kDa (Voilley et al., 1994; McDonald et al., 1994). To determine the optimal conditions for detecting ENaCα protein in A549 cells expressing endogenous hENaCα, untreated cells were harvested for total protein (Section 2.9.4) and a variety of blotting conditions tested. A primary anti-ENaCα rabbit monoclonal antibody (gift from Ken Clark. Clark et al., 2013) was chosen that targets hENaCα residues 49-64, the region constituting the greatest variation between ENaC subunits ensuring greater specificity for the ENaCα subunit. Furthermore, these residues are located in the intracellular N-terminus of hENaCα, thus allowing detection of full-length glycosylated and core glycosylated products (100kDa and 85kDa respectively) and the shorter furin cleavage product of ENaCα (~30kDa) (Hughey et al., 2004) (Section 1.2.1). Multiple protein bands could be detected for hENaCα under all conditions, with two distinct bands detected around 100kDa and 85kDa (Figure 5.5).

The optimal amount of total protein required for detection of a >50% decrease in hENaCα protein was determined: untreated A549 cells were harvested and protein extracted as previously. ENaCα was readily visualised when >2μg was loaded (Figure 5.6, upper panel) with the ~100 kDa putative mature hENaCα the easiest to detect.

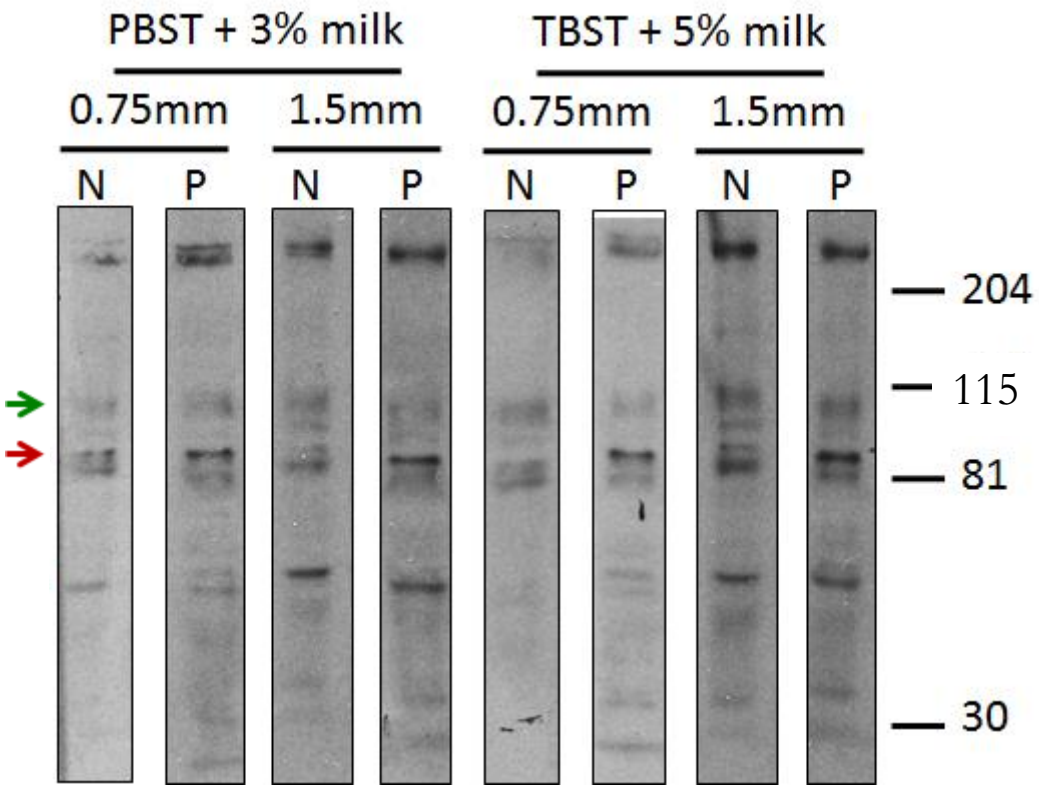

Figure 5.5. Images of hENaCα Western blots of protein extracted from A549 cells detected under different conditions.

Total protein (30 µg) from A549 cells was separated using either 0.75mm or 1.5mm thickness SDS-PAGE gels and protein transferred to either nitrocellulose (N) or PVDF (P) membranes, blocked with PBST/TBST plus milk. Primary anti-hENaCα rabbit antibody was diluted in blocking buffer (1:500) and added to the membranes. After washing, membranes were incubated with goat anti-rabbit IgG conjugated with HRP diluted in blocking buffer (1:10,000). Markers (Kaleidoscope ladder, Biorad, UK) are indicated in kDa. Bands could be detected for putative full length glycosylated (green arrow), and unglycosylated (red arrow) ENaCα at approximately 100kDa and 85kDa respectively, and could be detected to varying extents under the different conditions.

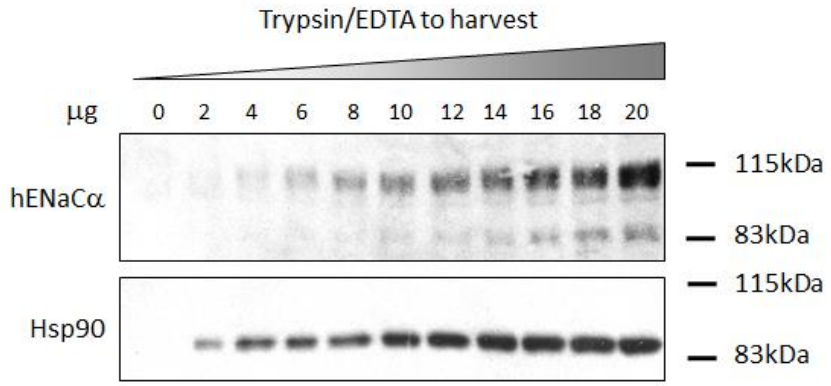

Figure 5.6. Images of ENaCα and Hsp90 proteins detected by Western blot with increasing quantities of input protein.

Between 2 and 20 µg of protein was extracted from untreated A549 cells, separated by SDS-PAGE and transferred to PVDF membranes. Human ENaCα (upper panel) and Hsp90 (lower panel) were detected using photographic film.

On a separate membrane the housekeeping protein Hsp90 (Greer et al., 2010) was detected using the primary antibody HSP90α/β (N-17) (Santa-Cruz Biotechnology, Inc.) (Section 2.9.4) and was easily detectable by eye at all quantities (Figure 5.6, lower panel). These data suggest that any protein input quantity between 8µg and 14µg would be appropriate for determining at least 50% knockdown of ENaCα protein under the conditions tested here. The loading control, Hsp90 was easily detected down to 2µg under the conditions tested however the signal was becoming saturated by 10µg of input protein. As the blot shown here was only given a flash exposure the protocol was adjusted for the experiments in section 5.2.6 to reduce the incubation time with ECL detection reagent from three minutes to one minute. The results here suggest that 14µg protein loaded onto the gel was sufficient to detect up to 85% knockdown of endogenous ENaCα (equivalent to 2µg input protein).

5.2.5 Detecting simultaneous CFTR protein expression and hENaCα protein knockdown in A549 cells transduced with dual-function rLV vectors

To determine whether CFTR expression and/or hENaCα knockdown could be detected at the protein level in A549 cells transduced with the dual function rLV, A549 cells were transduced with 1775 VP/cell of vScramble-EGFPLux2 (vGM084), vScramble-soCFTR2 (vGM087), vNash8-EGFPLux2 (vGM083) or vNash8-soCFTR2 (vGM086; Table 2.2) as previously. Cells were harvested at 72 hours post-transduction as previously, with an aliquot of cells from each well taken for RNA analyses and the remaining cells for each treatment combined and processed for protein extraction. Total protein (14 μg) was assayed for hENaCα, Hsp90 and CFTR by Western blot as previously (Figure 5.7A). CFTR protein could be detected at high levels after transduction with both of the soCFTR2-containing rLV vectors (Figure 5.7D). However, hENaCα protein knockdown could only be detected upon transduction of cells with the dual-function vNash8-soCFTR2 and not with vNash8-EGFPLux2 (Figure 5.7B and C). Both hENaCα bands were used to determine knockdown levels and densitometric analyses were performed separately for each band: for the ~100kDa band a knockdown of only ~25% could be detected, and with the ~85kDa band a knockdown of ~50% could be detected. Similar results were observed in a replicate experiment with a higher dose of virus (data not shown). The ENaCα quantitative results here were difficult to interpret due to apparent saturation of the Hsp90 signal (Figure 5.7A) meaning that densitometric analysis were likely inaccurate. Further optimisation of the Hsp90 detection, by altering primary and secondary antibody dilutions, would be required to confirm the knockdown observed.

A

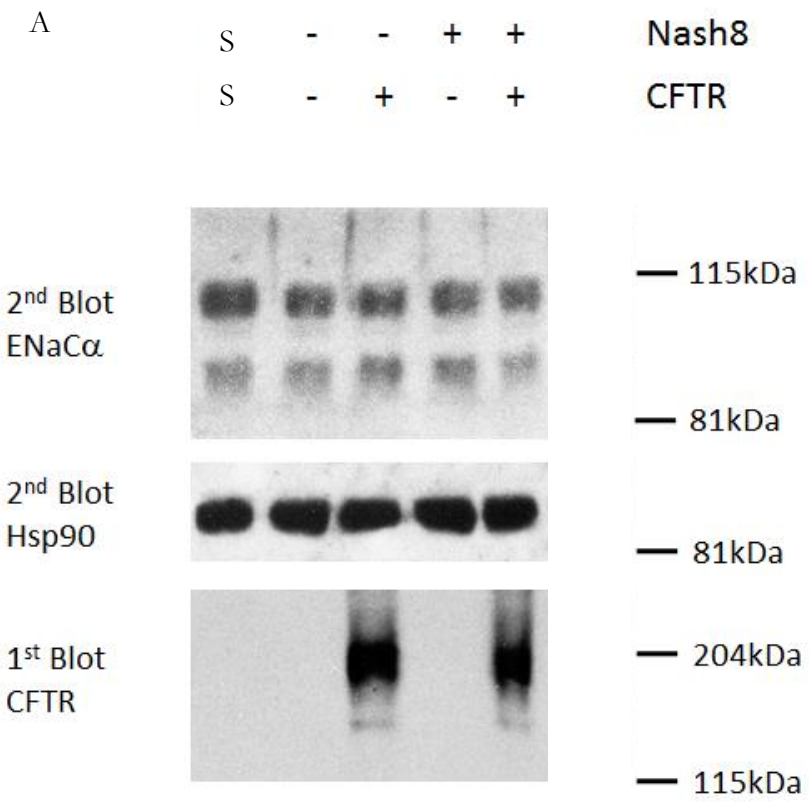
S - - + + Nash8
S - + - + CFTR
2nd Blot ENaCα
115kDa
81kDa
2nd Blot Hsp90
81kDa
1st Blot CFTR
204kDa
115kDa

B

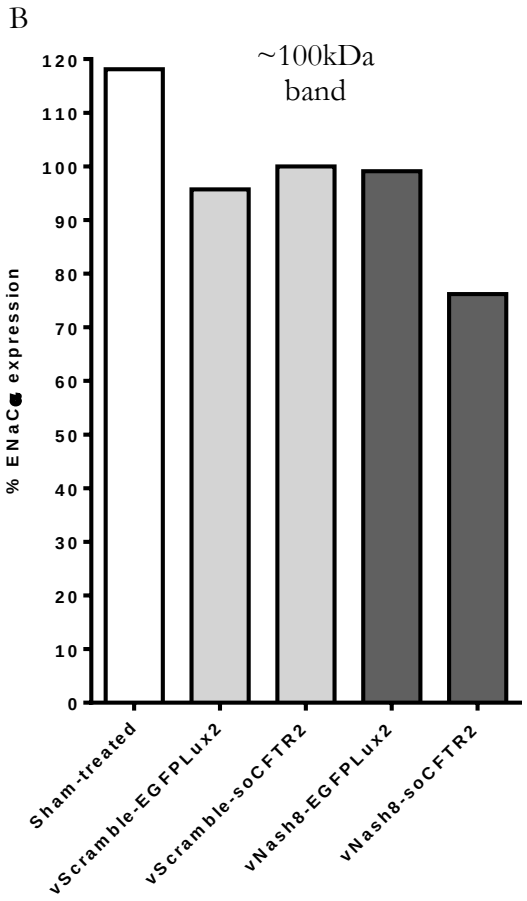
~100kDa band
% ENaCα expression
120
110
100
90
80
70
60
50
40
30
20
10
0
Sham-treated
vScramble-EGFPLux2
vScramble-soCFTR2
vNash8-EGFPLux2
vNash8-soCFTR2

C

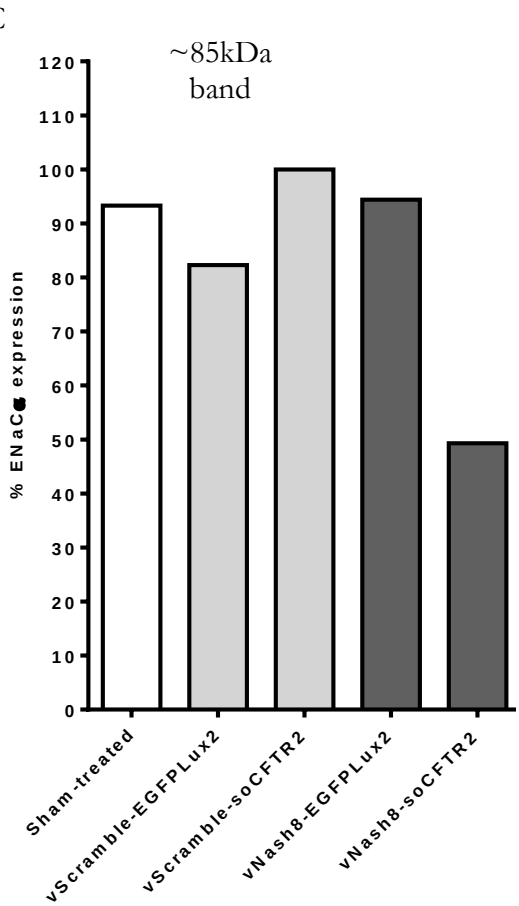
~85kDa band
% ENaCα expression
120
110
100
90
80
70
60
50
40
30
20
10
0
Sham-treated
vScramble-EGFPLux2
vScramble-soCFTR2
vNash8-EGFPLux2
vNash8-soCFTR2

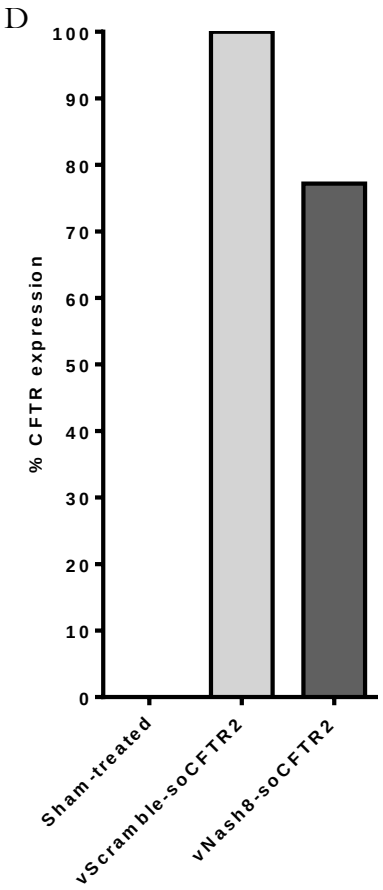

Figure 5.7. Images of hENaCα, Hsp90 and CFTR Western blots in A549 cells transduced with dual-function rLV vectors.

A549 cells were transduced with 1775 VP/cell of dual-function rLV vectors. Western blots were performed to detect hENaCα, Hsp90 and CFTR (A). The presence of the Nash8 shRNA or CFTR in the rLV vector is indicated by +. Sham-treated cells were also analysed. Densitometric analysis of ENaCα expression normalised to Hsp90 in the same blot (Section 2.9.4) was determined using the imageJ software, and % ENaCα protein expressed as percentage compared to vScramble-soCFTR2 (100%). The ~100kDa band (B) and the ~95kDa band (C) were analysed separately by densitometry. ImageJ analysis of CFTR expression was performed on a separate blot (D).

5.2.6 Simultaneous knockdown of mENaCα and CFTR transgene expression in M-1 cell culture.

The use of animal models is an important tool in gene therapy studies, particularly to determine possible immunological effects of a potential treatment for disease. Therefore the dual-function rLV vectors were also tested in M-1 (mouse kidney) cells, to screen and select suitable shRNA knockdown sequences (Section 5.2.6.1), and to assess the transduction efficiency of the dual-function rLV vectors on the mouse background (Section 5.2.6.3).

The M-1 mouse kidney cell line has previously been used for the determination of ENaCγ knockdown using mouse GAPDH as the housekeeping mRNA (Yueksekdag et al., 2010). Primer sets were used that could detect mENaCα (RPS-mENaCα-A; Table 2.7) and mGAPDH (RPS-GSKGAP-D, same as the set that can detect hGAPDH; Table 2.7) in samples harvested from the mouse lung (Clark et al., 2013). These primers were used to amplify mENaCα and mGAPDH in total RNA harvested from untransduced M-1 cells. Both primer sets amplified target mRNA with good efficiency (95% - 101%) for all the RNA input quantities tested (5 - 250ng per reaction; Figure 5.8). The data here led to the use of 50ng total RNA for detection of mENaCα knockdown by qRT-PCR as this would allow detection of up to 90% knockdown (5ng RNA).

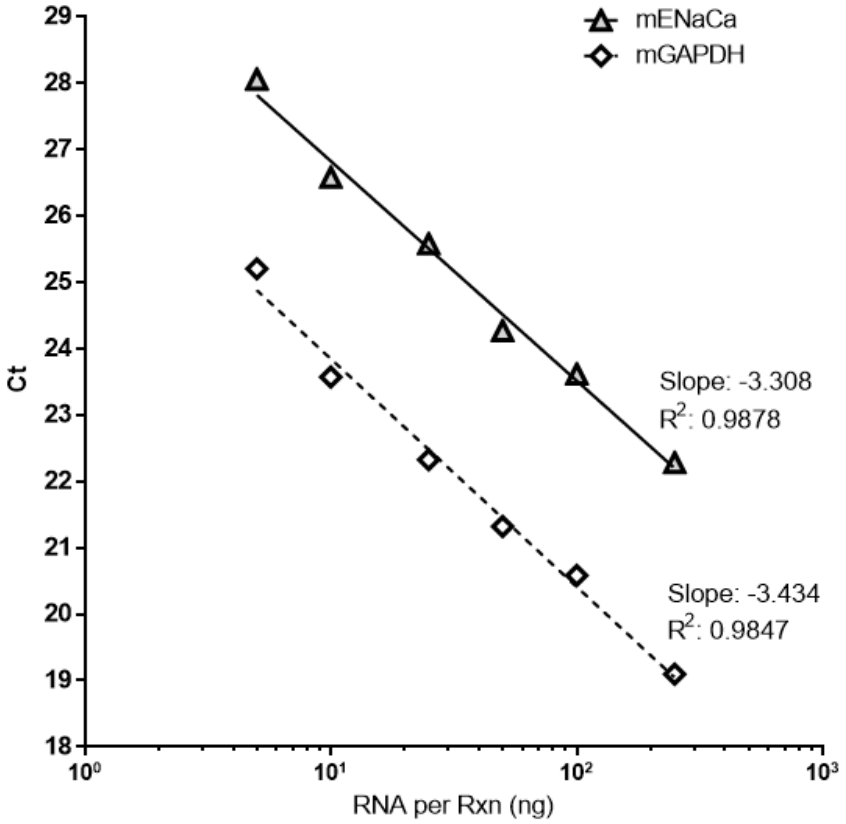

Figure 5.8. Graphs to show the efficiency of the RPS-mENaCα-A and RPS-GSKGAP-D TaqMan primer sets in M-1 cells.

Untreated M-1 cells were harvested for total RNA and a range of input RNA quantities (5, 10, 25, 50, 100 and 250 ng per reaction) analysed by qRT-PCR using the RPS-mENaCα-A and RPS-GSKGAP-D TaqMan primer sets (Table 2.7). The Ct values for the RPS-mENaCα-A (mENaCα) and RPS-GSKGAP-D (mGAPDH) assays were plotted against the RNA mass per qRT-PCR reaction (rxn). Non-linear regression was determined by semi-log analyses of mENaCα (solid line) and mGAPDH (dashed line), to determine the efficiency of the primers (A; slope of -3.33 indicates 100% efficiency). Symbols represent the mean ± SEM of three PCR wells.

To determine whether knockdown of *mENaCa* mRNA could be detected using this assay, lung homogenates were obtained from mice from a previous study, that had received either an anti-RSV siRNA (si-RSV), an anti-ENaCα siRNA (si-ENaCα) or no siRNA (naïve). These homogenates had previously shown mENaCα knockdown of approximately 50% using an absolute quantification method compared to the naïve (Clark et al., 2013) and si-RSV groups (unpublished data from the same study). Here, total RNA was extracted from lung homogenates and qRT-PCR performed using the RPS-mENaCα-A and RPS-GSKGAP-D primer sets. The relative expression of mENaCα was significantly lower in the si-ENaCα treated lungs than in naïve lungs or those from mice treated with si-RSV by at least 42% ($p<0.05$, ANOVA with Tukey's post-hoc multiple comparison test), suggesting that this assay is capable of detecting mENaCα knockdown.

5.2.6.1 Screening anti-mENaCα sequences in M-1 cells using pLKO viruses

Five LKO-based viral genome plasmids were obtained from Open Biosystems (pLKO-Nash1 to pLKO-Nash5; Table 2.1) containing shRNA sequences targeting the *mENaCa* mRNA transcript (Figure 5.9). Recombinant LV particles were produced using these plasmids at titres >3 x 10^8 VP/ml (except vNash2; 1.15 x 10^8 VP/ml; Table 5.3). Transduction of M-1 cells with 600 VP/cell of vLKO-shRNA for 24 hours, followed by puromycin selection for 48 hours resulted in an estimated transduction efficiency of 100%. The addition of puromycin resulted in a ~50% decrease in *mENaCa* mRNA expression compared to no selection (Figure 5.10A), therefore the vLKO-Scramble with puromycin selection was used as the comparator for screening vLKO-Nash rLVs. vLKO-Nash4 and vLKO-Nash5 knocked down *mENaCa* mRNA expression by 94% and 96% respectively, relative to vLKO-Scramble (Figure 5.10B), therefore the Nash4 and Nash5 shRNA sequences were taken forward for insertion into the dual-function vector.

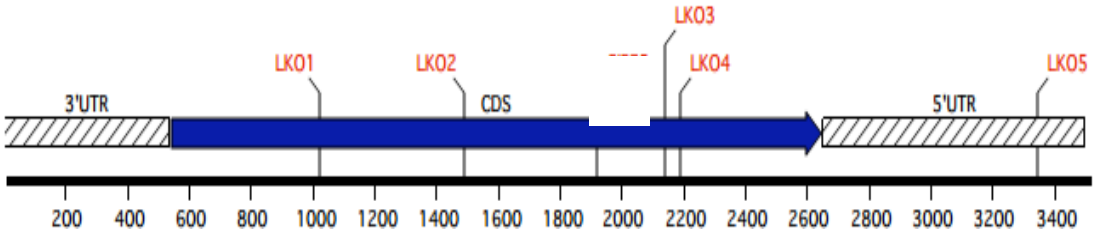

Figure 5.9. Diagram to indicate the targets of the anti-mENaCα shRNA sequences along the mENaCα transcript.

Five anti-mENaCα sequences were obtained as shRNA sequences in the pLKO.1 backbone. The target sequences of these shRNAs are indicated (LKO1 to LKO5) along the mENaCα transcript. Four of the sequences targeted the coding sequence (CDS) and one targeted the 5' untranslated region (5'UTR).

Virus name	Genome plasmid ref	Virus ref	VP/ml
vLKO-Nash1	pLKO-Nash1	vGM112	3.85E+08
vLKO-Nash2	pLKO-Nash2	vGM113	1.15E+08
vLKO-Nash3	pLKO-Nash3	vGM114	4.64E+08
vLKO-Nash4	pLKO-Nash4	vGM115	3.56E+08
vLKO-Nash5	pLKO-Nash5	vGM116	5.99E+08

Table 5.2. Viral particle titration of anti-mENaCα shRNA rLV vectors.

The anti-mENaCα shRNA viral genome plasmids were used to produce VSVG-pseudotyped rLV vectors. The viral particle number per ml virus supernatant (VP/ml) was determined for each virus using the HIVbb-B assay.

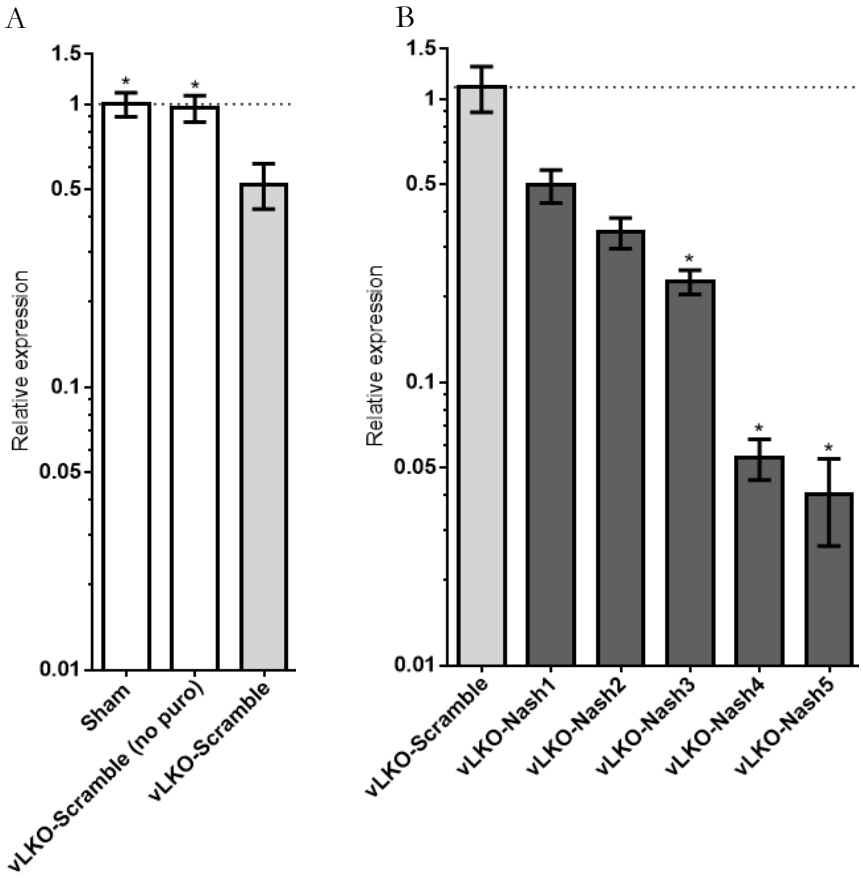

Figure 5.10. Relative mENaCα expression of in M-1 cells transduced with vLKO-Nash vectors.

M-1 cells were transduced with 700 VP/cell of anti-mENaCα vLKO-Nash vectors. Media was exchanged for puromycin selective media 24 hours post-transduction and cells harvested 72 hours post-transduction. Total RNA was extracted and relative *mENaCa* mRNA expression determined using sham-treated (A) or vLKO-Scramble treated (B) cells as the comparator. 'no puro' indicates that puromycin was not added to the media. Sham-treated cells also did not receive puromycin. Bars represent the mean ± SEM (n=6). * $p<0.05$ versus vLKO-Scramble, ANOVA with Tukey's post-hoc multiple comparison test

5.2.6.2 Transgene expression and dose determination in M-1 cell culture using the vEGFPLux2 vector

Prior to analysing the successful Nash sequences in the dual-function vector the appropriate dose with which to transduce the M-1 cells was determined. The vEGFPLux2 vector was used to transduce M-1 cells with doses ranging from 500 to 1250 VP/cell. The results showed a dose-dependent effect with increasing doses leading to increased transduction efficiency and decreased cell viability (Figure 5.11). Transduction efficiency reached a maximum of approximately 65% at 1000 VP/cell (Figure 5.11A). The decrease in cell viability from ~85% at 500 VP/cell to ~58% at 1250 VP/cell suggested that increasing doses of rLV led to cell death (Figure 5.11B). The relative expression of mENaCα revealed that transduction of M-1 cells with rLV significantly decreased mENaCα expression by as much as 50% compared with the sham-treated controls (Figure 5.11C), highlighting the importance of using an rLV control as the comparator when determining the relative expression of mENaCα.

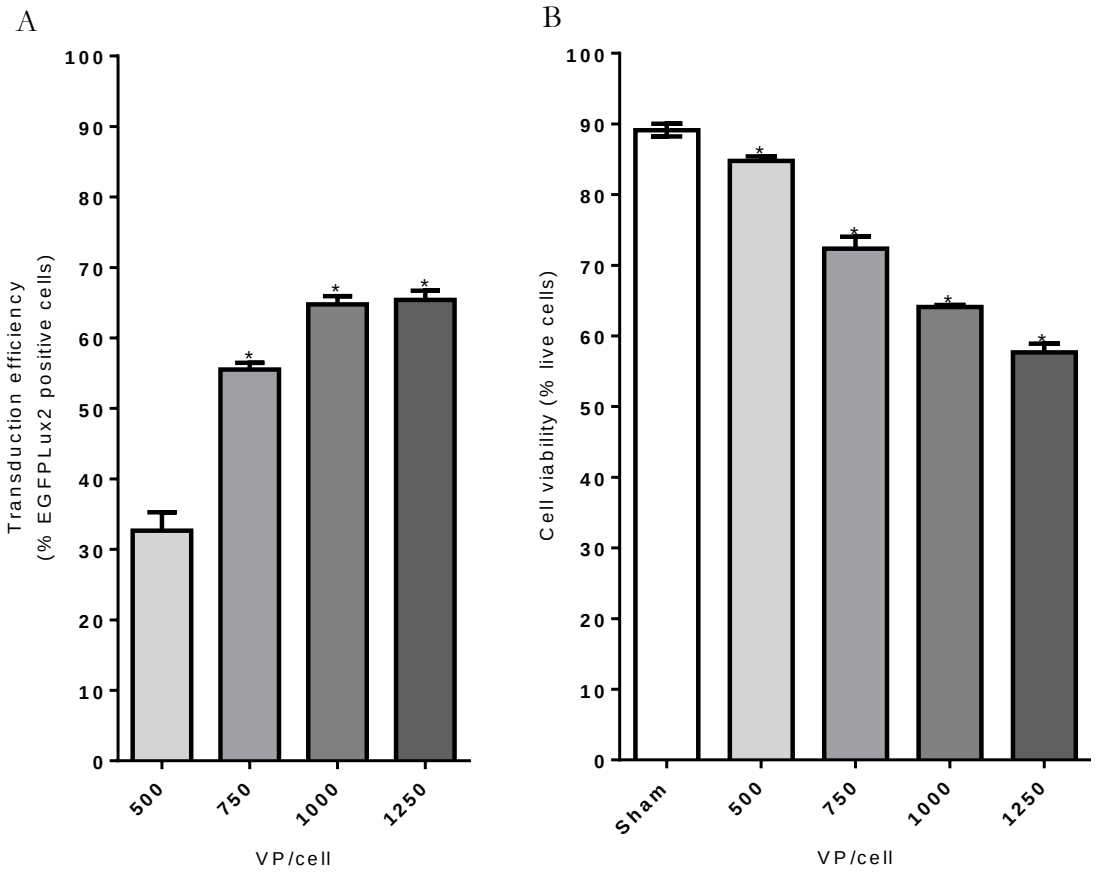
A
Transduction efficiency
(% EGFPLux2 positive cells)
100
90
80
70
60
50
40
30
20
10
0
500
750
1000
1250
VP/cell
B
Cell viability (% live cells)
100
90
80
70
60
50
40
30
20
10
0
Sham
500
750
1000
1250
VP/cell

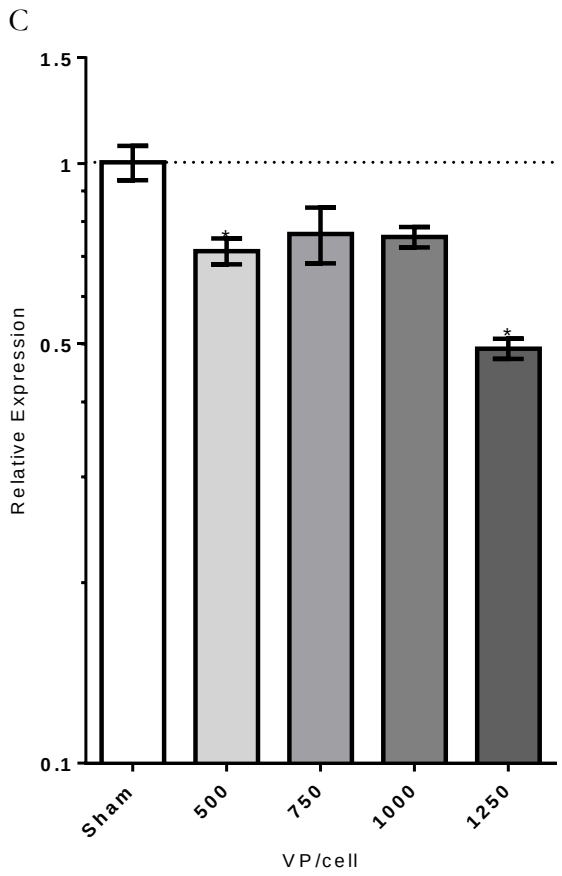
C
Relative Expression
1.5
1
0.5
0.1
Sham
500
750
1000
1250
VP/cell

Figure 5.11. Transduction efficiency, cell viability and relative mENaCα expression of M-1 cells transduced with vEGFPLux2.

M-1 cells were transduced with 500, 750, 1000 or 1250 VP/cell of vEGFPLux2, media changed at 24 hours post-transduction and cells harvested at 72 hours post-transduction. An aliquot of cells was taken for FACS analysis to determine the transduction efficiency (A) and cell viability (B) of transduced cells (n=3). Total RNA was extracted and relative *mENaCa* mRNA expression determined using sham-treated cells as the comparator (n=6). *$p<0.05$ versus 500 VP/cell (A) or sham-treated (B and C), Tukey's post-hoc multiple comparison test.

5.2.6.3 Knockdown of mENaCα mRNA in M-1 cells transduced with vNash4-soCFTR2 or vNash5-soCFTR2

To determine whether the Nash4 and Nash5 sequences could knock down mENaCα using the dual-function rLV vector, the Nash sequences were amplified out of the LKO backbone using specific primers (Figure 5.1; Table 2.2) and inserted into the pEGFPLux2 and psoCFTR2 backbones (Section 5.2.1) to create pNash4-EGFPLux2 (pGM416), pNash4-soCFTR2 (pGM417), pNash5-EGFPLux2 (pGM418) and pNash5-soCFTR2 (pGM419; Table 2.1) These rLV genome plasmids were then used to produce VSV-G pseudotyped rLV vectors at titres of between 5 x 10^8 VP/ml and 2 x 10^9 VP/ml (Table 5.3) which were suitable for transduction in cell culture.

The anti-mENaCα rLV particles were used to transduce M-1 cells with a dose of 1250 VP/cell. Results indicated that the transduction efficiency was not consistent between treatment groups, with vScramble-EGFPLux2 and vNash4-EGFPLux2 transducing only 30-35% of cells per well, and vNash5-EGFPLux2 transducing approximately 50% of cells per well Figure 5.13A). The cell viability for transduced wells was between 50 and 60% but no lower than the cell viability for untransduced cells (Figure 5.13B). No significant differences were observed in mENaCα relative expression between any of the dual-function treatments and the vScramble-EGFPLux2 control (Figure 5.13C). These data suggest that transgene expression was too low in M-1 cells to be able to detect target gene knockdown using the dual-function rLV vector therefore M-1 cells were no longer used as a tool for developing the dual-function rLV vector delivery.

Virus Name	Genome plasmid ref	Virus ref	VP/ml	EGFPLux2 to soCFTR2 fold difference
vNash4-EGFPLux2	pGM416	vGM128	2.06 x 10^9	4.06
vNash4-soCFTR2	pGM417	vGM129	5.07 x 10^8	
vNash5-EGFPLux2	pGM418	vGM130	1.16 x 10^9	1.58
vNash5-soCFTR2	pGM419	vGM131	7.34 x 10^8	
vScramble-EGFPLux2	pGM393	vGM084	1.26 x 10^9	

Table 5.3. Viral particle titration of dual-function rLV vectors.

The dual-function anti-mENaCα shRNA viral genome plasmids were used to produce VSVG-pseudotyped rLV vectors. The viral particle number per ml virus supernatant (VP/ml) was determined for each virus using the WPRE assay and the fold difference in titre between the EGFPLux2 and soCFTR2 transgenes determined.

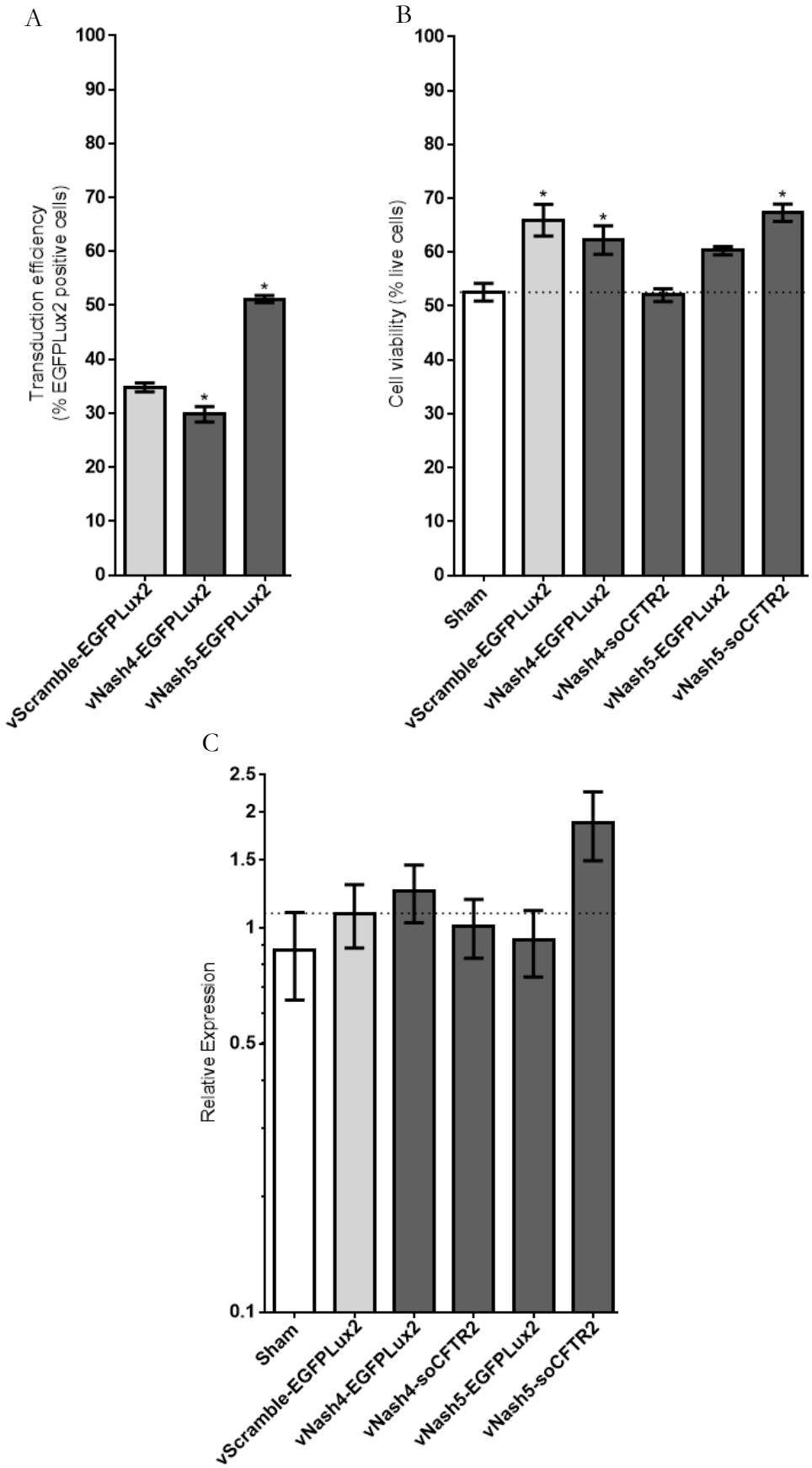
A
Transduction efficiency (% EGFPLux2 positive cells)
100
90
80
70
60
50
40
30
20
10
0
*
*
vScramble-EGFPLux2
vNash4-EGFPLux2
vNash5-EGFPLux2
B
Cell viability (% live cells)
100
90
80
70
60
50
40
30
20
10
0
*
*
*
Sham
vScramble-EGFPLux2
vNash4-EGFPLux2
vNash4-soCFTR2
vNash5-EGFPLux2
vNash5-soCFTR2
C
Relative Expression
2.5
2
1.5
1
0.5
0.1
Sham
vScramble-EGFPLux2
vNash4-EGFPLux2
vNash4-soCFTR2
vNash5-EGFPLux2
vNash5-soCFTR2

Figure 5.12. Relative expression of mENaCα in M-1 cells transduced with dual-function rLV

M-1 cells were transduced with dual-function rLV targeting mENaCα (1250 VP/cell) and harvested at 72 hours post-transduction. The transduction efficiency of viruses expressing EGFP was determined (A) and transgene expression was also determined for all wells by calculating the WPRE mRNA copies per ng total RNA (B). The relative expression of *mENaCa* mRNA was determined using qRT-PCR with normalisation against mGAPDH, and vScramble-EGFPLux2 as the comparator (A). Bars represent the mean ± SEM of n=3 (A) or n=6 (B and C) cell culture wells. * $p<0.05$ ANOVA versus vScramble-EGFPLux2 (A and C) or sham (B) with Tukey's post-hoc multiple comparison test.

5.2.7 Analysis of BACH1 as a target for knockdown in A549 cells

In order to evaluate a second target for knockdown using the rLV vector, the BACH1 gene was targeted for two reasons: 1) the upregulation of this gene is associated with lung emphysema, and 2) downregulation of BACH1 causes a concomitant upregulation of HMOX1, which can act as an internal control for specific knockdown (Section 5.1).

To determine an appropriate RNA input for detecting hBACH1 and *hHMOX1* mRNA expression in A549 cells, the TaqMan primer sets RPS-hBACH1-A and RPS-hHMOX1-A (Table 2.7) were used to amplify 5 to 250 ng of total RNA (5, 10, 25, 50, 100 and 250 ng) from untreated cells. Both primer sets amplified target mRNA with good efficiency (99% - 102%) for 10 to 250 ng of total input RNA (Figure 5.13A). Including the 5ng of total input RNA in these analyses reduced the efficiency to between 86% and 94.6%. The relative expression of hBACH1 and hHMOX1 was determined for each sample (using GAPDH as the normaliser) using the average ΔCt of all samples within each assay as the comparator: the relative expression of all samples should be close to 1. The 5 ng input RNA varied the most from the average in the hBACH1 and hHMOX1 assays (Figure 5.13B) confirming that the 5ng input could be below the range of the assay. These data suggest that the 50ng total RNA input used for previous qRT-PCR assays was also an appropriate input quantity for use in the hBACH1 and hHMOX1 and would allow detection of up to 80% knockdown.

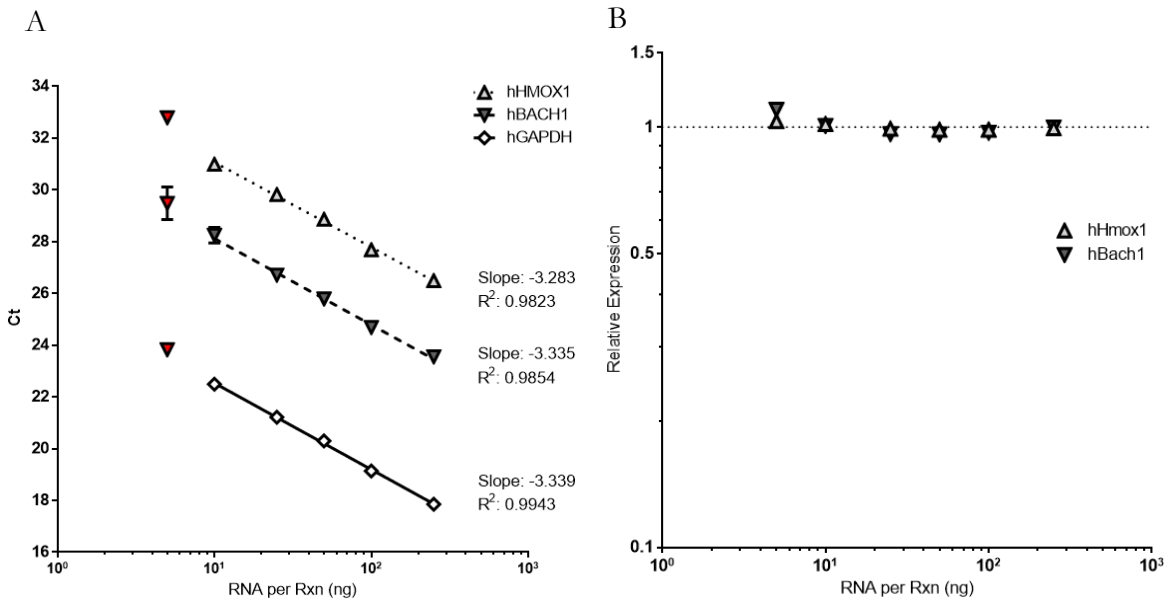

Figure 5.13. Graphs to show the efficiency of the RPS-hBACH1-A, RPS-hHMOX1-A and RPS-GSKGAP-D TaqMan primer sets in A549 cells.

Untreated A549 cells were harvested for total RNA and a range of input RNA quantities (5, 10, 25, 50, 100 and 250 ng per reaction) analysed by qRT-PCR using the RPS-hBACH1-A, RPS-hHMOX1-A and RPS-GSKGAP-D TaqMan primer sets (Table 2.7). The Ct values for the RPS-hHMOX1-A (hHMOX1), RPS-hBACH1-A (hBACH1) and RPS-GSKGAP-D (hGAPDH) assays were plotted against the RNA mass per qRT-PCR reaction (rxn) (A). Non-linear regression was determined by semi-log analyses of hHMOX1 (dotted line), hBACH1 (dashed line) and hGAPDH (solid line) with samples excluded from the analyses indicated by the red symbols, to determine the efficiency of the primers (A; slope of -3.33 indicates 100% efficiency). Symbols represent the mean ± SEM of three PCR wells. The relative expression of hBACH1 and hHMOX1 were calculated using hGAPDH as the normaliser and the average of the ΔCt values within each assay as the comparator (B).

5.2.7.1 Knockdown of hBACH1 and up-regulation of hHMOX1 in A549 cells transduced with anti-BACH1 LKO rLV vectors

The Bash3 sequence (Table 2.4) was chosen to test initially in A549 cells as this sequence was proven previously by the manufacturers to knock down *hBACH1* mRNA expression by ~60% in M-1 cells. vLKO-Bash3 (vGM066; Table 2.1) was produced as previously with a VSV-G pseudotype resulting in a titre of ~7 x 108 VP/ml which was similar to the vLKO-Nash titres (Table 4.1). Cells were transduced with 600 VP/cell of vLKO-Bash3 and puromycin-selected after 24 hours. Total RNA was extracted 72 hours post-transduction for qRT-PCR analyses Results indicated that Bash3 could significantly decrease hBACH1 relative expression by 73%, and increase hHMOX1 relative expression by 186% (Figure 5.14). This concomitant up-regulation of hHMOX1 expression indicated that the Bash3 sequence specifically knocked down hBACH1 to a degree that reduced its suppression of hHMOX1 expression. Similar results were observed in at least three further experiments, including transduction with a higher dose (1200 VP/cell) and without puromycin selection (data not shown).

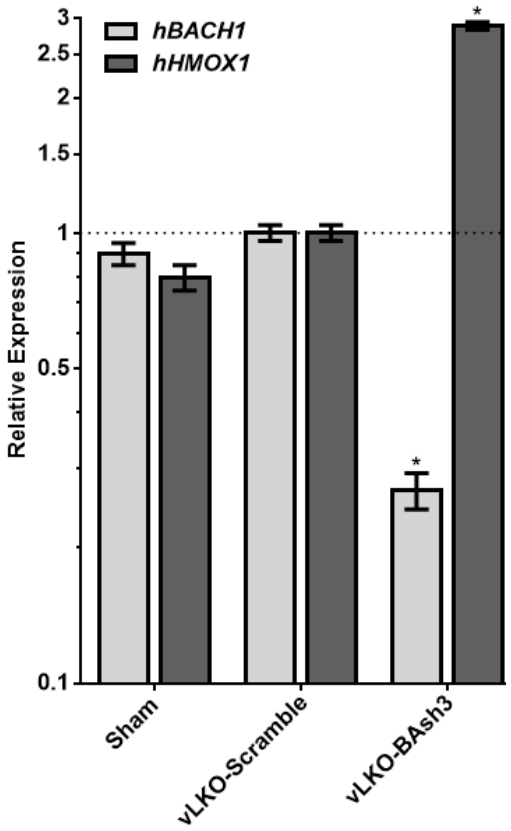

Figure 5.14. Relative expression of hBACH1 and hHMOX1 in A549 cells transduced with vLKO-Bash3

A549 cells were seeded at 2 x 10^5 cells/well for 24 hours prior to transduction with 600 VP/cell of vLKO-Bash3 or vLKO.Scramble with puromycin selection for 24 hours. Selective media was exchanged for fresh media at 24 hours post-transduction and cells were harvested at 72 hours post-transduction for RNA analyses. Relative expression of *hBACH1* and *hHMOX1* mRNA were determined. Bars represent the mean ± SEM for three separate wells. * $p<0.05$ versus vLKO.Scramble, ANOVA with Tukey's post-hoc multiple comparison test.

5.2.7.2 Knockdown of hBACH1 and up-regulation of hHMOX1 in A549 cells transduced with dual-function rLV vectors

The Bash3 sequence was amplified out of the LKO.1 backbone and inserted into vEGFPLux2, as described previously for Nash8 to create pBash3-EGFPLux2 (pGM391), which was subsequently used as the genome plasmid to produce rLV vectors with the VSV-G pseudotype as previously. The resultant vBash-EGFPLux2 (vGM082) rLV vector contained 1.86 x 10^9 VP/ml (3.09 x 10^7 FTU/ml). To determine whether vBash8-EGFPLux2 could concomitantly knock down *hBACH1* mRNA expression and upregulate *hHMOX1* mRNA expression, A549 cells were transduced with 3400 to 4200 VP/cell. Parallel transductions with vEGFPLux2 and vScramble-EGFPLux2 acted as the experimental controls. Treatment with the Bash3 containing vector resulted in significant *hBACH1* mRNA knockdown, by 83%, and concomitant *hHMOX1* mRNA upregulation, by 149% compared with vScramble-EGFPLux2 ($p<0.05$; Figure 5.15A). The transduction efficiency was ~85% in wells transduced with vBash3-EGFPLux2 compared to ~65% for wells transduced with vEGFPLux2 or vScramble-EGFPLux2 (Figure 5.15B). This discrepancy is likely due to the different doses delivered: ~3400 VP/cell for vEGFPLux2 and vScramble-EGFPLux2 and ~4200 VP/cell for vBash3-EGFPLux2. These data suggest that Bash3 expressed from this rLV vector can mediate significant specific target mRNA knockdown.

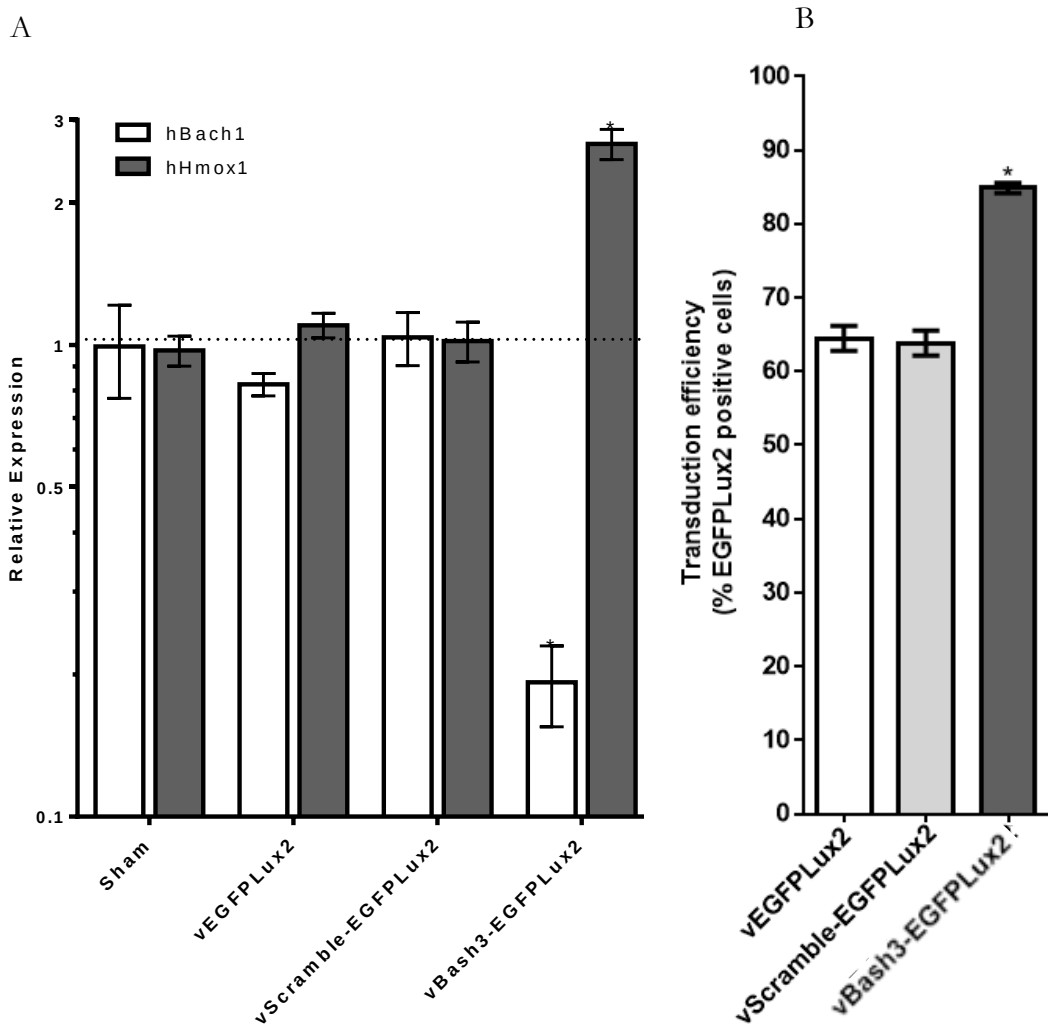

Figure 5.15. Relative *hBACH1*/*hHMOX1* expression and transgene expression in A549 cells transduced with dual-function anti-hBACH1 rLV vectors.

A549 cells were transduced with 4270, 3360 and 4220 VP/well of vEGFPLux2, vScramble-EGFPLux2 and vBash3-EGFPLux2 respectively, and harvested at 72 hours post-transduction. The relative expression of hBACH1 or *hHMOX1* mRNA was determined using qRT-PCR with normalisation against GAPDH, and vScramble-EGFPLux2 as the comparator (A). Transduction efficiency was determined using FACS analyses (B). Bars represent the mean ± SEM of n=6 (A) or 3 (B) cell culture wells. * $p<0.05$ versus vScramble-EGFPLux2, ANOVA with Tukey's post-hoc multiple comparison test.

5.3 Discussion

Due to the success of the Nash8 sequence in the LKO backbone in the chapter 4, the entire shRNA expression cassette (hU6-Nash8-cPPT) was extracted using PCR primers designed to allow subsequent insertion into the pEGFPLux2 vector genome plasmid, upstream of the EGFPLux2 transgene cassette, resulting in pNash8-EGFPLux2 (pGM392). Production of VSVG-pseudotyped virus using this vector genome plasmid and subsequent transduction in A549 cells led to a transduction efficiency of ~60%, and importantly the Nash8 sequence knocked down *hENaCa* mRNA expression by ~70% (Figure 5.3A).

To produce a dual-function rLV vector capable of simultaneous hENaCα knockdown and CFTR transgene expression, the soCFTR2 transgene was used to replace the EGFPLux2 transgene. soCFTR2 is the transgene currently in use in clinical trials for CF gene therapy and has shown a good safety profile when delivered to CF patients in a plasmid backbone using a cationic lipid for transient delivery to the lung via aerosolisation (Alton et al., 2013b). In addition there has been some evidence of mRNA expression in the lungs and nose, and, more encouragingly, nasal instillation of the same vector has been shown to produce transient correction of the nasal potential difference in CF patients (Gill et al., 1997). In parallel, mouse studies have indicated duration of expression of reporter genes in the mouse lung and nose following soCFTR2-expressing rLV vector intranasal delivery (Griesenbach et al., 2012).

Switching the soCFTR2 transgene for the EGFPLux2 transgene in the vector genome plasmids that were used to produce vNash8-EGFPLux2 and vScramble-EGFPLux2 resulted in the production of the dual-function rLV vector vNash8-soCFTR2 (vGM096) and the non-target shRNA control vScramble-soCFTR2 (vGM087). These rLV vectors were able to transduce A549 cells, although transgene expression was 3x lower than transduction using the EGFPLux2-containing rLV vectors (Figure 5.3B). This lower transduction efficiency could be due to the use of viral particle titre to determine doses: viral particle titres of rLV vectors containing the soCFTR transgene were 4- to 5-fold lower than the titres of rLV vectors

expressing the EGFPLux2 transgene suggesting that the soCFTR2 transgene has a detrimental effect on virus particle production (Table 5.1). This effect is likely mediated by the large size of the soCFTR2 transgene (4453bp) compared to the EGFPLux2 transgene (2420bp) which could also lead to the presence of defective virus particles due to incomplete packaging of the genomic viral RNA during production: these viruses would be detected by virus particle titration but would not contribute to the transduction efficiency of the rLV vector resulting in lower transgene expression following transduction of the same VP/well. The soCFTR2 transgene expression detected was sufficient to produce mature CFTR protein (Figure 5.7) which could form fully functional CFTR channels at the cell surface (Figure 5.2).

Although the soCFTR2-expressing rLV vectors mediated lower transgene expression in A549 cells, greater hENaCα knockdown was observed than with the EGFPLux2-expressing rLV vectors (71% and 85% knockdown compared to vScramble-EGFPLux2 respectively). Expression of CFTR appeared to account for a 31% and 48% decrease in *hENaCa* mRNA expression in combination with the Scramble or anti-hENaCα shRNAs respectively, compared to the EGFPLux2-expressing rLV vectors (Figure 5.3A). This enhanced knockdown was surprising, considering that the CFTR-containing rLV vectors mediated 3x lower transgene expression than the EGFPLux2-containing rLV vectors, therefore they would be expected to also mediate reduced knockdown of target gene expression. Whether this increased knockdown potential with expression of CFTR is due to CFTR-mediated down-regulation of *hENaCa* mRNA or due to vector-mediated toxicity from rLV vectors containing the larger CFTR transgene is uncertain.

Detection of hENaCα protein by Western blot resulted in observation of multiple bands, with two major bands at ~100kDa and ~85kDa (Figure 5.6 and Figure 5.7). Western blot analyses of ENaCα in the literature often display two bands of around 95-100kDa and 75-85kDa corresponding to the fully glycosylated and core glycosylated forms of hENaCα respectively (Knight et al., 2006; Caci et al., 2009; Alvarez de la Rosa et al., 2002; Gianotti et al., 2013). In

some studies the smaller band is referred to as the cleaved, activated ENaCα, however the antibody used in this study binds to the C-terminus, which is closer to the cleavage site, therefore the cleavage product would be observed at ~30kDa, not 75kDa. It is more likely that the smaller band is the core glycosylated form of the ENaCα protein. The bands observed here are similar to those observed previously in A549 cells using the same antibody (Clark et al., 2013). Both bands indicated hENaCα protein when cells were transduced with the vNash8-soCFTR2 rLV vector (40-50% decrease compared to vScramble-soCFTR2), however no indication of hENaCα knockdown was observed when cells were transduced with the vNash8-EGFPLux2 rLV vector (Figure 5.7). The low levels of hENaCα protein knockdown observed here could be due to the harvest time-point: although the half-life of newly synthesized ENaC channels at the apical surface of cells is ~2 hours, already established apical ENaCα expression remains stable for over 24 hours (Weisz et al., 2000) therefore the lack of protein knockdown observed with vNash8-EGFPLux2, and the decreased protein knockdown observed with vNash8-soCFTR2 (compared to the mRNA knockdown observed) could be due to the long half-life of the protein. Longer duration studies would have to be performed to determine whether greater knockdown could be observed at a later time-point once established ENaC proteins are turned over.

An alternative knockdown target to hENaCα was also tested in this chapter. BACH1 was chosen as for two main reasons: BACH1 upregulation is implicated in emphysema and COPD, and BACH1 knockdown causes upregulation of HMOX1 providing a secondary marker for specific BACH1 knockdown (Raval et al., 2012). Although increases in HMOX1 expression have been detected in the lungs of CF patients compared to non-CF patients, further augmenting HMOX1 expression could give greater protection against *Pseudomonas aeruginosa* cytotoxicity (Zhou et al., 2004) and could improve the oxidative stress response in CF patients (Zhang et al., 2013). It is also encouraging that $BACH1^{-/-}$ mice showed no decrease in longevity, nor increase in tumorigenesis compared to wild-type mice (Ota et al.,

2014), suggesting that knocking down BACH1 could be well tolerated. The anti-hBACH1 rLV vector vBash3-EGFPLux2 mediated concomitant *hBACH1* mRNA knockdown (83%) and *hHMOX1* mRNA upregulation in A549 cells, suggesting that the hBACH1 target could be a useful tool for detecting targeted knockdown in cell culture, and for developing this vector in further models.

Although these studies in A549 cells have provided sufficient evidence that the dual function vector can efficiently knock down target gene expression and produce transgene expression in immortalised cell culture, these data do not provide any evidence of the effect of the vector on lung physiology, neither do these data indicate whether the dual-function vector would be well tolerated by the immune system. The mouse model is a common choice for initial testing of the potential efficacy, duration of expression, target cells transduced, immune responses and physiological effects a disease treatment. Although the lungs of CFTR knockout mice do not exhibit lung disease, the nasal cavity does exhibit physiological properties similar to those in the nasal and lung epithelial surfaces of CF patients (Limberis et al., 2002), namely decreased nasal potential difference (nasal PD), the Cl^- transport defect, and Na^+ hyperabsorption. To determine whether shRNA sequences were available with the potential to knock down murine ENaCα, M-1 cells (mouse embryonic kidney), which express endogenous mENaCα, were used. Knockdown of mENaCα by ~95% was detected with the Nash4 and Nash5 shRNA sequences in the LKO backbone (Figure 5.10), however, once inserted into the dual-function vector no knockdown was observed (Figure 5.12). This lack of detectable knockdown was likely due to the poor transduction efficiency (<50%) of the rLV vector in M-1 cells (Figure 5.11).

The relative expression of mENaCα revealed that transduction of M-1 cells with rLV significantly decreased mENaCα expression by as much as 50% compared with the sham-treated controls (Figure 5.11C), highlighting the importance of using an rLV vector control as the comparator when determining the relative expression of mENaCα. These data suggest that M-1 cells are a poor model for detecting mENaCα knockdown using the dual-function vector. Rather than test the dual-function vectors in an alternative cell line, or directly in a mouse model, an alternative model was assessed in chapter 6: human bronchial epithelial cells grown at the air-liquid interface.

Chapter 6: Human bronchial Air-Liquid Interface (ALI) primary cultures as a tool to determine the efficacy of rLV vectors

6.1 Introduction

In Chapter 5 the dual-function vectors vNash8-soCFTR2 (vGM086) and vBash3-soCFTR2 (vGM085; section 2.1) were shown to knock down hENaCα and *BACH1* mRNA respectively, in A549 cells (Section 5.2.6 and 5.2.8). Dual-function vectors were also analysed in M-1 (mouse) cells to select a suitable vector for use in a mouse model, however, all of the chosen vectors were unsuccessful at knocking down target gene expression in M-1 cells, potentially due to low transduction efficiency (Section 5.2.7).

The use of animal disease models for testing gene therapy vectors can provide important information on the capability of the therapy to restore normal function to diseased cells/organs, and to assess the toxicity of the therapy. However, animal disease models of CF do not often fully reflect the pathophysiology of the human disease, and the larger animal models of CF (ferret and pig) that more closely represent humans in terms of lung physiology (airway total surface/size/lung pathophysiology) require extensive husbandry and have low life expectancies making studies into the efficacy of gene therapy in adult animals with CF lung disease both problematic and costly.

In this study, an alternative to animal CF models was examined: human primary bronchial epithelial cells grown at the air-liquid interface (ALI). This type of model has been useful for determining the physiological and bioelectrical differences in normal cultures versus disease cultures, including CF (Itani et al., 2011; Matsui et al., 1998a). To produce ALI cultures, human epithelial cells obtained from bronchial brushings of CF and non-CF individuals are mechanically dissociated and seeded onto a permeable filter in an insert that can be placed

into commercial tissue culture plates (Karp et al., 2002). The cells are initially grown to confluence with media in both the apical and basolateral compartments, known as submerged culture and, once fully confluent, the apical media is removed leaving the cells positioned at the air-liquid interface (ALI), with the apical cell surface in contact with the air, and the basolateral surface in contact with the media. Growth at this interface induces the cells to re-differentiate into airway epithelial cells resulting in a pseudostratified cell layer representative of the cellular morphology of the airway epithelium, where all cells adhere to the basolateral surface (the filter) yet some cells do not fully extend to the apical surface. Transmission electron microscopy (TEM) revealed the three distinct cell types present: basal cells, goblet cells and ciliated cells, and scanning electron microscopy (SEM) images displayed a confluent arrangement of goblet and ciliated cells (Karp et al., 2002). ALI cultures can also be produced using immortalised cell lines, but these cultures do not reproduce all the features of *in vivo* airway epithelia as well as primary cells (Karp et al., 2002). Instead, such cultures produce a gene expression profile more similar to primary airway cells maintained under submerged conditions, and different from primary airway cells maintained under ALI conditions, or from *in vivo* biopsies (Pezzulo et al., 2011) and were therefore not particularly suited here for use in assessing viral delivery to the airway epithelium. The use of human ALI culture in this study as opposed to ALI cultures derived from animal models was in part due to the differing pathophysiology in the lungs of CF animal models, and also due to the progression to testing dual-function rLV particles where the RNAi component targets human ENaCα or BACH1.

As early as 10 days following transfer to ALI culture, primary airway cells show similar properties to the airway epithelium *in vivo*; they have a complete covering of cilia (Zabner et al., 1996), a high transepithelial resistance (Rt) and intercellular impermeability caused by the formation of tight junctions (Lin et al., 2007), mucus production (Matsui et al., 1998b), and electrophysiological properties similar to those in the human nasal epithelium. Primary human nasal, tracheal and bronchial ALI cultures have been used to assess the differences in

morphology and ionic composition observed in CF epithelia: the apical solution on cultures derived from both CF and non-CF tissues samples were isotonic and exhibited similar apical ionic compositions to one another (Matsui et al., 1998a) providing evidence against the high salt hypothesis for CF (Section 1.1.3), however, the periciliary liquid (PCL) layer was greatly reduced in CF cultures with cilia unable to fully extend leading to reduced mucociliary transport rates compared to non-CF cultures (Matsui et al., 1998b), supporting the low volume hypothesis (Section 1.1.3).

In previous chapters, dual function rLV was produced (chapter 3) that could simultaneously knock down hENaCα and express CFTR in immortalised human cell culture (chapter 5) as a dual approach gene therapy to treat Cystic Fibrosis lung disease: Na^+ hyperabsorption via ENaC up-regulation is proposed to contribute to CF lung disease (Section 1.2.2). The expression profile of ENaC subunit mRNA is similar in ALI cultures, immortalised cell culture, and in lung tissues *in vivo*, with ENaCα expressed much more highly than ENaCβ, and ENaCγ expressed the least. Anti-hENaCα siRNA delivery to human bronchial ALI cultures using Lipofectamine2000 was shown to decrease target mRNA and protein expression by 65% and 40% respectively, with a concomitant decrease in the amiloride sensitive short circuit current (ENaC-specific) by 53%, leading to a 40-60% decrease in fluid absorption from the apical membrane (Caci et al., 2009). CF ALI cultures had reduced forskolin-stimulated short-circuit currents compared with non-CF ALI cultures which could be restored to normal levels by delivery of CFTR.

All rLV particles here were produced with the VSVG pseudotype, however, VSVG is an unsuitable pseudotype for delivery to fully-differentiated airway epithelia via the apical surface (mimicking delivery to the lung via the airways) as the VSVG receptors allow entry predominantly via the basolateral surface of ciliated epithelium (Fuller et al., 1984; Wang et al., 1999) (Section 1.4.3). An alternative pseudotype can be produced using Sendai virus (SeV) coat proteins, as wild-type SeV particles enter airway epithelia by binding to the sialic acid-

containing ganglioside receptors (SA-Rs) that are ubiquitously expressed on the apical surface of epithelial cells (Bitzer , 1997), via the fusion (F) and hemagglutinin/neuraminidase (HN) coat proteins (Kobayashi et al., 2003). Delivery of F/HN-pseudotyped rLV has been confirmed to the apical cells of the airway epithelium *in vivo* in mice (Mitomo et al., 2010) and *ex vivo* in human and sheep tissue (Griesenbach et al., 2012).

There is a history of poor apical transduction of primary fully-differentiated ALI cultures by rLV vectors (Aarbiou et al., 2012), therefore production of a high concentration of rLV particles was preferred to allow delivery of high viral doses in relatively small volumes so as not to flood the ALI surface. A method for the large-scale production, purification and concentration of rLV particles using a WAVE bioreactor (GE Healthcare Life Sciences, Little Chalfont, UK) has been developed within the UKCFGTC (Lee Davies, personal communication). The current protocol allows the production of approximately 1L of virus supernatant at an average concentration of 2 x 10^{10} VP/ml, which can be concentrated/purified to approximately 1 x 10^{12} VP/ml in a < 1ml volume, resulting in a typical VP loss of 20-30% (Lee Davies, personal communication). The purification process is carried out by anion-exchange membrane chromatography and tangential flow ultrafiltration/diafiltration and is designed to not only increase the concentration of the virus, but also to remove producer proteins, genomic DNA, producer plasmid DNA and other contaminations that may affect rLV particle quality and transduction efficiency. In this chapter, strategies to improve transduction of ALI cultures with F/HN-pseudotyped rLVs were explored, including interval dosing (Section 6.2.3), tight junction disruption (Section 6.2.4) and re-dosing at day 10 (Section 6.2.5). The improved multiple-EGTA dosing strategy was then used to assess target mRNA knockdown from an anti-hBACH1 rLV-F/HN (Section 6.2.6). To support these studies, commercial human bronchial MucilAir™ cultures were obtained (Epithelix-Sarl, Switzerland) that are fully differentiated ALI cultures that have

passed rigorous quality tests to ensure beating cilia, the presence of mucus, good Rt and correct morphology, with high batch to batch reproducibility (Epithelix, 2014).

6.2 Results

6.2.1 Large-scale rLV F/HN production and purification

Three rLV vectors, based on HIV pseudotyped with F and HN coat proteins, were produced in HEK293T suspension cells in 1L volumes and purified/concentrated to <1ml by Lee Davies for the studies in this chapter. All of the subsequent experiments described in this chapter, including the particle and functional virus titrations were performed by myself. The rLV vectors vEGFPLux2-F/HN (vGM035), vNash8.soCFTR2-F/HN (vGM096) and vBash3.EGFPLux2-F/HN (vGM123) were produced using the genome plasmids pEGFPLux2-NotMod (pGM290), pNash8-soCFTR2 (pGM395) and pBash3-EGFPLux2 (pGM391) respectively (Table 2.1). Particle titres of the purified viral supernatant from these production runs were within the expected range for viruses produced in this manner (Table 6.1). The functional titre was calculated by measuring the WPRE copy number ml of viral supernatant of HEK293T cells transduced with the virus. This titre reflects the number of integration events per ng DNA, and therefore a suitable functional value, and is expressed as TaqMan titration units per ml virus (TTU/ml) (Section 2.7.3); this method of functional titration (as opposed to FACS titration; Section 2.7.2) provides a closer comparison of doses containing different expression cassettes, and with published results (Section 6.2.2). The WAVE production technique provided virus quantities sufficient for several studies in ALI cultures.

Virus Name	vGM	Particle titre (VP/ml)	Functional titre (TTU/ml)	Volume of pure virus (µl)
vEGFPLux2-F/HN	vGM035	2.75×10^{12}	7.60×10^{9}	867
vNash8.soCFTR2-F/HN	vGM096	1.05×10^{12}	1.34×10^{8}	890
vBash3.EGFPLux2-F/HN	vGM123	1.37×10^{13}	1.20×10^{10}	929

Table 6.1 Titration results of rLV pseudotyped with F/HN using the Wave bioreactor

To determine particle titre (VP/ml), viral RNA was extracted from purified virus supernatant (n=2 from single production) and WPRE RNA copies determined by RT-PCR (Section 2.7.3). The WPRE copies per ml virus supernatant were then used to calculate the particle titre (VP/ml). Functional titre was determined following transduction of HEK293T cells with 1:10 and 1:100 dilutions of purified virus (n=3). Cells were harvested and cellular DNA extracted followed by RNase treatment. The WPRE DNA copies were determined by PCR the Functional titre determined as WPRE DNA copies per ml of cells (TaqMan Transducing Units; TTU/ml) as a functional indicator reflecting integrated viral sequences.

6.2.2 Dose determination in ALI cultures using vEGFPLux2-F/HN

To determine a suitable dose of virus for rLV transduction of ALI cultures a variety of different dosing strategies were employed (Figure 6.1A). Initial doses were chosen based on a published study using rLV-F/HN vectors (Mitomo et al., 2010). The authors reported that luciferase-expressing rLV-F/HN vectors at doses of 1.25 x 10^7 and 1.25 x 10^8 TTU/ALI permitted detection of bioluminescence at day 5 (D05) and luciferase activity at D10 and D26 with a detectable dose response in luciferase protein expression (Mitomo et al., 2010). The doses chosen here for the current study were 5 x 10^7 (Low dose), 2.5 x 10^8 (Mid dose) and 5 x 10^8 (High dose) TTU/ALI of vEGFPLux2-F/HN (vGM035) so that bioluminescence imaging (BLI) of the inserts could be used to quantify luciferase (Lux) expression over time with minimal disruption to the ALI cultures. The EGFPLux2 fusion protein also provides a method of determining the distribution of the transduced cells by microscopically monitoring EGFP fluorescence.

Non-CF ALI cultures were obtained (Epithelix, Switzerland) and maintained for at least 2 weeks, to allow recovery from any shipping related trauma, prior to transduction (Section 2.11.1). At this time, cilia movement could be observed microscopically and a small amount of mucus was visible on the surface of most cultures (data not shown). On day zero (D00) the apical surface of the cells were rinsed briefly with MucilAir™ media and then transduced with 100µl of Low, Mid or High doses of vEGFPLux2-F/HN in serum-free media by careful application to the apical surface and incubation for 4 hours (Section 2.11.2; this strategy will be referred to as 'normal dosing'; Figure 6.1A). Sham treatments were also included in all experiments, where the same volume media alone was added to cells. Following virus removal the apical surface was washed carefully with 200µl MucilAir™ media four times to remove any residual virus. Cells were analysed using BLI every 24 hours (Section 2.11.4) and images recorded at regular intervals to monitor GFP fluorescence.

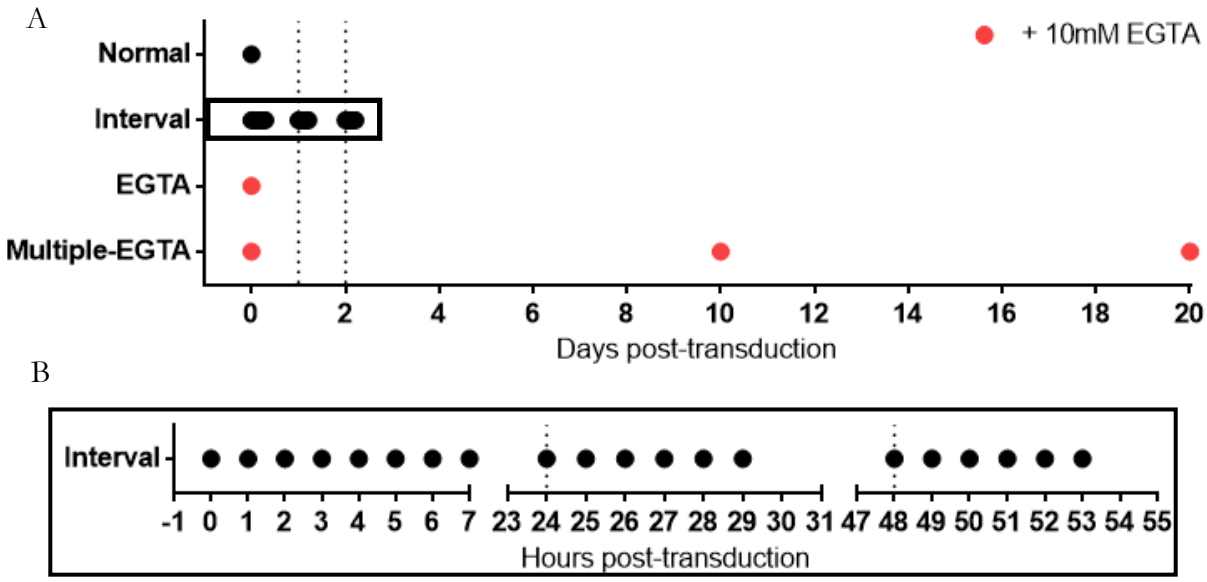

Figure 6.1. Outline of dosing strategies employed in chapter 6

Four different dosing strategies were used to transduce ALI cultures. The circles for the normal, EGTA and multiple-EGTA dosing strategies indicate 100µl doses of 5 x 10^7 TTU either with (red fill) or without (black fill) the addition of 10mM EGTA to the virus. The interval dosing was twenty 10µl doses of 2.5 x 10^6 TTU each; the boxed area in A is expanded in B to indicate hours post-transduction and vertical dashed lines are added at D01 and D02 for clarity.

Close inspection of the ALI cultures indicated that the addition of 100µl of media, either with or without rLV particles, caused 'gaps' to appear between cells in the layer (Figure 6.2A); however these gaps appeared to be re-populated and closed by 16 hours post-transduction.

The transduction efficiency, as indicated by the detection of EGFP-positive cells, was variable even amongst ALI cultures receiving a similar dose of virus (Figure 6.2B). The images shown, although from three separate ALI cultures transduced with the High dose only, are representative of all doses, highlighting that some inserts contained very low numbers of transduced cells (Figure 6.2: High 1 and 2) and/or contained clusters of transduced cells, usually around the perimeter of the ALI culture insert, with higher levels of fluorescence (Figure 6.2: High 3). The cell clusters were possibly caused by mechanical disruption of the cell layer during transduction, which has previously been shown to enhance gene transfer (Wang et al., 1999) and therefore may not reflect viral transduction from the apical surface, but from the basolateral surface of these cells.

Daily BLI measurements were taken to determine the average radiance ($p/s/cm^2/sr$) of each ALI culture following addition of luciferin to activate the luciferase in the EGFPLux2 fusion protein (Section 2.11.4). The mean average radiance of the sham samples was used to normalise the measurements, to account for auto-luminescence and day-to-day variability in background luminescence detection. For every ALI culture an increase in average radiance could be observed from D01 to D03 (Figure 6.3A) followed by relative stability until the cells were harvested on D12 (Figure 6.3B). A slight increase in average radiance was observed between D07 and D08, coinciding with the use of a new batch of Luciferin. No dose-dependence was observed at any time point due to the high variability within dosing groups therefore the average radiance within individual ALI cultures has been plotted (Figure 6.3B).

A

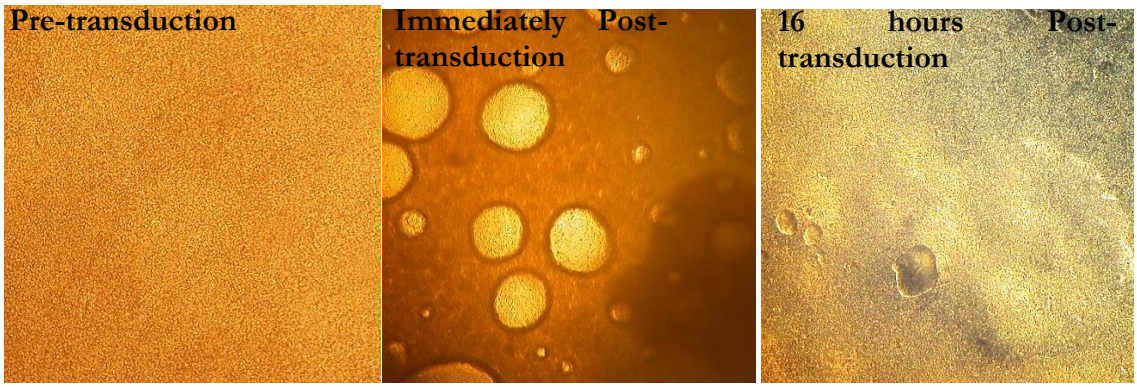

B

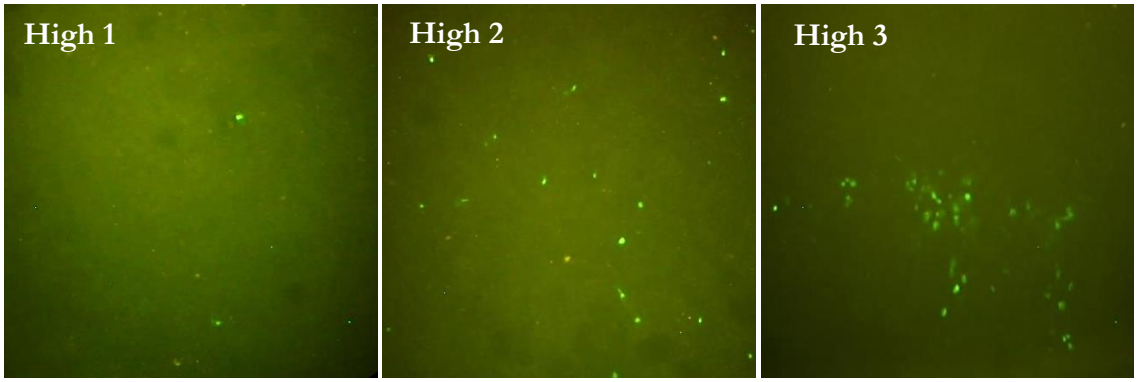

Figure 6.2. Micrographs of the EGFPLux2 fluorescence of ALI cultures transduced with High doses of vEGFPLux2-F/HN

Representative micrographs are shown of ALI cultures pre- and post-transduction showing the circular gaps formed in the cell layers upon transduction (A). Micrographs taken at D10 of three separate ALI cultures treated with the High dose virus were representative of all transduced cultures (B): areas of very low transduction in individual cells (High 1), areas of slightly more frequent transduction in individual cells (High 2) and clusters of transduced cells (High 3). All micrographs were taken at 10x magnification and images were scaled proportionally.

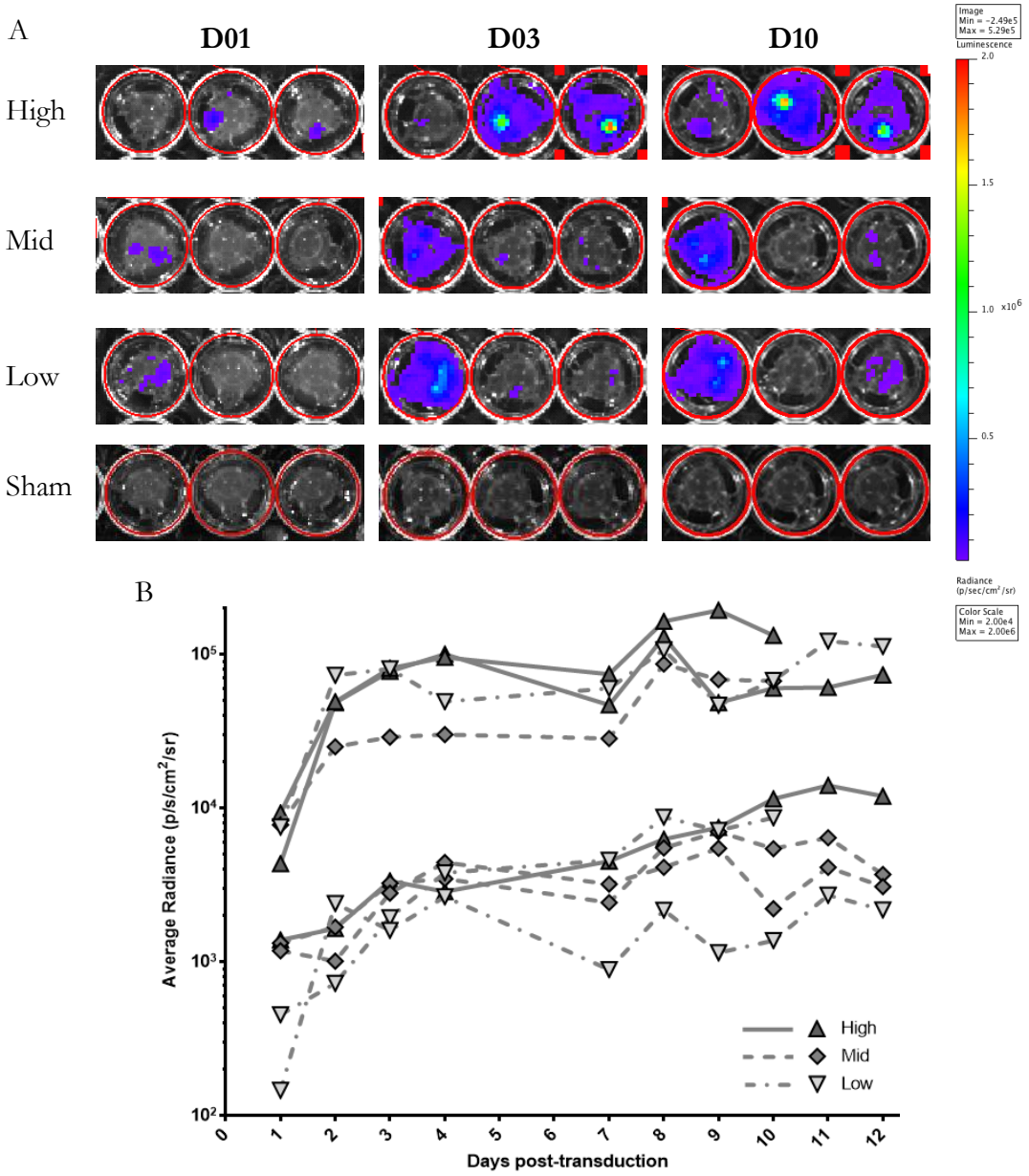

Figure 6.3. Bioluminescent imaging (BLI) and average radiance calculations of ALI cultures transduced with Low, Mid and High doses of vEGFPLux2-F/HN.

ALI cultures were transduced with either Low (5 x 10^7 TTU), Mid (2.5 x 10^8 TTU) or High (5 x 10^8 TTU) doses by apical administration of vEGFPLux2-F/HN in 100µl serum-free media for four hours followed by several washes with MucilAir media. Transduced cells were maintained up to D12 and BLI measurements performed at regular intervals. BLI data is shown as heat map photographs of radiance shown from the apical side of all cultures at D01, D03 and D10 (A; n=3). For each dose the ALI cultures 1 to 3 are shown left to right. The average radiance per ALI was calculated for the region of interest (ROI; red circle) and plotted for each individual well (B).

The inserts with the highest visible expression levels on the BLI heat map (High 2 and 3, Mid 1 and Low 1) emitted an average radiance of between 6 x 10^4 and 1.3 x 10^5 p/s/cm^2/sr per ALI culture, whereas the ALI cultures with low expression levels on the heat map (High 1, Mid 2 and 3, Low 2 and 3) emitted an average radiance of between 1.3 x 10^3 and 1.1 x 10^4 p/s/cm^2/sr per ALI culture.

The number of EGFP-positive cells in each insert was highly variable within doses (Figure 6.4). On day 12 Low 1, Mid 2 and High 1 inserts were harvested for RNA analyses (n=1) and Low 2, Mid 3 and High 3 harvested for protein analyses (n=1). Transgene mRNA expression was quantified using the WPRE mRNA assay (Section 2.9.2) and indicated that WPRE could be detected at similar levels in all three dosed groups (Figure 6.5).

These results indicated that although transduction with vEGFPLux2-F/HN was achievable in ALI cultures at these doses, the transduction efficiency was probably too low and too variable for subsequent knockdown studies with the dual-function rLV vectors using this normal dosing strategy.

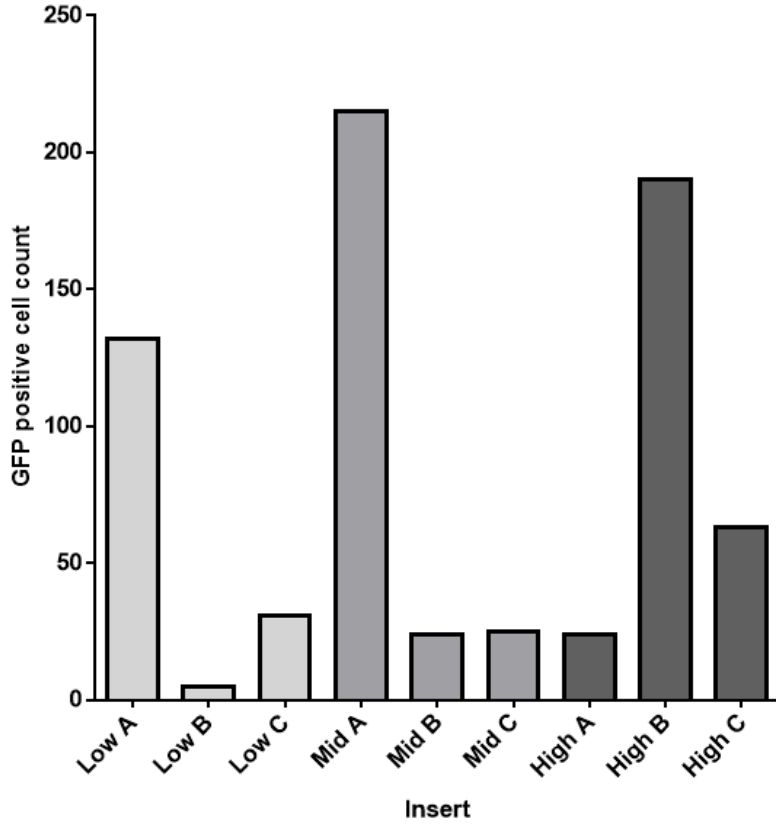

Figure 6.4. Number of EGFPLux2 positive cells determined by microscopy

ALI cultures were transduced with either Low (5 x 10^7 TTU), Mid (2.5 x 10^8 TTU) or High (5 x 10^8 TTU) doses by apical administration of vEGFPLux2-F/HN in 100µl serum-free media for four hours followed by several washes with MucilAir™ media. At D07 EGFPLux2 positive cells were counted by eye. Each bar represents measurements from a single culture.

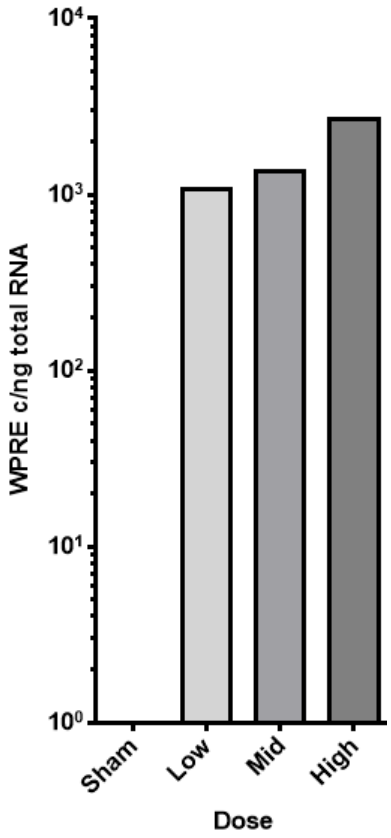

Figure 6.5. Transgene mRNA quantification of RNA harvested from ALI inserts transduced with Low, Mid or High doses of vEGFPLux2-F/HN

ALI cultures were transduced with either Low (5 x 10^7 TTU), Mid (2.5 x 10^8 TTU) or High (5 x 10^8 TTU) doses by apical administration of vEGFPLux2-F/HN in 100µl serum-free media for four hours followed by several washes with MucilAir™ media. ALI cultures Low 1, Mid 2 and High 1 were harvested on D12 using Trypsin/EDTA. RNA was extracted and WPRE copies per ng of total RNA (WPRE c/ng) detected by RT-PCR. Each bar represents a single ALI culture.

6.2.3 Effect of interval dosing on ALI culture transduction efficiency

A possible reason for the lack of dose response observed at the doses tested in section 6.2.2 could be the saturation/overcrowding of the ALI surface with viral particles (Section 6.3). In an attempt to improve transduction efficiency the Low dose of rLV particles (5 x 10^7 TTU/ALI) used in the previous study was divided into 20 aliquots (determined based on calculations outlined in section 2.11.3) and delivered repeatedly (Figure 6.1A and B; Interval). The dose aliquots were delivered over 3 days, with eight doses delivered on D00, and six each on D01 and D02; ALI cultures were washed prior to each dose to aid removal of residual virus particles. The volume added to the surface of the ALI culture was also reduced from 100µl to 10µl to try to minimise disruption of the ALI cell layer (Figure 6.2A).

The level of EGFPLux2 expression was determined by BLI at D02 and then at regular intervals up to D10. The average radiance was ~1.5 x 10^5 p/s/cm^2/sr by D02 and then steadily decreased to 4.3 x 10^4 p/s/cm^2/sr (a 3.5-fold decrease) by D10. There was a 10-fold difference in average radiance between the ALI cultures at early time-points, but by D05 the BLI measurements were similar (Figure 6.6). These data suggest that the strategy of dividing a total dose between multiple applications (a strategy that will be referred to as 'interval dosing') could increase rLV-dependent transduction and transgene expression in ALI cultures. However, the extent to which the interval dosing could increase virus transduction efficiencies (~1.65-fold compared to the Low normal dose; Figure 6.10) was not sufficient to warrant a change in the protocol from the normal dosing strategy.

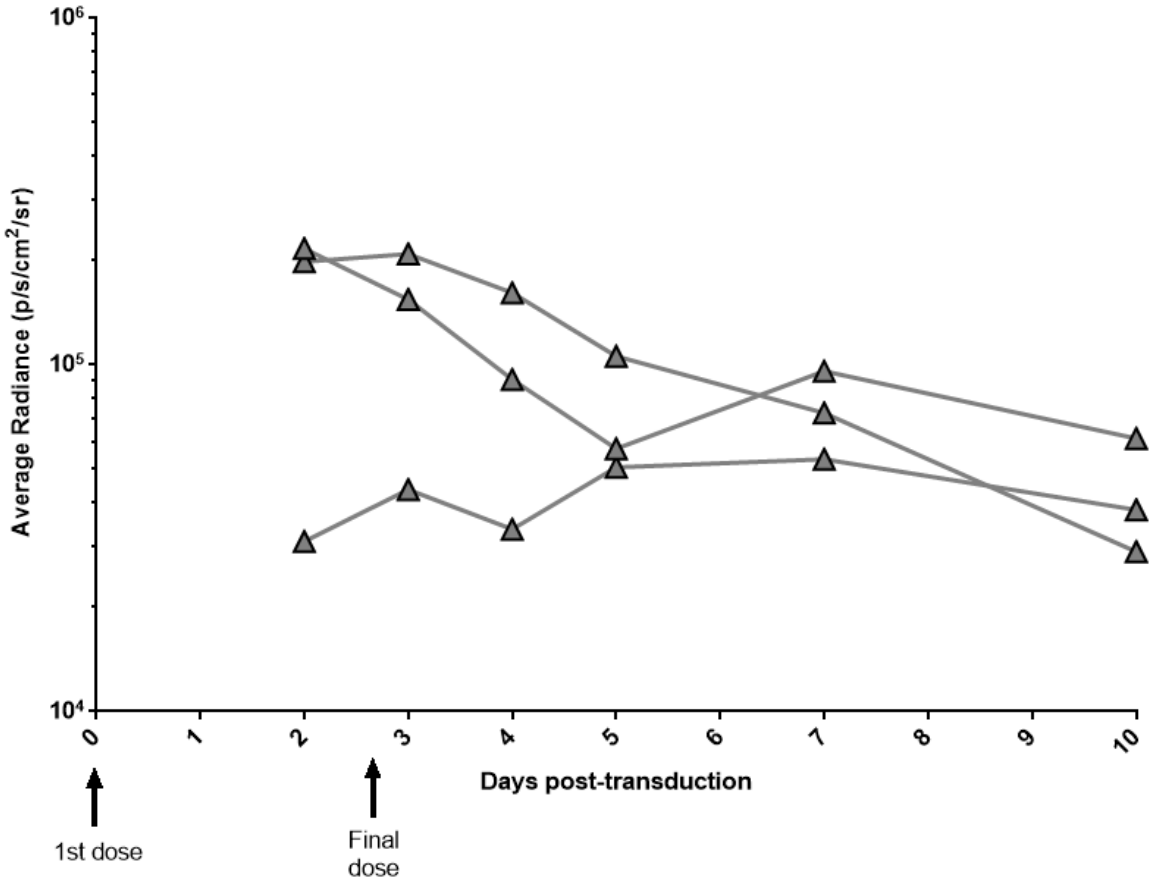

Figure 6.6. Average radiance calculations of ALI cultures transduced with interval doses of vEGFPLux2-F/HN

ALI cultures were transduced with a Low (5 x 10^7 TTU) dose by apical administration of vEGFPLux2-F/HN in twenty 10µl aliquots of 2.5 x 10^6 TTU in serum-free media delivered hourly and split over three days (Figure 6.10). The timing of the final dose is indicated on the x-axis. Each culture was washed with MucilAir™ media following 1hr incubation of the virus on the apical surface. BLI measurements were performed at regular intervals and the average radiance was calculated. The average radiance for each culture was plotted separately up to D10.

6.2.4 An EGTA dosing strategy to improve transduction in ALI cultures

The use of adjuvants to transiently disrupt tight junctions, or decrease mucociliary transport has been shown to facilitate increased virus transduction in primary ALI cultures (Sinn et al., 2005) and *in vivo*(Limberis et al., 2002). The addition of the Ca^{2+} chelating agent EGTA has been used to transiently disrupt tight junctions and increase gene transfer by allowing access to the receptors located on the basolateral surface as well as the apical surface (Wang , 1998, Wang , 1999, Walters , 1999, Thomas and Roth, 1994). To determine whether EGTA could also increase the transduction efficiency of vEGFPLux2-F/HN in ALI cultures, the Low dose of virus (5 x 10^7 TTU/ALI) was delivered as previously (Section 6.2.2) but with the addition of 10mM EGTA (referred here as 'EGTA dosing'; Figure 6.1A) to the virus mixture and a 4 hour incubation, followed by gentle washing of the ALI cell surface. Results indicated that the mean average radiance at D02 was 2.02 x 10^6 p/s/cm^2/sr, reaching a maximum at D03 of 5.82 x 10^6 p/s/cm^2/sr which then levelled off and declined steadily from D05 to 2.57 x 10^6 p/s/cm^2/sr at D10 (Figure 6.7). The addition of EGTA resulted in expression that was increased by ~60-fold compared with interval dosing (Figure 6.6), and by ~100-fold compared to normal dosing (Figure 6.3; Figure 6.10). This increase could be sufficient to detect changes in target gene expression from a dual-function rLV vector.

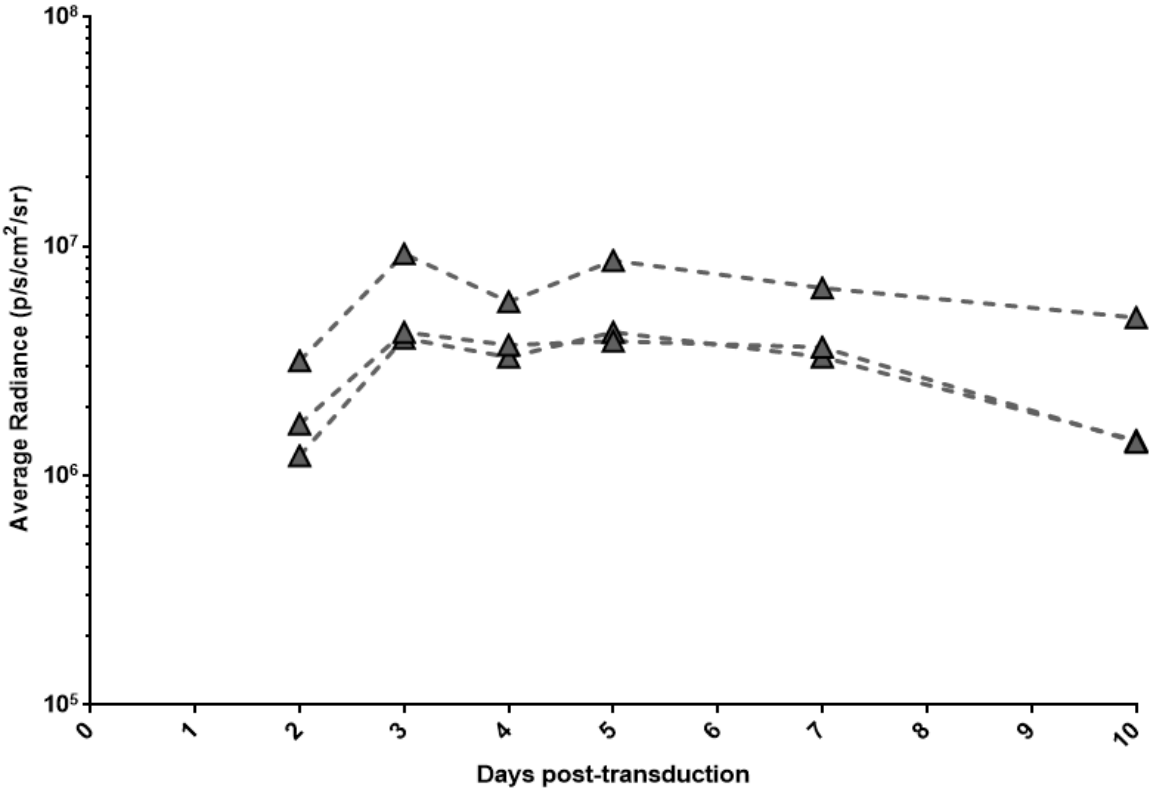

Figure 6.7. Average radiance of ALI cultures transduced with a single dose of vEGFPLux2-F/HN with addition of EGTA

ALI cultures were transduced with a Low (5 x 10^7 TTU) dose of vEGFPLux2-F/HN by apical administration in 100µl serum-free media with 10mM EGTA and each culture was washed with MucilAir media following 4hr incubation. BLI measurements were performed at regular intervals and the average radiance per ROI was calculated. The average radiance for each culture was plotted separately up to D10.

6.2.5 A multiple-EGTA dosing strategy to improve transduction in ALI cultures

Although the addition of EGTA increased BLI intensity by 2 log orders of magnitude (Section 6.2.4), attempts were made to further increase transgene expression in ALI culture by re-dosing with the Low dose (5 x 10^7 TTU/ALI) and EGTA at D10, and again at D20. Re-dosing at D10 led to an increase in average radiance by 4.8-fold by D19 which was 473-fold greater than the Low dose delivered using the normal dosing strategy (Figure 6.10). A third dose at D20 led to a further increase, but this was restricted to only 1.7-fold by D28 (Figure 6.8A) and was accompanied by a decline in ALI culture health including lower levels of cilia beating and altered cell morphology (Figure 6.8B)

To determine whether ALI cultures treated with the interval dosing strategy could also be re-dosed in this manner, at D10 and D20 the interval-dosed cultures from section 6.2.3 were also treated with the Low dose containing EGTA. The second dose at D10 resulted in an increase in average radiance 314-fold by D20 (Figure 6.8A). The third dose delivered at D20 resulted in a further 2.1-fold difference in average radiance by D28 (Figure 6.8A). These data suggest that two doses of virus with EGTA addition, delivered to ALI cultures at 10-day intervals are sufficient to increase transgene expression by at least 519-fold compared to a single Low dose without EGTA. However as the third dose led to a deterioration in cell health, subsequent studies were restricted to two EGTA doses of 5 x 10^7 TTU/ALI at D00 and D10 with harvesting at D20 for data collection (Figure 6.1). This approach is referred to as 'multiple-EGTA dosing' (Figure 6.1A).

A

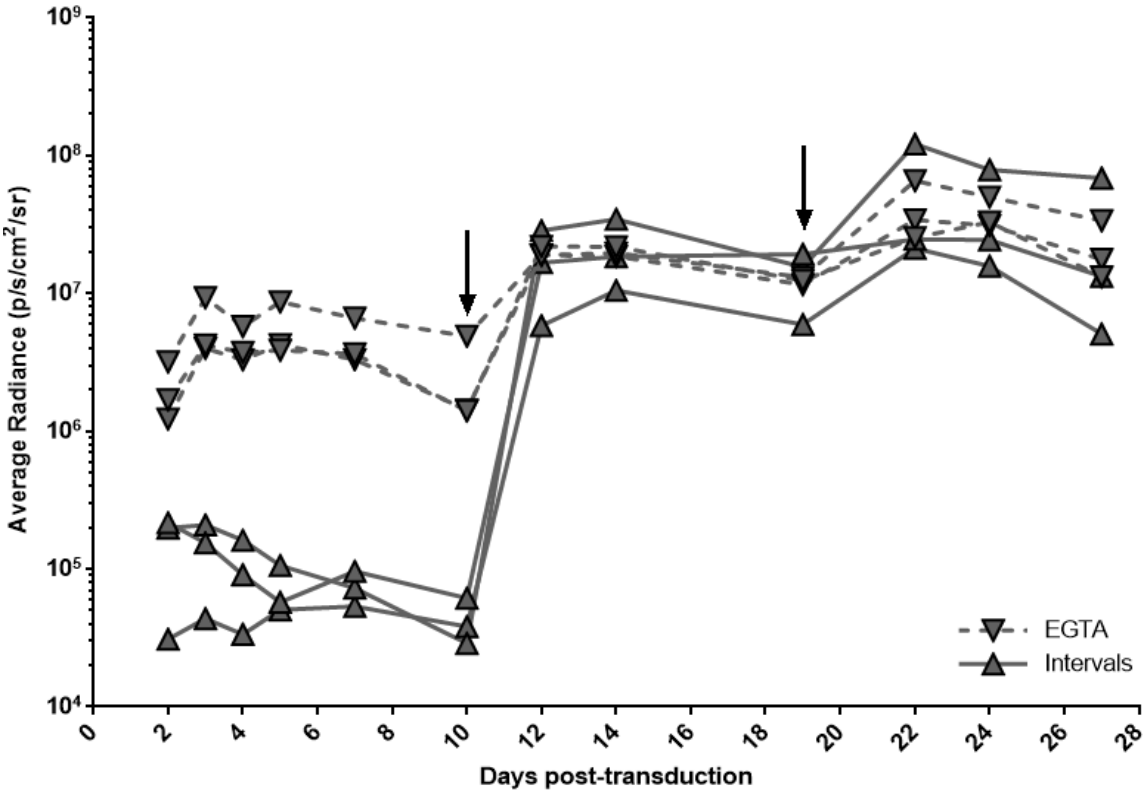

B

Figure 6.8. Average radiance of ALI inserts transduced with multiple-EGTA dosing of vEGFPLux2-F/HN and micrographs showing cell morphology after each dose.

ALI cultures were initially transduced with a Low (5 x 10^7 TTU) dose of vEGFPLux2-F/HN by EGTA dosing (EGTA; section 6.2.4) or interval dosing without EGTA (intervals; 6.2.3). At D10 and D20 both sets of ALI cultures were re-dosed with a further Low dose (5 x 10^7 TTU) using the EGTA dosing strategy (black arrows). BLI measurements were performed at regular intervals and the average radiance was calculated (A). The average radiance for each culture was plotted separately up to D28. Micrographs of a single ALI culture were also taken at 10x magnification after each dose (B) to show the change in cellular morphology with multiple doses.

6.2.6 Transduction of ALI cultures with anti-hBACH1 rLV

The improved multiple-EGTA dosing strategy (Section 6.2.5), was used to transduce ALI cultures with the shRNA-containing vector vBash3-EGFPLux2-F/HN (vGM123; Table 2.1). This rLV vector was specifically selected to evaluate potential knockdown in ALI cultures because the knockdown of hBACH1 results in concomitant hMOX1 up-regulation (Section 5.1), offering an increased opportunity to observe an effect with low levels of target knockdown. The use of the EGFPLux2 transgene rather than soCFTR2 enabled transgene expression detection by BLI throughout the transduction period. Two doses of vBash3-EGFPLux2-F/HN were delivered using the multiple-EGTA dosing strategy (Section 6.2.5; Figure 6.1). The initial dose (D00) led to an average radiance of 2.20 x 10^6 p/s/cm^2/sr by D09 that increased by a further 2-fold following the second dose to 4.22 x 10^6 p/s/cm^2/sr by D17 (Figure 6.9) when cultures were harvested. Total RNA was extracted and the relative expression of hBACH1 and hHMOX1 was determined as previously using RT-PCR (Section 2.9.1). The multiple-EGTA dosed samples from section 6.2.5 at D28 and a sham-treated group acted as negative hBACH1 knockdown controls. A modest, (~30%) but significant reduction in *hBACH1* mRNA levels was observed in ALI cultures transduced once with vBash3-EGFPLux2 when compared to the sham-treatment. However, no concomitant up-regulation of hHMOX1 expression was detected, and the relative hBACH1 expression was not significantly different from that detected in ALI cultures transduced with multiple-EGTA dosed vEGFPLux2-F/HN (Figure 6.9B). These data suggest that vBash3-EGFPLux2 may have the potential to substantially knock down hBACH1 in ALI cultures, but a higher transduction efficiency may be necessary to confidently detect this knockdown at the mRNA level. These data also suggest that a second EGTA-mediated dose may not be necessary. Regrettably, further investigation of this observation was curtailed by the expense of commercial ALI cultures and high-titre viral production. A summary figure of results from all of the ALI culture dosing strategies is provided below (Figure 6.10).

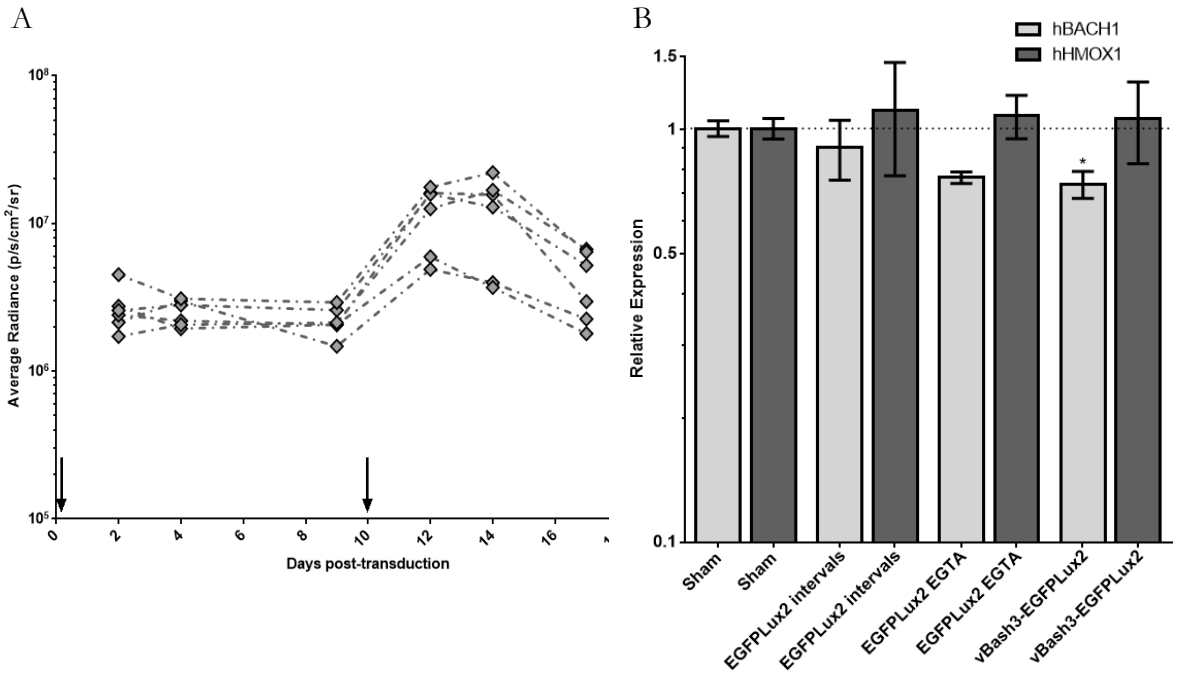

Figure 6.9. Average radiance and target mRNA relative expression in ALI cultures transduced with vBash3-EGFPLux2 using the multiple-EGTA dosing strategy.

ALI cultures were transduced with vBash3-EGFPLux2 using the multiple dosing strategy (Section 6.2.5; Figure 6.1) resulting in a delivery of 1 x 10^8 TTU/ALI over the course of the study. BLI measurements were performed at regular intervals and the average radiance was calculated (A). The average radiance for each culture was plotted separately up to D17 when cells were harvested for RNA extraction. The relative expression of hBACH1 and hHMOX1 was determined by RT-PCR. Samples harvested at D28 from the multiple-EGTA dosing study using vEGFPLux2-F/HN were also analysed to act as transduced controls alongside the sham-treated controls. * $p<0.05$ compared to sham-treated cells in the same assay, one-way ANOVA with Tukey's multiple comparisons test.

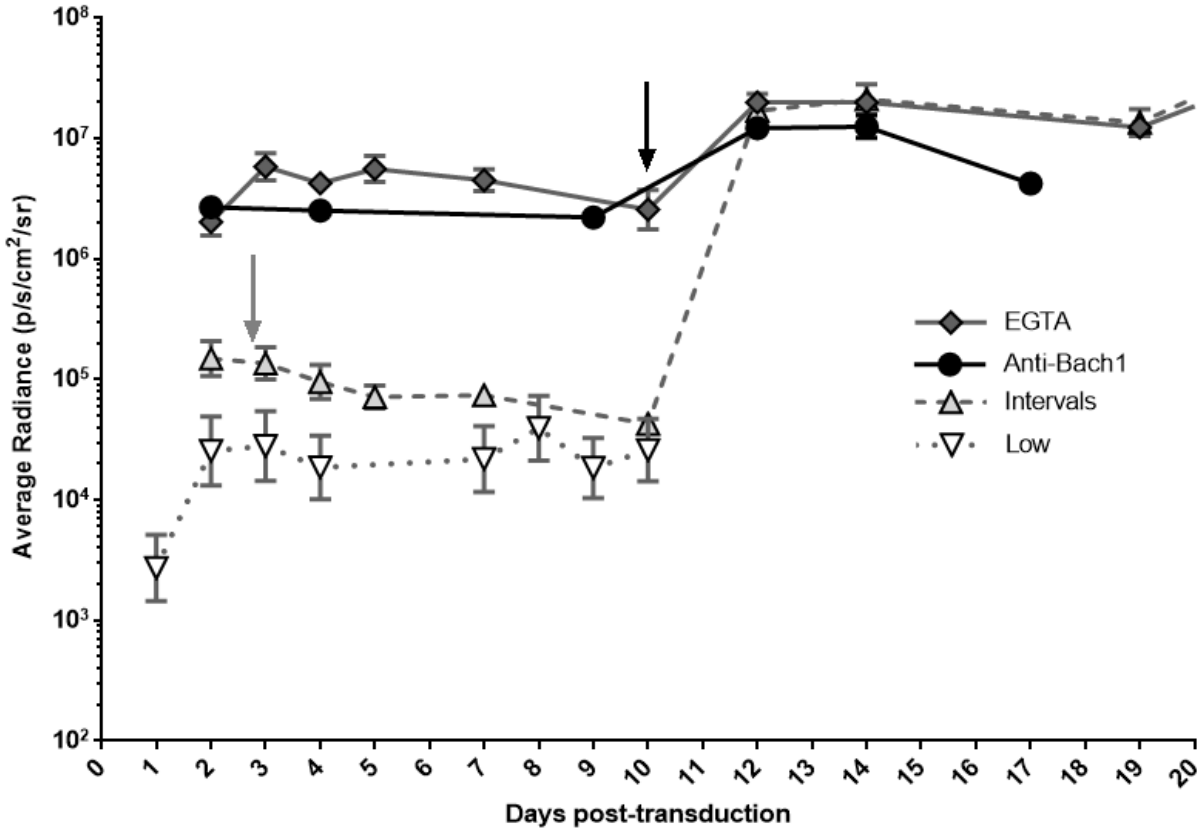

Figure 6.10. Summary chart of average radiances for the different dosing strategies

Three different dosing strategies were employed as outlined in Figure 6.1: normal dosing (dotted grey line; Low dose only indicated; n=3), interval dosing (dashed grey line; grey arrow indicates final interval dose delivery; n=3), and EGTA dosing (solid grey line; n=3) which is also the multiple-EGTA, with the black arrow indicating the second dose. The average radiance of the anti-BACH1 rLV vBash3-EGFPLux2 is also included (solid black line; n=6). Symbols represent the mean ± SEM.

6.3 Discussion

In this chapter various strategies were employed to increase transgene expression in non-CF ALI cultures (Figure 6.1A), for the development of a protocol that could detect target gene knockdown and transgene expression from a dual-function rLV vector. The effect of different dosing strategies was assessed using vEGFPLux2-F/HN rLV (vGM035), a vector that does not contain an shRNA sequence for target knockdown. The shRNA cassette was excluded to allow determination of the best dosing strategy without any potential detrimental effects that shRNA expression could have on viral yield during high-titre/purity production, transduction efficiency and ALI culture health.

The initial dosing strategy was based on published experiments performed by Mitomo and colleagues where 1.25 x 10^7 and 1.25 x 10^8 TTU/ALI were delivered directly to the apical surface of ALI cultures for 6 hours (Mitomo , 2010). The virus incubation time on ALI cultures was reduced to 4 hours in order to reduce ALI culture deterioration that has been observed by others (Uta Griesenbach, Imperial College, London, personal communication), and three doses were chosen: Low dose (5 x 10^7 TTU/ALI), Mid (2.5 x 10^8 TTU/ALI) and High dose (5 x 10^8 TTU/ALI) to determine a) whether reporter gene expression could be detected, and b) whether a dose response could be observed.

As early as D01 reporter gene expression could be detected by BLI (Figure 6.3A), reaching maximum expression by D02 which then persisted until D12 when the ALI cultures were harvested (Figure 6.3B). Transgene expression at D10 and D12 could also be detected by EGFP fluorescence imaging (Figure 6.2; Figure 6.4) and by RT-PCR analysis of transgene expression (Figure 6.5).

These results were difficult to compare directly with the results of Mitomo and colleagues as their published data largely focused on luciferase assays (transgene expression is expressed as relative light units per mg total protein (RLU/mg)) rather than BLI analysis (Mitomo et al.,

2010), however, the authors report a dose response between 1.25 x 10^7 and 1.25 x 10^8 TTU/ALI that was not detected in the current study. The lack of dose response observed here could be a result of inherent experimental variability due to the low number of ALI cultures transduced per dose (n=3) although this is similar to the Mitomo paper. Alternatively, it may reflect uneven transduction efficiency within ALIs as noted by the presence of clusters of transduced cells observed in disrupted areas of the ALI culture (Figure 6.2; High 3) that are also clearly visible as areas of high radiance in BLI images (Figure 6.3A; High 2, High 3, Mid 1 and Low 1). To reduce the impact of these clusters on the overall analyses, the average radiance per ALI in the region of interest (ROI) was calculated rather than the total radiance in the ROI as is used in some studies, despite this approach, the increase in the number of transduced cells (Figure 6.4) in the four cultures (High 2, High 3, Mid 1 and Low 1) resulted in at least a one log increase compared to the remaining cultures (Figure 6.3A).

One confounding factor, and possible cause of the observed mechanical disruption that appeared to lead to increased transduction efficiency, was the volume in which the virus is delivered. Virus doses were typically delivered in 100µl of serum-free media that remained in contact with the apical surface for 4 hours. At this point, 'gaps' could be observed in all ALI cultures, even controls receiving media alone (Figure 6.2A). While these gaps were largely re-populated by 16h post-transduction, the addition of 100µl media for 4 hours may well be detrimental to ALI cell health. Another reason for the lack of a dose response could be that the maximum level of transduction from a single dose had been reached, suggesting that the doses delivered could have been unnecessarily high: according to calculations based on the area of the membrane and HIV particle size the single 5 x 10^7 TTU dose (equivalent to 1.8 x 10^{10} VP; Table 6.1; section 2.11.3) would result in saturation of the ALI apical surface with 11-fold more virus than would be required to coat the ALI surface. These calculations also suggest that 5.3 x 10^6 TTU (1.87 x 10^9 VP) would provide a sufficient number of VP to coat the ALI surface. With this in mind, the Low dose was split into 20 aliquots of 2.5 x 10^6 TTU

delivered predominantly with 1 hour gaps over 3 days as indicated in Figure 6.1B. The use of this 1 hour gap was supported by studies with native SeV particles (Morgan and Howe, 1968) where almost complete virus entry to target cells was observed within 1 hour of infection.

The ALI apical surfaces were also washed gently immediately prior to each dose (and 1 hour following the final dose per day) to remove residual viral particles that are either in excess or had failed to enter the cells. This interval dosing strategy (20 x 10µl doses of 2.5 x 10^6 TTU/ALI at hourly intervals) resulted in a higher average radiance than the normal dosing strategy D02. However, in the limited studies performed, expression then fell to a similar level to the normal dosing strategy by D10 (Figure 6.6; Figure 6.10 summary). Intriguingly, although the interval dosing strategy involved virus addition up until D03, there was no apparent increase in transgene expression from D02 onwards (Figure 6.10), suggesting that the later doses of virus did not contribute to transgene expression. Using the data collected here it is not possible to rule out the possibility that all transgene expression observed is from the first day of dosing, or even the first 10µl aliquot. Due to the cost of the ALI cultures and high-titre virus it was decided, however, to switch to an alternate strategy (EGTA dosing) offering increased transgene expression, rather than investigate this phenomenon further.

The use of adjuvants to enhance gene transfer both *in vitro* and *in vivo* has resulted in the identification of Ca^{2+} chelators and ciliastatic agents that have the potential to enhance gene transfer to airway epithelial cells. In this study, the Ca^{2+} chelator EGTA was chosen, as this adjuvant disrupts the tight junctions allowing increased access to a greater surface area (Wang et al., 2000a). Although EGTA is more commonly used to increase the transduction efficiency of rLV pseudotypes targeting the basolateral surface of cells, such as VSVG (Wang et al., 1998; Wang et al., 1999; Wang et al., 2000b), it was hypothesised that the use of EGTA in this study would expose a greater surface area for virus adhesion to the epithelial cells; it is also possible that the SeV coat proteins could access epithelial cells via basolateral receptors as well as the apical SA-R (Bitzer et al., 1997). The addition of EGTA to the virus for simultaneous

application to the apical surface of ALI cultures resulted in greater transgene expression than with the normal or interval dosing strategy with the same dose (5 x 10^7 TTU/ALI) by two log orders of magnitude (Figure 6.7; Figure 6.10). A further increase was observed when a second dose of EGTA/virus was applied to the apical surface at D10 resulting in ~650-fold greater expression than the normal or interval dosing by D20 (Figure 6.8; Figure 6.10). The cultures that were interval-dosed were also re-dosed at D10 using the EGTA strategy and this resulted in an increase in average radiance matching the multiple-EGTA dosing strategy at D20 (Figure 6.8; Figure 6.10) suggesting that the level of transgene expression achieved from this D10 dose is the maximum possible when re-dosing in this manner. Further studies would be required to determine the most suitable quantity of virus and schedule of dosing to further increase transgene expression.

To determine whether the multiple-EGTA dosing strategy was a) reproducible, and b) increased transgene expression to a level that was suitable to detect target mRNA knockdown with an shRNA-expressing vector, this strategy was employed to deliver vBash3-EGFPLux2-F/HN to ALI cultures. The transgene expression profile was similar to that observed with vEGFPLux2-F/HN (Figure 6.9; Figure 6.10) except that the expression appeared to decrease by D17. A repeat of this study would be necessary to determine whether this decrease in expression is reproducible and to determine whether its cause is the addition of the shRNA cassette. While the vBash3-EGFPLux2-F/HN decreased hBACH1 expression by ~30% compared to the sham-treatment, no concomitant increase in hHMOX1 expression could be observed, suggesting that further increases in the number of cells transduced and/or shRNA cassette expression is required to achieve hHMOX1 up-regulation.

In summary, this chapter shows the improvement of the delivery of rLV pseudotyped with SeV to primary human airway epithelial cells grown at the air-liquid interface; whether this level of transgene expression is sufficient to knock down target gene expression is unresolved at present. Moving forward, functional studies using the anti-hENaCα dual-function rLV,

vNash8-soCFTR2-F/HN (Table 6.1) in ALI cultures derived from CF patient tissues, to reveal functional differences in Cl^- and Na^+ channel activities, may require further advances in ALI transduction efficiency and/or shRNA expression.

Chapter 7: Discussion

7.1 Development of vectors for gene therapy of CF lung disease

Since the discovery of the CFTR gene in 1989 (Riordan et al., 1989) CF has been considered a 'pathfinder' for gene therapy, although enthusiasm for CF lung gene therapy has been largely dampened due to inefficacy of both viral and non-viral vectors in the lung (Section 1.4), and the relatively slow progress over the last 25 years despite numerous clinical trials (reviewed in Prickett and Jain, 2013). The main problems associated with CF gene therapy are inefficiency of gene transfer to the target cells in the lung, possibly due to the mucus hyperviscosity encountered in the lungs of CF patients, and uncertainty over the most clinically relevant target cell type itself. In animal models pre-treatment with the mucolytic lysophosphatidylcholine (LPC) enhanced transduction efficiency of viral vectors following delivery to the lung, however, repeat administration was problematic due to the presence of neutralising antibodies against the virus coat proteins (Griesenbach et al., 2011), and toxic effects of the LPC treatment on the airway epithelia due to the disruption of tight junctions (Cmielewski et al., 2010).

Even though not proven to be clinically beneficial so far, many early clinical CF gene therapy trials using both viral and non-viral vectors have progressed the field for lung gene therapy and have encouraged the further refinement of gene transfer vectors (Section 1.4). Evaluation of non-viral formulations for CF has been extensive with many tested in the nasal epithelium, useful as a surrogate airway tissue, but only the GL67A liposome formulation has been evaluated in the lungs following aerosol delivery (Alton et al., 1999; Ruiz et al., 2001; Alton et al., 2013a; Alton et al., 2013b), and it is not yet known whether the resultant gene transfer efficiency, even after multiple administrations, is sufficient for clinical benefit. In terms of viral vectors, both recombinant Adenovirus (rAd) and adeno-associated virus (rAAV) vectors have been evaluated in the CF lung with varying degrees of success (Section 1.4.3) however

neither has so far been judged promising enough to take forward. There is still a possibility that a rAAV with a serotype displaying improved efficiency for lung gene transfer, such as rAAV6.2 or rAAV9 (Song et al., 2009; Bell et al., 2011), may be investigated in the future.

Recombinant Lentivirus (rLV) is a potentially exciting viral vector for airway gene transfer due to the development of pseudotypes with improved transduction efficiencies in the airways of animal models, including the use of F and HN coat proteins from Sendai virus (Section 1.4.3). Treatment of chronic CF lung disease will probably require the ability to repeatedly administer a gene transfer vector to the lung without loss of efficacy, a problem which has been observed with both rAd and rAAV vectors (Harvey et al., 1999; Moss et al., 2007). However, several studies suggest that rLV vectors may overcome this particular obstacle (Mitomo et al., 2010; Griesenbach et al., 2012) at least in the rodent airways. So far, the clinical use of rLV has been restricted to applications requiring only small quantities of vector, such as *ex vivo* delivery (Aiuti et al., 2013; Biffi et al., 2013), delivery to the eye (Bainbridge et al., 2008), or delivery to the brain (Palfi et al., 2014) *in vivo*. However improvements in the production of high purity, high titre rLV preparations are now being addressed (Lee Davies, personal communication; Merten et al., 2011), which means that the use of rLV for larger target organs, such as the lung, is becoming feasible.

The suitability of rLV for expression of CFTR in the airways as a treatment for CF lung disease is currently being evaluated in animal models (Mitomo et al., 2010; Griesenbach et al., 2012). However, expression of CFTR alone might not be sufficient for effective therapy. Studies summarised in Chapter 1 indicate that in addition to defective chloride (Cl^-) movement via the CFTR chloride channel, CF is associated with hyperabsorption of sodium ions (Na^+) across the airway epithelium by the epithelial sodium channel, ENaC (Section 1.2.2). Whereas CFTR and ENaC work together in normal airways to regulate airway surface liquid (ASL) hydration, thus supporting effective mucociliary clearance, in the CF airway

enhanced activity of ENaC leads to further dehydration of the epithelial surface. These observations led to the proposal to develop a dual function rLV vector capable of not only efficiently expressing the CFTR protein, but also of reducing expression of ENaC.

7.2 Generation of a modular recombinant lentivirus (rLV) for dual-function therapy

The majority of studies utilising rLV have evaluated vectors based on sequences derived from human immunodeficiency virus (HIV), rather than simian Immunodeficiency virus (SIV), feline immunodeficiency virus (FIV) or equine infectious anaemia virus (EIAV). SIV and FIV have not been assessed clinically, however this year a first-in-human trial for rLV gene therapy to treat Parkinson's disease shows great promise for the future of rLV gene therapy: patients receiving a tri-cistronic rEIAV (ProSavin) surgically delivered to the striatum resulted in significant improvement in motor function for up to 12 months post-delivery, with no clinically significant adverse effects (Palfi et al., 2014). Currently there are 86 open gene therapy trials worldwide using rLV as the vector, however only four of these trials involve *in vivo* delivery, all of which are for the treatment of ocular diseases via subretinal or intraocular delivery. The only other completed rLV gene therapy trial involved *ex vivo* delivery (Gene Therapy Clinical Trials Worldwide, 2014). Preliminary experiments have indicated that functional expression (at least in cell culture) is similar between SIV and HIV-based rLV vectors (Lee Davies, personal communication).

Studies in chapter 3 focused on the design of a modular recombinant HIV lentivirus (rLV) with the potential for expressing both transgenes and RNAi sequences, aiming to create dual-function vectors that can simultaneously produce transgene expression and knock down target gene expression. This vector was designed to contain strategically positioned restriction

sites to allow simple insertion of a) transgene sequences, b) transgene promoter sequences, and c) shRNA or shRNAmir sequences. A modular rLV vector genome plasmid was constructed (Figure 3.1) and a reporter transgene (enhanced green fluorescent protein-luciferase fusion; EGFPLux2) inserted along with a cytomegalovirus promoter/enhancer sequence (CMV-) to drive its expression (Figure 3.5). The resultant rLV vector (virus), vEGFPLux2 (vGM029; Table 2.2) successfully transduced both human (A549) and mouse (M-1) cell lines with transduction efficiencies of >85% and >50% respectively, with minimal reduction in cell viability at medium doses (Figure 3.7).

7.3 Screening of RNA interference (RNAi) sequences in A549 cells

Once the modular vectors had been constructed suitable knockdown sequences for use in the modular vectors were identified. In chapter 4 a screening protocol was developed to allow quick and simple knockdown analyses. The ENaC α-subunit (ENaCα) was chosen as the knockdown target for development of the screening protocol as this subunit appears to control ENaC gating, whereas ENaCβ and ENaCα appear to control channel conductance (Canessa et al., 1994a; Alvarez de la Rosa et al., 2000). Knockdown of the ENaCα subunit using short interfering RNA (siRNA) molecules has previously been shown to decrease both the amiloride-sensitive short circuit current (Isc_{amil}: representative of ENaC channel function) and fluid absorption from the ASL (Caci et al., 2009).

Initially, anti-ENaCα shRNA sequences were obtained in a pGIPZ vector genome plasmid (Figure 4.2), where each sequence was embedded within the endogenous miR-30 sequence (Section 4.2.2). RNA interference sequences such as these are known as shRNAmirs, and can be transcribed from the same expression cassette as the transgene. The expression cassette in the pGIPZ plasmid is in fact tri-cistronic, consisting of a turbo GFP (tGFP) reporter sequence, the puromycin resistance gene (PuroR) and the shRNAmir sequence, expressed

from CMV- and containing an internal ribosome entry site (IRES) upstream of the PuroR sequence (Figure 4.2). These expression cassettes allow indirect quantification of shRNAmir expression through assessment of tGFP expression. Attempts to screen these sequences by transient transfection of A549 cells directly with the pGIPZ plasmids initially resulted in significant knockdown of hENaCα with all constructs (data not shown), however, these initial results were obtained using sham-treated cells as the comparator. The use of the non-target shRNA-containing plasmid pLKO-Scramble as the comparator revealed that the hENaCα knockdown detected initially could also be detected when cells were transfected with pLKO-Scramble (Figure 4.4) and appeared to be an artefact of cellular toxicity. It was hypothesised that the toxicity observed was mediated by backbone sequences in the pGIPZ plasmid, possibly due to the fact that this plasmid constitutes a viral genome plasmid used to produce rLV vectors. Therefore, shRNAmir sequences were extracted from the pGIPZ backbone and inserted into the modular genome plasmid created in chapter 3, downstream of the EGFPLux2 transgene, which was then used to produce VSVG-pseudotyped rLV vectors. Unfortunately, significant knockdown of hENaCα could not be detected (Figure 4.12B). It was uncertain whether the lack of detectable knockdown was due to low/no expression of the shRNAmir sequences or inefficacy of the shRNAmir sequences, however analysis of WPRE mRNA (WPRE was downstream of the shRNAmir sequence) suggested that the entire expression cassette, which would include the shRNA sequence, was transcribed into mRNA (Figure 4.12C). Further studies would be required to determine whether the lack of knockdown observed is due to inefficacy of the shRNAmir sequence, or due to a fault in the downstream processing of the shRNAmir sequence from the transgene-shRNAmir-WPRE mRNA molecule. The latter could be demonstrated by extracting total RNA or miRNA (using a commercial kit such as mirVana miRNA isolation kit, Life Technologies) and designing primers for detecting the shRNAmir sequences; TaqMan primers and probes can be custom-

made to detect RNA as small as 17bp suitable for quantifying the downstream products of the shRNAmir, such as the Drosha-cleaved shRNA and even the Dicer-cleaved siRNA product.

To determine whether the insertion of an shRNA (rather than an shRNAmir) sequence, into the modular vector, could give detectable ENaCα knockdown, shRNA sequences were obtained in the pLKO.1 viral genome backbone, positioned downstream of human U6 pol II promoter. VSVG-pseudotyped rLV vectors were produced directly using the pLKO.1 sequences, which were then used to transduce A549 cells. This strategy could not be used with the pGIPZ viral genome plasmids as they are not compatible with the third-generation rLV production system. A dose of 1.2 x 10^8 VP/cell with puromycin selection for transduced cells resulted in significant knockdown of ENaCα 72 hours post-transduction, as determined by qRT-PCR of extracted mRNA (Figure 4.20).

7.4 Simultaneous transgene expression and target gene knockdown, with recombinant Lentivirus (rLV) in immortalised cell culture.

To determine whether the modular vector designed in chapter 3 could result in simultaneous ENaCα knockdown and CFTR expression, the anti-ENaCα shRNA expression cassette for Nash8, (hU6-Nash8-cPPT) was inserted upstream of the transgene cassette in pEGFPLux2 (pGM290) to create pNash8-EGFPLux2 (pGM392). The EGFPLux2 transgene was also replaced with soCFTR2 to create pNash8-soCFTR2 (pGM395). The dual-function pNash8-soCFTR2 was used to produce the VSVG-pseudotyped rLV vector, vNash8-soCFTR2 (vGM086) shown to knock down *hENaCa* mRNA and protein by <80% and <40% respectively in A549 cell culture (Figures 5.5 and 5.9). CFTR expression could also be detected at both the mRNA (Figure 5.4) and protein (Figure 5.5) levels. Furthermore, the dual-function vector was shown to express functional chloride channels when delivered to

A549 cells via transient transfection, measured by an increase in iodide efflux following transfection (Figure 5.3). The detection of a large band at ~160kDa by anti-CFTR antibody in Western blots suggested that a fully processed CFTR protein was also expressed upon transduction of A549 cells with the dual-function vector, as this band corresponded to the fully glycosylated CFTR bands observed in previous studies (Caldwell et al., 2011).

The vNash8-EGFPLux2 rLV vector was used to estimate the percentage of cells transduced with the dual-function vector, revealing high transduction efficiency (>80% GFP positive) in A549 cells. Quantification of transgene mRNA indicated that the rLV vectors expressing soCFTR2 produced lower transgene expression compared with those expressing EGFPLux2 (Figure 5.5), meaning that the transduction efficiency of the dual-function rLV could be lower than estimated. However, experienced workers in the CF field have observed that expression of the comparatively large CFTR mRNA is often routinely lower than expression of smaller reporter genes from the same configuration of transgene cassette (Deborah Gill, Personal Communication).

To determine whether knockdown of an alternative target could be achieved using the modular vector design, BACH1 was chosen, which is often up-regulated in pulmonary emphysema associated with lung diseases such as CF and chronic obstructive pulmonary disease (COPD). This target also offers an internal control in the form of the concomitant HMOX1 up-regulation that is observed with BACH1 knockdown (Section 5.1). Successful knockdown of hBACH1, with concomitant up-regulation of hHMOX1 was observed when the Bash3 anti-BACH1 shRNA was delivered to A549 cells using the dual-function vector, confirming that this vector can mediate significant target gene knockdown (Figure 5.17).

Attempts to identify a sequence that could knockdown mENaCα in M-1 (mouse kidney) cell culture, for use in mouse studies, were unsuccessful with the dual-function vector. Greater than 80% *mENaCa* mRNA knockdown was achieved with puromycin-selected anti-mENaCα

LKO.1 rLV transduction, but no significant knockdown was observed with the dual-function vector, possibly due to the low transduction efficiency observed compared with transduction in A549 cells (30-50% transduction efficiency compared to >80% at the same dose). It was thought that testing mBACH1 knockdown sequences in M-1 cell culture could produce more promising results, using the added mHMOX1 up-regulation, however, none of the five anti-mBACH1 shRNA sequences tested successfully knocked down mBACH1, even with puromycin selection (data not shown).

It would have been interesting to have identified mouse-specific sequences and generated dual-function vectors for testing in mice, but, with constraints on time and money, a decision was made to focus on only one species and testing model. Focus on the human sequences was originally prioritised because of the potential for investigating epithelial electrophysiology in human air-liquid interface (ALI) cultures. Furthermore, there was also an expectation that smaller quantities of rLV would be needed to generate efficient transduction levels in ALI cultures compared with the quantities required for transduction of the whole lung in mice. Studies described in section 6.2.2 show that a dose of 5×10^7 TTU of rLV is sufficient for transduction of ALI cultures as measured by bioluminescence imaging (BLI) of luciferase expression from the EGFPLux2 fusion protein but that transduction efficiency appears to be very low (Figure 6.3).

One published study has reported knockdown of hENaCα in cell culture upon delivery of an rLV vector showing a 27% decrease in ENaCα mRNA, leading to a 66% decrease in protein expression and a 37% decrease in amiloride-sensitive ENAC short circuit current (Isc_{amil}) in H441 cells (Aarbiou et al., 2012). The transduction efficiency achieved was ~90%; in contrast, in this thesis a transduction efficiency of >80% was observed in A549 cells, causing a >80% decrease in mRNA expression, but only ~50% decrease in protein expression. Aarbiou and colleagues do not state the post-transduction time-point for mRNA or protein extraction for

these analyses, therefore it is difficult to determine whether the protein results found here are comparable. Also, Aarbiou *et al* used different primary antibodies to detect ENaCα protein detecting a band of ~75kDa whereas in this thesis bands were observed at ~85 and ~100 kDa. Furthermore, the authors used β-actin as the housekeeping gene/protein for both qRT-PCR and Western blot, whereas in this thesis GAPDH and Hsp90 were used as the housekeeping gene and protein for qRT-PCR and Western blot respectively. Hsp90 has not previously been widely used as a 'housekeeping' protein for Western blot analysis, but has been shown to have stable expression at a wide range of cell densities, comparable to the stability of β-actin (Greer et al., 2010), and in our hands the expression of this protein in A549 cells appears to remain relatively constant, even following rLV transduction. Hsp90 was chosen due to its larger size, allowing detection of ENaCα, CFTR and the housekeeping protein in the same cells on the same Western blot. To detect distinct bands of the large, multi-glycosylated CFTR membrane protein, specific immuno-blotting conditions are required, which means that the small β-actin (30kDa) is difficult to use as the housekeeping protein.

At the submission of this thesis, no other published studies have attempted to simultaneously knock down ENaCα and express CFTR using the same vector.

7.5 The use of rLV vectors in human bronchial air-liquid interface (ALI) primary cultures

Human bronchial air-liquid interface (ALI) cultures have previously been used to determine the efficacy of gene transfer agents (Griesenbach et al., 2012; Suk et al., 2014), however the efficiency of transduction from the apical surface of these cultures using VSVG-pseudotyped rLV has resulted in poor efficacy, thought to be due to the location of the VSVG receptors on

the basolateral surface of the polarised epithelial cells (Johnson et al., 2000). Therefore, although the VSVG-pseudotyped rLV vectors assessed in earlier chapters were sufficient for transduction of immortalised cells grown in culture, this pseudotype was not suitable for transducing polarised ALI cultures with electrically tight junctions. As discussed previously the F and HN coat proteins from Sendai virus have shown great promise as a pseudotype for generating rLV vectors to efficiently transduce airway cells (Section 1.4.3); F/HN-pseudotyped rLV vectors have been shown to transduce ALI cultures (Griesenbach et al., 2012). To determine whether the dual-function rLV vector could potentially transduce the human airways for treatment of lung disease, ALI cultures were used as a model of the human airway epithelium.

To enable the development of an ALI transduction protocol without potential adverse effects from the expression of shRNA sequences, the non-shRNA-containing rLV vector vEGFPLux2 was produced with the F/HN pseudotype (vEGFPLux2-F/HN; vGM035). Delivery of increasing doses of vEGFPLux2-F/HN directly to the apical surface of the ALI cultures resulted in transgene expression detectable by BLI, but there was no evidence of a dose response (Figure 6.3). The levels of BLI achieved here were similar to those observed previously in this model with similar, and lower, doses of rLV (Uta Griesenbach, personal communication.). The low number of EGFPLux2-expressing cells detected by fluorescence microscopy (Figure 6.4) and the pattern of BLI expression observed in the BLI photographs (Figure 6.3) suggested that although the transduced cells were few in number they produced high levels of transgene expression. The absence of a dose response and to increase the number of cells transduced, calculations were performed to examine in the number of viral particles delivered relative to the surface area of the ALI insert. Such calculations revealed that it was possible that 10x more virus particles were delivered to the ALI surface than would fit snugly on the surface of the cells, suggesting that virus overcrowding was occurring with even the lowest dose. An alternative dosing strategy, termed 'interval dosing', was designed in

which the lowest dose of virus was divided and delivered at hourly intervals in a lower volume (10µl, rather than 100µl), in order to minimise virus overcrowding with each dose. Interestingly, the same level of expression was observed with this dosing strategy than with a single low dose in 100µl, with peak expression observed 48 hours post-transduction and no further increase in expression even though dosing was continued at intervals for a further 24 hours. Further investigation would be required to determine whether the first dose, or the first day of dosing, was responsible for the observed transgene expression, and also whether delivery of even lower doses could improve transgene expression by further reducing virus overcrowding.

In an effort to further enhance transgene expression the tight junction disrupter EGTA was used in conjunction with the low dose in a 100µl volume. Although the receptors for F/HN are predominantly on the apical surface of the epithelial cells, addition of EGTA to open the tight junctions between cells leads to an increased surface area for transduction and resulted in greater transgene expression than delivering virus alone (Figure 6.7). However, it is unclear whether the increased expression observed was due to increased virus entry at the basolateral surface of the epithelia, or cell layer damage; enhanced gene expression was observed in areas of mechanical disruption of cells without the addition of EGTA. In addition, the majority of transduced cells appeared to be broader (possibly basal cells) with the addition of EGTA, rather than the columnar epithelial target cells, although further investigation would be required to confirm the cell types transduced with either interval or EGTA dosing. Even though EGTA dosing achieved greater transduction efficiency in ALI cultures overall, disrupting the tight junctions appeared to compromise cellular morphology, and repeat dosing resulted in progressively fewer ciliated epithelia cells, with observable cilia beating. Four doses resulted in complete absence of beating cilia and only basal cells were visible, with many cells becoming detached from the insert membrane (data not shown). Two doses of vBash3-EGFPLux2-F/HN delivered with EGTA resulted in similar transgene expression to that

observed with vEGFPLux2-F/HN, however there was no evidence of concomitant BACH1 knockdown and HMOX1 up-regulation (Figure 6.9).

Aarbiou and colleagues detected a significant decrease in ENaCα mRNA and ENaC-specific current in human bronchial ALI cells transduced with the anti-ENaCα rLV, which resulted in a significant decrease in fluid reabsorption from the apical surface (Aarbiou et al., 2012). However, the rLV vector was not delivered directly to the surface of the ALI culture, mimicking the transduction of the human airway epithelium, rather the rLV was used to transduce isolated cells before seeding onto inserts and subsequent differentiation into polarised epithelia. This strategy did result in ~50% transduction efficiency, whereas rLV vector delivery directly to the apical surface of ALI cells led to only 1.4% of cells transduced (Aarbiou et al., 2012), which is similar to the low levels of transduction observed in this thesis (Figure 6.4). Quantifying the transduction efficiency observed using FACS analysis of transduced cultures could allow greater detection of cells expressing the EGFPLux2 transgene at levels too low to detect using standard fluorescence microscopy.

In this thesis EGTA was used during rLV delivery to ALI cultures in an attempt to increase transduction efficiency, but there was also deterioration in cell health and a reduction in cilia beating. These phenomena were also observed when Aarbiou and colleagues used LPC to enhance rLV delivery; high concentration of LPC (300μg/ml) caused destabilisation of tight junctions (similar effect to EGTA), and resulted in significant cilia shedding indicating cell damage. The authors state that higher concentrations caused substantial loss of cell integrity and therefore were not used in further studies. Importantly, lower levels of LPC (75μg/ml) did not have these damaging effects and led to an increase in transduction efficiency to 14.6%. It is possible that decreasing the concentration of EGTA used in chapter 6 could increase transduction efficiency of the rLV vectors in ALI cells without compromising cell morphology and ALI composition. Furthermore, using LPC instead of EGTA would be

preferable as low concentrations of LPC co-delivered with rLV-F/HN have been shown to enhance gene transfer in the sheep lung, and was well-tolerated (Liu et al., 2010).

Another important finding was that knockdown of ENaCα reduced ENaC-specific fluid re-absorption in CF ALI cells without inducing the expression of dsRNA-induced pro-inflammatory cytokines (Aarbiou et al., 2012). Caci and colleagues also reported decreased fluid re-absorption in human bronchial ALIs transfected with anti-ENaCα siRNA when >50% ENaCα knockdown was achieved (Caci et al., 2009). The same group went on to show that this strategy increases ASL height in non-CF ALI cells to an extent similar to pharmacological rescue of mutant CFTR, although additional stimulation of CFTR activity was required (Gianotti et al., 2013).

7.6 Implications

At the time of submission of this thesis there were no published studies combining the knockdown of ENaC subunits with CFTR transgene expression. None of the studies cited in this thesis achieved >2% transduction efficiency upon apical application of vectors to ALI cultures and this would need to be improved, perhaps using strategies described above, in order to proceed to use this model for functional studies. This would permit an evaluation of the potential for the dual-function rLV vectors to rescue ASF height in CF mutant ALI cells and to compare the effects of anti-ENaCα activity, CFTR expression and both together using the dual-function rLV vectors. The effect of these different rLV vectors on ENaC-specific current, CFTR-specific current and overall ionic composition in CF mutant cells would also be interesting.

The findings presented in this thesis indicate that there is much promise for using knockdown of ENaCα as a treatment for CF lung disease.

7.7 Future applications and conclusions

The studies presented in this thesis provide proof-of-principle that dual-function rLV vectors can be developed. Evidence was shown of significant knockdown of two different targets (hENaCα and hBACH1) and expression of two different genes (EGFPLux2 and soCFTR2) demonstrating the versatility of the vector. Future work would require further developing the protocol for transduction of rLV vectors to human bronchial ALI cells. Avoiding the use of tight junction disruptors would be preferable in individuals with CF, where the lungs are damaged and contain large numbers of resident bacteria, as this could further exacerbate lung disease pathology.

A future direction would be to develop these vectors for use in animal models of CF lung disease. Attempts in this thesis to transduce mouse M-1 cells with the dual-function vector were unsuccessful due to low transduction efficiency, but these vectors could be tested directly in a mouse model. CF transgenic mice are generally considered to be poor models of CF lung disease but other CF animal models have been developed including pigs (Rogers et al., 2008), ferrets (Li and Engelhardt, 2003) and, most recently rats (Tuggle et al., 2014), some of which have lung characteristics which more closely match the human CF pathology. These CF animal models are not yet widely available in sufficient numbers, largely due to the prevalence of intestinal blockage at birth which, similar to meconium ileus in human babies, requires immediate surgery if the animal is to survive. However improved husbandry and treatment of these CF models are beginning to increase the availability of these animals and it might be feasible to test the dual function vector in these CF animals and evaluate the impact of simultaneous expression of CFTR and anti-ENaC sequences on CF epithelial electrophysiology. Alternatively, the intestinal organoid model, which is a three-dimensional polarised structure surrounding a lumen, with apical cells facing inwards and basal cells facing the culture media, is becoming more available (Dekkers et al., 2013b; Dekkers et al., 2013a).

Organoids have been produced using CF intestinal stem cells and show promise for use in the development of novel CF therapies.

Prime candidates for the treatment of CF could include shRNA targeting pro-inflammatory cytokines: Interleukin-8 (IL-8) has been shown to be up-regulated in the lungs of CF patients (Bonfield et al., 1995) and is involved in neutrophil recruitment during the inflammatory response. Suppression of IL-8 in CF patients was shown to reduce the number of neutrophils (McElvaney et al., 1992) therefore knockdown of this cytokine could help to break the cycle of chronic inflammation in CF lungs. Another target for knockdown could be neutrophil elastase (NE), which is released from neutrophils upon apoptosis and is thought to be the dominant inducer of IL-8 expression in the CF lung (Nakamura et al., 1992). NE has also been shown to activate near-silent ENaC channels (Caldwell et al., 2005), increasing airway sodium transport; therefore knockdown of NE could not only aid in reducing IL-8 production, but also reduce sodium hyperabsorption via ENaC. Considering the recent flurry of research into the lack of functional SPLUNC1 as a major contributor to CF lung disease (Section 1.2.2), it would be interesting to assess SPLUNC1 expression as a therapeutic tool. SPLUNC1 normally inhibits the activation of ENaC, however, its effect is pH-dependent and the acidification that occurs in the CF lung renders SPLUNC1 inactive, contributing to the hyperactivation of ENaC observed therein (Garland et al., 2013; Garcia-Caballero et al., 2009). Recently it was discovered that an 18 amino acid peptide (S18), corresponding to a section of the N-terminus of SPLUNC1, could mediate pH-independent specific inhibition of ENaC activation (Hobbs et al., 2013a). Future work could involve expressing this S18 peptide as the transgene in the dual-function vector, along with knockdown of ENaCα, to reduce both ENaC channel number and ENaC activation.

Another example of a lung disease where the dual-function approach could be promising is alpha-1 anti-trypsin (AAT) deficiency. Patients with AAT deficiency develop emphysema; in

chapter 6 hBACH1 was assessed as a knockdown target as it is overexpressed in emphysema, therefore knockdown of hBACH1 and expression of AAT in the lungs of patients with AAT deficiency could help to reduce emphysema and restore AAT action. There is currently ongoing research into developing a dual-function approach in the liver of patients with a gain-of-function mutation in AAT, where accumulation of this protein can cause hepatotoxicity. Simultaneous knockdown of the mutant AAT using shRNAmir, and expression of AAT that is not targeted by the shRNAmir, significantly reduced mutant AAT in the mouse liver, and reduced inflammation (Mueller et al., 2012). However, lung pathophysiology in AAT deficiency is caused by lack of AAT in the lung (AAT is an anti-protease that normally inhibits NE activity), therefore knockdown of mutant AAT in the lung is unnecessary. A dual function vector expressing AAT and knocking down NE or IL-8 could be tested for AAT-deficiency. A dual therapy for CF could be developed expressing shRNAs targeting either ENaCα, NE or IL-8, and expressing the AAT transgene. If NE and IL-8 are indeed major mediators of CF lung pathology then increased AAT would increase inhibition of NE and therefore also down-regulate IL-8 production. The latter approach could be preferable over expressing CFTR in the dual-function vector as AAT is a secreted protein and therefore a small proportion of cells expressing AAT could have a greater effect on the airway epithelium than the same number of cells expressing the CFTR channel. AAT has also been shown to inhibit epithelial sodium transport via ENaC (Lazrak et al., 2009), possibly due to its activity in inhibiting NE, therefore the combination of ENaCα knockdown and AAT expression could have a significant effect on CF epithelia.

In conclusion, the dual-function vector designed and tested in this thesis can successfully mediate transgene expression and target gene knockdown in cell culture. The modular design of this vector offers flexibility in combining different transgene and shRNA combinations, with potential for developing treatments for many lung diseases. In addition, the ability to pseudotype rLV vectors for transduction of different tissues offers further versatility in developing vector configurations suitable for treatment of diseases in other organs. With the recent European market approval of a gene therapeutic (Glybera) for human disease, the future potential for commercially available gene therapy is becoming more widely-recognised. Focus on the rational design and utility of vectors, such as the dual-function vector, for specific therapeutic effects will aid the development of the field and translation to human studies.

References

Aarbiou, J., Copreni, E., Buijs-Offerman, R. M., van der Wegen, P., Castellani, S., Carbone, A., Tilesi, F., Fradiani, P., Hiemstra, P. S., Yueksekdag, G., Diana, A., Rosenecker, J., Ascenzioni, F., Conese, M. & Scholte, B. J. 2012. **Lentiviral small hairpin RNA delivery reduces apical sodium channel activity in differentiated human airway epithelial cells**. *J Gene Med,* 14**,** 733-45.

Accurso, F. J., Rowe, S. M., Clancy, J. P., Boyle, M. P., Dunitz, J. M., Durie, P. R., Sagel, S. D., Hornick, D. B., Konstan, M. W., Donaldson, S. H., Moss, R. B., Pilewski, J. M., Rubenstein, R. C., Uluer, A. Z., Aitken, M. L., Freedman, S. D., Rose, L. M., Mayer-Hamblett, N., Dong, Q., Zha, J., Stone, A. J., Olson, E. R., Ordonez, C. L., Campbell, P. W., Ashlock, M. A. & Ramsey, B. W. 2010. **Effect of VX-770 in persons with cystic fibrosis and the G551D-CFTR mutation**. *N Engl J Med,* 363**,** 1991-2003.

Ahmed, I. S., Rohe, H. J., Twist, K. E. & Craven, R. J. 2010. **Pgrmc1 (progesterone receptor membrane component 1) associates with epidermal growth factor receptor and regulates erlotinib sensitivity**. *J Biol Chem,* 285**,** 24775-82.

Aitken, M. L., Moss, R. B., Waltz, D. A., Dovey, M. E., Tonelli, M. R., McNamara, S. C., Gibson, R. L., Ramsey, B. W., Carter, B. J. & Reynolds, T. C. 2001. **A phase I study of aerosolized administration of tgAAVCF to cystic fibrosis subjects with mild lung disease**. *Hum Gene Ther,* 12**,** 1907-16.

Aiuti, A., Biasco, L., Scaramuzza, S., Ferrua, F., Cicalese, M. P., Baricordi, C., Dionisio, F., Calabria, A., Giannelli, S., Castiello, M. C., Bosticardo, M., Evangelio, C., Assanelli, A., Casiraghi, M., Di Nunzio, S., Callegaro, L., Benati, C., Rizzardi, P., Pellin, D., Di Serio, C., Schmidt, M., Von Kalle, C., Gardner, J., Mehta, N., Neduva, V., Dow, D. J., Galy, A., Miniero, R., Finocchi, A., Metin, A., Banerjee, P. P., Orange, J. S., Galimberti, S., Valsecchi, M. G., Biffi, A., Montini, E., Villa, A., Ciceri, F., Roncarolo, M. G. & Naldini, L. 2013. **Lentiviral hematopoietic stem cell gene therapy in patients with Wiskott-Aldrich syndrome**. *Science,* 341**,** 1233151.

Akusjarvi, G., Svensson, C. & Nygard, O. 1987. **A mechanism by which adenovirus virus-associated RNAI controls translation in a transient expression assay**. *Mol Cell Biol,* 7**,** 549-51.

Alba, R., Bosch, A. & Chillon, M. 2005. **Gutless adenovirus: last-generation adenovirus for gene therapy**. *Gene Ther,* 12 Suppl 1**,** S18-27.

Almaca, J., Faria, D., Sousa, M., Uliyakina, I., Conrad, C., Sirianant, L., Clarke, L. A., Martins, J. P., Santos, M., Heriche, J. K., Huber, W., Schreiber, R., Pepperkok, R., Kunzelmann, K. & Amaral, M. D. 2013. **High-content siRNA screen reveals global ENaC regulators and potential cystic fibrosis therapy targets**. *Cell,* 154**,** 1390-400.

Alton, E. W., Baker, A., Baker, E., Boyd, A. C., Cheng, S. H., Coles, R. L., Collie, D. D., Davidson, H., Davies, J. C., Gill, D. R., Gordon, C., Griesenbach, U., Higgins, T., Hyde, S. C., Innes, J. A., McCormick, D., McGovern, M., McLachlan, G., Porteous, D. J., Pringle, I., Scheule, R. K., Shaw, D. J., Smith, S., Sumner-Jones, S. G., Tennant, P. & Vrettou, C. 2013a. **The safety profile of a cationic lipid-mediated cystic fibrosis gene transfer agent following repeated monthly aerosol administration to sheep**. *Biomaterials,* 34**,** 10267-77.

Alton, E. W., Boyd, A. C., Cheng, S. H., Cunningham, S., Davies, J. C., Gill, D. R., Griesenbach, U., Higgins, T., Hyde, S. C., Innes, J. A., Murray, G. D. & Porteous, D. J. 2013b. **A randomised, double-blind, placebo-controlled phase IIB clinical trial of repeated application of gene therapy in patients with cystic fibrosis**. *Thorax,* 68**,** 1075-7.

Alton, E. W., Boyd, A. C., Cheng, S. H., Davies, J. C., Davies, L. A., Dayan, A., Gill, D. R., Griesenbach, U., Higgins, T., Hyde, S. C., Innes, J. A., McLachlan, G., Porteous, D., Pringle, I., Scheule, R. K. & Sumner-Jones, S. 2014. **Toxicology study assessing efficacy and safety of repeated administration of lipid/DNA complexes to mouse lung**. *Gene Ther,* 21**,** 89-95.

Alton, E. W., Stern, M., Farley, R., Jaffe, A., Chadwick, S. L., Phillips, J., Davies, J., Smith, S. N., Browning, J., Davies, M. G., Hodson, M. E., Durham, S. R., Li, D., Jeffery, P. K., Scallan, M., Balfour, R., Eastman, S. J., Cheng, S. H., Smith, A. E., Meeker, D. & Geddes, D. M. 1999. **Cationic lipid-mediated CFTR gene transfer to the lungs and nose of patients with cystic fibrosis: a double-blind placebo-controlled trial**. *Lancet,* 353**,** 947-54.

Alvarez de la Rosa, D., Canessa, C. M., Fyfe, G. K. & Zhang, P. 2000. **Structure and regulation of amiloride-sensitive sodium channels**. *Annu Rev Physiol,* 62**,** 573-94.

Alvarez de la Rosa, D., Li, H. & Canessa, C. M. 2002. **Effects of aldosterone on biosynthesis, traffic, and functional expression of epithelial sodium channels in A6 cells**. *J Gen Physiol,* 119**,** 427-42.

Anderson, M. P., Berger, H. A., Rich, D. P., Gregory, R. J., Smith, A. E. & Welsh, M. J. 1991. **Nucleoside triphosphates are required to open the CFTR chloride channel**. *Cell,* 67**,** 775-84.

Azad, A. K., Rauh, R., Vermeulen, F., Jaspers, M., Korbmacher, J., Boissier, B., Bassinet, L., Fichou, Y., des Georges, M., Stanke, F., De Boeck, K., Dupont, L., Balascakova, M., Hjelte, L., Lebecque, P., Radojkovic, D., Castellani, C., Schwartz, M., Stuhrmann, M., Schwarz, M., Skalicka, V., de Monestrol, I., Girodon, E., Ferec, C., Claustres, M., Tummler, B., Cassiman, J. J., Korbmacher, C. & Cuppens, H. 2009. **Mutations in the amiloride-sensitive epithelial sodium channel in patients with cystic fibrosis-like disease**. *Hum Mutat,* 30**,** 1093-103.

Bachhuber, T., Konig, J., Voelcker, T., Murle, B., Schreiber, R. & Kunzelmann, K. 2005. **Cl- interference with the epithelial Na+ channel ENaC**. *J Biol Chem,* 280**,** 31587-94.

Bainbridge, J. W., Smith, A. J., Barker, S. S., Robbie, S., Henderson, R., Balaggan, K., Viswanathan, A., Holder, G. E., Stockman, A., Tyler, N., Petersen-Jones, S., Bhattacharya, S. S., Thrasher, A. J., Fitzke, F. W., Carter, B. J., Rubin, G. S., Moore, A. T. & Ali, R. R. 2008. **Effect of gene therapy on visual function in Leber's congenital amaurosis**. *N Engl J Med,* 358**,** 2231-9.

Bazzani, R. P., Cai, Y., Hebel, H. L., Hyde, S. C. & Gill, D. R. 2011. **The significance of plasmid DNA preparations contaminated with bacterial genomic DNA on inflammatory responses following delivery of lipoplexes to the murine lung**. *Biomaterials,* 32**,** 9854-65.

Bell, C. L., Vandenberghe, L. H., Bell, P., Limberis, M. P., Gao, G. P., Van Vliet, K., Agbandje-McKenna, M. & Wilson, J. M. 2011. **The AAV9 receptor and its modification to improve in vivo lung gene transfer in mice**. *J Clin Invest,* 121**,** 2427-35.

Berdiev, B. K., Cormet-Boyaka, E., Tousson, A., Qadri, Y. J., Oosterveld-Hut, H. M., Hong, J. S., Gonzales, P. A., Fuller, C. M., Sorscher, E. J., Lukacs, G. L. & Benos, D. J. 2007. **Molecular proximity of cystic fibrosis transmembrane conductance regulator and epithelial sodium channel assessed by fluorescence resonance energy transfer**. *J Biol Chem,* 282**,** 36481-8.

Biffi, A., Montini, E., Lorioli, L., Cesani, M., Fumagalli, F., Plati, T., Baldoli, C., Martino, S., Calabria, A., Canale, S., Benedicenti, F., Vallanti, G., Biasco, L., Leo, S., Kabbara, N., Zanetti, G., Rizzo, W. B., Mehta, N. A., Cicalese, M. P., Casiraghi, M., Boelens, J. J., Del Carro, U., Dow, D. J., Schmidt, M., Assanelli, A., Neduva, V., Di Serio, C., Stupka, E., Gardner, J., von Kalle, C., Bordignon, C., Ciceri, F., Rovelli, A., Roncarolo, M. G., Aiuti, A., Sessa, M. & Naldini, L. 2013. **Lentiviral hematopoietic stem cell gene therapy benefits metachromatic leukodystrophy**. *Science,* 341**,** 1233158.

Bingle, L., Barnes, F. A., Cross, S. S., Rassl, D., Wallace, W. A., Campos, M. A. & Bingle, C. D. 2007. **Differential epithelial expression of the putative innate immune molecule SPLUNC1 in cystic fibrosis**. *Respir Res,* 8**,** 79.

Birket, S. E., Chu, K. K., Liu, L., Houser, G. H., Diephuis, B. J., Wilsterman, E. J., Dierksen, G., Mazur, M., Shastry, S., Li, Y., Watson, J. D., Smith, A. T., Schuster, B. S., Hanes, J., Grizzle, W. E., Sorscher, E. J., Tearney, G. J. & Rowe, S. M. 2014. **A Functional Anatomic Defect of the Cystic Fibrosis Airway**. *Am J Respir Crit Care Med.*

Bitzer, M., Lauer, U., Baumann, C., Spiegel, M., Gregor, M. & Neubert, W. J. 1997. **Sendai virus efficiently infects cells via the asialoglycoprotein receptor and requires the presence of cleaved F0 precursor proteins for this alternative route of cell entry**. *J Virol,* 71**,** 5481-6.

Bompadre, S. G., Sohma, Y., Li, M. & Hwang, T. C. 2007. **G551D and G1349D, two CF-associated mutations in the signature sequences of CFTR, exhibit distinct gating defects**. *J Gen Physiol,* 129**,** 285-98.

Bonfield, T. L., Panuska, J. R., Konstan, M. W., Hilliard, K. A., Hilliard, J. B., Ghnaim, H. & Berger, M. 1995. **Inflammatory cytokines in cystic fibrosis lungs**. *Am J Respir Crit Care Med,* 152**,** 2111-8.

Bosworth, D. G. & Nielson, D. W. 1997. **Effectiveness of home versus hospital care in the routine treatment of cystic fibrosis**. *Pediatr Pulmonol,* 24**,** 42-7.

Boucher, R. C., Cotton, C. U., Gatzy, J. T., Knowles, M. R. & Yankaskas, J. R. 1988. **Evidence for reduced Cl- and increased Na+ permeability in cystic fibrosis human primary cell cultures**. *J Physiol,* 405**,** 77-103.

Boucher, R. C., Stutts, M. J., Knowles, M. R., Cantley, L. & Gatzy, J. T. 1986. **Na+ transport in cystic fibrosis respiratory epithelia. Abnormal basal rate and response to adenylate cyclase activation**. *J Clin Invest,* 78**,** 1245-52.

Boudreau, R. L., Martins, I. & Davidson, B. L. 2009. **Artificial microRNAs as siRNA shuttles: improved safety as compared to shRNAs in vitro and in vivo**. *Mol Ther,* 17**,** 169-75.

Boudreau, R. L., Monteys, A. M. & Davidson, B. L. 2008. **Minimizing variables among hairpin-based RNAi vectors reveals the potency of shRNAs**. *RNA,* 14**,** 1834-44.

Boue, A., Muller, F., Nezelof, C., Oury, J. F., Duchatel, F., Dumez, Y., Aubry, M. C. & Boue, J. 1986. **Prenatal diagnosis in 200 pregnancies with a 1-in-4 risk of cystic fibrosis**. *Hum Genet,* 74**,** 288-97.

Boyle, M. P., Bell, S. C., Konstan, M. W., McColley, S. A., Rowe, S. M., Rietschel, E., Huang, X., Waltz, D., Patel, N. R., Rodman, D. & group, V. X. s. 2014. **A CFTR corrector (lumacaftor) and a CFTR potentiator (ivacaftor) for treatment of patients with cystic fibrosis who have a phe508del CFTR mutation: a phase 2 randomised controlled trial**. *Lancet Respir Med,* 2**,** 527-38.

Boyle, M. P. & De Boeck, K. 2013. **A new era in the treatment of cystic fibrosis: correction of the underlying CFTR defect**. *Lancet Respir Med,* 1**,** 158-63.

Bridge, A. J., Pebernard, S., Ducraux, A., Nicoulaz, A. L. & Iggo, R. 2003. **Induction of an interferon response by RNAi vectors in mammalian cells**. *Nat Genet,* 34**,** 263-4.

Brooks, D. A. 1999. **Introduction: molecular chaperones of the ER: their role in protein folding and genetic disease**. *Semin Cell Dev Biol,* 10**,** 441-2.

Brunetti-Pierri, N., Ng, T., Iannitti, D., Cioffi, W., Stapleton, G., Law, M., Breinholt, J., Palmer, D., Grove, N., Rice, K., Bauer, C., Finegold, M., Beaudet, A., Mullins, C. & Ng, P. 2013. **Transgene expression up to 7 years in nonhuman primates following hepatic transduction with helper-dependent adenoviral vectors**. *Hum Gene Ther,* 24**,** 761-5.

Bruns, J. B., Carattino, M. D., Sheng, S., Maarouf, A. B., Weisz, O. A., Pilewski, J. M., Hughey, R. P. & Kleyman, T. R. 2007. **Epithelial Na+ channels are fully activated by furin- and prostasin-dependent release of an inhibitory peptide from the gamma-subunit**. *J Biol Chem,* 282**,** 6153-60.

Burns, J. C., Friedmann, T., Driever, W., Burrascano, M. & Yee, J. K. 1993. **Vesicular stomatitis virus G glycoprotein pseudotyped retroviral vectors: concentration to very high titer and efficient gene transfer into mammalian and nonmammalian cells**. *Proc Natl Acad Sci U S A,* 90**,** 8033-7.

Burns, J. C., Matsubara, T., Lozinski, G., Yee, J. K., Friedmann, T., Washabaugh, C. H. & Tsonis, P. A. 1994. **Pantropic retroviral vector-mediated gene transfer, integration, and expression in cultured newt limb cells**. *Dev Biol,* 165**,** 285-9.

Caci, E., Melani, R., Pedemonte, N., Yueksekdag, G., Ravazzolo, R., Rosenecker, J., Galietta, L. J. & Zegarra-Moran, O. 2009. **Epithelial sodium channel inhibition in primary human bronchial epithelia by transfected siRNA**. *Am J Respir Cell Mol Biol,* 40**,** 211-6.

Caldwell, R. A., Boucher, R. C. & Stutts, M. J. 2005. **Neutrophil elastase activates near-silent epithelial Na+ channels and increases airway epithelial Na+ transport**. *Am J Physiol Lung Cell Mol Physiol,* 288**,** L813-9.

Caldwell, R. A., Grove, D. E., Houck, S. A. & Cyr, D. M. 2011. **Increased folding and channel activity of a rare cystic fibrosis mutant with CFTR modulators**. *Am J Physiol Lung Cell Mol Physiol,* 301**,** L346-52.

Campos, M. A., Abreu, A. R., Nlend, M. C., Cobas, M. A., Conner, G. E. & Whitney, P. L. 2004. **Purification and characterization of PLUNC from human tracheobronchial secretions**. *Am J Respir Cell Mol Biol,* 30**,** 184-92.

Canessa, C. M., Merillat, A. M. & Rossier, B. C. 1994a. **Membrane topology of the epithelial sodium channel in intact cells**. *Am J Physiol,* 267**,** C1682-90.

Canessa, C. M., Schild, L., Buell, G., Thorens, B., Gautschi, I., Horisberger, J. D. & Rossier, B. C. 1994b. **Amiloride-sensitive epithelial Na+ channel is made of three homologous subunits**. *Nature,* 367**,** 463-7.

Carattino, M. D., Hughey, R. P. & Kleyman, T. R. 2008a. **Proteolytic processing of the epithelial sodium channel gamma subunit has a dominant role in channel activation**. *J Biol Chem,* 283**,** 25290-5.

Carattino, M. D., Passero, C. J., Steren, C. A., Maarouf, A. B., Pilewski, J. M., Myerburg, M. M., Hughey, R. P. & Kleyman, T. R. 2008b. **Defining an inhibitory domain in the alpha-subunit of the epithelial sodium channel**. *Am J Physiol Renal Physiol,* 294**,** F47-52.

Carthew, R. W. & Sontheimer, E. J. 2009. **Origins and Mechanisms of miRNAs and siRNAs**. *Cell,* 136**,** 642-55.

Castanotto, D., Sakurai, K., Lingeman, R., Li, H., Shively, L., Aagaard, L., Soifer, H., Gatignol, A., Riggs, A. & Rossi, J. J. 2007. **Combinatorial delivery of small interfering RNAs reduces RNAi efficacy by selective incorporation into RISC**. *Nucleic Acids Res,* 35**,** 5154-64.

Cebotaru, L., Vij, N., Ciobanu, I., Wright, J., Flotte, T. & Guggino, W. B. 2008. **Cystic fibrosis transmembrane regulator missing the first four transmembrane segments increases wild type and DeltaF508 processing**. *J Biol Chem,* 283**,** 21926-33.

Chadwick, S. L., Kingston, H. D., Stern, M., Cook, R. M., O'Connor, B. J., Lukasson, M., Balfour, R. P., Rosenberg, M., Cheng, S. H., Smith, A. E., Meeker, D. P., Geddes, D. M. & Alton, E. W. 1997. **Safety of a single aerosol administration of escalating doses of the cationic lipid GL-67/DOPE/DMPE-PEG5000 formulation to the lungs of normal volunteers**. *Gene Ther,* 4**,** 937-42.

Chang, H. & Fujita, T. 1996. **Lack of mutations in epithelial sodium channel beta-subunit gene in human subjects with hypertension**. *J Hypertens,* 14**,** 1417-9.

Chang, S. S., Grunder, S., Hanukoglu, A., Rosler, A., Mathew, P. M., Hanukoglu, I., Schild, L., Lu, Y., Shimkets, R. A., Nelson-Williams, C., Rossier, B. C. & Lifton, R. P. 1996. **Mutations in subunits of the epithelial sodium channel cause salt wasting with hyperkalaemic acidosis, pseudohypoaldosteronism type 1**. *Nat Genet,* 12**,** 248-53.

Cheng, S. H., Gregory, R. J., Marshall, J., Paul, S., Souza, D. W., White, G. A., O'Riordan, C. R. & Smith, A. E. 1990. **Defective intracellular transport and processing of CFTR is the molecular basis of most cystic fibrosis**. *Cell,* 63**,** 827-34.

Chernick, W. S. & Barbero, G. J. 1959. **Composition of tracheobronchial secretions in cystic fibrosis of the pancreas and bronchiectasis**. *Pediatrics,* 24**,** 739-45.

Clancy, J. P., Rowe, S. M., Accurso, F. J., Aitken, M. L., Amin, R. S., Ashlock, M. A., Ballmann, M., Boyle, M. P., Bronsveld, I., Campbell, P. W., De Boeck, K., Donaldson, S. H., Dorkin, H. L., Dunitz, J. M., Durie, P. R., Jain, M., Leonard, A., McCoy, K. S., Moss, R. B., Pilewski, J. M., Rosenbluth, D. B., Rubenstein, R. C., Schechter, M. S., Botfield, M., Ordonez, C. L., Spencer-Green, G. T., Vernillet, L., Wisseh, S., Yen, K. & Konstan, M. W. 2012. **Results of a phase IIa study of VX-809, an investigational CFTR corrector compound, in subjects with cystic fibrosis homozygous for the F508del-CFTR mutation**. *Thorax,* 67**,** 12-8.

Clark, K. L., Hughes, S. A., Bulsara, P., Coates, J., Moores, K., Parry, J., Carr, M., Mayer, R. J., Wilson, P., Gruenloh, C., Levin, D., Darton, J., Weber, W. M., Sobczak, K., Gill, D. R., Hyde, S. C., Davies, L. A., Pringle, I. A., Sumner-Jones, S. G., Jadhav, V., Jamison, S., Strapps, W. R., Pickering, V. & Edbrooke, M. R. 2013. **Pharmacological Characterization of a Novel ENaCalpha siRNA (GSK2225745) With Potential for the Treatment of Cystic Fibrosis**. *Mol Ther Nucleic Acids,* 2**,** e65.

Cmielewski, P., Anson, D. S. & Parsons, D. W. 2010. **Lysophosphatidylcholine as an adjuvant for lentiviral vector mediated gene transfer to airway epithelium: effect of acyl chain length**. *Respir Res,* 11**,** 84.

Coakley, R. D., Grubb, B. R., Paradiso, A. M., Gatzy, J. T., Johnson, L. G., Kreda, S. M., O'Neal, W. K. & Boucher, R. C. 2003. **Abnormal surface liquid pH regulation by cultured cystic fibrosis bronchial epithelium**. *Proc Natl Acad Sci U S A,* 100**,** 16083-8.

Consortium, T. R. 2012. **Validation of target gene knockdown with quantitative PCR**. *In:* INSTITUTE, T. B. (ed.) *http://www.broadinstitute.org/rnai/public/resources/protocols*. The RNAi Consortium.

Crossley, J. R., Elliott, R. B. & Smith, P. A. 1979. **Dried-blood spot screening for cystic fibrosis in the newborn**. *Lancet,* 1**,** 472-4.

Crossley, J. R., Smith, P. A., Edgar, B. W., Gluckman, P. D. & Elliott, R. B. 1981. **Neonatal screening for cystic fibrosis, using immunoreactive trypsin assay in dried blood spots**. *Clin Chim Acta,* 113**,** 111-21.

Crystal, R. G., McElvaney, N. G., Rosenfeld, M. A., Chu, C. S., Mastrangeli, A., Hay, J. G., Brody, S. L., Jaffe, H. A., Eissa, N. T. & Danel, C. 1994. **Administration of an adenovirus containing the human CFTR cDNA to the respiratory tract of individuals with cystic fibrosis**. *Nat Genet,* 8**,** 42-51.

Dai, Y., Schwarz, E. M., Gu, D., Zhang, W. W., Sarvetnick, N. & Verma, I. M. 1995. **Cellular and humoral immune responses to adenoviral vectors containing factor IX gene: tolerization of factor IX and vector antigens allows for long-term expression**. *Proc Natl Acad Sci U S A,* 92**,** 1401-5.

Dalemans, W., Barbry, P., Champigny, G., Jallat, S., Dott, K., Dreyer, D., Crystal, R. G., Pavirani, A., Lecocq, J. P. & Lazdunski, M. 1991. **Altered chloride ion channel kinetics associated with the delta F508 cystic fibrosis mutation**. *Nature,* 354**,** 526-8.

Database, C. F. M. 2014. *CF Mutations Database Statistics* [Online]. Available: http://www.genet.sickkids.on.ca/cftr/StatisticsPage.html [Accessed 9th September 2014].

Davidson, D. J. & Dorin, J. R. 2001. **The CF mouse: an important tool for studying cystic fibrosis**. *Expert Rev Mol Med,* 2001**,** 1-27.

Davies, L. A., Hyde, S. C., Nunez-Alonso, G., Bazzani, R. P., Harding-Smith, R., Pringle, I. A., Lawton, A. E., Abdullah, S., Roberts, T. C., McCormick, D., Sumner-Jones, S. G. & Gill, D. R. 2012. **The use of CpG-free plasmids to mediate persistent gene expression following repeated aerosol delivery of pDNA/PEI complexes**. *Biomaterials,* 33**,** 5618-27.

Davies, L. A., Seguela, C., Varathalingam, A., Cheng, S. H., Hyde, S. C. & Gill, D. R. 2007. **Identification of transfected cell types following non-viral gene transfer to the murine lung**. *J Gene Med,* 9**,** 184-96.

Davis, H. E., Morgan, J. R. & Yarmush, M. L. 2002. **Polybrene increases retrovirus gene transfer efficiency by enhancing receptor-independent virus adsorption on target cell membranes**. *Biophys Chem,* 97**,** 159-72.

Deglon, N., Tseng, J. L., Bensadoun, J. C., Zurn, A. D., Arsenijevic, Y., Pereira de Almeida, L., Zufferey, R., Trono, D. & Aebischer, P. 2000. **Self-inactivating lentiviral vectors with enhanced transgene expression as potential gene transfer system in Parkinson's disease**. *Hum Gene Ther,* 11**,** 179-90.

Dekkers, J. F., van der Ent, C. K. & Beekman, J. M. 2013a. **Novel opportunities for CFTR-targeting drug development using organoids**. *Rare Dis,* 1**,** e27112.

Dekkers, J. F., Wiegerinck, C. L., de Jonge, H. R., Bronsveld, I., Janssens, H. M., de Winter-de Groot, K. M., Brandsma, A. M., de Jong, N. W., Bijvelds, M. J., Scholte, B. J., Nieuwenhuis, E. E., van den Brink, S., Clevers, H., van der Ent, C. K., Middendorp, S. & Beekman, J. M. 2013b. **A functional CFTR assay using primary cystic fibrosis intestinal organoids**. *Nat Med,* 19**,** 939-45.

Demeneix, B., Behr, J., Boussif, O., Zanta, M. A., Abdallah, B. & Remy, J. 1998. **Gene transfer with lipospermines and polyethylenimines**. *Adv Drug Deliv Rev,* 30**,** 85-95.

Dodge, J. A., Morison, S., Lewis, P. A., Coles, E. C., Geddes, D., Russell, G., Littlewood, J. M. & Scott, M. T. 1997. **Incidence, population, and survival of cystic fibrosis in the UK, 1968-95. UK Cystic Fibrosis Survey Management Committee**. *Arch Dis Child,* 77**,** 493-6.

Drwinga, H. L., Toji, L. H., Kim, C. H., Greene, A. E. & Mulivor, R. A. 1993. **NIGMS human/rodent somatic cell hybrid mapping panels 1 and 2**. *Genomics,* 16**,** 311-4.

Dubois, B. L. & Naylor, S. L. 1993. **Characterization of NIGMS human/rodent somatic cell hybrid mapping panel 2 by PCR**. *Genomics,* 16**,** 315-9.

Dull, T., Zufferey, R., Kelly, M., Mandel, R. J., Nguyen, M., Trono, D. & Naldini, L. 1998. **A third-generation lentivirus vector with a conditional packaging system**. *J Virol,* 72**,** 8463-71.

Duneclift, S., Wells, U. & Widdicombe, J. 1997. **Estimation of thickness of airway surface liquid in ferret trachea in vitro**. *J Appl Physiol (1985),* 83**,** 761-7.

Dykxhoorn, D. M. & Lieberman, J. 2005. **The silent revolution: RNA interference as basic biology, research tool, and therapeutic**. *Annu Rev Med,* 56**,** 401-23.

Dykxhoorn, D. M., Novina, C. D. & Sharp, P. A. 2003. **Killing the messenger: short RNAs that silence gene expression**. *Nat Rev Mol Cell Biol,* 4**,** 457-67.

Elbashir, S. M., Lendeckel, W. & Tuschl, T. 2001. **RNA interference is mediated by 21- and 22-nucleotide RNAs**. *Genes Dev,* 15**,** 188-200.

Engelhardt, J. F., Zepeda, M., Cohn, J. A., Yankaskas, J. R. & Wilson, J. M. 1994. **Expression of the cystic fibrosis gene in adult human lung**. *J Clin Invest,* 93**,** 737-49.

Enuka, Y., Hanukoglu, I., Edelheit, O., Vaknine, H. & Hanukoglu, A. 2012. **Epithelial sodium channels (ENaC) are uniformly distributed on motile cilia in the oviduct and the respiratory airways**. *Histochem Cell Biol,* 137**,** 339-53.

Espinosa, M., Noe, G., Troncoso, C., Ho, S. B. & Villalon, M. 2002. **Acidic pH and increasing [Ca(2+)] reduce the swelling of mucins in primary cultures of human cervical cells**. *Hum Reprod,* 17**,** 1964-72.

Farrell, P. M. 2008. **The prevalence of cystic fibrosis in the European Union**. *J Cyst Fibros,* 7**,** 450-3.

Felgner, P. L., Barenholz, Y., Behr, J. P., Cheng, S. H., Cullis, P., Huang, L., Jessee, J. A., Seymour, L., Szoka, F., Thierry, A. R., Wagner, E. & Wu, G. 1997. **Nomenclature for synthetic gene delivery systems**. *Hum Gene Ther,* 8**,** 511-2.

Ferrari, S., Griesenbach, U., Iida, A., Farley, R., Wright, A. M., Zhu, J., Munkonge, F. M., Smith, S. N., You, J., Ban, H., Inoue, M., Chan, M., Singh, C., Verdon, B., Argent, B. E., Wainwright, B., Jeffery, P. K., Geddes, D. M., Porteous, D. J., Hyde, S. C., Gray, M. A., Hasegawa, M. & Alton, E. W. 2007. **Sendai virus-mediated CFTR gene transfer to the airway epithelium**. *Gene Ther,* 14**,** 1371-9.

Firsov, D., Gautschi, I., Merillat, A. M., Rossier, B. C. & Schild, L. 1998. **The heterotetrameric architecture of the epithelial sodium channel (ENaC)**. *EMBO J,* 17**,** 344-52.

Firsov, D., Schild, L., Gautschi, I., Merillat, A. M., Schneeberger, E. & Rossier, B. C. 1996. **Cell surface expression of the epithelial Na channel and a mutant causing Liddle syndrome: a quantitative approach**. *Proc Natl Acad Sci U S A,* 93**,** 15370-5.

Fish, R. J. & Kruithof, E. K. 2004. **Short-term cytotoxic effects and long-term instability of RNAi delivered using lentiviral vectors**. *BMC Mol Biol,* 5**,** 9.

Flotte, T. R., Zeitlin, P. L., Reynolds, T. C., Heald, A. E., Pedersen, P., Beck, S., Conrad, C. K., Brass-Ernst, L., Humphries, M., Sullivan, K., Wetzel, R., Taylor, G., Carter, B. J. & Guggino, W. B. 2003. **Phase I trial of intranasal and endobronchial administration of a recombinant adeno-associated virus serotype 2 (rAAV2)-CFTR vector in adult cystic fibrosis patients: a two-part clinical study**. *Hum Gene Ther,* 14**,** 1079-88.

Flume, P. A., Mogayzel, P. J., Jr., Robinson, K. A., Goss, C. H., Rosenblatt, R. L., Kuhn, R. J., Marshall, B. C. & Clinical Practice Guidelines for Pulmonary Therapies, C. 2009. **Cystic fibrosis pulmonary guidelines: treatment of pulmonary exacerbations**. *Am J Respir Crit Care Med,* 180**,** 802-8.

Freedman, S. D. & Scheele, G. A. 1994. **Acid-base interactions during exocrine pancreatic secretion. Primary role for ductal bicarbonate in acinar lumen function**. *Ann N Y Acad Sci,* 713**,** 199-206.

Freimark, B. D., Blezinger, H. P., Florack, V. J., Nordstrom, J. L., Long, S. D., Deshpande, D. S., Nochumson, S. & Petrak, K. L. 1998. **Cationic lipids enhance cytokine and cell influx levels in the lung following administration of plasmid: cationic lipid complexes**. *J Immunol,* 160**,** 4580-6.

Fuchs, H. J., Borowitz, D. S., Christiansen, D. H., Morris, E. M., Nash, M. L., Ramsey, B. W., Rosenstein, B. J., Smith, A. L. & Wohl, M. E. 1994. **Effect of aerosolized recombinant human DNase on exacerbations of respiratory symptoms and on pulmonary function in patients with cystic fibrosis. The Pulmozyme Study Group**. *N Engl J Med,* 331**,** 637-42.

Fuller, S., von Bonsdorff, C. H. & Simons, K. 1984. **Vesicular stomatitis virus infects and matures only through the basolateral surface of the polarized epithelial cell line, MDCK**. *Cell,* 38**,** 65-77.

Gaillard, E. A., Kota, P., Gentzsch, M., Dokholyan, N. V., Stutts, M. J. & Tarran, R. 2010. **Regulation of the epithelial Na+ channel and airway surface liquid volume by serine proteases**. *Pflugers Arch,* 460**,** 1-17.

Garcia-Caballero, A., Rasmussen, J. E., Gaillard, E., Watson, M. J., Olsen, J. C., Donaldson, S. H., Stutts, M. J. & Tarran, R. 2009. **SPLUNC1 regulates airway surface liquid volume by protecting ENaC from proteolytic cleavage**. *Proc Natl Acad Sci U S A,* 106**,** 11412-7.

Garland, A. L., Walton, W. G., Coakley, R. D., Tan, C. D., Gilmore, R. C., Hobbs, C. A., Tripathy, A., Clunes, L. A., Bencharit, S., Stutts, M. J., Betts, L., Redinbo, M. R. & Tarran, R. 2013. **Molecular basis for pH-dependent mucosal dehydration in cystic fibrosis airways**. *Proc Natl Acad Sci U S A,* 110**,** 15973-8.

Gautam, A., Densmore, C. L., Golunski, E., Xu, B. & Waldrep, J. C. 2001. **Transgene expression in mouse airway epithelium by aerosol gene therapy with PEI-DNA complexes**. *Mol Ther,* 3**,** 551-6.

Gentzsch, M., Dang, H., Dang, Y., Garcia-Caballero, A., Suchindran, H., Boucher, R. C. & Stutts, M. J. 2010. **The cystic fibrosis transmembrane conductance regulator impedes proteolytic stimulation of the epithelial Na+ channel**. *J Biol Chem,* 285**,** 32227-32.

George, P. M., Banya, W., Pareek, N., Bilton, D., Cullinan, P., Hodson, M. E. & Simmonds, N. J. 2011. **Improved survival at low lung function in cystic fibrosis: cohort study from 1990 to 2007**. *BMJ,* 342**,** d1008.

Gianotti, A., Melani, R., Caci, E., Sondo, E., Ravazzolo, R., Galietta, L. J. & Zegarra-Moran, O. 2013. **Epithelial sodium channel silencing as a strategy to correct the airway surface fluid deficit in cystic fibrosis**. *Am J Respir Cell Mol Biol,* 49**,** 445-52.

Gibson, L. E. & Cooke, R. E. 1959. **A test for concentration of electrolytes in sweat in cystic fibrosis of the pancreas utilizing pilocarpine by iontophoresis**. *Pediatrics,* 23**,** 545-9.

Giglio, L., Candusso, M., D'Orazio, C., Mastella, G. & Faraguna, D. 1997. **Failure to thrive: the earliest feature of cystic fibrosis in infants diagnosed by neonatal screening**. *Acta Paediatr,* 86**,** 1162-5.

Gill, D. R., Pringle, I. A. & Hyde, S. C. 2009. **Progress and prospects: the design and production of plasmid vectors**. *Gene Ther,* 16**,** 165-71.

Gill, D. R., Smyth, S. E., Goddard, C. A., Pringle, I. A., Higgins, C. F., Colledge, W. H. & Hyde, S. C. 2001. **Increased persistence of lung gene expression using plasmids containing the ubiquitin C or elongation factor 1alpha promoter**. *Gene Ther,* 8**,** 1539-46.

Gill, D. R., Southern, K. W., Mofford, K. A., Seddon, T., Huang, L., Sorgi, F., Thomson, A., MacVinish, L. J., Ratcliff, R., Bilton, D., Lane, D. J., Littlewood, J. M., Webb, A. K., Middleton, P. G., Colledge, W. H., Cuthbert, A. W., Evans, M. J., Higgins, C. F. & Hyde, S. C. 1997. **A placebo-controlled study of liposome-mediated gene transfer to the nasal epithelium of patients with cystic fibrosis**. *Gene Ther,* 4**,** 199-209.

Goven, D., Boutten, A., Lecon-Malas, V., Marchal-Somme, J., Amara, N., Crestani, B., Fournier, M., Leseche, G., Soler, P., Boczkowski, J. & Bonay, M. 2008. **Altered Nrf2/Keap1-Bach1 equilibrium in pulmonary emphysema**. *Thorax,* 63**,** 916-24.

Greer, S., Honeywell, R., Geletu, M., Arulanandam, R. & Raptis, L. 2010. **Housekeeping genes; expression levels may change with density of cultured cells**. *J Immunol Methods,* 355**,** 76-9.

Gregory, R. J., Rich, D. P., Cheng, S. H., Souza, D. W., Paul, S., Manavalan, P., Anderson, M. P., Welsh, M. J. & Smith, A. E. 1991. **Maturation and function of cystic fibrosis transmembrane conductance regulator variants bearing mutations in putative nucleotide-binding domains 1 and 2**. *Mol Cell Biol,* 11**,** 3886-93.

Griesenbach, U., Inoue, M., Hasegawa, M. & Alton, E. W. 2005. **Sendai virus for gene therapy and vaccination**. *Curr Opin Mol Ther,* 7**,** 346-52.

Griesenbach, U., Inoue, M., Meng, C., Farley, R., Chan, M., Newman, N. K., Brum, A., You, J., Kerton, A., Shoemark, A., Boyd, A. C., Davies, J. C., Higgins, T. E., Gill, D. R., Hyde, S. C., Innes, J. A., Porteous, D. J., Hasegawa, M. & Alton, E. W. 2012. **Assessment of F/HN-pseudotyped lentivirus as a clinically relevant vector for lung gene therapy**. *Am J Respir Crit Care Med,* 186**,** 846-56.

Griesenbach, U., McLachlan, G., Owaki, T., Somerton, L., Shu, T., Baker, A., Tennant, P., Gordon, C., Vrettou, C., Baker, E., Collie, D. D., Hasegawa, M. & Alton, E. W. 2011. **Validation of recombinant Sendai virus in a non-natural host model**. *Gene Ther,* 18**,** 182-8.

Griesenbach, U., Munkonge, F. M., Sumner-Jones, S., Holder, E., Smith, S. N., Boyd, A. C., Gill, D. R., Hyde, S. C., Porteous, D., Alton, E. W. & Consortium, U. K. C. F. G. T. 2008. **Assessment of CFTR function after gene transfer in vitro and in vivo**. *Methods Mol Biol,* 433**,** 229-42.

Grimm, D., Streetz, K. L., Jopling, C. L., Storm, T. A., Pandey, K., Davis, C. R., Marion, P., Salazar, F. & Kay, M. A. 2006. **Fatality in mice due to oversaturation of cellular microRNA/short hairpin RNA pathways**. *Nature,* 441**,** 537-41.

Grubb, B. R. & Boucher, R. C. 1999. **Pathophysiology of gene-targeted mouse models for cystic fibrosis**. *Physiol Rev,* 79**,** S193-214.

Grubb, B. R., Pickles, R. J., Ye, H., Yankaskas, J. R., Vick, R. N., Engelhardt, J. F., Wilson, J. M., Johnson, L. G. & Boucher, R. C. 1994. **Inefficient gene transfer by adenovirus vector to cystic fibrosis airway epithelia of mice and humans**. *Nature,* 371**,** 802-6.

Haerteis, S., Schaal, D., Brauer, F., Bruschke, S., Schweimer, K., Rauh, R., Sticht, H., Rosch, P., Schwarzinger, S. & Korbmacher, C. 2012. **An inhibitory peptide derived from the alpha-subunit of the epithelial sodium channel (ENaC) shows a helical conformation**. *Cell Physiol Biochem,* 29**,** 761-74.

Halbert, C. L., Allen, J. M. & Miller, A. D. 2001. **Adeno-associated virus type 6 (AAV6) vectors mediate efficient transduction of airway epithelial cells in mouse lungs compared to that of AAV2 vectors**. *J Virol,* 75**,** 6615-24.

Halbert, C. L., Lam, S. L. & Miller, A. D. 2007. **High-efficiency promoter-dependent transduction by adeno-associated virus type 6 vectors in mouse lung**. *Hum Gene Ther,* 18**,** 344-54.

Harvey, B. G., Leopold, P. L., Hackett, N. R., Grasso, T. M., Williams, P. M., Tucker, A. L., Kaner, R. J., Ferris, B., Gonda, I., Sweeney, T. D., Ramalingam, R., Kovesdi, I., Shak, S. & Crystal, R. G. 1999. **Airway epithelial CFTR mRNA expression in cystic fibrosis patients after repetitive administration of a recombinant adenovirus**. *J Clin Invest,* 104**,** 1245-55.

Hay, J. G., McElvaney, N. G., Herena, J. & Crystal, R. G. 1995. **Modification of nasal epithelial potential differences of individuals with cystic fibrosis consequent to local administration of a normal CFTR cDNA adenovirus gene transfer vector**. *Hum Gene Ther,* 6**,** 1487-96.

Henry, S. D., van der Wegen, P., Metselaar, H. J., Tilanus, H. W., Scholte, B. J. & van der Laan, L. J. 2006. **Simultaneous targeting of HCV replication and viral binding with a single lentiviral vector containing multiple RNA interference expression cassettes**. *Mol Ther,* 14**,** 485-93.

Hobbs, C. A., Blanchard, M. G., Alijevic, O., Tan, C. D., Kellenberger, S., Bencharit, S., Cao, R., Kesimer, M., Walton, W. G., Henderson, A. G., Redinbo, M. R., Stutts, M. J. & Tarran, R. 2013a. **Identification of the SPLUNC1 ENaC-inhibitory domain yields novel strategies to treat sodium hyperabsorption in cystic fibrosis airway epithelial cultures**. *Am J Physiol Lung Cell Mol Physiol,* 305**,** L990-L1001.

Hobbs, C. A., Da Tan, C. & Tarran, R. 2013b. **Does epithelial sodium channel hyperactivity contribute to cystic fibrosis lung disease?** *J Physiol,* 591**,** 4377-87.

Hoegger, M. J., Fischer, A. J., McMenimen, J. D., Ostedgaard, L. S., Tucker, A. J., Awadalla, M. A., Moninger, T. O., Michalski, A. S., Hoffman, E. A., Zabner, J., Stoltz, D. A. & Welsh, M. J. 2014. **Cystic fibrosis. Impaired mucus detachment disrupts mucociliary transport in a piglet model of cystic fibrosis**. *Science,* 345**,** 818-22.

Hopf, A., Schreiber, R., Mall, M., Greger, R. & Kunzelmann, K. 1999. **Cystic fibrosis transmembrane conductance regulator inhibits epithelial Na+ channels carrying Liddle's syndrome mutations**. *J Biol Chem,* 274**,** 13894-9.

Hou, W., Tian, Q., Steuerwald, N. M., Schrum, L. W. & Bonkovsky, H. L. 2012. **The let-7 microRNA enhances heme oxygenase-1 by suppressing Bach1 and attenuates oxidant injury in human hepatocytes**. *Biochim Biophys Acta,* 1819**,** 1113-22.

Huang, S. Y., Bolser, D., Liu, H. Y., Hwang, T. C. & Zou, X. 2009. **Molecular modeling of the heterodimer of human CFTR's nucleotide-binding domains using a protein-protein docking approach**. *J Mol Graph Model,* 27**,** 822-8.

Hughey, R. P., Bruns, J. B., Kinlough, C. L., Harkleroad, K. L., Tong, Q., Carattino, M. D., Johnson, J. P., Stockand, J. D. & Kleyman, T. R. 2004. **Epithelial sodium channels are activated by furin-dependent proteolysis**. *J Biol Chem,* 279**,** 18111-4.

Hughey, R. P., Carattino, M. D. & Kleyman, T. R. 2007. **Role of proteolysis in the activation of epithelial sodium channels**. *Curr Opin Nephrol Hypertens,* 16**,** 444-50.

Hughey, R. P., Mueller, G. M., Bruns, J. B., Kinlough, C. L., Poland, P. A., Harkleroad, K. L., Carattino, M. D. & Kleyman, T. R. 2003. **Maturation of the epithelial Na+ channel involves proteolytic processing of the alpha- and gamma-subunits**. *J Biol Chem,* 278**,** 37073-82.

Hutson, T. H., Foster, E., Dawes, J. M., Hindges, R., Yanez-Munoz, R. J. & Moon, L. D. 2012. **Lentiviral vectors encoding short hairpin RNAs efficiently transduce and knockdown LINGO-1 but induce an interferon response and cytotoxicity in central nervous system neurones**. *J Gene Med,* 14**,** 299-315.

Hyde, S. C., Pringle, I. A., Abdullah, S., Lawton, A. E., Davies, L. A., Varathalingam, A., Nunez-Alonso, G., Green, A. M., Bazzani, R. P., Sumner-Jones, S. G., Chan, M., Li, H., Yew, N. S., Cheng, S. H., Boyd, A. C., Davies, J. C., Griesenbach, U., Porteous, D. J., Sheppard, D. N., Munkonge, F. M., Alton, E. W. & Gill, D. R. 2008. **CpG-free plasmids confer reduced inflammation and sustained pulmonary gene expression**. *Nat Biotechnol,* 26**,** 549-51.

Hyde, S. C., Southern, K. W., Gileadi, U., Fitzjohn, E. M., Mofford, K. A., Waddell, B. E., Gooi, H. C., Goddard, C. A., Hannavy, K., Smyth, S. E., Egan, J. J., Sorgi, F. L., Huang, L., Cuthbert, A. W., Evans, M. J., Colledge, W. H., Higgins, C. F., Webb, A. K. & Gill, D. R. 2000. **Repeat administration of DNA/liposomes to the nasal epithelium of patients with cystic fibrosis**. *Gene Ther,* 7**,** 1156-65.

Itani, O. A., Chen, J. H., Karp, P. H., Ernst, S., Keshavjee, S., Parekh, K., Klesney-Tait, J., Zabner, J. & Welsh, M. J. 2011. **Human cystic fibrosis airway epithelia have reduced Cl- conductance but not increased Na+ conductance**. *Proc Natl Acad Sci U S A,* 108**,** 10260-5.

Jain, L., Chen, X. J., Ramosevac, S., Brown, L. A. & Eaton, D. C. 2001. **Expression of highly selective sodium channels in alveolar type II cells is determined by culture conditions**. *Am J Physiol Lung Cell Mol Physiol,* 280**,** L646-58.

Jasti, J., Furukawa, H., Gonzales, E. B. & Gouaux, E. 2007. **Structure of acid-sensing ion channel 1 at 1.9 A resolution and low pH**. *Nature,* 449**,** 316-23.

Ji, H. L., Chalfant, M. L., Jovov, B., Lockhart, J. P., Parker, S. B., Fuller, C. M., Stanton, B. A. & Benos, D. J. 2000. **The cytosolic termini of the beta- and gamma-ENaC subunits are involved in the functional interactions between cystic fibrosis transmembrane conductance regulator and epithelial sodium channel**. *J Biol Chem,* 275**,** 27947-56.

Jiang, C., Finkbeiner, W. E., Widdicombe, J. H., McCray, P. B., Jr. & Miller, S. S. 1993. **Altered fluid transport across airway epithelium in cystic fibrosis**. *Science,* 262**,** 424-7.

Johnson, L. G., Olsen, J. C., Naldini, L. & Boucher, R. C. 2000. **Pseudotyped human lentiviral vector-mediated gene transfer to airway epithelia in vivo**. *Gene Ther,* 7**,** 568-74.

Johnson, L. G., Olsen, J. C., Sarkadi, B., Moore, K. L., Swanstrom, R. & Boucher, R. C. 1992. **Efficiency of gene transfer for restoration of normal airway epithelial function in cystic fibrosis**. *Nat Genet,* 2**,** 21-5.

Jones, A. P. & Wallis, C. 2010. **Dornase alfa for cystic fibrosis**. *Cochrane Database of Systematic Reviews*.

Joris, L., Dab, I. & Quinton, P. M. 1993. **Elemental composition of human airway surface fluid in healthy and diseased airways**. *Am Rev Respir Dis,* 148**,** 1633-7.

Karp, P. H., Moninger, T. O., Weber, S. P., Nesselhauf, T. S., Launspach, J. L., Zabner, J. & Welsh, M. J. 2002. **An in vitro model of differentiated human airway epithelia. Methods for establishing primary cultures**. *Methods Mol Biol,* 188**,** 115-37.

Kashlan, O. B. & Kleyman, T. R. 2011. **ENaC structure and function in the wake of a resolved structure of a family member**. *Am J Physiol Renal Physiol,* 301**,** F684-96.

Kerem, E., Bistritzer, T., Hanukoglu, A., Hofmann, T., Zhou, Z., Bennett, W., MacLaughlin, E., Barker, P., Nash, M., Quittell, L., Boucher, R. & Knowles, M. R. 1999. **Pulmonary epithelial sodium-channel dysfunction and excess airway liquid in pseudohypoaldosteronism**. *N Engl J Med,* 341**,** 156-62.

Kerem, E., Corey, M., Kerem, B., Durie, P., Tsui, L. C. & Levison, H. 1989. **Clinical and genetic comparisons of patients with cystic fibrosis, with or without meconium ileus**. *J Pediatr,* 114**,** 767-73.

Kingsman, S. M., Mitrophanous, K. & Olsen, J. C. 2005. **Potential oncogene activity of the woodchuck hepatitis post-transcriptional regulatory element (WPRE)**. *Gene Ther,* 12**,** 3-4.

Kleyman, T. R., Carattino, M. D. & Hughey, R. P. 2009. **ENaC at the cutting edge: regulation of epithelial sodium channels by proteases**. *J Biol Chem,* 284**,** 20447-51.

Knight, K. K., Olson, D. R., Zhou, R. & Snyder, P. M. 2006. **Liddle's syndrome mutations increase Na+ transport through dual effects on epithelial Na+ channel surface expression and proteolytic cleavage**. *Proc Natl Acad Sci U S A,* 103**,** 2805-8.

Knowles, M. R., Church, N. L., Waltner, W. E., Yankaskas, J. R., Gilligan, P., King, M., Edwards, L. J., Helms, R. W. & Boucher, R. C. 1990. **A pilot study of aerosolized amiloride for the treatment of lung disease in cystic fibrosis**. *N Engl J Med,* 322**,** 1189-94.

Knowles, M. R., Hohneker, K. W., Zhou, Z., Olsen, J. C., Noah, T. L., Hu, P. C., Leigh, M. W., Engelhardt, J. F., Edwards, L. J., Jones, K. R. & et al. 1995a. **A controlled study of adenoviral-vector-mediated gene transfer in the nasal epithelium of patients with cystic fibrosis**. *N Engl J Med,* 333**,** 823-31.

Knowles, M. R., Paradiso, A. M. & Boucher, R. C. 1995b. **In vivo nasal potential difference: techniques and protocols for assessing efficacy of gene transfer in cystic fibrosis**. *Hum Gene Ther,* 6**,** 445-55.

Knowles, M. R., Robinson, J. M., Wood, R. E., Pue, C. A., Mentz, W. M., Wager, G. C., Gatzy, J. T. & Boucher, R. C. 1997. **Ion composition of airway surface liquid of patients with cystic fibrosis as compared with normal and disease-control subjects**. *J Clin Invest,* 100**,** 2588-95.

Knowles, M. R., Stutts, M. J., Yankaskas, J. R., Gatzy, J. T. & Boucher, R. C., Jr. 1986. **Abnormal respiratory epithelial ion transport in cystic fibrosis**. *Clin Chest Med,* 7**,** 285-97.

Kobayashi, M., Iida, A., Ueda, Y. & Hasegawa, M. 2003. **Pseudotyped lentivirus vectors derived from simian immunodeficiency virus SIVagm with envelope glycoproteins from paramyxovirus**. *J Virol,* 77**,** 2607-14.

Konig, J., Schreiber, R., Voelcker, T., Mall, M. & Kunzelmann, K. 2001. **The cystic fibrosis transmembrane conductance regulator (CFTR) inhibits ENaC through an increase in the intracellular Cl- concentration**. *EMBO Rep,* 2**,** 1047-51.

Konstan, M. W., Davis, P. B., Wagener, J. S., Hilliard, K. A., Stern, R. C., Milgram, L. J., Kowalczyk, T. H., Hyatt, S. L., Fink, T. L., Gedeon, C. R., Oette, S. M., Payne, J. M., Muhammad, O., Ziady, A. G., Moen, R. C. & Cooper, M. J. 2004. **Compacted DNA nanoparticles administered to the nasal mucosa of cystic fibrosis subjects are safe and demonstrate partial to complete cystic fibrosis transmembrane regulator reconstitution**. *Hum Gene Ther,* 15**,** 1255-69.

Kopeikin, Z., Yuksek, Z., Yang, H. Y. & Bompadre, S. G. 2014. **Combined effects of VX-770 and VX-809 on several functional abnormalities of F508del-CFTR channels**. *J Cyst Fibros,* 13**,** 508-14.

Kosari, F., Sheng, S., Li, J., Mak, D. O., Foskett, J. K. & Kleyman, T. R. 1998. **Subunit stoichiometry of the epithelial sodium channel**. *J Biol Chem,* 273**,** 13469-74.

Kovesi, T. A., Swartz, R. & MacDonald, N. 1998. **Transient renal failure due to simultaneous ibuprofen and aminoglycoside therapy in children with cystic fibrosis**. *N Engl J Med,* 338**,** 65-6.

Lazrak, A., Nita, I., Subramaniyam, D., Wei, S., Song, W., Ji, H. L., Janciauskiene, S. & Matalon, S. 2009. **Alpha(1)-antitrypsin inhibits epithelial Na+ transport in vitro and in vivo**. *Am J Respir Cell Mol Biol,* 41**,** 261-70.

Lee, S. H. & Sinko, P. J. 2006. **siRNA--getting the message out**. *Eur J Pharm Sci,* 27**,** 401-10.

Lee, Y., Ahn, C., Han, J., Choi, H., Kim, J., Yim, J., Lee, J., Provost, P., Radmark, O., Kim, S. & Kim, V. N. 2003. **The nuclear RNase III Drosha initiates microRNA processing**. *Nature,* 425**,** 415-9.

Lewis, H. A., Buchanan, S. G., Burley, S. K., Conners, K., Dickey, M., Dorwart, M., Fowler, R., Gao, X., Guggino, W. B., Hendrickson, W. A., Hunt, J. F., Kearins, M. C., Lorimer, D., Maloney, P. C., Post, K. W., Rajashankar, K. R., Rutter, M. E., Sauder, J. M., Shriver, S., Thibodeau, P. H., Thomas, P. J., Zhang, M., Zhao, X. & Emtage, S. 2004. **Structure of**

nucleotide-binding domain 1 of the cystic fibrosis transmembrane conductance regulator. *EMBO J,* 23**,** 282-93.

Li, T. & Folkesson, H. G. 2006. **RNA interference for alpha-ENaC inhibits rat lung fluid absorption in vivo**. *Am J Physiol Lung Cell Mol Physiol,* 290**,** L649-L660.

Li, Z. & Engelhardt, J. F. 2003. **Progress toward generating a ferret model of cystic fibrosis by somatic cell nuclear transfer**. *Reprod Biol Endocrinol,* 1**,** 83.

Limberis, M., Anson, D. S., Fuller, M. & Parsons, D. W. 2002. **Recovery of airway cystic fibrosis transmembrane conductance regulator function in mice with cystic fibrosis after single-dose lentivirus-mediated gene transfer**. *Hum Gene Ther,* 13**,** 1961-70.

Lin, H., Li, H., Cho, H. J., Bian, S., Roh, H. J., Lee, M. K., Kim, J. S., Chung, S. J., Shim, C. K. & Kim, D. D. 2007. **Air-liquid interface (ALI) culture of human bronchial epithelial cell monolayers as an in vitro model for airway drug transport studies**. *J Pharm Sci,* 96**,** 341-50.

Liu, C., Wong, E., Miller, D., Smith, G., Anson, D. & Parsons, D. 2010. **Lentiviral airway gene transfer in lungs of mice and sheep: successes and challenges**. *J Gene Med,* 12**,** 647-58.

Liu, G., Li, D., Pasumarthy, M. K., Kowalczyk, T. H., Gedeon, C. R., Hyatt, S. L., Payne, J. M., Miller, T. J., Brunovskis, P., Fink, T. L., Muhammad, O., Moen, R. C., Hanson, R. W. & Cooper, M. J. 2003. **Nanoparticles of compacted DNA transfect postmitotic cells**. *J Biol Chem,* 278**,** 32578-86.

Loo, T. W., Bartlett, M. C. & Clarke, D. M. 2013. **Corrector VX-809 stabilizes the first transmembrane domain of CFTR**. *Biochem Pharmacol,* 86**,** 612-9.

Lorenz, C., Hadwiger, P., John, M., Vornlocher, H. P. & Unverzagt, C. 2004. **Steroid and lipid conjugates of siRNAs to enhance cellular uptake and gene silencing in liver cells**. *Bioorg Med Chem Lett,* 14**,** 4975-7.

Lund, E., Guttinger, S., Calado, A., Dahlberg, J. E. & Kutay, U. 2004. **Nuclear export of microRNA precursors**. *Science,* 303**,** 95-8.

Lyczak, J. B., Cannon, C. L. & Pier, G. B. 2002. **Lung infections associated with cystic fibrosis**. *Clin Microbiol Rev,* 15**,** 194-222.

Ma, H. P., Saxena, S. & Warnock, D. G. 2002. **Anionic phospholipids regulate native and expressed epithelial sodium channel (ENaC)**. *J Biol Chem,* 277**,** 7641-4.

Mall, M., Grubb, B. R., Harkema, J. R., O'Neal, W. K. & Boucher, R. C. 2004. **Increased airway epithelial Na+ absorption produces cystic fibrosis-like lung disease in mice**. *Nat Med,* 10**,** 487-93.

Mall, M. A., Button, B., Johannesson, B., Zhou, Z., Livraghi, A., Caldwell, R. A., Schubert, S. C., Schultz, C., O'Neal, W. K., Pradervand, S., Hummler, E., Rossier, B. C., Grubb, B. R. & Boucher, R. C. 2010. **Airway surface liquid volume regulation determines different airway phenotypes in liddle compared with betaENaC-overexpressing mice**. *J Biol Chem,* 285**,** 26945-55.

Mano, I. & Driscoll, M. 1999. **DEG/ENaC channels: a touchy superfamily that watches its salt**. *Bioessays,* 21**,** 568-78.

Mastrangeli, A., Harvey, B. G., Yao, J., Wolff, G., Kovesdi, I., Crystal, R. G. & Falck-Pedersen, E. 1996. **"Sero-switch" adenovirus-mediated in vivo gene transfer: circumvention of anti-adenovirus humoral immune defenses against repeat adenovirus vector administration by changing the adenovirus serotype**. *Hum Gene Ther,* 7**,** 79-87.

Matsui, H., Grubb, B. R., Tarran, R., Randell, S. H., Gatzy, J. T., Davis, C. W. & Boucher, R. C. 1998a. **Evidence for periciliary liquid layer depletion, not abnormal ion composition, in the pathogenesis of cystic fibrosis airways disease**. *Cell,* 95**,** 1005-15.

Matsui, H., Randell, S. H., Peretti, S. W., Davis, C. W. & Boucher, R. C. 1998b. **Coordinated clearance of periciliary liquid and mucus from airway surfaces**. *J Clin Invest,* 102**,** 1125-31.

McBride, J. L., Boudreau, R. L., Harper, S. Q., Staber, P. D., Monteys, A. M., Martins, I., Gilmore, B. L., Burstein, H., Peluso, R. W., Polisky, B., Carter, B. J. & Davidson, B. L. 2008. **Artificial miRNAs mitigate shRNA-mediated toxicity in the brain: implications for the therapeutic development of RNAi**. *Proc Natl Acad Sci U S A,* 105**,** 5868-73.

McDonald, F. J., Snyder, P. M., McCray, P. B., Jr. & Welsh, M. J. 1994. **Cloning, expression, and tissue distribution of a human amiloride-sensitive Na+ channel**. *Am J Physiol,* 266**,** L728-34.

McElvaney, N. G., Nakamura, H., Birrer, P., Hebert, C. A., Wong, W. L., Alphonso, M., Baker, J. B., Catalano, M. A. & Crystal, R. G. 1992. **Modulation of airway inflammation in cystic fibrosis. In vivo suppression of interleukin-8 levels on the respiratory epithelial surface by aerosolization of recombinant secretory leukoprotease inhibitor**. *J Clin Invest,* 90**,** 1296-301.

McLachlan, G., Davidson, H., Holder, E., Davies, L. A., Pringle, I. A., Sumner-Jones, S. G., Baker, A., Tennant, P., Gordon, C., Vrettou, C., Blundell, R., Hyndman, L., Stevenson, B., Wilson, A., Doherty, A., Shaw, D. J., Coles, R. L., Painter, H., Cheng, S. H., Scheule, R. K., Davies, J. C., Innes, J. A., Hyde, S. C., Griesenbach, U., Alton, E. W., Boyd, A. C., Porteous, D. J., Gill, D. R. & Collie, D. D. 2011. **Pre-clinical evaluation of three non-viral gene transfer agents for cystic fibrosis after aerosol delivery to the ovine lung**. *Gene Ther,* 18**,** 996-1005.

McShane, D., Davies, J. C., Davies, M. G., Bush, A., Geddes, D. M. & Alton, E. W. 2003. **Airway surface pH in subjects with cystic fibrosis**. *Eur Respir J,* 21**,** 37-42.

Meisler, M. H., Barrow, L. L., Canessa, C. M. & Rossier, B. C. 1994. **SCNN1, an epithelial cell sodium channel gene in the conserved linkage group on mouse chromosome 6 and human chromosome 12**. *Genomics,* 24**,** 185-6.

Mekus, F., Ballmann, M., Bronsveld, I., Dork, T., Bijman, J., Tummler, B. & Veeze, H. J. 1998. **Cystic-fibrosis-like disease unrelated to the cystic fibrosis transmembrane conductance regulator**. *Hum Genet,* 102**,** 582-6.

Melchior, W. B., Jr. & Von Hippel, P. H. 1973. **Alteration of the relative stability of dA-dT and dG-dC base pairs in DNA**. *Proc Natl Acad Sci U S A,* 70**,** 298-302.

Merten, O. W., Charrier, S., Laroudie, N., Fauchille, S., Dugue, C., Jenny, C., Audit, M., Zanta-Boussif, M. A., Chautard, H., Radrizzani, M., Vallanti, G., Naldini, L., Noguiez-Hellin, P. & Galy, A. 2011. **Large-scale manufacture and characterization of a lentiviral vector produced for clinical ex vivo gene therapy application**. *Hum Gene Ther,* 22**,** 343-56.

Mitomo, K., Griesenbach, U., Inoue, M., Somerton, L., Meng, C., Akiba, E., Tabata, T., Ueda, Y., Frankel, G. M., Farley, R., Singh, C., Chan, M., Munkonge, F., Brum, A., Xenariou, S., Escudero-Garcia, S., Hasegawa, M. & Alton, E. W. 2010. **Toward gene therapy for cystic fibrosis using a lentivirus pseudotyped with Sendai virus envelopes**. *Mol Ther,* 18**,** 1173-82.

Moffat, J., Grueneberg, D. A., Yang, X., Kim, S. Y., Kloepfer, A. M., Hinkle, G., Piqani, B., Eisenhaure, T. M., Luo, B., Grenier, J. K., Carpenter, A. E., Foo, S. Y., Stewart, S. A., Stockwell, B. R., Hacohen, N., Hahn, W. C., Lander, E. S., Sabatini, D. M. & Root, D. E. 2006. **A lentiviral RNAi library for human and mouse genes applied to an arrayed viral high-content screen**. *Cell,* 124**,** 1283-98.

Morgan, C. & Howe, C. 1968. **Structure and development of viruses as observed in the electron microscope. IX. Entry of parainfluenza I (Sendai) virus**. *J Virol,* 2**,** 1122-32.

Moss, R. B., Milla, C., Colombo, J., Accurso, F., Zeitlin, P. L., Clancy, J. P., Spencer, L. T., Pilewski, J., Waltz, D. A., Dorkin, H. L., Ferkol, T., Pian, M., Ramsey, B., Carter, B. J., Martin, D. B. & Heald, A. E. 2007. **Repeated aerosolized AAV-CFTR for treatment of cystic fibrosis: a randomized placebo-controlled phase 2B trial**. *Hum Gene Ther,* 18**,** 726-32.

Mueller, C., Tang, Q., Gruntman, A., Blomenkamp, K., Teckman, J., Song, L., Zamore, P. D. & Flotte, T. R. 2012. **Sustained miRNA-mediated knockdown of mutant AAT with simultaneous augmentation of wild-type AAT has minimal effect on global liver miRNA profiles**. *Mol Ther,* 20**,** 590-600.

Nakamura, H., Yoshimura, K., McElvaney, N. G. & Crystal, R. G. 1992. **Neutrophil elastase in respiratory epithelial lining fluid of individuals with cystic fibrosis induces interleukin-8 gene expression in a human bronchial epithelial cell line**. *J Clin Invest,* 89**,** 1478-84.

NHS 2014. **A Laboratory Guide to Newborn Screening in the UK for Cystic Fibrosis (CF)**. *In:* NHS (ed.) 4th ed. UK.

Nishikawa, M. & Hashida, M. 2002. **Nonviral approaches satisfying various requirements for effective in vivo gene therapy**. *Biol Pharm Bull,* 25**,** 275-83.

Nykanen, A., Haley, B. & Zamore, P. D. 2001. **ATP requirements and small interfering RNA structure in the RNA interference pathway**. *Cell,* 107**,** 309-21.

O'Neal, W. K., Zhou, H., Morral, N., Langston, C., Parks, R. J., Graham, F. L., Kochanek, S. & Beaudet, A. L. 2000. **Toxicity associated with repeated administration of first-generation adenovirus vectors does not occur with a helper-dependent vector**. *Mol Med,* 6**,** 179-95.

Ogden, R. C. & Adams, D. A. 1987. **Electrophoresis in agarose and acrylamide gels**. *Methods Enzymol,* 152**,** 61-87.

Ota, K., Brydun, A., Itoh-Nakadai, A., Sun, J. & Igarashi, K. 2014. **Bach1 deficiency and accompanying overexpression of heme oxygenase-1 do not influence aging or tumorigenesis in mice**. *Oxid Med Cell Longev,* 2014**,** 757901.

Painter, H. 2007. *An investigation of mRNA as a gene transfer agent.* DPhil DPhil, University of Oxford.

Palfi, S., Gurruchaga, J. M., Ralph, G. S., Lepetit, H., Lavisse, S., Buttery, P. C., Watts, C., Miskin, J., Kelleher, M., Deeley, S., Iwamuro, H., Lefaucheur, J. P., Thiriez, C., Fenelon, G., Lucas, C., Brugieres, P., Gabriel, I., Abhay, K., Drouot, X., Tani, N., Kas, A., Ghaleb, B., Le Corvoisier, P., Dolphin, P., Breen, D. P., Mason, S., Guzman, N. V., Mazarakis, N. D., Radcliffe, P. A., Harrop, R., Kingsman, S. M., Rascol, O., Naylor, S., Barker, R. A., Hantraye, P., Remy, P., Cesaro, P. & Mitrophanous, K. A. 2014. **Long-term safety and tolerability of ProSavin, a lentiviral vector-based gene therapy for Parkinson's disease: a dose escalation, open-label, phase 1/2 trial**. *Lancet,* 383**,** 1138-46.

Palmer, D. H., Chen, M. J., Searle, P. F., Kerr, D. J. & Young, L. S. 2005. **Inhibition of NF-kappaB enhances the cytotoxicity of virus-directed enzyme prodrug therapy and oncolytic adenovirus cancer gene therapy**. *Gene Ther,* 12**,** 1187-97.

Perez-Vilar, J., Olsen, J. C., Chua, M. & Boucher, R. C. 2005. **pH-dependent intraluminal organization of mucin granules in live human mucous/goblet cells**. *J Biol Chem,* 280**,** 16868-81.

Pezzulo, A. A., Starner, T. D., Scheetz, T. E., Traver, G. L., Tilley, A. E., Harvey, B. G., Crystal, R. G., McCray, P. B., Jr. & Zabner, J. 2011. **The air-liquid interface and use of primary cell cultures are important to recapitulate the transcriptional profile of in vivo airway epithelia**. *Am J Physiol Lung Cell Mol Physiol,* 300**,** L25-31.

Phuan, P. W., Veit, G., Tan, J., Roldan, A., Finkbeiner, W. E., Lukacs, G. L. & Verkman, A. S. 2014. **Synergy-based small-molecule screen using a human lung epithelial cell line yields DeltaF508-CFTR correctors that augment VX-809 maximal efficacy**. *Mol Pharmacol,* 86**,** 42-51.

Poulsen, J. H., Fischer, H., Illek, B. & Machen, T. E. 1994. **Bicarbonate conductance and pH regulatory capability of cystic fibrosis transmembrane conductance regulator**. *Proc Natl Acad Sci U S A,* 91**,** 5340-4.

Prickett, M. & Jain, M. 2013. **Gene therapy in cystic fibrosis**. *Transl Res,* 161**,** 255-64.

Pringle, I. A., Hyde, S. C. & Gill, D. R. 2009. **Non-viral vectors in cystic fibrosis gene therapy: recent developments and future prospects**. *Expert Opin Biol Ther,* 9**,** 991-1003.

Ramachandran, P. V. & Ignacimuthu, S. 2013. **RNA interference--a silent but an efficient therapeutic tool**. *Appl Biochem Biotechnol,* 169**,** 1774-89.

Ramsey, B. W., Farrell, P. M. & Pencharz, P. 1992. **Nutritional assessment and management in cystic fibrosis: a consensus report. The Consensus Committee**. *Am J Clin Nutr,* 55**,** 108-16.

Rauh, R., Diakov, A., Tzschoppe, A., Korbmacher, J., Azad, A. K., Cuppens, H., Cassiman, J. J., Dotsch, J., Sticht, H. & Korbmacher, C. 2010. **A mutation of the epithelial sodium channel associated with atypical cystic fibrosis increases channel open probability and reduces Na+ self inhibition**. *J Physiol,* 588**,** 1211-25.

Rauh, R., Soell, D., Haerteis, S., Diakov, A., Nesterov, V., Krueger, B., Sticht, H. & Korbmacher, C. 2013. **A mutation in the beta-subunit of ENaC identified in a patient with cystic fibrosis-like symptoms has a gain-of-function effect**. *Am J Physiol Lung Cell Mol Physiol,* 304**,** L43-55.

Raval, C. M., Zhong, J. L., Mitchell, S. A. & Tyrrell, R. M. 2012. **The role of Bach1 in ultraviolet A-mediated human heme oxygenase 1 regulation in human skin fibroblasts**. *Free Radic Biol Med,* 52**,** 227-36.

Rawlins, E. L. & Hogan, B. L. 2008. **Ciliated epithelial cell lifespan in the mouse trachea and lung**. *Am J Physiol Lung Cell Mol Physiol,* 295**,** L231-4.

Rees, W. A., Yager, T. D., Korte, J. & von Hippel, P. H. 1993. **Betaine can eliminate the base pair composition dependence of DNA melting**. *Biochemistry,* 32**,** 137-44.

Renier, M., Tamanini, A., Nicolis, E., Rolfini, R., Imler, J. L., Pavirani, A. & Cabrini, G. 1995. **Use of a membrane potential-sensitive probe to assess biological expression of the cystic fibrosis transmembrane conductance regulator**. *Hum Gene Ther,* 6**,** 1275-83.

Riordan, J. R., Rommens, J. M., Kerem, B., Alon, N., Rozmahel, R., Grzelczak, Z., Zielenski, J., Lok, S., Plavsic, N., Chou, J. L. & et al. 1989. **Identification of the cystic fibrosis gene: cloning and characterization of complementary DNA**. *Science,* 245**,** 1066-73.

Rogers, C. S., Stoltz, D. A., Meyerholz, D. K., Ostedgaard, L. S., Rokhlina, T., Taft, P. J., Rogan, M. P., Pezzulo, A. A., Karp, P. H., Itani, O. A., Kabel, A. C., Wohlford-Lenane, C. L., Davis, G. J., Hanfland, R. A., Smith, T. L., Samuel, M., Wax, D., Murphy, C. N., Rieke, A., Whitworth, K., Uc, A., Starner, T. D., Brogden, K. A., Shilyansky, J., McCray, P. B., Jr., Zabner, J., Prather, R. S. & Welsh, M. J. 2008. **Disruption of the CFTR gene produces a model of cystic fibrosis in newborn pigs**. *Science,* 321**,** 1837-41.

Rommens, J. M., Iannuzzi, M. C., Kerem, B., Drumm, M. L., Melmer, G., Dean, M., Rozmahel, R., Cole, J. L., Kennedy, D., Hidaka, N. & et al. 1989. **Identification of the cystic fibrosis gene: chromosome walking and jumping**. *Science,* 245**,** 1059-65.

Rose, A. C., Goddard, C. A., Colledge, W. H., Cheng, S. H., Gill, D. R. & Hyde, S. C. 2002. **Optimisation of real-time quantitative RT-PCR for the evaluation of non-viral mediated gene transfer to the airways**. *Gene Ther,* 9**,** 1312-20.

Rowe, S. M., Heltshe, S. L., Gonska, T., Donaldson, S. H., Borowitz, D., Gelfond, D., Sagel, S. D., Khan, U., Mayer-Hamblett, N., Van Dalfsen, J. M., Joseloff, E., Ramsey, B. W. & Network, G. I. o. t. C. F. F. T. D. 2014. **Clinical Mechanism of the Cystic Fibrosis Transmembrane Conductance Regulator Potentiator Ivacaftor in G551D-mediated Cystic Fibrosis**. *Am J Respir Crit Care Med,* 190**,** 175-84.

Rudolph, C., Lausier, J., Naundorf, S., Muller, R. H. & Rosenecker, J. 2000. **In vivo gene delivery to the lung using polyethylenimine and fractured polyamidoamine dendrimers**. *J Gene Med,* 2**,** 269-78.

Ruiz, F. E., Clancy, J. P., Perricone, M. A., Bebok, Z., Hong, J. S., Cheng, S. H., Meeker, D. P., Young, K. R., Schoumacher, R. A., Weatherly, M. R., Wing, L., Morris, J. E., Sindel, L., Rosenberg, M., van Ginkel, F. W., McGhee, J. R., Kelly, D., Lyrene, R. K. & Sorscher, E. J. 2001. **A clinical inflammatory syndrome attributable to aerosolized lipid-DNA administration in cystic fibrosis**. *Hum Gene Ther,* 12**,** 751-61.

Ryter, S. W. & Choi, A. M. 2005. **Heme oxygenase-1: redox regulation of a stress protein in lung and cell culture models**. *Antioxid Redox Signal,* 7**,** 80-91.

Ryter, S. W., Kim, H. P., Nakahira, K., Zuckerbraun, B. S., Morse, D. & Choi, A. M. 2007. **Protective functions of heme oxygenase-1 and carbon monoxide in the respiratory system**. *Antioxid Redox Signal,* 9**,** 2157-73.

Samuel, C. E. 2001. **Antiviral actions of interferons**. *Clin Microbiol Rev,* 14**,** 778-809, table of contents.

Schaedel, C., Marthinsen, L., Kristoffersson, A. C., Kornfalt, R., Nilsson, K. O., Orlenius, B. & Holmberg, L. 1999. **Lung symptoms in pseudohypoaldosteronism type 1 are associated with deficiency of the alpha-subunit of the epithelial sodium channel**. *J Pediatr,* 135**,** 739-45.

Schambach, A., Bohne, J., Baum, C., Hermann, F. G., Egerer, L., von Laer, D. & Giroglou, T. 2006. **Woodchuck hepatitis virus post-transcriptional regulatory element deleted from X protein and promoter sequences enhances retroviral vector titer and expression**. *Gene Ther,* 13**,** 641-5.

Scheule, R. K. 2000. **The role of CpG motifs in immunostimulation and gene therapy**. *Adv Drug Deliv Rev,* 44**,** 119-34.

Schild, L., Canessa, C. M., Shimkets, R. A., Gautschi, I., Lifton, R. P. & Rossier, B. C. 1995. **A mutation in the epithelial sodium channel causing Liddle disease increases channel activity in the Xenopus laevis oocyte expression system**. *Proc Natl Acad Sci U S A,* 92**,** 5699-703.

Schmittgen, T. D. & Livak, K. J. 2008. **Analyzing real-time PCR data by the comparative C(T) method**. *Nat Protoc,* 3**,** 1101-8.

Shah, P. L., Scott, S. F., Geddes, D. M. & Hodson, M. E. 1995. **Two years experience with recombinant human DNase I in the treatment of pulmonary disease in cystic fibrosis**. *Respir Med,* 89**,** 499-502.

Shankar, P., Manjunath, N. & Lieberman, J. 2005. **The prospect of silencing disease using RNA interference**. *JAMA,* 293**,** 1367-73.

Shao, P. L., Lu, M. Y., Liau, Y. J., Chao, M. F., Chang, L. Y., Lu, C. Y., Kao, C. L., Chang, S. Y., Chi, Y. H. & Huang, L. M. 2011. **Argonaute-2 enhances suppression of human cytomegalovirus replication by polycistronic short hairpin RNAs targeting UL46, UL70 and UL122**. *Antivir Ther,* 16**,** 741-9.

Sheppard, D. N. & Welsh, M. J. 1999. **Structure and function of the CFTR chloride channel**. *Physiol Rev,* 79**,** S23-45.

Shimkets, R. A., Lifton, R. P. & Canessa, C. M. 1997. **The activity of the epithelial sodium channel is regulated by clathrin-mediated endocytosis**. *J Biol Chem,* 272**,** 25537-41.

Shimkets, R. A., Warnock, D. G., Bositis, C. M., Nelson-Williams, C., Hansson, J. H., Schambelan, M., Gill, J. R., Jr., Ulick, S., Milora, R. V., Findling, J. W. & et al. 1994. **Liddle's syndrome: heritable human hypertension caused by mutations in the beta subunit of the epithelial sodium channel**. *Cell,* 79**,** 407-14.

Silva, J. M., Li, M. Z., Chang, K., Ge, W., Golding, M. C., Rickles, R. J., Siolas, D., Hu, G., Paddison, P. J., Schlabach, M. R., Sheth, N., Bradshaw, J., Burchard, J., Kulkarni, A., Cavet, G., Sachidanandam, R., McCombie, W. R., Cleary, M. A., Elledge, S. J. & Hannon, G. J. 2005. **Second-generation shRNA libraries covering the mouse and human genomes**. *Nat Genet,* 37**,** 1281-8.

Sinn, P. L., Shah, A. J., Donovan, M. D. & McCray, P. B., Jr. 2005. **Viscoelastic gel formulations enhance airway epithelial gene transfer with viral vectors**. *Am J Respir Cell Mol Biol,* 32**,** 404-10.

Smith, A. L., Redding, G., Doershuk, C., Goldmann, D., Gore, E., Hilman, B., Marks, M., Moss, R., Ramsey, B., Rubio, T. & et al. 1988. **Sputum changes associated with therapy for endobronchial exacerbation in cystic fibrosis**. *J Pediatr,* 112**,** 547-54.

Smith, J. J., Travis, S. M., Greenberg, E. P. & Welsh, M. J. 1996. **Cystic fibrosis airway epithelia fail to kill bacteria because of abnormal airway surface fluid**. *Cell,* 85**,** 229-36.

Snyder, P. M., Cheng, C., Prince, L. S., Rogers, J. C. & Welsh, M. J. 1998. **Electrophysiological and biochemical evidence that DEG/ENaC cation channels are composed of nine subunits**. *J Biol Chem,* 273**,** 681-4.

Snyder, P. M., Price, M. P., McDonald, F. J., Adams, C. M., Volk, K. A., Zeiher, B. G., Stokes, J. B. & Welsh, M. J. 1995. **Mechanism by which Liddle's syndrome mutations increase activity of a human epithelial Na+ channel**. *Cell,* 83**,** 969-78.

Song, Y., Lou, H. H., Boyer, J. L., Limberis, M. P., Vandenberghe, L. H., Hackett, N. R., Leopold, P. L., Wilson, J. M. & Crystal, R. G. 2009. **Functional cystic fibrosis transmembrane conductance regulator expression in cystic fibrosis airway epithelial cells by AAV6.2-mediated segmental trans-splicing**. *Hum Gene Ther,* 20**,** 267-81.

Stewart, A. P., Haerteis, S., Diakov, A., Korbmacher, C. & Edwardson, J. M. 2011. **Atomic force microscopy reveals the architecture of the epithelial sodium channel (ENaC)**. *J Biol Chem*.

Stocker, A. G., Kremer, K. L., Koldej, R., Miller, D. S., Anson, D. S. & Parsons, D. W. 2009. **Single-dose lentiviral gene transfer for lifetime airway gene expression**. *J Gene Med,* 11**,** 861-7.

Stoltz, D. A., Meyerholz, D. K., Pezzulo, A. A., Ramachandran, S., Rogan, M. P., Davis, G. J., Hanfland, R. A., Wohlford-Lenane, C., Dohrn, C. L., Bartlett, J. A., Nelson, G. A. t., Chang, E. H., Taft, P. J., Ludwig, P. S., Estin, M., Hornick, E. E., Launspach, J. L., Samuel, M., Rokhlina, T., Karp, P. H., Ostedgaard, L. S., Uc, A., Starner, T. D., Horswill, A. R., Brogden, K. A., Prather, R. S., Richter, S. S., Shilyansky, J., McCray, P. B., Jr., Zabner, J. & Welsh, M. J.

2010. **Cystic fibrosis pigs develop lung disease and exhibit defective bacterial eradication at birth**. *Sci Transl Med,* 2**,** 29ra31.

Stoos, B. A., Naray-Fejes-Toth, A., Carretero, O. A., Ito, S. & Fejes-Toth, G. 1991. **Characterization of a mouse cortical collecting duct cell line**. *Kidney Int,* 39**,** 1168-75.

Stutts, M. J., Canessa, C. M., Olsen, J. C., Hamrick, M., Cohn, J. A., Rossier, B. C. & Boucher, R. C. 1995a. **CFTR as a cAMP-dependent regulator of sodium channels**. *Science,* 269**,** 847-50.

Stutts, M. J., Lazarowski, E. R., Paradiso, A. M. & Boucher, R. C. 1995b. **Activation of CFTR Cl- conductance in polarized T84 cells by luminal extracellular ATP**. *Am J Physiol,* 268**,** C425-33.

Stutts, M. J., Rossier, B. C. & Boucher, R. C. 1997. **Cystic fibrosis transmembrane conductance regulator inverts protein kinase A-mediated regulation of epithelial sodium channel single channel kinetics**. *J Biol Chem,* 272**,** 14037-40.

Su, H., Trombly, M. I., Chen, J. & Wang, X. 2009. **Essential and overlapping functions for mammalian Argonautes in microRNA silencing**. *Genes Dev,* 23**,** 304-17.

Suk, J. S., Kim, A. J., Trehan, K., Schneider, C. S., Cebotaru, L., Woodward, O. M., Boylan, N. J., Boyle, M. P., Lai, S. K., Guggino, W. B. & Hanes, J. 2014. **Lung gene therapy with highly compacted DNA nanoparticles that overcome the mucus barrier**. *J Control Release,* 178**,** 8-17.

Tanimoto, T., Hattori, N., Senoo, T., Furonaka, M., Ishikawa, N., Fujitaka, K., Haruta, Y., Yokoyama, A., Igarashi, K. & Kohno, N. 2009. **Genetic ablation of the Bach1 gene reduces hyperoxic lung injury in mice: role of IL-6**. *Free Radic Biol Med,* 46**,** 1119-26.

Tarran, R. & Redinbo, M. R. 2014. **Mammalian short palate lung and nasal epithelial clone 1 (SPLUNC1) in pH-dependent airway hydration**. *Int J Biochem Cell Biol,* 52C**,** 130-135.

Tarran, R., Trout, L., Donaldson, S. H. & Boucher, R. C. 2006. **Soluble mediators, not cilia, determine airway surface liquid volume in normal and cystic fibrosis superficial airway epithelia**. *J Gen Physiol,* 127**,** 591-604.

Thomas, D. C. & Roth, M. G. 1994. **The basolateral targeting signal in the cytoplasmic domain of glycoprotein G from vesicular stomatitis virus resembles a variety of intracellular targeting motifs related by primary sequence but having diverse targeting activities**. *J Biol Chem,* 269**,** 15732-9.

Touw, D. J., Brimicombe, R. W., Hodson, M. E., Heijerman, H. G. & Bakker, W. 1995. **Inhalation of antibiotics in cystic fibrosis**. *Eur Respir J,* 8**,** 1594-604.

Trust, C. 2014. **UK Cystic Fibrosis Resgistry Annual data report 2013**. *In:* TRUST, U. C. (ed.) *cysticfibrosis.org.uk/Registry.* cysticfibrosis.org.uk/Registry.

Tuggle, K. L., Birket, S. E., Cui, X., Hong, J., Warren, J., Reid, L., Chambers, A., Ji, D., Gamber, K., Chu, K. K., Tearney, G., Tang, L. P., Fortenberry, J. A., Du, M., Cadillac, J. M., Bedwell, D. M., Rowe, S. M., Sorscher, E. J. & Fanucchi, M. V. 2014. **Characterization of**

defects in ion transport and tissue development in cystic fibrosis transmembrane conductance regulator (CFTR)-knockout rats. *PLoS One,* 9**,** e91253.

Van Goor, F., Hadida, S., Grootenhuis, P. D., Burton, B., Cao, D., Neuberger, T., Turnbull, A., Singh, A., Joubran, J., Hazlewood, A., Zhou, J., McCartney, J., Arumugam, V., Decker, C., Yang, J., Young, C., Olson, E. R., Wine, J. J., Frizzell, R. A., Ashlock, M. & Negulescu, P. 2009. **Rescue of CF airway epithelial cell function in vitro by a CFTR potentiator, VX-770**. *Proc Natl Acad Sci U S A,* 106**,** 18825-30.

Van Goor, F., Hadida, S., Grootenhuis, P. D., Burton, B., Stack, J. H., Straley, K. S., Decker, C. J., Miller, M., McCartney, J., Olson, E. R., Wine, J. J., Frizzell, R. A., Ashlock, M. & Negulescu, P. A. 2011. **Correction of the F508del-CFTR protein processing defect in vitro by the investigational drug VX-809**. *Proc Natl Acad Sci U S A,* 108**,** 18843-8.

Verdugo, P., Deyrup-Olsen, I., Aitken, M., Villalon, M. & Johnson, D. 1987. **Molecular mechanism of mucin secretion: I. The role of intragranular charge shielding**. *J Dent Res,* 66**,** 506-8.

Voilley, N., Lingueglia, E., Champigny, G., Mattei, M. G., Waldmann, R., Lazdunski, M. & Barbry, P. 1994. **The lung amiloride-sensitive Na+ channel: biophysical properties, pharmacology, ontogenesis, and molecular cloning**. *Proc Natl Acad Sci U S A,* 91**,** 247-51.

Wagner, J. A., Messner, A. H., Moran, M. L., Daifuku, R., Kouyama, K., Desch, J. K., Manley, S., Norbash, A. M., Conrad, C. K., Friborg, S., Reynolds, T., Guggino, W. B., Moss, R. B., Carter, B. J., Wine, J. J., Flotte, T. R. & Gardner, P. 1999. **Safety and biological efficacy of an adeno-associated virus vector-cystic fibrosis transmembrane regulator (AAV-CFTR) in the cystic fibrosis maxillary sinus**. *Laryngoscope,* 109**,** 266-74.

Wagner, J. A., Reynolds, T., Moran, M. L., Moss, R. B., Wine, J. J., Flotte, T. R. & Gardner, P. 1998. **Efficient and persistent gene transfer of AAV-CFTR in maxillary sinus**. *Lancet,* 351**,** 1702-3.

Wang, G., Davidson, B. L., Melchert, P., Slepushkin, V. A., van Es, H. H., Bodner, M., Jolly, D. J. & McCray, P. B., Jr. 1998. **Influence of cell polarity on retrovirus-mediated gene transfer to differentiated human airway epithelia**. *J Virol,* 72**,** 9818-26.

Wang, G., Sinn, P. L. & McCray, P. B., Jr. 2000a. **Development of retroviral vectors for gene transfer to airway epithelia**. *Curr Opin Mol Ther,* 2**,** 497-506.

Wang, G., Slepushkin, V., Zabner, J., Keshavjee, S., Johnston, J. C., Sauter, S. L., Jolly, D. J., Dubensky, T. W., Jr., Davidson, B. L. & McCray, P. B., Jr. 1999. **Feline immunodeficiency virus vectors persistently transduce nondividing airway epithelia and correct the cystic fibrosis defect**. *J Clin Invest,* 104**,** R55-62.

Wang, G., Zabner, J., Deering, C., Launspach, J., Shao, J., Bodner, M., Jolly, D. J., Davidson, B. L. & McCray, P. B., Jr. 2000b. **Increasing epithelial junction permeability enhances gene transfer to airway epithelia In vivo**. *Am J Respir Cell Mol Biol,* 22**,** 129-38.

Wang, Q., Dai, X. Q., Li, Q., Tuli, J., Liang, G., Li, S. S. & Chen, X. Z. 2013. **Filamin interacts with epithelial sodium channel and inhibits its channel function**. *J Biol Chem,* 288**,** 264-73.

Wang, S., Hannafon, B. N., Wolf, R. F., Zhou, J., Avery, J. E., Wu, J., Lind, S. E. & Ding, W. Q. 2014. **Characterization of docosahexaenoic acid (DHA)-induced heme oxygenase-1 (HO-1) expression in human cancer cells: the importance of enhanced BTB and CNC homology 1 (Bach1) degradation**. *J Nutr Biochem,* 25**,** 515-25.

Warnatz, H. J., Schmidt, D., Manke, T., Piccini, I., Sultan, M., Borodina, T., Balzereit, D., Wruck, W., Soldatov, A., Vingron, M., Lehrach, H. & Yaspo, M. L. 2011. **The BTB and CNC homology 1 (BACH1) target genes are involved in the oxidative stress response and in control of the cell cycle**. *J Biol Chem,* 286**,** 23521-32.

Weisz, O. A., Wang, J. M., Edinger, R. S. & Johnson, J. P. 2000. **Non-coordinate regulation of endogenous epithelial sodium channel (ENaC) subunit expression at the apical membrane of A6 cells in response to various transporting conditions**. *J Biol Chem,* 275**,** 39886-93.

Wine, J. J. 2001. **Cystic fibrosis: the 'bicarbonate before chloride' hypothesis**. *Curr Biol,* 11**,** R463-6.

Winter, M. C., Sheppard, D. N., Carson, M. R. & Welsh, M. J. 1994. **Effect of ATP concentration on CFTR Cl- channels: a kinetic analysis of channel regulation**. *Biophys J,* 66**,** 1398-403.

Wiseman, J. W., Goddard, C. A., McLelland, D. & Colledge, W. H. 2003. **A comparison of linear and branched polyethylenimine (PEI) with DCChol/DOPE liposomes for gene delivery to epithelial cells in vitro and in vivo**. *Gene Ther,* 10**,** 1654-62.

Worldwide, G. T. C. T. 2014. **Gene Therapy Clinical Trials Worldwide**. www.wiley.com: Journal of Gene Therapy.

Wu, J. V., Joo, N. S., Krouse, M. E. & Wine, J. J. 2001. **Cystic fibrosis transmembrane conductance regulator gating requires cytosolic electrolytes**. *J Biol Chem,* 276**,** 6473-8.

Yan, W., Samaha, F. F., Ramkumar, M., Kleyman, T. R. & Rubenstein, R. C. 2004. **Cystic fibrosis transmembrane conductance regulator differentially regulates human and mouse epithelial sodium channels in Xenopus oocytes**. *J Biol Chem,* 279**,** 23183-92.

Yang, Y., Janich, S., Cohn, J. A. & Wilson, J. M. 1993. **The common variant of cystic fibrosis transmembrane conductance regulator is recognized by hsp70 and degraded in a pre-Golgi nonlysosomal compartment**. *Proc Natl Acad Sci U S A,* 90**,** 9480-4.

Yee, J. K., Friedmann, T. & Burns, J. C. 1994a. **Generation of high-titer pseudotyped retroviral vectors with very broad host range**. *Methods Cell Biol,* 43 Pt A**,** 99-112.

Yee, J. K., Miyanohara, A., LaPorte, P., Bouic, K., Burns, J. C. & Friedmann, T. 1994b. **A general method for the generation of high-titer, pantropic retroviral vectors: highly efficient infection of primary hepatocytes**. *Proc Natl Acad Sci U S A,* 91**,** 9564-8.

Yew, N. S., Wysokenski, D. M., Wang, K. X., Ziegler, R. J., Marshall, J., McNeilly, D., Cherry, M., Osburn, W. & Cheng, S. H. 1997. **Optimization of plasmid vectors for high-level expression in lung epithelial cells**. *Hum Gene Ther,* 8**,** 575-84.

Yi, R., Qin, Y., Macara, I. G. & Cullen, B. R. 2003. **Exportin-5 mediates the nuclear export of pre-microRNAs and short hairpin RNAs**. *Genes Dev,* 17**,** 3011-6.

Yonemitsu, Y., Kitson, C., Ferrari, S., Farley, R., Griesenbach, U., Judd, D., Steel, R., Scheid, P., Zhu, J., Jeffery, P. K., Kato, A., Hasan, M. K., Nagai, Y., Masaki, I., Fukumura, M., Hasegawa, M., Geddes, D. M. & Alton, E. W. 2000. **Efficient gene transfer to airway epithelium using recombinant Sendai virus**. *Nat Biotechnol,* 18**,** 970-3.

Yueksekdag, G., Drechsel, M., Rossner, M., Schmidt, C., Kormann, M., Illenyi, M. C., Rudolph, C. & Rosenecker, J. 2010. **Repeated siRNA application is a precondition for successful mRNA gammaENaC knockdown in the murine airways**. *Eur J Pharm Biopharm,* 75**,** 305-10.

Zabner, J., Cheng, S. H., Meeker, D., Launspach, J., Balfour, R., Perricone, M. A., Morris, J. E., Marshall, J., Fasbender, A., Smith, A. E. & Welsh, M. J. 1997. **Comparison of DNA-lipid complexes and DNA alone for gene transfer to cystic fibrosis airway epithelia in vivo**. *J Clin Invest,* 100**,** 1529-37.

Zabner, J., Couture, L. A., Gregory, R. J., Graham, S. M., Smith, A. E. & Welsh, M. J. 1993. **Adenovirus-mediated gene transfer transiently corrects the chloride transport defect in nasal epithelia of patients with cystic fibrosis**. *Cell,* 75**,** 207-16.

Zabner, J., Ramsey, B. W., Meeker, D. P., Aitken, M. L., Balfour, R. P., Gibson, R. L., Launspach, J., Moscicki, R. A., Richards, S. M., Standaert, T. A. & et al. 1996. **Repeat administration of an adenovirus vector encoding cystic fibrosis transmembrane conductance regulator to the nasal epithelium of patients with cystic fibrosis**. *J Clin Invest,* 97**,** 1504-11.

Zabner, J., Seiler, M., Walters, R., Kotin, R. M., Fulgeras, W., Davidson, B. L. & Chiorini, J. A. 2000. **Adeno-associated virus type 5 (AAV5) but not AAV2 binds to the apical surfaces of airway epithelia and facilitates gene transfer**. *J Virol,* 74**,** 3852-8.

Zabner, J., Smith, J. J., Karp, P. H., Widdicombe, J. H. & Welsh, M. J. 1998. **Loss of CFTR chloride channels alters salt absorption by cystic fibrosis airway epithelia in vitro**. *Mol Cell,* 2**,** 397-403.

Zanta-Boussif, M. A., Charrier, S., Brice-Ouzet, A., Martin, S., Opolon, P., Thrasher, A. J., Hope, T. J. & Galy, A. 2009. **Validation of a mutated PRE sequence allowing high and sustained transgene expression while abrogating WHV-X protein synthesis: application to the gene therapy of WAS**. *Gene Ther,* 16**,** 605-19.

Zeng, Y., Wagner, E. J. & Cullen, B. R. 2002. **Both natural and designed micro RNAs can inhibit the expression of cognate mRNAs when expressed in human cells**. *Mol Cell,* 9**,** 1327-33.

Zhang, P. X., Murray, T. S., Villella, V. R., Ferrari, E., Esposito, S., D'Souza, A., Raia, V., Maiuri, L., Krause, D. S., Egan, M. E. & Bruscia, E. M. 2013. **Reduced caveolin-1 promotes hyperinflammation due to abnormal heme oxygenase-1 localization in lipopolysaccharide-challenged macrophages with dysfunctional cystic fibrosis transmembrane conductance regulator**. *J Immunol,* 190**,** 5196-206.

Zhou, H., Lu, F., Latham, C., Zander, D. S. & Visner, G. A. 2004. **Heme oxygenase-1 expression in human lungs with cystic fibrosis and cytoprotective effects against Pseudomonas aeruginosa in vitro**. *Am J Respir Crit Care Med,* 170**,** 633-40.

Zhou, Z., Wang, X., Liu, H. Y., Zou, X., Li, M. & Hwang, T. C. 2006. **The two ATP binding sites of cystic fibrosis transmembrane conductance regulator (CFTR) play distinct roles in gating kinetics and energetics**. *J Gen Physiol,* 128**,** 413-22.

Zuckerman, J. B., Robinson, C. B., McCoy, K. S., Shell, R., Sferra, T. J., Chirmule, N., Magosin, S. A., Propert, K. J., Brown-Parr, E. C., Hughes, J. V., Tazelaar, J., Baker, C., Goldman, M. J. & Wilson, J. M. 1999. **A phase I study of adenovirus-mediated transfer of the human cystic fibrosis transmembrane conductance regulator gene to a lung segment of individuals with cystic fibrosis**. *Hum Gene Ther,* 10**,** 2973-85.

Zufferey, R., Donello, J. E., Trono, D. & Hope, T. J. 1999. **Woodchuck hepatitis virus posttranscriptional regulatory element enhances expression of transgenes delivered by retroviral vectors**. *J Virol,* 73**,** 2886-92.

Zufferey, R., Dull, T., Mandel, R. J., Bukovsky, A., Quiroz, D., Naldini, L. & Trono, D. 1998. **Self-inactivating lentivirus vector for safe and efficient in vivo gene delivery**. *J Virol,* 72**,** 9873-80.